THE ROLE OF GIBBERELLIN IN THE REPRODUCTIVE DEVELOPMENT OF *ARABIDOPSIS THALIANA*

ANDREW R. G. PLACKETT, BA.

Thesis submitted to the University of Nottingham

for the degree of Doctor of Philosophy

DECEMBER 2011

ABSTRACT

The plant hormone gibberellin (GA) promotes several processes during *Arabidopsis* reproductive development, including the transition to flowering, floral organ growth and fertility. GA functions during stamen development to promote degradation of the tapetum cell layer through programmed cell death (PCD) and in post-anthesis pollen development. Bioactive GA is synthesised through a multi-step pathway, in which the last two biosynthetic steps are expressed as conserved multigene families. One of these, the GA 20-oxidases (GA20ox) consists of five paralogues in *Arabidopsis*, though physiological functions have only been ascribed to two (*AtGA20ox1* and *-2*). Through a reverse genetics approach, this project demonstrates that AtGA20ox1, -2 and -3 account for almost all GA20ox activity in *Arabidopsis*, with very little evidence of any functions for AtGA20ox4 or -5. Unlike AtGA20ox1, -2, -3 and -4, AtGA20ox5 possesses only partial GA20ox activity, performing the first two out of three sequential catalytic conversions *in vitro*.

Partial functional redundancy occurs between AtGA20ox1, -2 and -3 across *Arabidopsis* development, although AtGA20ox1 and -2 dominate. Mapping of floral *AtGA20ox* expression through qPCR and the creation of transgenic GUS reporter lines found that the relationship between these three paralogues is complex, and not explicable through the simple hypothesis of co-expression in the same tissues. During anther development, the reported expression of *AtGA20ox1*, *-2*, *-3* and *-4* is mainly restricted to the tapetum cell layer, and loss of *AtGA20ox1*, *-2* and *-3* results in an anther developmental arrest in which the tapetum does not degrade.

This project demonstrates that stamen development is dependent on an optimum level of GA, with GA-deficiency restricting filament elongation to prevent pollination and GA-overdose negatively affecting anther development. DELLA repression of GA signalling is necessary for successful pollen development, with two of the five DELLA paralogues, RGA and GAI, critical to this process in the Columbia ecotype.

Word count: 83,910

ACKNOWLEDGEMENTS

Firstly, I want to acknowledge and thank my supervisors Peter, Steve and Zoe for their help, expertise and guidance, as well as for putting me forward to do this project in the first place. I hope that I've repaid their trust. Thanks also to Andy Phillips for his advice and input at all the progress meetings he had to sit through, even though *Arabidopsis* isn't his favourite thing.

The members of our lab all deserve special mention: Simon "Chop Chop!" Vaughan; Ian "Scone" Prosser; Anne "Princess Hair" Grønlund; Jayne "I'm Not Playing Any More!" Griffiths; Ellen "Pastry Lattice" Colebrook; Dennis "Cider" Ward; Stephen "Singing" Pearce; Aakriti "Don't Kill Everyone!" Wanchoo; Rob "Enthusiast" Jackson; Barbora "Late Nights" Gallova; Archana "Fume Cupboard" Patil and Richard "Unforgettable" Barker. I particularly want to thank Simon, Ian and Jayne for pointing out when I was being stupid- though it could have been done with a bit less laughter- and Ellen for finding everything so amazing. Others who should get recognition for their help are Helen and Ian, who've done all the washing up, Ian and Anthony, who've prepared countless trays of soil in which to grow all those ruddy plants, Sue and Helen, for really running the show, Rothamsted Bioimaging, Graham Shephard for all the pretty pictures, and Steve Powers, for being a statistical superhero. Thanks too to the members of Zoe's lab, particularly Caiyun and Gema, for sharing their microscopy expertise and making me so welcome on my visits up there.

I also want to thank the regulars of the 11:00 Coffee Group, who's conversation made up for the 'coffee', and lately the Afternoon Coffee Group, by which time we were all just clinging on to sanity. Thanks too to all the other good people, student or otherwise, whom I've met at Rothamsted over four years (Lucia, Till, Clare, Becky, Emma, Emma, Nina, James, Nick, Neil, Charlie, Sam, Mary, Carlos and Freddy to name but a few) for the *in*sanity, laughter, and occasionally alcohol. And thank you Gwyn, Carolina, Dave, Izzy, Martin, Jo, Gareth, Rhi, James and Debbie for reminding me to be me from time to time during all this.

Finally, to all my family and especially Jan Plackett, who wanted a doctor and a solicitor. She's wound up with a plant scientist and a particle physicist. Sorry, Mum...

CONTENTS

LIST OF FIGURES AND TABLES

LIST OF ABBREVIATIONS

2-ODD	2-oxoglutarate-dependent dioxygenase
ANOVA	Analysis of variance
bp	Base pair
C_x-GA	GA molecule with X carbon atoms
cDNA	Complementary DNA
Col-0	Columbia-0
CPS	*ent*-COPALYL DIPHOSPHATE SYNTHASE
C-X	Carbon position X
dH_2O	Deionised water
DNA	Deoxyribonucleic acid
dNTP	Deoxynucleotide triphosphate
FM	Floral meristem
$GA_{(x)}$	Gibberellin (species X)
GA2ox	GA 2-oxidase
GA20ox	GA 20-oxidase
GA3ox	GA 3-oxidase
GAI	GA INSENSITIVE
GC-MS	Combined gas chromatography-mass spectrometry
gDNA	Genomic DNA
GFP	Green fluorescent protein
GID1	GIBBERELLIN INSENSITIVE DWARF 1
GUS	β-Glucuronidase
HPLC	High performance liquid chromatography
IM	Inflorescence meristem
KAO	*ent*-KAURENOIC ACID OXIDASE
kb	Kilobase
KO	*ent*-KAURENE OXIDASE
KS	*ent*-KAURENE SYNTHASE
L*er*	Landsberg *erecta*

LSD	Least significant difference
ml	Millilitre
mm	Millimetre
mM	Millimolar
ng	Nanogram
PCD	Programmed cell death
PCR	Polymerase chain reaction
PMC	Pollen mother cell
qPCR	Quantitative real-time PCR
RGA	REPRESSOR OF *ga1-3*
RGL1, -2, -3	RGA LIKE 1, -2, -3
RNA	Ribonucleic acid
RT-PCR	Reverse transcription-PCR
SAM	Shoot apical meristem
S.E.	Standard Error
SNP	Single nucleotide polymorphism
µg	Microgram
µl	Microlitre
µm	Micrometre
µM	Micromolar

CHAPTER 1: GIBBERELLIN AND *ARABIDOPSIS* REPRODUCTIVE DEVELOPMENT

1.1 GIBBERELLIN: CHEMICAL STRUCTURE AND BIOLOGICAL ACTIVITY

The phytohormone gibberellin (GA) acts to regulate plant growth and development throughout the various phases of the plant lifecycle, promoting germination, growth of plant tissues, organogenesis and both male and female fertility (Fleet & Sun, 2005). The importance of GA to the fertility of flowering plants is demonstrated by the phenotype of a GA-deficient mutant of the genetic model *Arabidiopsis thaliana*, *ga1-3*, which, although it produces flowers, is both male and female sterile (Koornneef & Van der Veen, 1980, see Figure 1.1). The presence of GA has been shown to enhance both expansion and division of plant cells (Ubeda-Tomas et al., 2009), providing a mechanism through which morphogenesis is controlled at a supracellular level. These responses arise from widespread, tissue-specific transcriptional changes triggered by GA signalling, the targets of which include many different transcription factors (Cao et al., 2006; Zentella et al., 2007). Some bacterial and fungal species also produce GAs, but comparison between the biosynthesis pathways in higher plants and the fungus *Gibberella fujikuroi* indicates that the ability to synthesise GA did not evolve from a common ancestral origin (Hedden et al., 2002). Although the presence of GAs has been reported in plant species as diverse as algae, mosses and ferns (Radley, 1961; Kato et al., 1962; Ergün et al., 2002), evolutionary studies of GA signalling components suggest that the co-option of GA as a signalling molecule (at least via the signalling mechanism conserved across angiosperms, see section 1.3) occurred in land plants after the divergence of bryophytes (mosses) but prior to the emergence of vascular plants (Hirano et al. 2007, Yasumura et al. 2007), and thus also prior to the evolution of flowering plants.

The GAs comprise a large family of related molecular structures within a class of organic compounds called the diterpenes, derived from the 20-carbon (C_{20}) compound geranylgeranyl diphosphate (GGDP, Bohlmann et al., 1998). 136 different gibberellins have been isolated from a variety of plant, fungal and bacterial species (http://www.plant-hormones.info/

Figure 1.1: The effect of GA-deficiency on flowering plant growth and development. *Comparison of the phenotypes of a mature wild-type* Arabidopsis *plant (Columbia-0 ecotype) and the GA-deficient mutant* ga1-3 *(backcrossed into Col-0), showing vegetative (a,b) and floral (c) phenotypes.*

gibberellins.htm), the specific structure of each designated through a standardised numerical nomenclature (Macmillan & Takahashi, 1968). Of these, four GAs are the main biologically active forms in plant species: GA_1, GA_4 , GA_3 and GA_7 (Hedden & Phillips, 2000; see Figure 1.2). GA_1 and GA_4 are the two predominant bioactive forms of GA found in plant tissues, with *Arabidopsis* mainly producing GA_4 in both vegetative and reproductive tissues (Talon et al., 1990). In rice (*Oryza sativa*), a dichotomy has been identified between the vegetative and

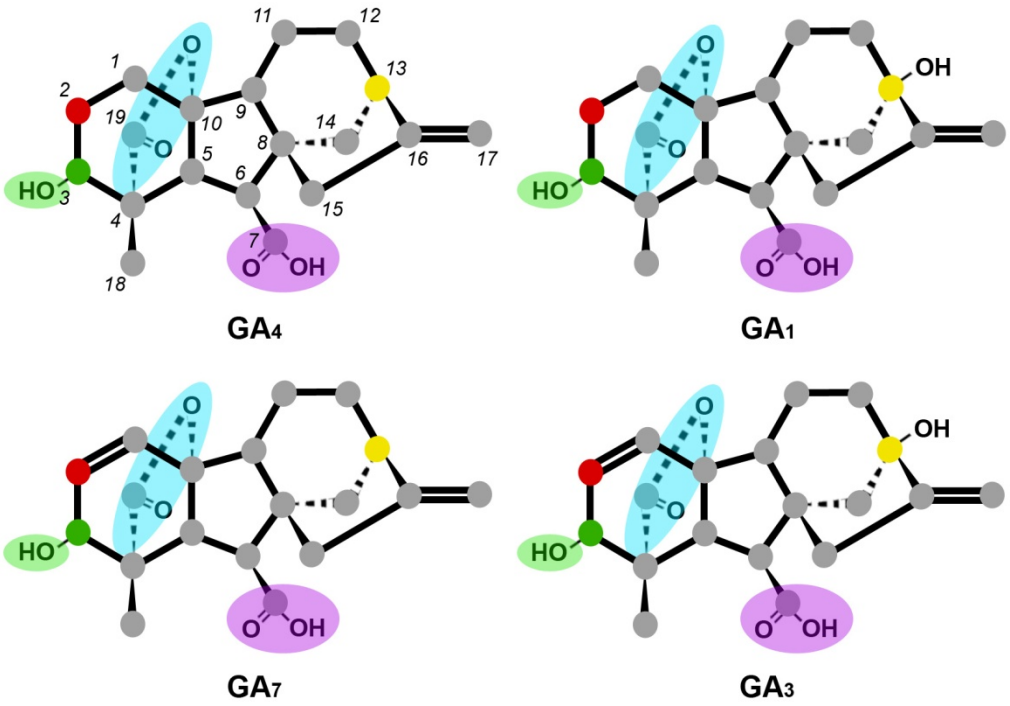

Figure 1.2: Molecular structure of bioactive GA species.

Numerals in italics shown on GA_4 denote carbon positions (grey circles). Carbon positions with structural or biological signficance (C_2, C_3 and C_{13}) are indicated in red, green and yellow, respectively. Common structural features that confer bioactivity on these species are highlighted in blue (lactone group) green (3 hydroxyl group) and purple (6 carboxyl group), respectively.

reproductive phases: GA_1 predominates during vegetative growth whilst GA_4 is the most abundant bioactive GA in reproductive tissues (Kurogochi et al., 1979; Kobayashi et al., 1984, 1988). As such, it appears that GA_4 is more important to reproductive development than GA_1, although based on their signalling responses plants do not seem to actually distinguish between these two forms (Macmillan, 2001) and so the reason for this preference in rice is as yet unclear. GA molecules do not in themselves have any innate biological activity- in order to elicit a physiological response in plants there needs to be both a mechanism for perceiving GA (the GID1 receptor, see section 1.3.1) and for effecting a downstream response to that signal (see section 1.3.2). Recent progress in resolving the crystal structure of the GID1 protein (Murase et al., 2008; Shimada et al, 2008) has determined that the structural basis underlying bioactivity of some GA species and not others is due to the structure of the GA

binding site of GID1, which results in close binding of certain GA conformations. Particular features that confer bioactivity on a GA molecule are their oxidation to a C_{19} structure, a lactone group bridging carbons 4 and 10 in place of carbon 20, a carboxyl group at carbon 6 and the β-hydroxylation of carbon 3 (Hoad, 1983; Figure 1.2). Importantly, bioactive and intermediate forms of GA can be rendered inactive by β-hydroxylation of carbon 2 (Thomas et al. 1999), resulting in stearic hindrance between the GA molecule and the GID1 GA binding site (Shimada et al, 2008). This mechanism for GA deactivation via GA 2-oxidase (GA2ox) activity plays an important role in regulating the production of bioactive GA in plant tissues (see section 1.2.2, Rieu et al., 2008a).

1.2 GA BIOSYNTHESIS AND CATABOLISM

Components of a single, conserved GA biosynthesis pathway have been identified in both *Arabidopsis* and rice (Figure 1.3, Hedden & Phillips 2000; Yamaguchi, 2008), implying that the same pathway exists in both monocot and dicot flowering plants. Although we now understand the steps through which plants produce their predominant forms of bioactive GA, it is believed that later stages of the pathway would best be represented as a metabolic grid as opposed to a linear pathway (MacMillan, 1997; Hedden & Phillips, 2000). Regulation of this pathway has been shown to be complex, involving the interaction of developmental, environmental and homeostatic factors to determine the level of bioactive GA. Bioactive GA is not synthesised uniformly across all tissues: in the floral context, measurements taken in rice identified high concentrations of GA_4 in anther tissue but not in the lemma (sepal/petal analogue, Kobayashi et al, 1988). Petal growth is also correlated to that of stamens in *Arabidopsis* GA biosynthesis and signalling mutant phenotypes (Figure 1.1). As such, certain plant tissues may be dependent on others for the production of a GA signal. The mobility of bioactive GA has been previously demonstrated in *Arabidopsis* during the transition to reproductive development (see section 1.5.1). The level of bioactive GA in specific tissues is controlled by regulating synthesis and deactivation rather than intracellular sequestration of bioactive forms: analysis of the relative concentrations of bioactive and intermediate GA species in rice indicates that some intermediate GAs are more abundant in plant tissues than bioactive GA (Kobayashi et al., 1988). When a GA signal is required, bioactive GA is

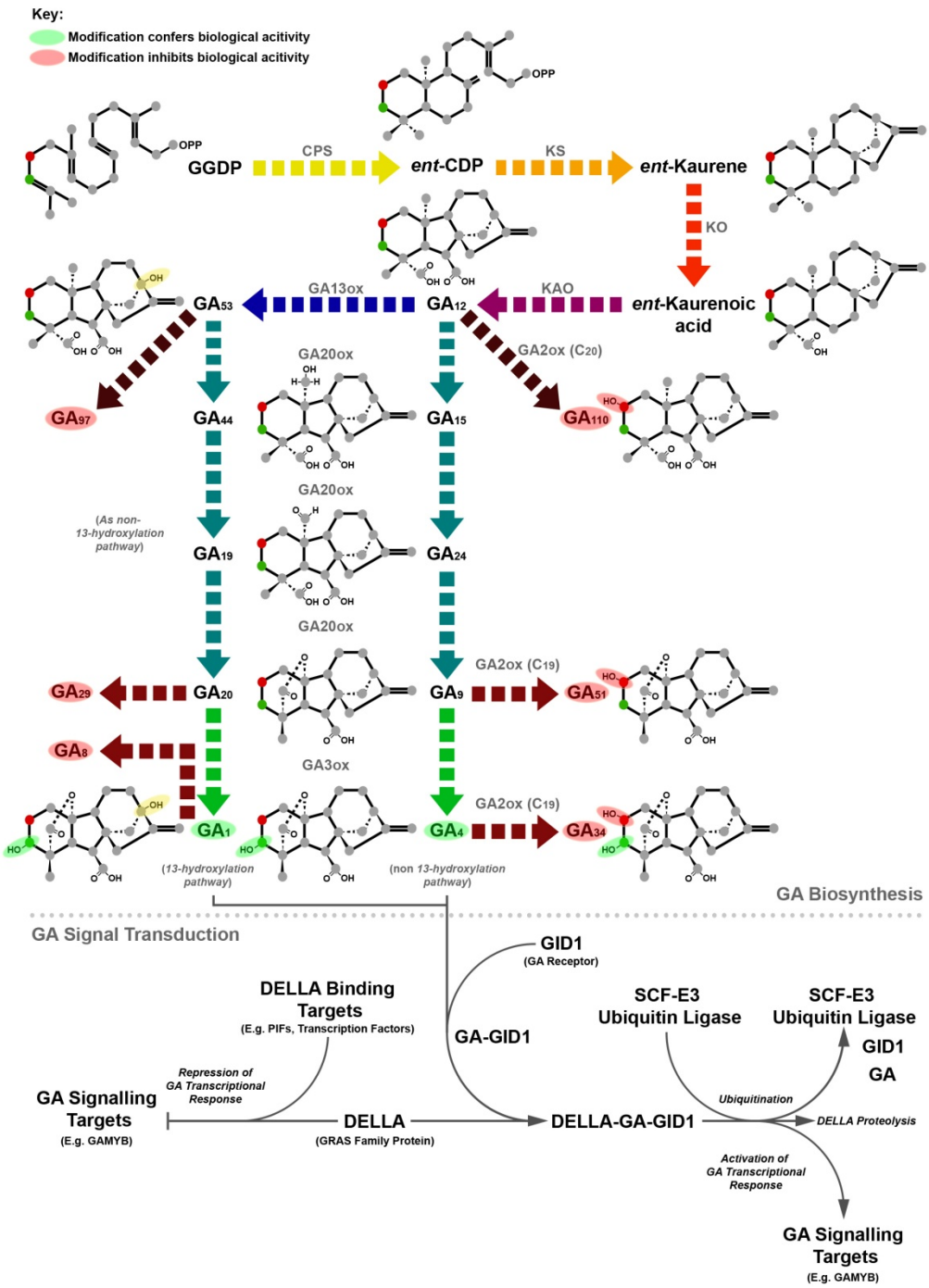

Figure 1.3: Schematic of the GA biosynthesis and signal transduction pathway. *Coloured arrows represent steps catabolised by individual enzymes (specified in grey). Carbon skeleton structures included are of representative GA species, demonstrating important structural modifications at each step. Modifications that confer bioactivity are highlighted in green, those that inhibit bioactivity in red. Hydroxylation of carbon-13 is highlighted in yellow. Adapted from Plackett et al. (2011).*

synthesised from this pool of existing intermediates. Consequently, regulation of the enzymes catalysing the final steps of GA biosynthesis has been shown to exert significant influence on the level and spatial distribution of bioactive GA (see section 1.2.1). *Arabidopsis* growth and development is not saturated for GA response: application of exogenous GA to the Columbia ecotype causes significant increases in final plant size (Jacobsen & Olszewski, 1993). This implies that the level of bioactive GA produced in plant tissues is tightly regulated.

The GA biosynthesis pathway can be subdivided into three broad stages. The common diterpenoid metabolite *trans*-geranlygeranly diphosphate (GGDP, Figure 1.3) is catalysed to *ent*-kaurene by terpene cyclases, which occur as single copy genes in both *Arabidopsis* and rice (Table 1.1, Hedden & Phillips, 2000; Sakamoto et al., 2004). *ent*-copalyl diphosphate synthase (CPS) catalyses the first recognised step of GA biosynthesis, the conversion of GGDP to *ent*-copalyl diphosphate (Figure 1.3, Sun & Kamiya, 1994), and deletion of *AtCPS* (also referred to as *GA1*) in the *Arabidopsis* mutant *ga1-3* (Sun et al., 1992) causes a severely GA-deficient, dwarfed phenotype. The second stage (conversion of *ent*-kaurene to GA_{12}) is catalysed by the P450 monooxygenases KO and KAO. The final stage of biosynthesis is catalysed by 2-oxogluterate dependent dioxygenases (2-ODD's), which exist as two conserved families of isozymes: the GA 20-oxidases (GA20ox's) and GA 3-oxidases (GA3ox's, see section 1.2.1). Environmental regulation of early GA biosynthetic steps including *ent*-kaurene synthesis has been demonstrated in some species, with particular enhancement of expression by light and photoperiod (Sun & Kamiya, 1997; Zeevaart & Gage, 1993).

Comparisons between the tissue expression patterns of early and late *Arabidopsis* GA biosynthetic genes demonstrates that the GA biosynthesis pathway is spatially distributed. In roots, for example, analysis of *AtCPS* expression through transgenic β-glucuronidase (GUS) reporter lines indicate that expression is restricted to the growing tip (root apical meristem (RAM) and division zone/early elongation zone, but excluded from the root cap and vasculature, Silverstone et al., 1997), whilst *AtGA3ox* expression is localised to vascular tissues above the root elongation zone as well as the elongation zone, quiescent centre (QC) of the RAM and the root cap (Mitchum et al., 2006). Unpublished GUS expression data

Gene Function	Number of Paralogues	
	Arabidopsis thaliana	Rice (*Oryza sativa*)
ent-Copalyl Diphosphate Synthase (CPS)	1 (*GA1*)	1 (*OsCPS*)
Kaurene Synthase (KS)	1 (*AtKS*)	1 (*OsKS*)
Kaurene Oxidase (KO)	1 (*AtKO*)	1 (*OsKO*)
Kaurenoic Acid Oxidase (KAO)	2 (*AtKAO1, -2*)	1 (*OsKAO*)
GA 20-Oxidase (GA20ox)	5 (*AtGA20ox1, -2, -3, -4, -5*)	4 (*OsGA20ox1, -2, -3, -4*)
GA 3-Oxidase (GA3ox)	4 (*AtGA3ox1, -2, -3, -4*)	2 (*OsGA3ox1, -2*)
C_{19} GA 2-Oxidase (C_{19}-GA2ox)	5 (*AtGA2ox1, -2, -3, -4, -6*)	7 (*OsGA2ox1, -2, -3, -4, -7, -8, 10*)
C_{20} GA 2-oxidase (C_{20}-GA2ox)	2 (*AtGA2ox7, -8*)	3 (*OsGA2ox5, -6, -9*)
Gibberellin Insitive Dwarf 1(GID1) (GA receptor)	3 (*AtGID1A, AtGID1B, AtGID1C*)	1 (*OsGID1*)
DELLA (GA Response Repressor)	5 (*GAI, RGA, RGL1, -2 -3*)	1 (*SLR1*)
F-Box (GA Signal Transduction)	2 (*SLY1, SNZ*)	1 (*GID2*)
GAMYB (Downstream DELLA Target)	2 (*MYB33, MYB65*)	1 (*OsGAMYB*)

Table 1.1: Comparison of GA biosynthetic and GA signalling gene numbers between *Arabidopsis* and rice.

indicates that *AtGA20ox* expression may partially bridge this divide in root tissues, with expression in the root meristem, elongation zone and root vasculature (A. Phillips). In developing floral tissues *AtCPS* and *AtGA3ox* expression patterns are reported to overlap to a greater extent than in roots, but not completely (Figure 1.10, Silverstone et al., 1997; Mitchum et al., 2006; Hu et al., 2008). The intercellular mobility of particular GA intermediates remains a subject for debate, though the differential expression patterns of *AtCPS* and *AtKO* seen at germination (Yamaguchi et al, 2001) identifies *ent*-kaurane as a mobile intermediate. Grafting experiments in pea (*Pisum sativum*, Proebsting et al., 1992) between GA-deficient shoots and wild type rootstocks support this principle: a wild type root was unable to rescue growth of an *le* shoot (a *GA3ox* knockout mutant), but growth of *na* mutant shoots (a *KAO* knockout, Ingram & Reid, 1987; Davidson et al. 2003) was rescued, indicating differential mobility of different GA species over long distances. Evidence suggests a further compartmentalisation of GA biosynthesis within plant cells. Both CPS and KS proteins have been localised to plastids (Sun & Kamiya, 1994; Aach et al., 1995, Helliwell et al., 2001) and KAO to the endoplasmic reticulum (ER, Helliwell, 2001), whilst 2-ODDs are believed to be cytosolic (Yamaguchi, 2008).

1.2.1 The *GA 20-Oxidase*, *GA 3-Oxidase* and *GA 2-Oxidase* Gene Families

The activity of the last stage of GA biosynthesis governs the production of bioactive GA, with GA20ox activity in particular limiting the rate of biosynthesis. Ectopic expression of *GA20ox* genes drives an increase in the concentration of bioactive GA in *Arabidopsis* tissues (Huang et al., 1998; Coles et al., 1999), whilst increasing expression of earlier biosynthetic genes such as *AtCPS* causes an increase in GA_{12} concentration, but not that of bioactive GA (Fleet et al., 2003). Whilst loss of *AtGA3ox* expression causes dwarfed phenotypes (Mitchum et al., 2006), attempts to overexpress *AtGA3ox* genes in *Arabidopsis* to date have not produced obvious GA-overdosed phenotypes (Phillips, 2004). That said, ectopic expression of the pumpkin (*Cucurbita maxima*) gene *CmGA3ox1* (which demonstrates unusual catalytic activity *in vitro*) in *Arabidopsis* has since been shown to cause GA-overdosed growth phenotypes (Radi et al., 2006). Overexpression of a native GA3ox in hybrid aspen (*Populus tremula x Populus tremuloides*) was shown to cause only minor changes to growth and the amount of bioactive GA present (Israelsson et al., 2004), whilst overexpression of *PttGA20ox* caused a 20-fold increase in bioactive GA and dramatically increased internode elongation (Eriksson et al., 2000), suggesting that GA20ox activity is rate limiting within the GA biosynthesis pathway. GA analysis of specific rice plant tissues and whole *Arabidopsis* plants supports this model, with GA20ox substrates (GA_{53}, GA_{44}, GA_{19} and GA_{24} in *Arabidopsis*, GA_{19} in rice) being more abundant than those of GA3ox in both species (Kurogochi et al., 1979; Kobayashi et al., 1988; Xu et al. 1997).

2-ODD enzymes catalyse oxidative reactions, with the GA20ox, GA3ox and GA2ox families oxidising carbon positions 20, 3 and 2, respectively (Figures 1.2 and 1.3). Each GA20ox enzyme catalyse a series of oxidative reactions, ultimately resulting in the loss of carbon-20 to create a C_{19} molecule, whilst most GA3ox enzymes apparently catalyse the final oxidative step to create GA_4 and GA_1 (Hedden, 1997). Two distinct functional sub-groups of GA2ox enzyme have been identified in both *Arabidopsis* and rice, one preferring C_{20} GA species as substrates and the other C_{19} GAs (Schomburg et al., 2003; Lee & Zeevaart, 2005; Lo et al.,

2008). In all three of these families each enzyme catalyses oxidation of both 13-hydroxylated and non-13-hydroxylated substrates (Hedden & Phillips, 2000).

Genome sequence analysis indicates that multiple, copies of *GA20ox*, *GA3ox* and *GA2ox* genes exist in both *Arabidopsis* and rice (Hedden & Phillips, 2000; Sakamoto et al., 2004; Lo et al., 2008), but although the existence of multigene families is conserved between these two species the number of genes within these families varies (Table 1.1). Based on sequence similarity, *Arabidopsis* carries five *GA20ox*, four *GA3ox* and seven *GA2ox* genes. Tissue expression pattern analysis using GUS reporter lines demonstrates that members of the *AtGA3ox* gene family are differentially expressed, leading to functional specialisation: *AtGA3ox1* and *-2* are primarily expressed in vegetative tissues, whilst expression of *AtGA3ox3* and *-4* is restricted to the reproductive phase of development, in flowers and siliques (Mitchum et al., 2006, Hu et al., 2008). Mutant analysis indicates that, as well as having specialist functions in plant development, *AtGA3ox1* and *-2* have partially overlapping functions, for example in leaf expansion and root growth (Mitchum et al., 2006). Although loss-of-function alleles for *AtGA3ox3* and *-4* have been identified and analysed (see section 1.5.4, Hu et al., 2008), the *AtGA3ox2* and *-4* loci are immediately adjacent on chromosome 1, presenting a technical barrier to creating combinatorial mutants in which all four paralogues are non-functional.

Functional specialisation and redundancy between these four paralogues is also evident in the floral context, most notably during stamen development. *AtGA3ox1* expression is restricted to the stamen filament (Mitchum et al., 2006) whilst *AtGA3ox2*, *-3* and *-4* are expressed in developing anther tissues (Figure 1.10, Hu et al., 2008). Within the anther expression of *AtGA3ox2* diverges compared to that of *AtGA3ox3* and *-4* (Hu et al., 2008): although all are expressed from the same developmental stage (meiosis), expression of *AtGA3ox3* and *-4* is strongest in the tapetum cell layer, expression declining after the degeneration of this layer until only occurring in mature pollen by the time anther development is complete. In contrast, when expression of *AtGA3ox3* and *-4* is at its strongest, *AtGA3ox2* expression has declined, reappearing in developing pollen and the surrounding anther wall tissues after tapetal

degeneration, a peak in expression coinciding with anther dehiscence. Interestingly, despite not being expressed in anther tissues, mutant analysis indicates that the action of *AtGA3ox1* can compensate for the absence of both *AtGA3ox2* and *-3* or both *AtGA3ox3* and *-4*, whereas the *ga3ox1 ga3ox2 ga3ox3* and *ga3ox1 ga3ox3 ga3ox4* triple mutants display stamen developmental defects (Hu et al., 2008, see section 1.5.4). Conversely, the *ga3ox1* single mutant demonstrates normal stamen filament elongation whilst *ga3ox1 ga3ox3* double mutant flowers have short stamens (Hu et al., 2008). As such, the effect of these different paralogues on phenotype is not entirely constrained to the tissues in which they are expressed, a phenomenon that can be explained by the mobility of bioactive GA from the site of synthesis. This further reinforces the point that the sites of GA action are not necessarily restricted to the sites of GA biosynthesis.

As yet the floral tissue expression patterns of the five *AtGA20ox* paralogues have not been reported, representing a significant gap in our knowledge. Broad scale expression analysis by qPCR (Rieu et al., 2008) indicates that *AtGA20ox1* and *-2* are the most abundantly and consistently expressed paralogues across *Arabidopsis* development. *AtGA20ox3* expression is more varied, being most highly expressed in developing seeds, during germination and early vegetative growth, whilst only minor roles are predicted for *AtGA20ox4* and *-5*, though both are expressed in inflorescence tissue. Mutant analysis of *AtGA20ox1* and *-2* in the same paper demonstrates a mixture of specialisation and functional redundancy between these two paralogues, including during floral development, where the *ga20ox1* and *ga20ox2* single mutants have no reported phenotype, but *ga20ox1 ga20ox2* flowers demonstrate stamen developmental defects (see section 1.5.4). The semi-dwarf phenotype of *ga20ox1 ga20ox2* (Rieu et al., 2008) indicates remaining functions for the other *AtGA20ox* paralogues, for which loss-of-function alleles have not yet been published.

The expression of specific *AtGA20ox*, *AtGA3ox* and *AtGA2ox* paralogues, as well as differing spatially and temporally, is differentially regulated by a number of different environmental factors. The expression of *AtGA3ox1* and *-2* during germination is photo-reversibly up-regulated by red light, mediated in the case of *AtGA3ox2* (but not *AtGA3ox1*) through

phytochrome B (Yamaguchi et al., 1998). In the same tissues, *AtGA2ox2* is down-regulated in response to red light and upregulated in the dark (Yamauchi et al., 2007). Thus, co-ordinated changes in expression between GA biosynthesis and catabolism genes exacerbates the effect of light regulation on the levels of bioactive GA within the seed. Conversely, evidence has been published indicating that *AtGA20ox2* and, to a lesser extent, *AtGA20ox1*, are up-regulated in response to far-red light to promote petiole elongation (Hisamatsu et al., 2005), with up-regulation apparently dependent on the inactivation of PhyB. The same study also saw up-regulation of *AtGA20ox2* (but not *AtGA20ox1*) under long day photoperiods. Increased expression of *GA20ox* and *GA3ox* paralogues in response to photoperiod has also been observed in spinach (Wu et al., 1996; Lee & Zeevaart, 2002). During germination, Yamauchi et al. (2004) demonstrated that low temperature specifically up-regulates *AtGA20ox1*, *-2* and *AtGA3ox1* expression in imbibed seed, but not expression of *AtGA20ox3* or *AtGA3ox2*, which are also expressed at this stage. Interestingly, *AtGA3ox1* was shown to respond independently to these two simultaneous environmental stimuli, with red light causing an additive increase in *AtGA3ox1* expression in conjunction with cold treatment (Yamauchi et al., 2004). Circadian regulation of specific paralogues has also been demonstrated, with both *AtGA3ox1* (Penfield & Hall, 2009) and *AtGA20ox1* (but not *AtGA20ox2*, Hisamatsu et al., 2005) expression demonstrating periodicity in specific developmental contexts. It can be concluded from this combined evidence that, although each paralogue within the same family appears to perform the same biochemical function, the timing, position and manner in which they are expressed can result in profoundly different developmental roles for individual paralogues.

Although GA2ox-mediated 2β-hydroxylation appears to be a major pathway of GA inactivation, with loss of multiple paralogues resulting in GA-overdosed phenotypes and reduced fertility (Rieu et al., 2008a), evidence for other mechanisms of GA inactivation is now being uncovered. These include *ELONGATED UPPERMOST INTERNODE* (*EUI*, Zhu et al. 2006) in rice, which inactivates non-13-hydroxylated GAs by epoxidation of the C-16,17 double bond and, in *Arabidopsis*, methylation of a broad range of GA species by two gibberellin methyltransferase enzymes, GAMT1 and GAMT2 (Varbanova et al., 2007). The

presence of multiple mechanisms for GA inactivation may be an indication of the importance to successful plant development of preventing inappropriate GA responses. Importantly, it has been demonstrated through exogenous GA application that excess GA is sub-optimal to *Arabidopsis* fertility, reducing the number of seeds set per silique (Jacobsen & Olszewski, 1993). The mechanism of GA signal transduction as we now understand it also seems geared to this philosophy, working through a constant negative signal that is relieved by the presence of GA, thus potentially reducing the risk of 'leaky' downstream signalling in the absence of GA. The following sections summarise our current model of the mechanism of GA signal transduction and how regulation of its components is integrated with that of the GA biosynthesis pathway.

1.3 GA SIGNALLING

The presence of bioactive GA alone is insufficient to cause plants cells to respond- they must also have the capacity to perceive the presence of bioactive GA and a mechanism through which GA-dependent changes can be effected. With recent advances in our understanding of GA signalling components in both *Arabidopsis* and rice, a conserved model of GA signal transduction has emerged, based on the principle of relief of repression (Harberd et al., 2009; Sun, 2010; Ueguchi-Tanaka & Matsuoka, 2010). In the absence of a GA signal, a particular transcriptomic state is maintained by interaction of the DELLA proteins with target transcription factors and other partners (see section 1.3.3). Binding of bioactive GA to the receptor protein GIBBERELLIN INSENSITIVE DWARF 1 (GID1) promotes its association with DELLA proteins, which are subsequently targeted for degradation via the 26S proteasome (Figure 1.3). Removal of the DELLA proteins alters the balance of interactions between transcription factors, which in turn changes the transcriptional output of that responding cell. Although other hormone signal transduction pathways share this paradigm (for example auxin and jasmonate signalling, Spartz & Gray, 2008), this particular signal transduction pathway responds solely to GA, with separate signal transduction pathways responding to the presence other hormones. Points of interaction between GA signalling and other signal transduction pathways during reproductive development are still being identified (see section 1.5.4)

Given the mobility of bioactive GA once it has been synthesised (see section 1.2), another experimental approach to identifying where and when GA plays a role in plant developmental is to locate the sites of GA action via the tissue expression patterns of the signal transduction machinery. Analysis of GA signalling mutants is complicated in *Arabidopsis* due to the presence of multiple paralogues of both GID1 and DELLA (Table 1.1, see sections 1.3.1 and 1.3.2), whilst rice carries a single GID1 and DELLA proteins (SLENDER RICE 1, Ikeda et al. 2001). The contrast in the number of GA signalling components between these two species, unlike the conservation of multigene families in GA biosynthesis, is interesting. Loss of *SLR1* in rice causes vegetative phenotypes resembling plants chemically overdosed with bioactive GA (i.e. excessive growth) and male sterility (Ikeda et al., 2001). The precise nature of the male sterility phenotype in rice is not described, but in barley (which also carries a single DELLA gene, *SLENDER 1*, Lanahan & Ho, 1988), where a similar male sterility phenotype is reported in *sln1*, the phenotype is described as pollenless (Lanahan & Ho, 1988). This suggests that repression of GA responses is very important to maintaining successful pollen development in some way.

1.3.1 GA Signal Perception: The GID1 Receptor

First identified through a loss of function mutation in rice (Ueguchi-Tanaka et al., 2005), three paralogues of GID1 have been independently identified in *Arabidopsis*: *AtGID1a*, *-b* and *-c* (Griffiths et al., 2006; Nakajima et al., 2006; Iuchi et al., 2007). Protein interactions between GID1 and DELLA proteins have been demonstrated *in vitro* by yeast-2-hybrid screens for both rice (Ueguchi-Tanaka et al., 2007, also *in planta*) and (all three) *Arabidopsis* orthologues (Griffiths et al., 2006; Nakajima et al., 2006), the binding affinity enhanced in both systems by the presence of bioactive GA. Interestingly, a low background level of protein interaction was detected in the yeast-2-hybrid assays between DELLA proteins and AtGID1b and -c even in the absence of GA (Griffiths et al., 2006; Nakajima et al., 2006). GA-independent interaction between GID1 and DELLA has since been demonstrated *in vitro* and *in planta* in rice using a mutant form of *OsGID1* (Yamamoto et al., 2010), identifying a key amino-acid residue shared with AtGID1b and homologues from other plant species that also demonstrated GA-

independent DELLA interaction *in vitro*. Interaction between GID1 and DELLA protein is nevertheless dramatically enhanced by the presence of bioactive GA, a process that can now be explained by a conformational change induced in the GID1 receptor protein on binding with a bioactive GA molecule (Murase et al., 2008; Shimada et al., 2008).

Loss of GID1 in rice confers an extreme dwarf phenotype, similar to severely GA-deficient mutants, but unlike biosynthesis mutants growth cannot be rescued by exogenous GA treatment (Ueguchi-Tanaka et al., 2005). The severity of this phenotype suggests that GID1 is the predominant (and potentially the only) GA receptor present in rice. In *Arabidopsis*, both expression analysis and phenotypic analysis of combinatorial mutants indicates that *AtGID1A, -B* and *-C* are functionally redundant, requiring the loss of all three to produce a similar extreme dwarf phenotype (Griffiths et al., 2006; Iuchi et al. 2007; Willige et al. 2007). Some phenotypic differences are observed between these reports, most notably with regards to flowering. Iuchi et al. (2007) and Willige et al. (2007) found that the *gid1* triple mutant failed to flower whilst Griffiths et al. (2006) report that it eventually does (see section 1.5.2 for further discussion). The rice *gid1* mutant does flower, although the flowers are sterile (Ueguchi-Tanaka et al., 2005; Aya et al., 2009, see section 1.5.2). Only small differences in vegetative phenotype occur between the *AtGID1* single and double mutants compared to wild-type plants (although stem elongation is reduced in the *Atgid1a Atgid1c* double mutant, Griffiths et al., 2006; Iuchi et al. 2007), demonstrating that the function of these three paralogues overlaps to a large extent. Analysis of floral phenotypes showed that loss of *AtGID1a* and *-b* reduces stamen filament elongation, but only slightly, again indicating functional redundancy between all three paralogues in this context. The precise tissue expression patterns of these three paralogues has not yet been reported, but quantitative and semi-quantitative RT-PCR analysis of expression levels found that the three paralogues are expressed (at varying levels) in all of the tissues sampled during plant development (Griffiths et al., 2006; Nakajima et al., 2006). Functional redundancy and the apparently broad-ranging (cumulative) expression of *AtGID1* may make its distribution less informative about the sites of GA signalling than the expression patterns of other components of the GA signal transduction pathway.

Although the severely dwarfed phenotypes of the *gid1* mutants suggest that GID1 is the primary GA receptor throughout angiosperm development, the soluble nature of this protein and its reported nuclear localisation in rice (Ueguchi-Tanaka et al., 2005) contrasts with evidence from experiments on barley aleurone cell layers, where a GA receptor was predicted to associate with the plasma membrane (Hooley et al., 1991; Gilroy & Jones, 1994). Loss-of-function mutant alleles of the barley *GID1* orthologue have been identified and characterised (Chandler et al., 2008), finding residual sensitivity to exogenous GA treatment of both vegetative and aleurone tissues in these mutants. As such, the possible existence of another GA receptor cannot be explicitly ruled out, although from the evidence outlined above any such receptor is likely to play an extremely minor role in GA signalling.

1.3.2 GA Signal Transduction: DELLA Proteins and Proteolysis

The DELLA proteins are a conserved phylogenetic group belonging to a protein superfamily defined by the presence of a C terminal GRAS domain, encoding a basic leucine zipper (bZIP) DNA binding motif (Pysh et al., 1999). Loss of the C-terminal GRAS domain in DELLA proteins results in a loss of DELLA function (Silverstone et al., 1998), which in turn causes a rescue of growth in GA-deficient mutant backgrounds (Silverstone et al., 1997a; Dill & Sun, 2001), clearly demonstrating the role of DELLA proteins as negative regulators of plant growth. Within the GRAS family, DELLA proteins share the unique feature of GA-responsiveness, which is conferred by an N-terminal domain defined by the presence of the amino-acid sequence aspartate (D) glutamate (E) leucine (L) leucine (L) alanine (A). Loss of this domain creates a dominant-negative dwarf phenotype in both *Arabidopsis* (the *ga insensitive* (*gai*) allele, Peng et al., 1997; Dill et al., 2001) and wheat (*reduced height* (*rht*), Peng et al. 1999) in which there is constitutive repression of downstream GA responses by the truncated DELLA protein which cannot be alleviated by exogenous GA treatment. We now know that this N-terminal region of the DELLA protein binds to the GA-bound form of GID1 (Murase et al., 2008), a conclusion supported by *in vitro* deletion studies that demonstrate the necessity of the N-terminal region to the DELLA-GID1 interaction (Willige et al., 2007).

The nature of DELLA protein action to repress GA transcriptional responses is as yet less clearly understood. Despite the identification of early downstream targets through microarray and RT-PCR-based techniques (Cao et al. 2006, Zentella et al. 2007, Hou et al., 2008, see section 1.3.3) *in planta* studies have failed to demonstrate direct DNA binding by DELLA proteins to target promoters (Feng et al., 2008). DELLAs have been demonstrated to interact with targets at the protein level, forming complexes with transcription factors that in turn can bind DNA (see section 1.3.3). As such, it appears that DELLA proteins act to modify GA transcriptional responses indirectly through interaction with other proteins that themselves regulate transcription. This group of proteins could be specified as 'DELLA binding proteins' rather than downstream targets, although they are not precluded from also being eventual transcriptional targets downstream of GA signalling.

Five DELLA paralogues have now been identified in *Arabidopsis*, based on sequence similarity: *GAI*, *REPRESSOR OF GA1-3* (*RGA*), *RGA-LIKE1* (*RGL1*), *RGL2* and *RGL3* (Dill & Sun, 2001). All five have been shown to bind to AtGID1 *in vitro* (Nakajima et al., 2006) and mutant analysis in the Landsberg *erecta ga1-3* GA-deficient background has so far demonstrated growth-regulating functions for all but *RGL3* (Dill & Sun, 2001; Wen & Chang, 2002; Lee et al., 2002; Tyler et al., 2004). This approach has also demonstrated partial functional redundancy between these paralogues: loss of *RGA* partially restores vegetative growth to *ga1-3* plants, whilst loss of *GAI* does not, but loss of both restores growth to that of L*er* wild type (Dill & Sun, 2001; King et al. 2001). Both of these studies found that loss of *RGA* and *GAI* was not sufficient to rescue floral development in the *ga1-3* background, which is otherwise arrested at an early stage (see section 1.5.2). In contrast, a combined loss of *RGA* and *RGL2* was sufficient to partially restore fertility in late *ga1-3* flowers, whilst loss of *RGA*, *RGL1* and *RGL2* completely restored floral development (Cheng et al., 2004). This same conclusion was reached through independent mutant analysis in the Columbia ecotype (Tyler et al., 2004). However, apparent ecotype-specific differences have been uncovered, with loss of *RGA* alone substantially rescuing *ga1-3* floral development in Col-0 (Tyler et al., 2004), which was not observed in L*er* (Dill & Sun, 2001). Interestingly, despite the apparent predominance of *RGA*, *RGL1* and *RGL2*, Dill and Sun (2001) report a reduced fertility

phenotype when *RGA* and *GAI* are lost in the L*er* background, with reduced amounts of pollen and stamen length reduced relative to pistil growth at flower opening. Recent work indicates that loss of *RGA* and *GAI* from Col-0 results in complete male sterility (Thomas, S., personal communication).

These results cumulatively demonstrate that the relative importance of particular DELLA paralogues in regulating GA responses varies between different tissues, with Tyler et al. (2004) demonstrating differential expression patterns of the various paralogues across development using qPCR analysis. As well as functional specialisation through spatial separation, however, recent attempts to identify downstream targets of DELLAs via screening yeast-2-hybrid libraries suggest that different DELLA paralogues may also have preferences for different binding partners (Thomas, S., personal communication). GFP tagging demonstrates that both RGA and GAI are nuclear-localised proteins (Silverstone et al., 2001; Fleck & Harberd, 2002), but discrepancies have arisen relating to their behaviour in response to a GA signal: RGA-GFP is reported to be completely degraded (Silverstone et al., 2001), Zentella et al. (2007) quantifying the RGA response to within minutes of GA application, whilst GAI (and RGL1)-GFP fusions seem more resistant to GA-dependent degradation (Fleck & Harberd, 2002; Wen & Chang, 2002). In contrast, Feng et al. (2008) demonstrate through immunoblot analysis that GA treatment of seedlings reduces the level of all native DELLA proteins. These results are not conclusive and may reflect experimental artefacts, but again questions whether all DELLA proteins are functionally similar. This has recently been addressed directly in work by Gallego-Bartolomé et al. (2010). Their analysis of known angiosperm DELLA gene sequences identified two phylogenetic clades of DELLAs in dicots, with the *Arabidopsis* paralogues *GAI* and *RGA* falling into clade I and *RGL1*, *-2* and *-3* falling into clade II. However, they demonstrate that RGA is able to complement RGL2-specific functions (repression of germination) when driven by the *RGL2* promoter sequence, and *vice versa*, indicating that the site of expression has a greater impact on DELLA function *in planta* than the identity of the paralogue involved.

Logically, the sites of DELLA expression could be used to indicate plant tissues capable of responding to GA signalling, and thus contribute to our understanding of the sites of GA action. To date, the tissue expression patterns of DELLA genes during *Arabidopsis* floral development has not been mapped, except in the case of *RGL2* where a GUS reporter indicates expression in most floral tissues, with expression highest in stamen filaments, sepals and in stylar tissue just beneath the stigma (Lee et al., 2002). Interestingly, in stamens expression of *RGL2* appears to be excluded from the developing anther during development, where GA signalling is predicted to occur (see section 1.5.2).

Silverstone et al. (2001) demonstrated that in response to a GA signal DELLA proteins are degraded rather than being relocalised or sequestered. Degradation of DELLAs occurs through proteolysis by the 26S proteasome, a process mediated by Skp-Cullin-F-box (SCF) E3 ubiquitin ligase protein complexes that target proteins for degradation through ubiquitination. The target specificity of the complex is provided by different species of F-box protein (Petroski & Deshaies, 2005). To date, a single F-box protein targeting DELLAs for degradation has been identified in rice (GIBBERELLIN INSENSITIVE DWARF 2, Gomi et al., 2004), with two found in *Arabidopsis* (SLEEPY1 (SLY1), McGinnis et al., 2003, and SNEEZY (SNE), Strader et al., 2004- also named SLY2, Fu et al. 2004). Mutations in these genes cause dwarf phenotypes and increased concentrations of DELLA protein to accumulate. SLY1 protein interacts with GAI *in vitro* via the GRAS domain (Dill et al., 2004), whilst yeast-3-hybrid experiments have shown that GA-GID1 enhances the interaction between SLY1 and RGA (Griffiths et al., 2006). A similar three-way GA-dependent interaction has been recently demonstrated in rice (Hirano et al., 2010), supporting the model that the creation of the GID1-GA-DELLA complex directly recruits F-box proteins and thus targets DELLAs for degradation. Interestingly, recent analysis of *Arabidopsis* and rice F-box mutants suggests that, although proteolysis of DELLAs is an important component of GA signal transduction, binding of DELLAs to GID1 is sufficient to relieve DELLA repression of downstream GA signalling (Ariizumi et al., 2008; Ueguchi-Tanaka et al., 2008), a phenomenon which may represent an ancestral component of the GA signalling mechanism. The relative contribution

of this mechanism is demonstrated by the relatively mild phenotypes associated with F-box mutants in comparison with the quantity of DELLA protein that they accumulate.

Overexpression of *SNE* can complement *sly1* mutants and reduce the accumulation of DELLA protein in this background (Strader et al., 2004; Ariizumi et al., 2011), suggesting that SLY1 and SNE both target DELLA proteins for proteolysis. Importantly, however, the suppression of the mutant phenotype is only partial (Ariizumi et al., 2011), and whilst accumulation of RGA and GAI protein was reduced when *SNE* was overexpressed in the *sly1* background, RGL2 levels remained abnormally high (Ariizumi et al., 2011), in contrast to when functional SLY1 was reintroduced. As such, these two F-box proteins appear to have different DELLA target preferences. *SLY1* appears to be expressed throughout the plant (McGinnis et al, 2003; Strader et al., 2004), with floral expression strongest in the stamen filament (Ariizumi et al., 2011). In contrast, *SNE* mRNA is far less abundant and mainly present in flowers (Strader et al., 2004), results from a GUS reporter line indicating that expression is restricted to anther tissues (Ariizumi et al., 2011). This is an interesting parallel with *RGL2* expression, which is apparently excluded from the anther (see above). The conclusions drawn are that SLY1 is the dominant F-box protein in *Arabidopsis* GA signalling, but that SNE may also play some specialist roles. Furthermore, analysis of this pathway has revealed differences between the different DELLA paralogues, which may turn out to have repercussions for GA signalling *in planta*.

It has been shown that the DELLA proteins are another point at which GA signalling can be regulated by endogenous and environmental factors. Fu and Harberd (2003) demonstrated in roots that reduced auxin signalling or transport increased the stability of an RGA-GFP fusion protein, making it less susceptible to GA-induced proteolysis. Ethylene signalling has been shown to delay GA-mediated degradation of RGA-GFP, with further genetic evidence of an interaction with GAI as well (Achard et al., 2003). Ethylene is frequently associated with environmental stress, and the interaction between ethylene signalling and DELLA proteins has been shown to delay the transition to flowering in *Arabidopsis* (Achard et al., 2007). Similarly, salt-stress-induced abscisic acid (ABA, another hormone associated with

environmental stress) increases the resistance of RGA-GFP to GA-induced degradation (Achard et al., 2006), leading to the proposition that DELLA proteins act to integrate environmental and endogenous signals to regulate plant growth. The mechanism(s) through which DELLA stability is modulated are not yet known, but these results clearly show that GA-dependent growth responses can be modulated by other hormone signalling pathways downstream of GA biosynthesis.

1.3.3 DELLA Binding Proteins and Downstream Signalling Targets

Relief of DELLA repression by a GA signal results in large-scale transcriptional changes in responding cells (Zentella et al., 2007). It has been demonstrated that different populations of downstream targets respond in different tissue types (for example between imbibed seed and developing flowers, Ogawa et al., 2003; Cao et al., 2006; Hou et al., 2008), though to what extent this is due to target availability or DELLA target preference has not been fully explored. Time-course analyses of GA responses have identified different phases of transcriptional response to GA (Zentella et al., 2007), with target genes whose transcription alters soon after GA induction considered to be among the immediate targets of GA signalling, and genes that respond later potentially being indirect targets further downstream. Interestingly, the transcriptional response to GA signalling includes both up-regulation and down-regulation, indicating that the presence of DELLA proteins maintains the transcription of some downstream targets, as well as repressing others (Zentella et al., 2007). In floral tissues, of 806 genes identified as RGA-dependent targets by Hou et al. (2008), 393 were down-regulated and 413 up-regulated by the introduction of RGA through dexamethasone (DEX) treatment. Comparing against other microarray experiments found that 34.4% of the RGA-down-regulated genes (and thus are normally up-regulated in response to GA signalling) identified from this dataset were specifically or predominantly expressed in stamens, compared to 4.6% of the RGA-up-regulated genes. Hou et al. (2008) report that a low percentage of the floral GA target genes that they identified were specific to other floral organs, and infer from their results that stamen development is regulated by a specific subset of GA targets.

An important target of GA signalling is the GAMYB family of transcription factors, which regulate anther development in rice (Kaneko et al., 2004), barley (Murray et al., 2003) and *Arabidopsis* (Millar & Gubler, 2005). In rice, which carries a single GAMYB orthologue (*OsGAMYB*), it has been demonstrated that OsGAMYB is solely responsible for transmitting GA signalling during stamen development, the *gamyb-2* loss-of-function mutant phenocopying the rice GA-deficient mutant *oscps1-1* (Aya et al., 2009). A number of GAMYB targets that regulate stamen developmental processes have also been identified in rice (see section 1.5.2 for further discussion). Three putative homologues of GAMYB have been identified in *Arabidopsis* based on sequence similarity and complementation of HvGAMYB in barley (*AtMYB33*, *AtMYB65* and *AtMYB101*, Gocal et al., 2001), of which two, *AtMYB33* and *AtMYB65*, have redundant roles in regulating stamen development (Millar & Gubler, 2005). Loss of these two paralogues results in male sterility (see section 1.5.2). Interestingly, *AtMYB33* and *-65* were not identified as DELLA-regulated targets by floral transcriptomics studies (Cao et al., 2006; Hou et al., 2008), and *AtMYB33* expression was not significantly different when comparing between wild type L*er*, *ga1-3* (GA deficient), *gai* (GA insensitive) and *ga1-3 gai-t6 rga-24* (loss of DELLA repression in GA-deficient background) plants (Achard et al., 2004, although the same study reports that exogenous GA treatment increased *AtMYB33* expression in all of these lines). Expression of *OsGAMYB* was not altered by GA treatment of rice aleurone cells (where *OsGAMYB* is also expressed, Tsuji et al., 2006), though evidence from the barley aleurone system indicates that *HvGAMYB* is transcriptionally regulated by GA signalling (Gubler et al., 1995; Gubler et al., 2002). However, the late response time (1 hour) suggests that *HvGAMYB* is not a direct target of GA signalling in this system (Gubler et al., 2002). *AtMYB33*, *AtMYB65* and *OsGAMYB* expression has been shown to be regulated post-transcriptionally through microRNA-directed mRNA cleavage (Achard et al., 2004; Millar & Gubler, 2005; Tsuji et al., 2006; Allen et al., 2007), restricting expression to developing anthers. *OsGAMYB* expression is not similarly regulated in rice aleurone (Tsuji et al., 2006), suggesting that post-transcriptional regulation of GAMYBs is specific to the reproductive context. Expression of miR159, the conserved microRNA enacting this regulation, appears to be responsive to GA signalling in *Arabidopsis* (Achard et al., 2004) but

not in rice (Tsuji et al., 2006). As such, the status of GAMYBs as transcriptional targets in *Arabidopsis* is still not clearly defined, and their regulation appears to be complex.

Only a small number of proteins have as yet been confirmed as DELLA-binding. It has been demonstrated that two basic helix-loop-helix (bHLH) transcription factors, PHYTOCHROME INTERACTING FACTOR (PIF)3 and PIF4, bind to RGA protein *in vitro* and *in planta* (de Lucas et al, 2008; Feng et al., 2008). Both of these proteins act to promote cell expansion in seedlings in response to red light. GA signalling has been shown to interact with this pathway, with the accumulation of DELLA protein inhibiting hypocotyl growth in response to red light (Feng et al., 2008). RGA was shown to interfere with the binding of these PIFs to their target promoter sequences through competing for the conserved bHLH DNA-recognition domain (de Lucas et al., 2008; Feng et al., 2008). Other, closely-related PIF proteins have been shown to interact with both RGA and RGL2 (Gallego-Bartolomé et al., 2010), including SPATULA (Gallego-Bartolomé et al., 2010; Josse et al., 2011), a negative regulator of cotyledon growth in seedlings and petal growth in flowers (Penfield et al., 2005). However, Josse et al. (2011) demonstrate that, in the context of seedling growth, regulation of SPT by DELLAs appears to be dominated instead by a post-transcriptional mechanism that inhibits accumulation of SPT transcript. It has been recently demonstrated that DELLA proteins also bind to JA ZIM (JAZ) domain proteins (the functional equivalent to DELLA proteins in JA signalling, Spartz & Gray, 2008), inhibiting JAZ repression of the transcription factor MYC2 and thus promoting a JA downstream transcriptional response (Hou et al., 2010). In both of these cases DELLA binding has a repressive action on the activity of its binding partner. Recent experimental work has identified a situation in which, whilst binding of a transcription factor to a promoter sequence occurs in the absence of DELLA, transcription of that gene is only induced on binding of DELLA to that transcription factor (Hedden, P., personal communication). Thus DELLA-protein binding can have positive or inhibitory effects on proteins whose effect on growth can itself be either positive or inhibitory, indicating that this could be a highly flexible mechanism for regulating transcription factor activity. It should also be noted that many of the DELLA binding proteins identified so far are involved with the integration of environmental information and plant growth, at a level separate from either the

modulation of GA biosynthesis (see section 1.2.1) or DELLA protein stability (see section 1.3.2).

1.4 GA HOMEOSTASIS

An important outcome of GA signalling is the transcriptional regulation of the GA biosynthesis and signalling pathways themselves. *AtGA20ox* and *AtGA3ox* homologues in various species are both down-regulated in response to GA treatment and up-regulated in GA-deficient or -insensitive mutants (Phillips et al., 1995; Martin et al., 1996; Carrera et al., 1999), whilst conversely it has been shown that numerous *AtGA2ox* paralogues (targeting both C_{19}- and C_{20}-GAs) are up-regulated by GA treatment (Thomas et al., 1999; Rieu et al., 2008a). As yet there is no evidence for earlier steps of GA biosynthesis being under similar transcriptional regulation (Silverstone et al., 1997; Helliwell et al., 1998). The GA biosynthesis pathway is therefore responsive to the amount of bioactive GA produced, the overall effect being to reduce GA biosynthesis and increase GA catabolism in the presence of bioactive GA (Figure 1.4) and *vice versa* in the absence of GA. This regulation is referred to as GA homeostasis, which in particular may act as an efficient mechanism to limit the response of tissues to a GA signal to a shorter period of time. The integration of homeostatic regulation with other developmental and environmental inputs to GA biosynthesis has not yet been fully resolved, but in *Arabidopsis*, it has been demonstrated that some paralogues amongst the *GA20ox* and *GA3ox* gene families are not subject to feedback regulation. For example, *AtGA20ox4* and *-5* are not feedback-regulated (Rieu et al., 2008), nor are *AtGA3ox2* (Yamaguchi et al., 1998), *AtGA3ox3* and *-4* (Matsushita et al., 2007). *AtGA2ox3* expression is also unresponsive to GA treatment, whilst the four other C_{19}-GA 2-oxidases in *Arabidopsis* are (Rieu et al., 2008a). Consequently, this may represent a mechanism by which GA homeostasis can be overridden by other inputs when a GA signal is required.

Homeostatic regulation of GA biosynthesis is mediated through the GA signalling pathway: high *AtGA3ox1* expression in the *ga1-3* background is reduced in the absence of RGA

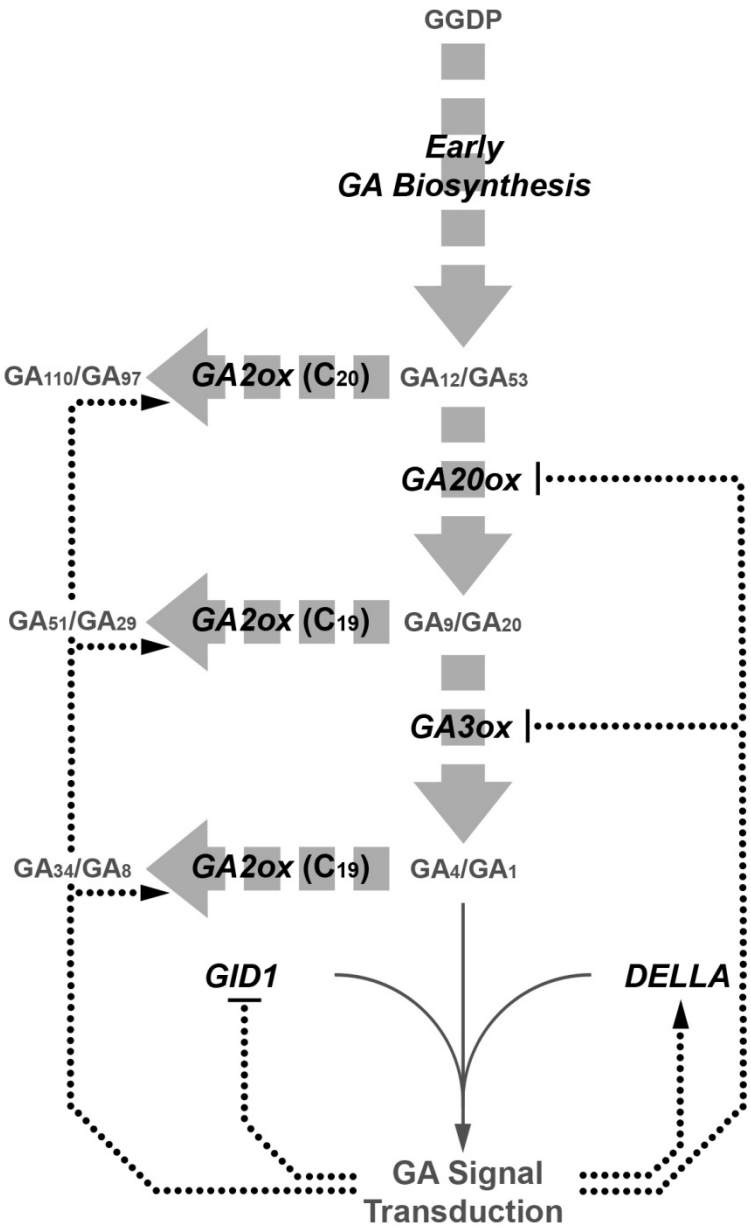

Figure 1.4: Homeostatic regulation of GA biosynthetic and signalling genes.

Transcriptional regulatory loops of GA biosynthetic and signalling genes are indicated by black dotted arrows or bars, representing positive regulation ('feed-forward') or negative regulation ('feedback'), respectively, in response to GA signalling.

(Silverstone et al., 2001), and down-regulation of *AtGA3ox1* expression in response to GA treatment is abolished in the *gid1a gid1b gid1c* GA-insensitive mutant (Griffiths et al., 2006). *AtGA3ox1* and *AtGA20ox2* have further been identified as early downstream transcriptional targets of DELLA signalling in transcriptomics analysis (Zentella et al., 2007). No *AtGA2ox* paralogues were identified as early targets, suggesting that there may be important temporal

elements to GA homeostasis. The same study identified *AtGID1a* and *-1b* as being negatively-regulated by GA signalling, and Griffiths et al. (2006) demonstrate that expression of all three *AtGID1* paralogues is reduced in response to GA treatment, with a corresponding up-regulation in GA-deficient and DELLA-repressed backgrounds. As such, as well as modulating GA biosynthesis the sensitivity of the GA signalling pathway is also responsive to GA signalling. With the aid of F-box mutants it has been demonstrated that the expression of DELLA genes themselves increases in response to GA signalling (Ueguchi-Tanaka et al., 2008), suggesting that they too are linked to GA homeostasis via a feedback loop that makes the plant more resistant to the presence of bioactive GA. We can also conclude that the GA signalling pathway is co-ordinately regulated with the GA biosynthesis pathway through GA signalling itself. The downstream mechanisms by which components of the GA biosynthetic and signalling pathways are homeostatically regulated are still being determined. Interestingly, it appears that *GA3ox1* feedback regulation may be mediated through a separate mechanism to *GA20ox* genes: an AT-hook protein identified in relation to negatively regulating *AtGA3ox1* expression in response to GA signalling does not affect *AtGA20ox* expression (Matsushita et al., 2007), whilst in tobacco a dominant-negative form of the leucine-zipper transcription factor REPRESSION OF SHOOT GROWTH (RSG) inhibits feedback regulation of *NtGA20ox* but not *NtGA3ox* (Ishida et al., 2004). It may be possible in future to exploit these functional differences to further explore and understand the effects of GA homeostasis on these two gene families.

1.5 FUNCTIONS OF GA SIGNALLING DURING REPRODUCTIVE DEVELOPMENT

Arabidopsis development can be divided into two distinct phases: a vegetative phase in which the plant exists as a rosette, and a reproductive phase (marked by the transition to flowering, see section 1.5.1), during which the plant behaves very differently, producing flowers instead of leaves at the apical meristem and with subsequent elongation of internode tissues both between flowers (inflorescence internodes) and between some pre-existing leaves directly beneath the point of floral transition (vegetative internodes, see Figure 1.5), a process known as ‘bolting’. Phenotypic analysis of GA biosynthesis and signalling mutants has identified

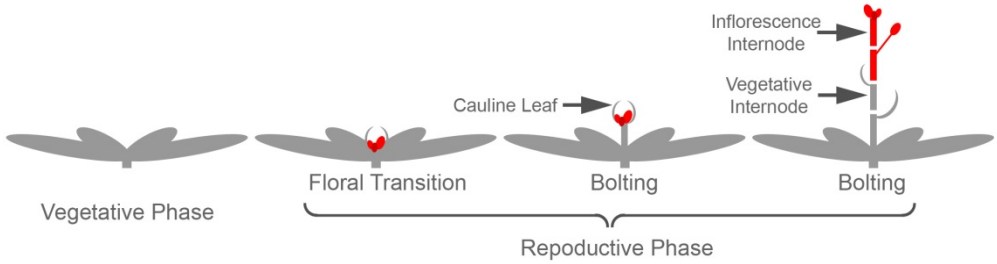

Figure 1.5: Progression of flowering in *Arabidopsis thaliana*.

roles for GA at numerous points during this reproductive phase of development, which will be outlined in the sections below.

The reliance of plants on GA for growth and expansion of vegetative tissues (including stem elongation) is well documented, typified by the severely dwarfed nature of GA-deficient mutants such as *ga1-3* in *Arabidopsis* (Koornneef & Van der Veen, 1980, Figure 1.1) and similarly *oscps-1* in rice (Sakamoto et al., 2004). The link between internode elongation and flowering is not well understood, though the two are associated in many rosette plants (Mutasa-Göttgens & Hedden, 2009). In *Arabidopsis*, bolting only occurs after the shoot apical meristem (SAM) has altered to the reproductive developmental programme (GA-treatment prior to flowering fails to induce internode elongation), whilst in some other species such as sugar beet stem elongation precedes the transition to flowering (Mutasa-Göttgens et al., 2008). Internode elongation in *Arabidopsis* begins basally and travels up the stem (Yates, T., unpublished data), although the factors determining both the timing and position of release of repression of stem elongation are currently unknown.

1.5.1 Floral Transition and Organogenesis

The transition from vegetative to reproductive development is caused by a change of identity at the apical meristem, from the vegetative Shoot Apical Meristem (SAM) which produces vegetative organs (leaves), to the reproductive Inflorescence Meristem (IM), which instead of leaves produces floral meristems (FM) that go on to produce floral organs and thus constitute a flower. The transition to flowering is subject to regulation by endogenous and environmental signals, a major environmental factor in *Arabidopsis* being photoperiod (Searle

& Coupland, 2004). These cues act through a number of different pathways (reviewed in Boss et al., 2004), which are integrated by regulating the expression of a number of key genes that confer IM identity: *FLOWERING LOCUS T* (*FT*), *SUPPRESSOR OF OVEREXPRESSION OF CONSTANS 1* (*SOC1*) and *LEAFY* (*LFY*). *LFY* is also important for subsequently determining FM identity (Weigel et al., 1992; Weigel & Nilsson, 1995) through antagonising the expression of *TERMINAL FLOWER 1* (*TFL1*) in conjunction with the floral identity gene *APETALA 1* (*AP1*, Weigel et al., 1992; Ratcliffe et al., 1999).

GA signalling promotes flowering, but its importance is dependent on other factors. Flowering is promoted under a long day (LD) photoperiod in *Arabidopsis* through the LD pathway which acts via light signalling and circadian regulation to promote expression of *CONSTANS* (*CO*), which in turn promotes both *SOC1* and *FT* (Searle & Coupland, 2004). Under short days (SD), which are not permissive to flowering, the failure of the GA-deficient mutant *ga1-3* to flower in contrast to L*er* wild type (Wilson et al., 1992, Rieu et al., 2008) demonstrates that under SD conditions GA is essential for the floral transition to occur. Under LD, *ga1-3* eventually flowers without GA treatment (though it is still delayed compared to L*er*), demonstrating that the reliance of the floral transition on GA is reduced under LD. The failure of *ga1-3* to flower under SD is due to an absence of *LFY* expression in this mutant, constitutive expression of which can restore flowering, whereas under LD *LFY* expression in *ga1-3* is reduced compared to L*er*, but not abolished (Blázquez et al. 1998). Under SD, GA promotes expression of *SOC1* (Moon et al., 2003), constitutive expression of which can also rescue flowering in *ga1-3*. *SOC1* has since been shown to directly activate *LFY* expression (Lee et al., 2008), and as such GA may act indirectly to regulate *LFY* through this pathway. Interestingly, although *SOC1* integrates signals from the autonomous/vernalisation pathway (Moon et al., 2003), loss of GA biosynthesis in the *ga1-3* mutant does not inhibit flowering responses to vernalization in vernalization-sensitive *Arabidopsis* backgrounds (Michaels & Amasino, 1999).

The delayed flowering of GA-deficient mutants under LD demonstrates that GA still acts to promote flowering under these conditions. As well as the links to *LFY* (see above) GA

treatment has been shown to promote *FT* expression in *ga1-3* under LD (Hisamatsu & King, 2008). *FT* expression is up-regulated under LD conditions by combined CONSTANS (CO) and light signalling to promote flowering (Boss et al. 2004). The inductive effect on *FT* by GA treatment was found to be far greater under LD than SD (Hisamatsu & King, 2008), suggesting that *FT* is repressed by the photoperiod pathway under SD (i.e. non-permissive) conditions, even in the presence of GA. Hisamatsu and King (2008) also found evidence that GA promotes flowering under LD independently of *FT* regulation: GA treatment accelerated flowering of a *ft* mutant under LD conditions. However, as mentioned in section 1.3.1, two reports on the *Arabidopsis gid1a gid1b gid1c* GA-insensitive mutant indicate that this mutant does not flower even under inductive LD conditions (Iuchi et al., 2007; Willige et al., 2007), implying an absolute reliance of *Arabidopsis* on GA signalling to flower. These contrast with a third report (Griffiths et al., 2006), which describes flowering (albeit delayed) of a *gid1a gid1b gid1c* mutant under LD. This discrepancy has yet to be resolved. Two of these conflicting reports (Griffiths et al., 2006; Iuchi et al., 2007) utilise the same triple mutant, so the described phenotypic differences are unlikely to be due to allelic variation and may instead be due to differing growth conditions between the two studies, given the influence that environment has in the making the decision to flower.

High levels of GA_4 have been recorded at the SAM just prior to the floral transition under SD conditions, but the expression of GA biosynthesis genes at the SAM at this time do not correlate with this (Eriksson et al., 2006), suggesting that the SAM is not the source of GA synthesis to induce flowering. Eriksson et al. (2006) demonstrated through radiolabelling studies that GA_4 can travel from rosette leaves to the SAM, which means that it is feasible for remote vegetative tissues to promote the floral transition via GA. A precedent for this type of signalling already exists, with the photoperiod inductive signal originating in rosette leaves rather than the SAM (Zeevaart, 1976). Furthermore, *AtGA2ox4* has been shown through mutant analysis to delay the transition to flowering under SD conditions (Rieu et al., 2008a). This GA2ox paralogue is expressed in stem tissues directly beneath the SAM (Jasinski et al., 2005, Figure 1.6), and so it may act to delay flowering by inactivating remotely-synthesised GA_4, preventing it from reaching the SAM. Similarly, expression of GA-deactivating

enzymes (GA2ox's and a putative 16,17-epoxidase) beneath the SAM has been observed during vegetative growth of *Lolium temulentum* (King et al., 2008) and rice (Sakamoto et al., 2001a; Zhu et al. 2006).

GA promotes organogenesis and antagonises meristematic identity (Hay et al., 2002), necessitating its exclusion from the SAM. The KNOX gene *SHOOTMERISTEMLESS* (*STM*), which is necessary for maintenance of the meristematic indeterminate cell fate (Endrizzi et al., 1996), acts to repress *AtGA20ox1* expression within the SAM (Hay et el., 2002) and to upregulate *AtGA2ox* expression at the SAM boundary, this latter function acting through upregulation of cytokinin (CK) biosynthesis and signalling (Jasinski et al., 2005, Figure 1.6). The repression of *GA20ox* expression by KNOX proteins has been observed in other species (Sakamoto et al., 2001; Chen et al., 2004). Conversely, *AtGA20ox1* is expressed in developing leaf primordia outside the SAM (Hay et al., 2002). Interestingly, at a similar stage of development *AtGA3ox1* is reported as being expressed in the SAM (Mitchum et al., 2006), though primarily in the rib meristem beneath the indeterminate meristematic cells. This contradiction has yet to be reconciled, but may hinge on the availability of GA_9 for GA3ox to convert into bioactive GA_4. A similar antagonistic relationship between KNOX and GA is likely to exist between the IM and developing floral primordia: weak *stm* alleles demonstrate that STM is required for the maintenance of inflorescence and floral meristems (Endrizzi et al., 1996) and the severity of the floral phenotype is enhanced when CK signalling is also impaired (Jasinski et al., 2005). Bartrina et al. (2011) further demonstrate that inhibiting degradation of CK in the meristematic results in a larger IM, whilst overexpressing CK degrading genes reduces IM size. The expression pattern of *AtGA20ox1* in the reproductive context is not reported, but consistent with this model *AtGA3ox1* is expressed in early floral primordia and not in the IM (Hu et al., 2008).

1.5.2 Early Floral Development and Floral Organ Identity

Floral development in *Arabidopsis* is determinate and highly uniform, allowing precise characterisation of development with important morphological events marking particular stages (Smyth et al., 1990, see Appendix 1). Floral organ primordia arise from the floral

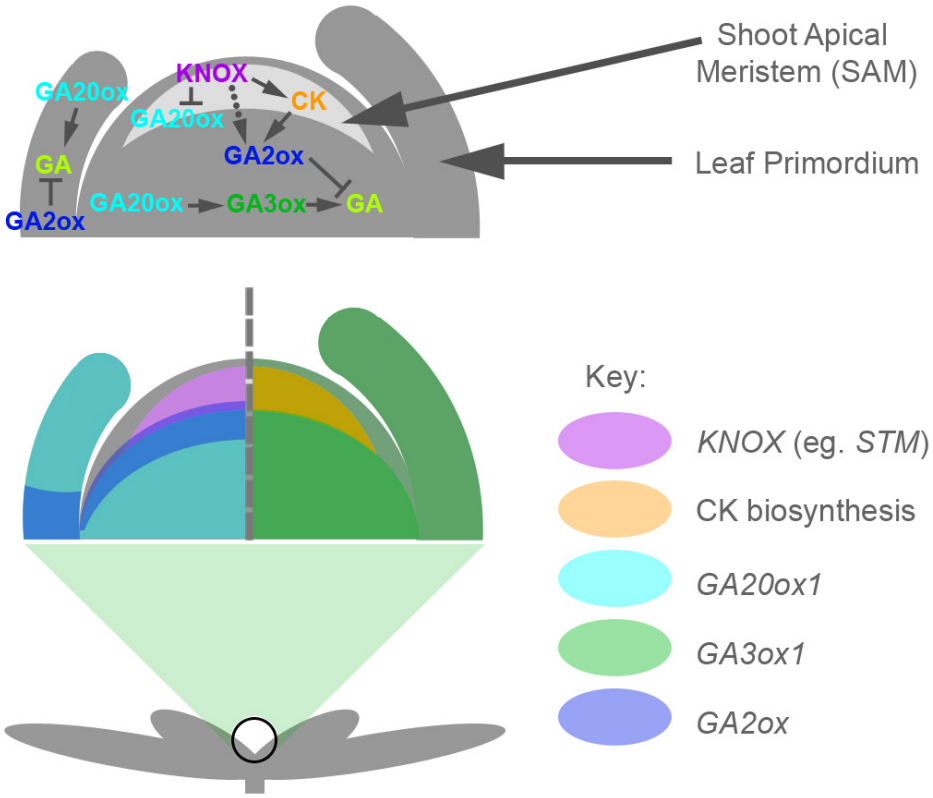

Figure 1.6: Model of the antagonistic regulation of GA biosynthesis during organogenesis and meristematic maintenance.

meristem in concentric rings or 'whorls' near the start of floral development (stages 3-5), their identity determined through interactions between MADS-box transcription factors which are expressed in specific domains across the floral meristem (Figure 1.7), a mechanism referred to as the ABCE model (the subject of recent reviews, Airoldi, 2010; Irish, 2010). LFY promotes expression of a number of these key floral homeotic genes, including *APETALA1* (*AP1*, A class, Parcy et al., 1998), *APETELA3* (*AP3*, B class, Ng & Yanofsky, 2001; Lamb et al., 2002) and *AGAMOUS* (*AG*, C class, Lohmann et al., 2001). GA-deficient and -insensitive mutant flowers are not reported to demonstrate defects in floral organ identity or floral organ numbers, suggesting that GA is not necessary for successful establishment of the floral plan in *Arabidopsis*. Interestingly, the GA-deficient tomato mutant *stamenless-2* exhibits partial conversion from stamen to carpel identity (Sawhney, 1992), suggesting that in other species GA can have greater influence over floral organ identity. In maize, loss of the *CPS* orthologue *ANTHER EAR1* (*AN1*) causes partial reversion from monoecy, with normally-female florets of the ear inflorescence also producing stamens (Bensen et al., 1995).

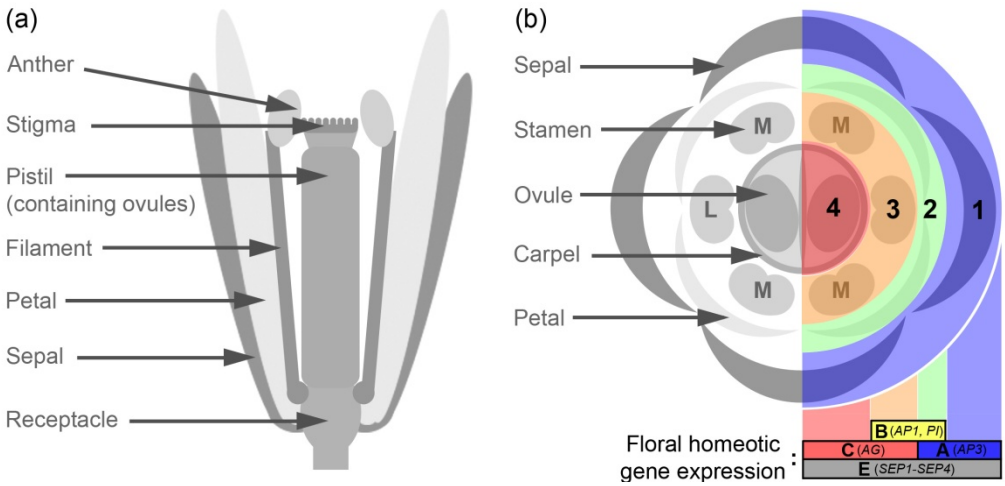

Figure 1.7: The *Arabidopsis* flower and establishment of floral organ identity.

(a) Diagram of Arabidopsis *floral structure (longitudinal section), listing major components.* *(b)* Arabidopsis *floral plan. Floral organs and arranged in concentric whorls (1, 2, 3 and 4, marked with blue, green orange and red, respectively), each corresponding to a different floral organ type (sepal, petal, stamen and carpel). Floral organ identity is determined by combinations of A, B and C-class floral homeotic genes expressed in each whorl, as shown. E.g., stamen identity is specified by a combination of B (yellow) and C (red). The number of floral organs in each whorl is invariant (Bowman et al., 1994). Stamens are classified into 'medial' (long) stamens (M) and lateral (short) stamens (L). The appearance of short stamen primordia is fractionally delayed compared to those of long stamens, and development of the short stamens is consistently behind that of long stamens in the same flower (Smyth et al., 1990).*

Unlike the floral transition, during early floral development *LFY* expression is not responsive to GA signalling (Yu et al., 2004) and becomes down-regulated in floral tissues by floral stage 5 when stamen and petal primordia arise (Weigel et al., 1992). It has been demonstrated that *AG* expression continues throughout floral development even once *LFY* is no longer expressed (Bowman et al., 1991), and that sustained *AG* expression beyond stage 5 is necessary for successful stamen development (Ito et al., 2007). Yu et al. (2004) demonstrate that expression of both *AP3* and *AG* is reduced in *ga1-3*, and that they are up-regulated by GA signalling, suggesting that GA acts to maintain floral growth and development through maintaining expression of the floral homeotic genes. Furthermore, *AtGA3ox1* has been identified as a

downstream transcriptional target of AG (Gómez-Mena et al., 2005), suggesting that GA biosynthesis and *AG* expression may be mutually self-sustaining during floral development via a positive feedback loop. Evidence suggests that AG maintains numerous separate positive feedback loops involving its downstream targets (Ito, 2011), and may act as a master regulator of development once its expression is established.

1.5.3 Stamen Development: Microsporogenesis and Tapetum Function

Mutant analysis suggests that male reproductive development of *Arabidopsis* is more dependent on GA than female reproductive development, with male fertility being impaired in less severely GA-deficient mutants whilst female fertility remains apparently unaffected (Rieu et al., 2008; Hu et al., 2008). Common *Arabidopsis* GA-deficient stamen phenotypes include reduced filament elongation and delayed or failed anther dehiscence (Figure 1.8). Arrests in anther and pollen development have been reported in GA-deficient backgrounds of several species (Nester & Zeevaart, 1988; Goto & Pharis, 1999; Aya et al., 2009), indicating that GA functions to promote microgametophyte development. Loss of GA biosynthesis in both *Arabidopsis* and rice (as represented by the *ga1-3* and *oscps1-1* mutants) results in pollen development arresting once haploid microspores have been released from tetrads, at the young microspore stage in rice (Aya et al., 2009) and further characterised in *Arabidopsis* as prior to entry into pollen mitosis (Cheng et al., 2004). The immediate cause for developmental arrest at this stage is unknown. Interestingly, the GA-insensitive rice mutant *gid1-4* exhibits an earlier block in anther development, prior to the completion of meiosis and the appearance of tetrads (Aya et al., 2009). Stamen development in the *Arabidopsis gid1a gid1b gid1c* mutant has not yet been studied. This indicates the existence of a potential second checkpoint in anther development dependent on GA signalling. This difference in phenotype between GA-deficient and GA-insensitive mutants may be explained by GA-independent interaction between GID1 and DELLA proteins in GA-deficient plants, resulting in a low basal level of GA signal transduction in these backgrounds (see section 1.3.1). In contrast to *Arabidopsis* and rice, anther development in the GA-deficient tomato mutant *gib-1* is blocked prior to meiosis (Jacobsen & Olszewski, 1991). The pollen mother cells (PMCs) in this mutant were

Figure 1.8: Floral organ phenotypes associated with *Arabidopsis* GA-deficient and GA-insensitive mutants. *Adapted from Plackett et al. (2011).*

found to be arrested in the G1 stage of premeiotic interphase, suggesting that the GA-dependent developmental block is at least partially enacted through the cell cycle. However, clear developmental differences have been identified between anthers of tomato and other model plant species, as demonstrated by the tapetum, which arises from one L2 tissue layer in *Arabidopsis* (Scott et al., 2004, Figure 1.9, see further discussion below), but is derived from two separate histological sources in tomato (Jacobsen & Olszewski, 1991). There may also be divergence in some plant species' response to GA signalling during anther development.

Analysis of *AtGA3ox::GUS* reporter lines (Mitchum et al., 2006, Hu et al., 2008) indicates that bioactive GA is synthesised in both the stamen filament and anthers across much of floral development, from floral stage 9 onwards (Figure 1.10). Weak *AtGA3ox* expression is seen in anther and microspore tissues from anther stage 6 (Sanders et al., 1999), at the point that PMCs enter meiosis. The four *AtGA3ox* paralogues display differential expression patterns during stamen development (see section 1.2.1), with two peaks of expression seen: one in the tapetum prior to degeneration (see below) and one in mature pollen prior to anther dehiscence. Tapetal expression of GA-biosynthetic genes has been observed in rice via *in situ* hybridisation (*OsGA20ox1* and *-2*, *OsGA3ox1* and *-2*, Kaneko et al. 2003) and in tobacco via GUS reporting (*NtGA3ox*, Itoh et al., 1999). These results indicate that GA is synthesised in

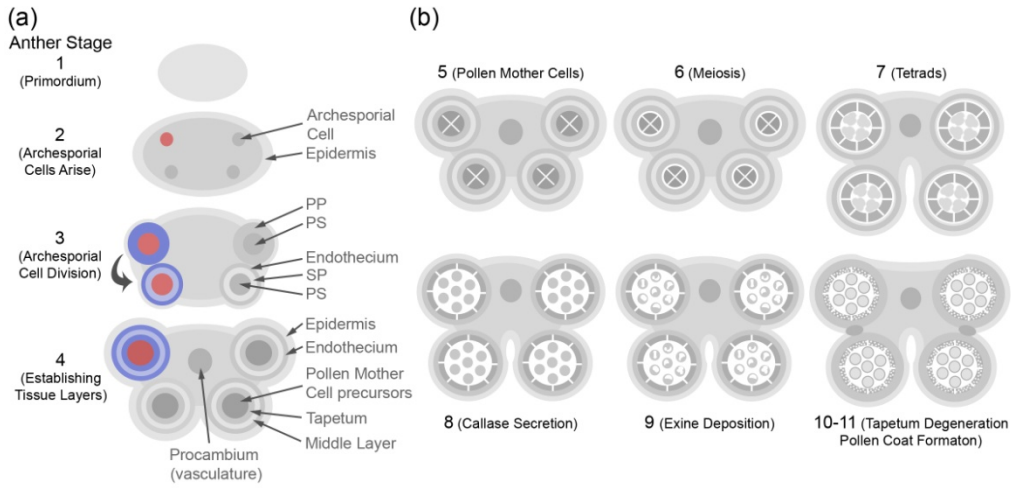

Figure 1.9: Development of *Arabidopsis* anther tissues and tapetum function. *Developmental stages taken from Sanders et al. (1999), showing (a) establishment of anther tissue layers and (b) subsequent meiosis and tapetum-dependent pollen development through to tapetum degeneration. In (a), descendents of the archesporial cell are highlighted in colour. At anther stage 3 the archesporial cell divides into a Primary Sporogenous (PS, red) and Primary Parietal (PP, blue) lineages, the PP subsequently differentiating to establish the endothecium and Secondary Parietal (SP) layers. The SP subsequently differentiates into the tapetum and middle layer. PS cells become pollen mother cells by anther stage 5.*

both the tapetum cell layer and developing microspores, though potentially at different developmental stages. The stamen expression patterns of the *AtGA20ox* family are currently unknown. Recent trancriptomic analyses performed specifically on anther tissues in rice suggest that GA biosynthesis is specifically down-regulated in both the tapetum and meiotic PMCs until after meiosis is complete and unicellular microspores are released from tetrads (Chhun et al., 2007; Hirano et al., 2008; Tang et al., 2010), after which time we see up-regulation of numerous components of GA biosynthesis in both cell types. Conversely, Hirano et al. (2008) showed up-regulation of *SLR1* in both the tapetum and PMCs during meiosis, with a concomitant down-regulation from the unicellular stage. This may indicate that GA responses are being tightly regulated during this phase of microspore development. *OsGAMYB::GUS* reporter lines show expression in anthers from the pre-meiotic stage onward, indicative of GA signalling (Aya et al., 2009, see section 1.3.3). GUS reporter lines indicate that both *OsGAMYB* and *AtMYB33* are expressed in developing microspores and the

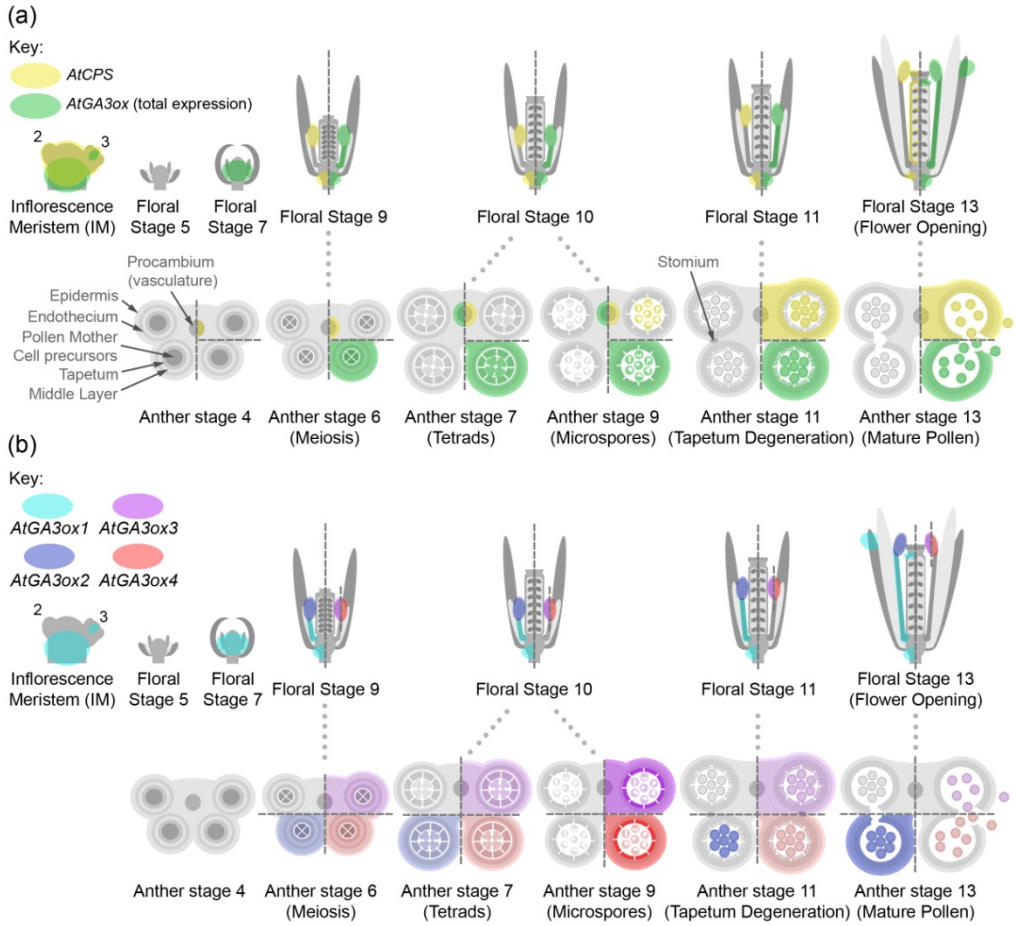

Figure 1.10: Expression of *Arabidopsis* GA biosynthesis genes during floral and anther development.

*Expression patterns are based on evidence from GUS reporter lines (Silverstone et al., 1997; Mitchum et al., 2006; Hu et al., 2008), demonstrating differential tissue expression patterns between (a) early (*AtCPS*) and late (*AtGA3ox*) biosynthetic stages and (b) the four separate* AtGA3ox *paralogues. The intensity of colour shown reflects the reported intensity of GUS staining, and by inference the intensity of gene expression. Floral and anther developmental stages given are as listed by Smyth et al. (1990) and Sanders et al. (1999), respectively. Floral stages 2 and 3are marked as primordia on the inflorescence meristem (IM). Adapted from Plackett et al. (2011).*

surrounding tapetal cells (Millar & Gubler, 2005; Aya et al., 2009), suggesting that a GA response is occurring simultaneously in both cell types. However, it is as yet unclear whether the developmental blocks observed during pollen development in GA biosynthesis/signalling

mutants are due to loss of GA signalling directly in the PMCs, indirectly due to a loss of GA signalling in the tapetum, or both.

The tapetum cell layer is crucial to the successful development of pollen. The innermost sporophytic tissue layer surrounding the anther locule (Figure 1.9), the tapetum acts as a nurse tissue for the developing microspores, secretes callase enzymes necessary to release the microspores from the callose wall surrounding the haploid cells at the end of meiosis (tetrads), and both synthesises and releases key elements of the outer pollen coat into the locule, an action which necessitates the timely degeneration of tapetal cells via programmed cell death (PCD, Scott et al., 2004, see further discussion below). Generally speaking, two broad categories of tapetal types have been classified within angiosperms (Huysmans et al., 1998): amoeboid, in which tapetal protoplasts move into the locule, and secretory, in which tapetal cells remain *in situ* until they degenerate. Both *Arabidopsis* and rice develop secretory tapeta, and it is for these two species that most is known about the action of GA signalling on tapetum function.

In *Arabidopsis*, the development of the tapetum is tightly interlinked with the pollen that it surrounds. Derived from two distinct cell lineages (the tapetum from primary parietal cells and PMCs from primary sporogenous cells, Figure 1.9, Scott et al., 2004), mutant analysis in *Arabidopsis* demonstrates that their respective identities and future cell fates are established by signalling between the two. A tapetally-expressed leucine-rich repeat receptor-like kinase EXTRA SPOROGENOUS CELLS/EXCESS MICROSPORES (EXS/EMS, Canales et al., 2002; Zhao et al., 2002) interacts with the protein ligand TAPETUM DETERMINANT1 (TPD1) secreted by nascent PMCs to establish and maintain tapetum cell fate: loss of either component results in the tapetal precursors forming additional PMCs instead (Yang et al., 2003, Yang et al., 2005, Jia et al., 2008). Development of the PMC lineage is also affected in *exs/ems* and *tpd1* mutants, with development blocking in meiosis prior to cytokinesis. This developmental block is reminiscent of the *osgid1-4* GA-insensitive phenotype described above, but the presence of a clearly defined tapetum cell layer suggests that GA signalling acts

downstream of the EXS/EMS-TPD1 signalling module and is not required to specify tapetum cell identity.

A critical function of the tapetum is synthesis of pollen coat components. These processes have been studied most closely in species belonging to the Brassicaceae family, which includes *Arabidopsis*. In *Brassica napus* (which also possesses a secretory tapetum, Huysmans et al., 1998) the tapetum has been demonstrated to be the predominant contributor of sporopollenin (a major structural component of the exine pollen wall layer) and pollen coat lipids (Piffanelli et al., 1997). During formation of the *Brassica* exine, tapetally-synthesised structural lipids and proteins are secreted into the anther locule, whilst components of the pollen coat are mostly released into the locule later in development, upon tapetum cell death (Piffanelli et al., 1998). These components, which include long-chain fatty acids and large lipid-associated proteins, are sequestered in two tapetal organelles (tapetosomes and elaioplasts) prior to tapetal cell degeneration (Hernández-Pinzón et al., 1999). The importance of these functions to pollen development is clearly demonstrated by *Arabidopsis* male-sterile mutants with defects in either lipid biosynthesis (*male sterility 2*, Aarts et al., 1997) or tapetal PCD (Kawanabe et al., 2006), which result in pollen abortion or collapse. It has recently been demonstrated in rice that *oscps1-1* displays defects in tapetum secretory function (with corresponding differences to the pollen exine layer) and that GA is necessary for the tapetum to enter PCD (Aya et al., 2009). Developing microspores in this mutant are reported as being morphologically normal at the time that tapetum function is disrupted, suggesting that the action of GA on these two cell types is separable and that the GA signalling controlling tapetum function most likely occurs within the tapetum. Both the GA-deficient tomato mutants *gib-2* and *sl-2* also demonstrate delayed or abnormal tapetum degeneration (Nester & Zeevaart, 1988; Sawhney, 1992).

In rice, it has been determined through mutant and transcriptomic analysis that GA signalling in anthers acts almost solely through *OsGAMYB* (Aya et al., 2009, see section 1.3.3). This same study identified a number of immediate downstream targets of OsGAMYB involved directly in lipid biosynthesis, transport, and the signalling cascade that leads to PCD, as well

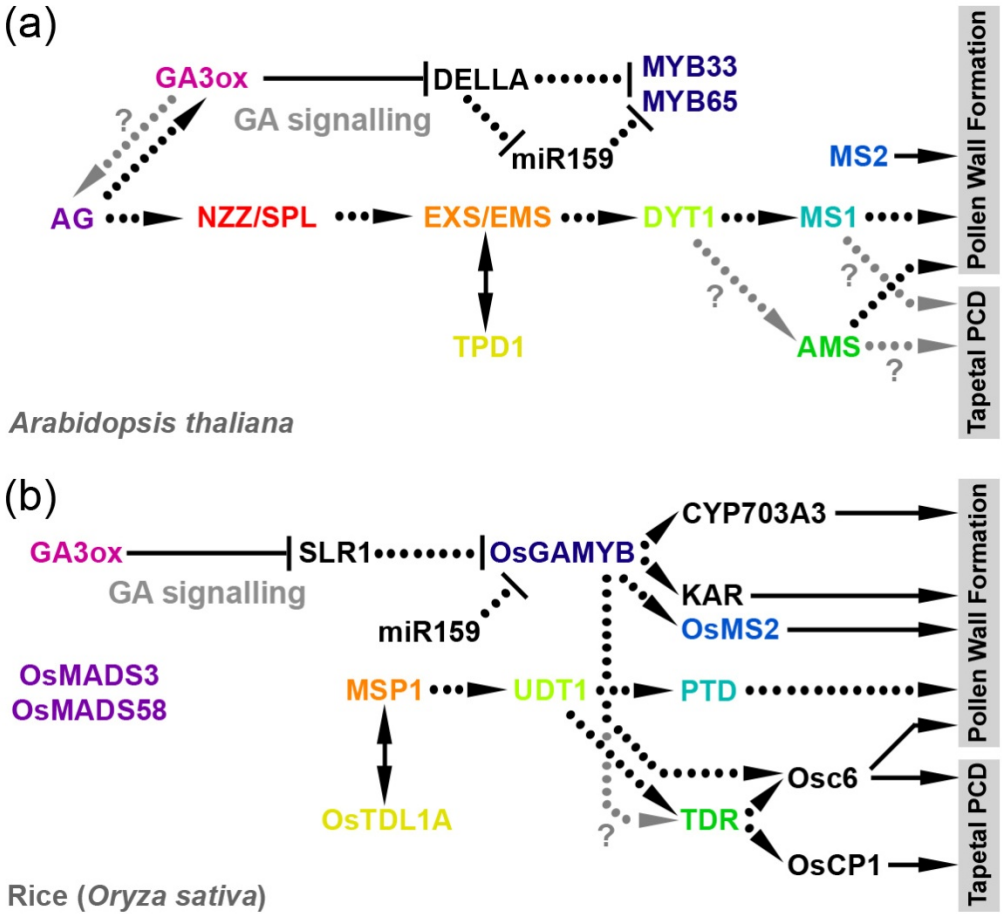

Figure 1.11: Regulation of tapetum development and function by GA signalling.

Genetic pathways showing known transcription factors and downstream targets involved in anther/tapetum development in Arabidopsis *(a) and rice (b). Putative homologues between the two systems are indicated by matching colours. Dotted arrows indicate transcriptional or indirect regulation. Solid arrows indicate direct enzymatic function or protein-protein interaction (double headed arrow). Black arrows indicate confirmed interactions, grey arrows indicate possible interactions. Adapted from Plackett et al. (2011).*

as other transcription factors (Figure 1.11). Recent developments in our understanding of the transcriptional cascade regulating anther development suggest the existence of a conserved genetic framework underpinning anther development in both rice and *Arabidopsis* (Wilson & Zhang, 2009). Points of integration between this pathway and GA signalling are now being identified. One transcription factor identified as a putative target of OsGAMYB is *TAPETUM DEGENERATION RETARDATION* (*TDR*, Li et al., 2006, Aya et al., 2009), which shares sequence homology with the *Arabidopsis* transcription factor *ABORTED MICROSPORES*

(*AMS*, Figure 1.11, Sorensen et al., 2003). Downstream targets of AtMYB33 and AtMYB65 have not yet been identified in *Arabidopsis* anther development, and comparisons with the rice system may well provide an important starting point. The expression of *AtMYB33* and *AtMYB65* has been shown not to be regulated by the NZZ/SPL-EXS/EMS-DYT1 cascade (Zhang et al., 2006). Coupled with this, similarities between the anther phenotypes of *myb33 myb65* and *dyt1* (tapetum hypertrophy and failure of PMC development at meiosis, Millar & Gubler, 2005; Zhang et al., 2006) have led to speculation that AtGAMYBs and DYT1 interact at the protein level, forming heterodimers to regulate common downstream targets (Zhang et al., 2006). However, as yet no such protein interaction has been demonstrated *in vitro* or *in planta*, and the evidence from rice so far suggests that instead these two signalling pathways independently regulate common downstream targets. Interestingly, Millar and Gubler (2005) report a low level of sporadic recovery of pollen development in the *myb33 myb65* mutant. This recovery is specific to individual locules within an anther, indicative of a highly localised effect. This suggests that the cause may be to do with downstream targets of GA signalling rather than the signalling mechanism itself. The rescue of fertility can be enhanced by altering environmental conditions such as light intensity and temperature (Millar & Gubler, 2005), which suggests interaction between GA signalling and another signalling pathway in anther development. The role of known DELLA binding targets such as PIFs (see section 1.3.3) in reproductive development has not yet been investigated, and these may in time be found to play a role in this phenomenon.

All of the examples given above relate to the effect of the absence of GA signalling on pollen development. In rice and barley, which each possess only one DELLA protein to repress GA downstream responses, loss of DELLA function (therefore leading to constitutive GA signalling) also causes male sterility (Ikeda et al., 2001; Lanahan & Ho, 1988). This phenotype is not well described in published literature, but in the case of barley anthers are recorded as being 'pollenless' (Lanahan & Ho, 1988), suggesting that inappropriate GA signalling in anther tissues also disrupts pollen development. The fact that *Arabidopsis* carries five DELLA paralogues has made it difficult to recreate similar constitutive GA signalling in this species, and to date no published combination of DELLA loss-of-function mutant alleles

has resulted in serious pollen developmental defects (see section 1.3.2). However, a recent combination of *RGA* and *GAI* loss-of-function alleles in the Columbia-0 ecotype of *Arabidopsis* unexpectedly caused severe defects in male fertility (Thomas, S., personal communication). If confirmed as having defects in pollen development, this mutant may allow the effects of constitutive GA signalling on tapetum function and pollen development to be investigated more closely.

1.5.4 Late Stamen Development: Maturation and Post-Pollination Growth

Arabidopsis mutants with less severe GA-related phenotypes allow us to examine the direct effects of GA on later stages of floral development beyond tapetum degeneration, encompassing stamen maturation and pollination. In self-fertilising species such as *Arabidopsis*, coordination of development between the male and female reproductive organs of a flower determines pollination success (and hence successful seed set), as the pistil is receptive to pollen for only a short window of time (reported as three to five days after flower opening for the Col-0 ecotype, Vivian-Smith & Kolutnow, 1999). The *ga20ox1 ga20ox2* semi-dwarf double mutant, which has only a partially-reduced capacity for GA biosynthesis (as demonstrated by a 50% reduction in shoot GA_4 content) in contrast to mutants such as *ga1-3*, displays a reduced fertility phenotype despite the successful production of mature, viable pollen (Rieu et al., 2008). This is due to a mechanical block in pollination caused by reduced filament elongation and a failure of the anther to undergo dehiscence (Figure 1.8, Rieu et al., 2008). A similar floral phenotype has been observed in the *ga3ox1 ga3ox3* double and *ga3ox1 ga3ox3 ga3ox4* triple mutants, where a late block in anther development (floral stage 11-12) has been proposed (Hu et al., 2008). Very interestingly, successful seed set is eventually restored in both *ga20ox* and *ga3ox* combinatorial mutants without rescue by exogenous GA treatment. Stamen growth and development in *ga3ox1 ga3ox3* flowers apparently increases gradually in flowers produced later on the inflorescence until development is substantially rescued (Hu et al., 2008). The underlying cause for this phenotypic rescue has not yet been explained. In all of the examples listed, however, functional paralogues from within the same family are still present in these mutant

backgrounds (and in the case of the *AtGA3ox* family, expression of all four paralogues is seen through to anther dehiscence, Figure 1.10), so one possible explanation could be up-regulation of the remaining paralogues to compensate for the absence of the others.

The mechanisms through which GA signalling acts to promote late stage filament elongation and anther dehiscence are beginning to be elucidated. It has not been directly proven that GA signalling at this stage is transmitted through GAMYB, but *AtMYB33::GUS* expression has been reported in both anther tissues and mature pollen at dehiscence (Millar & Gubler, 2005). GA-dependent promotion of stamen filament elongation has recently been shown to act partially through jasmonate (JA) signalling. JA biosynthesis and signalling mutants display similar reduced filament elongation and delayed dehiscence floral phenotypes (Stintzi & Browse, 2000; Ishiguro et al., 2001; Mandaokar et al., 2006). GA signalling acts by increasing JA biosynthesis, specifically up-regulating the JA biosynthesis gene *DELAYED ANTHER DEHISCENCE1* (*DAD1*) (Cheng et al., 2009), which is expressed in the stamen filament (Ishiguro et al., 2001). A number of MYB transcription factors have been identified during filament elongation as downstream targets of both GA and JA signalling, including *MYB21*, *MYB24* and *MYB57* (Cheng et al., 2009). Both MYB21 and MYB24 have been shown to be binding targets of the JA-signal-repressing JAZ proteins (Song et al., 2011), and so the possibility exists that their activity is also regulated through DELLA binding to JAZ proteins (see section 1.3.3).

Although *DAD1* expression is limited to the filament, *MYB21* is expressed in the anther vasculature and anther-filament junction (Cheng et al., 2009), *MYB24* is expressed in the filament vasculature (Cheng et al., 2009), and *MYB108* (whose expression has been shown to be strongly dependent on *MYB21*) is expressed in anther tissues, with strongest expression in the anther vasculature (Mandaokar & Browse., 2009). Furthermore, loss of *MYB21* and *MYB24* creates a functional male-sterile phenotype, in which pollen develops normally but anther dehiscence fails to occur (Mandoakar et al., 2006). This raises the possibility that GA signalling acts to promote both anther dehiscence and filament elongation through the JA pathway. However, treatment of GA-deficient mutants with exogenous JA cannot rescue

floral phenotypes (Cheng et al., 2009), which suggests that GA signalling simultaneously acts on other, JA-independent targets that are required for stamen maturation.

A combinatorial, loss-of-function auxin-response mutant (*arf6 arf8*) demonstrates similar late stamen phenotypes to those listed above (Nagpal et al., 2005). The same study demonstrates that *arf6 arf8* synthesises less JA than wild type, but ARF6 and -8 were not found to regulate any of a series of known JA-biosynthetic genes examined in anther tissues. Exogenous JA treatment rescued anther dehiscence but not filament elongation in this mutant, again suggesting that JA may transmit some of the auxin signal at this stage of development, but other crucial targets are independently regulated by auxin. The floral and vegetative semi-dwarf phenotypes of this mutant are tantalizingly reminiscent of the *ga20ox1 ga20ox2* GA-deficient mutant, but to date it is not known whether auxin and GA signalling interact at this stage of stamen development.

Whilst pollination represents one potential barrier to plant reproduction, overcome by successful delivery of pollen to the stigma, fertilisation represents another, requiring successful pollen development post-anthesis. Pollen germination is dependent on *de novo* GA biosynthesis by the pollen grain, as evidenced by the failure of pollen from rice GA-deficient mutants to germinate (Chhun et al., 2007). Pollen tube growth is also promoted by GA, demonstrated both in GA-deficient mutants (Chhun et al., 2007) and pollen overexpressing *GA2ox* (Singh et al., 2002). GA signalling during pollen tube growth is apparently mediated through the established GA signal transduction pathway, with loss of *RGA* function partially rescuing growth of GA-deficient pollen tubes (Swain et al., 2004). Unlike most other plant tissues except root hairs, pollen tube elongation does not occur by cell expansion but by polarised tip growth (Hepler et al., 2001), representing a novel system, and possibly novel downstream transcriptional targets, on which GA signalling acts. Pollen tube growth is also unusual in that it has been found that high levels of bioactive GA can in fact be inhibitory to pollen tube growth *in vitro* (Singh et al., 2002), though the reasons for this are not yet understood.

Taking advantage of the haploid nature of the gametophyte stage, using transmission ratios of mutant alleles in heterozygous backgrounds Chhun et al. (2007) demonstrated an interesting division between GA-deficient rice mutants, in which mutant pollen developed successfully but suffered a fitness penalty during post-anthesis development, and GA signalling mutants where most pollen failed during development and was subsequently inviable, but mutant pollen that did survive did not incur a fitness penalty post-anthesis. The explanation that they provide for this relates to the division between expression of GA signalling and GA biosynthesis genes seen in rice anthers before and after meiosis (discussed in section 1.5.3). They propose a model whereby components of the GA signal transduction machinery are synthesised prior to meiosis by the diploid PMCs, with the protein being divided between the subsequent haploid microspores during cytokinesis. Consequently, mutant microspores that do not carry a functional copy of a GA signalling gene can still contain functional, sporophytically-produced GA signalling protein, and thus develop without displaying a severe phenotype. In contrast, GA biosynthesis genes are not highly expressed until after meiosis and cytokinesis has separated the microspores, and as such microspores lacking a functional copy of a GA biosynthesis gene will reflect that genotype in their phenotype. This model also explains the 3:1 segregation ratios observed during the production of the *gid1a gid1b gid1c* GA-insensitive triple mutant (Griffiths et al., 2006), which otherwise paradoxically implies relatively normal post-anthesis development of GA-insensitive pollen.

1.6 QUESTIONS ARISING AND PROJECT AIMS

This review of the current literature raises a number of important points for further investigation:

- GA 20-oxidase activity appears to represent an important, rate-limiting step in the GA biosynthesis pathway, regulating the final amount of bioactive GA produced in plant tissues in response to endogenous and environmental stimuli. The presence of a multigene family governing this step is conserved between species, and evidence exists for both functional specialisation and redundancy between paralogues. Despite this, information regarding the respective roles and relative importance of individual paralogues within the *Arabidopsis GA20ox* multigene family during reproductive

development is lacking compared to other stages of this pathway. Only two out of five paralogues have been characterised through mutant analysis, with the vegetative and floral phenotypes of the double mutant clearly demonstrating that one or more of the remaining paralogues has significant functions in floral development (Figure 1.8, Rieu et al., 2008). This project aims to identify loss-of-function alleles for the remaining *AtGA20ox* paralogues and characterise their developmental roles using reverse-genetic techniques to create novel combinatorial mutants.

- Gene expression analysis has revealed distributed expression of the first (*CPS*) and final (*GA3ox*) steps of the GA biosynthesis pathway in *Arabidopsis*, as well as differential expression between the *AtGA3ox* paralogues in floral tissues. However, we do not know how this relates to expression of intermediate steps in the pathway, particularly the *AtGA20ox* gene family. This project will characterise the tissue expression patterns of the *AtGA20ox* gene family during floral development through the creation and analysis of transgenic promoter::GUS reporter lines.

- Much of past research has focussed on analysing the effects of GA-deficiency or insensitivity on reproductive development and fertility, particularly that relating to stamen development. This review has highlighted evidence that excess or inappropriate GA signalling, produced either through chemical treatment, signalling mutants or transgenic approaches, also has negative impacts on plant fertility, the reasons for which have not been determined. Furthermore, there is evidence from barley and rice that constitutive GA signalling has a strong and specific negative effect on male fertility, though again the cause of this has never been investigated in detail. The recent discovery of a similar male-sterile phenotype in an *Arabidopsis* GA signalling mutant provides the opportunity to examine this phenomenon in more detail. To better understand the importance of GA signalling and its repression on stamen development, this project aims to characterise the phenotype of this new mutant and to also try to explain differences between it and similar mutants in the L*er* ecotype.

CHAPTER 2: MATERIALS AND METHODS

2.1 PLANT MATERIAL AND GROWTH CONDITIONS

2.1.1 Mutant Alleles

All characterisation of gene function *in planta* was performed in the model plant *Arabidopsis thaliana* through phenotypic analysis of mutant plant lines. Table 2.1 lists those mutant alleles used in phenotypic characterisation experiments during this project, either singly or in combination with other alleles. Where possible, mutant alleles that were to be combined into combinatorial mutant lines were sourced from the Columbia-0 ecotype. Where this was not possible (as in the case of the *ga20ox3-3*, *ga20ox4-2* and *ga20ox5-2* alleles, Table 2.1), mutant alleles were introgressed into the Col-0 background by sequential backcrossing (six times in total) prior to crossing into a combinatorial line. The *ga1-3* mutant allele was originally generated in the L*er* ecotype, but has been similarly introgressed into Col-0 (Tyler et al., 2004). All experimental work presented in this project uses *ga1-3*(Col-0). Novel alleles characterised for the first time in this project were identified through searches of existing mutant collections via the *Arabidopsis* Information Resource (TAIR) database (http://www.arabidopsis.org/index.jsp) and SALK Institute Genomic Analysis Laboratory (SIGnAL) T-DNA express gene mapping tool (http://signal.salk.edu/cgi-bin/tdnaexpress). Seed stocks were ordered from the National Arabidopsis Stock Centre (NASC, Nottingham) or the Arabidopsis Biological Resource Centre (ABRC, USA) where possible. CSHL mutant lines were obtained by request directly from Cold Spring Harbor Laboratories (U.S.A.). Where single or combinatorial mutant lines have been previously characterised and published (Table 2.1), seed stocks were obtained by request from the relevant research groups.

Mutant alleles used in this project confer loss-of-function of the relevant gene, either through physical interruption to the coding sequence or associated regulatory elements via insertion of transposable elements (T-DNA, Martienssen, 1998; Alonso et al., 2003; Rosso et al., 2003), large-scale deletions/chromosomal rearrangement induced by fast-neutron mutagenesis (e.g. *ga1-3*, Sun et al., 1992) or single nucleotide polymorphisms (SNPs) either generated artificially via induced mutagenesis (Colbert et al., 2001; Till et al., 2003) or identified as natural ecotypic variations in gene sequence (Ossowski et al., 2008). Depending on the nature

Gene	Locus	Mutant Allele	Mutation Type	Source Ecotype	First Publication
GA20ox1	At4g25420	*ga20ox1-3*	T-DNA (SALK)	Col-0	Rieu et al., 2008
GA20ox2	At5g51810	*ga20ox2-1*	T-DNA (GABI-kat)	Col-0	Rieu et al., 2008
GA20ox3	At5g07200	*ga20ox3-1*	SNP (Q165*)	Col-0	Unpublished
GA20ox3	At5g07200	*ga20ox3-2*	SNP (L208F)	Col-0	Unpublished
GA20ox3	At5g07200	*ga20ox3-3*	T-DNA (CSHL)	L*er*	Unpublished
GA20ox4	At1g60980	*ga20ox4-1*	SNP (P233S)	Col-0	Unpublished
GA20ox4	At1g60980	*ga20ox4-2*	Indel (-1bp)	Bur-0	Unpublished
GA20ox5	At1g44090	*ga20ox5-1*	T-DNA (SALK)	Col-0	Unpublished
GA20ox5	At1g44090	*ga20ox5-2*	T-DNA (CSHL)	L*er*	Unpublished
***CPS* (*'GA1'*)**	At4g02780	*ga1-3*	Indel (-5kb)	L*er*	Sun et al., 1992
ERECTA	At2g26330	*er105*	Indel (+4kb)	Col-0	Torii et al., 1996
RGA	At2g01570	*rga-28*	T-DNA (SALK)	Col-0	Tyler et al., 2004
RGA	At2g01570	*rga-24*	Indel (-8.4kb)	L*er*	Silverstone et al., 1998
RGA	At2g01570	*rga-t2*	T-DNA (CSHL)	L*er*	Lee et al., 2002
GAI	At1g14920	*gai-td1*	T-DNA (SAIL)	Col-0	Unpublished
GAI	At1g14920	*gai-t6*	T-DNA (Ds)	L*er*	Peng et al., 1997
GID1a	At3g05120	*gid1a-1*	T-DNA (SALK)	Col-0	Griffiths et al., 2006
GID1b	At3g63010	*gid1b-1*	T-DNA (SM)	Col-0	Griffiths et al., 2006
GID1c	At5g27320	*gid1c-1*	T-DNA (SALK)	Col-0	Griffiths et al., 2006

Table 2.1: Summary of *Arabidopsis* mutant alleles used during this project.

of the mutation, SNPs can also impair gene function, potentially by causing the substitution of an amino acid residue critical to protein function but more reliably through mechanisms such as frameshift mutations, disruption to mRNA processing signals or the introduction of a premature stop codon.

New combinatorial mutants lines were generated by crossing mutant lines, performed by manual pollen transfer between flowers of separate parent plants. Unopened, late-stage buds

of the female recipient were emasculated to prevent self-pollination, leaving the pistil intact. Newly-opened flowers of the male donor were used to apply fresh pollen directly to the stigma of the female recipient. Siliques that successfully developed from these crossing events were harvested, the seed they contained designated as F_1 seed and the immediate offspring of the cross designated as F_1 plants. Homozygous mutant lines were identified in subsequent generations by genotyping PCR (see section 2.2.2).

2.1.2 Transgenic Lines

Transgenic *Arabidopsis* plant lines (plants carrying heterologous T-DNA sequence) were generated as part of this project through *Agrobacterium*-mediated transformation (see section 2.2.6). The details of the transgenic lines produced during this project are listed in Table 2.2.

AtGA20ox::GUS transcriptional fusion reporter constructs were designed to drive GUS expression under the native 5' promoter of each *AtGA20ox* paralogue (see section 5.2.2), with the *AtGA20ox* promoter sequence inserted immediately adjacent to the GUS CDS using an *Nde*I restriction site where possible. In the case of *AtGA20ox3*, it proved necessary to use an adjacent *Xma*I site. These constructs were built using a pre-existing GUS expression binary vector, pBI101.2 (Silverstone et al., 1997), making two single nucleotide modifications to introduce an *Nde*I site at the GUS ATG and to delete an *Nde*I site in the surrounding vector sequence. The restriction sites used for cloning into pBI101.2(modified) are given in Table 2.2, with terminal restriction sites being incorporated into the promoter sequence via PCR where necessary. In circumstances where native *Nde*I sites occurred within the target promoter sequence, the promoter was incorporated as two separate restriction fragments, taking advantage of a native restriction site within the target promoter sequence (Table 2.2). The maximum length of *AtGA20ox* 5' promoter sequence was captured by each construct, taking up to half the non-coding sequence between that paralogue and the preceding gene. Two separate *AtGA20ox5* variants were generated due to the presence of a predicted small ORF in this promoter region (Figure 5.3a)

35S::GA20ox1 and *35S::GA20ox5* constructs were designed to drive constitutive expression

(a)

Transgene	5' Promoter Fragment	Restriction Sites	Binary Vector	Vector Published
pGA20ox1-TC-GUS	-3074bp to -1bp	*Hind*III-*Spe*I-*Nde*I	pBI101.2 (modified)	Silverstone et al., 1997
pGA20ox2-TC-GUS	-1514bp to -1bp	*Xma*I-*Nde*I	pBI101.2 (modified)	Silverstone et al., 1997
pGA20ox3-TC-GUS	-2618bp to -1bp	*Sal*I-*Xma*I	pBI101.2 (modified)	Silverstone et al., 1997
pGA20ox4-TC-GUS	-2122bp to -1bp	*Sal*I-*Bam*HI-*Nde*I	pBI101.2 (modified)	Silverstone et al., 1997
pGA20ox5S-TC-GUS	-608bp to -1bp	*Xma*I-*Nde*I	pBI101.2 (modified)	Silverstone et al., 1997
pGA20ox5L-TC-GUS	-1873bp to -1bp	*Xma*I-*Nde*I	pBI101.2 (modified)	Silverstone et al., 1997
35S::GA20ox1	(pMS37)	*Not*I-(*Eco*RI-*Bam*HI)-*Not*I	pMLBART	Gleave, 1992
35S::GA20ox5	(pMS37)	*Not*I-(*Xho*I-*Kpn*I)-*Not*I	pMLBART	Gleave, 1992
LTP12::RGA(cDNA)::GFP	-1096bp to -15bp	*att*L-*att*R Recombination	pGWB450	Nakagawa et al., 2007
LAT52::RGA(cDNA)::GFP	-603bp to -5bp	*att*L-*att*R Recombination	pGWB450	Nakagawa et al., 2007

(b)

Transgenic line	Plant Antibiotic Selection	T_0 Background
pGA20ox1-TC-GUS	Kanamycin ($50\mu gml^{-1}$)	Wild type (Col-0)
pGA20ox2-TC-GUS	Kanamycin ($50\mu gml^{-1}$)	Wild type (Col-0)
pGA20ox3-TC-GUS	Kanamycin ($50\mu gml^{-1}$)	Wild type (Col-0)
pGA20ox4-TC-GUS	Kanamycin ($50\mu gml^{-1}$)	Wild type (Col-0)
pGA20ox5S-TC-GUS	Kanamycin ($50\mu gml^{-1}$)	Wild type (Col-0)
pGA20ox5L-TC-GUS	Kanamycin ($50\mu gml^{-1}$)	Wild type (Col-0)
35S::GA20ox1 (cDNA)	BASTA (50µM)	*ga20ox1 ga20ox2 ga20ox3-1*
35S::GA20ox5 (cDNA)	BASTA (50µM)	*ga20ox1 ga20ox2 ga20ox3-1*
LTP12::RGA(cDNA)::GFP	Kanamycin ($50\mu gml^{-1}$)	*rga-28*; segregating *gai-td1* (Col-0)
LAT52::RGA(cDNA)::GFP	Kanamycin ($50\mu gml^{-1}$)	*rga-28*; segregating *gai-td1* (Col-0)

Table 2.2: Summary of *Arabidopsis* transgenic lines.

Tables describe the functional elements and construction method of each plasmid construct (a), as well as selection marker for subsequent plant breeding and the genetic background transformed (b). Promoter fragments are described by relative position to their native ATG.

of these two paralogues separately in the *ga20ox1 ga20ox2 ga20ox3-1* mutant background. *AtGA20ox1* and *AtGA20ox5* cDNA clones were amplified and inserted into plasmid pMS37 (Gleave, 1992, see Table 2.2 for restriction sites), which carries the CaMV 35S promoter and ocs 3' sequence. These expression cassettes were then inserted into the pMLBART binary vector (Gleave, 1992) as a *Not*I fragment.

The final transgenic constructs produced for this project, designed to express a C-terminal RGA::GFP fusion protein in specific anther tissues, were constructed using the Invitrogen Gateway System (Invitrogen Corporation, California, U.S.A.), which utilises site-specific recombination of *att* sites derived from bacteriophage lambda (Landy, 1989; Hartley et al., 2000). An RGA cDNA clone (excluding stop codon) was amplified and cloned into the shuttle vector pENTR11 (Invitrogen Corporation, California, U.S.A.) as a *Sal*I-*Not*I fragment before recombination into the final destination vectors such that the GFP coding sequence is in-frame with RGA. The plant-expression Gateway-compatible vector pGWB450 (Nakagawa et al., 2007, kindly donated by Zoe Wilson) was modified to contain one of two promoter fragments 5' of the *att* recombination site, taken from the *Arabidopsis* gene *Lipid Transport Protein 12* (*LTP12*, Ariizumi et al., 2002) and the tomato gene *LAT52* (Twell et al., 1989), respectively. GUS reporter analysis of these promoter fragments has previously demonstrated tissue-specificity in developing *Arabidopsis* anthers, with *LTP12* expressed in the tapetum (Ariizumi et al., 2002) and *LAT52* expressed in developing pollen (Twell et al., 1990; Eady et al., 1994). The *LTP12* promoter fragment was amplified from Col-0 genomic DNA whilst the *LAT52* fragment was amplified from the plasmid pLAT52 (kindly donated by David Twell). Each promoter was cloned into pGWB450 using a pre-existing *Xba*I site.

The parent populations of plants that were transformed were designated the T_0 generation, with the resulting seed produced post-transformation as T_1 seed, etc. Where possible, T-DNA constructs were transformed into pure-breeding T_0 populations, but due to the nature of the *rga-28 gai-td1* male-sterile phenotype (see section 6.2.2), *LTP12::RGA::pGWB450* and *LAT52::RGA::pGWB450* were by necessity transformed into an *rga-28* population segregating for the *gai-td1* allele. Screening for successful transformation events in T_1

progeny was achieved by antibiotic resistance selection in germinating seedlings on agar media, with individual seedlings that showed resistance after five days transplanted to soil and subsequent T_2 seed harvested separately from each. Antibiotic resistance screening of T_2 lines (each line descended from an individual T_1 plant) identified lines exhibiting a 3:1 Mendelian ratio of antibiotic resistance to susceptibility, indicative of a single hemizygous T-DNA insertion. Populations of approximately 180 plants were screened and tested against the null hypothesis of a 3:1 resistance segregation pattern using a X^2 statistical analysis. Individual resistant seedlings from single-insertion lines were taken forward to set T_3 seed. Antibiotic-resistance screening of T_3 lines (each line descended from a single T_2 plant) was used to identify lines homozygous for the inserted DNA (in which no antibiotic susceptibility was detected), which would be pure-breeding in subsequent generations. The identity of the inserted transgene was confirmed *in planta* at the T_3 generation by amplification of T-DNA-specific PCR products from genomic DNA samples (not shown). In addition, promoter::RGA::GFP T_1 and T_2 transgenic plants were genotyped at the *GAI* locus to identify genetic individuals lacking both native *RGA* and *GAI*.

T-DNA constructs were transformed into at least three independent T_0 populations of plants, each designated a separate 'transformation pot'. Transformant progeny descended from these separate pots (and therefore representing independent transformation events) were tracked, and characterisation experiments were performed using one homozygous T_3 line from each transformation pot to independently verify the effect of the T-DNA on phenotype. In the case of the *AtGA20ox::GUS* reporter lines, inflorescence GUS-staining patterns were compared both within and between transgenic lines to identify the most common expression pattern for that particular reporter (Table 5.2). Individual T_3 lines displaying a representative expression pattern were then selected as representative lines and subjected to further characterisation.

2.1.3 Growth Conditions

All *Arabidopsis* plant lines were grown to maturity on soil comprising Levingtons F2 commercial soil mix containing Suscon green™ (Fargo, Littlehampton, U.K.), treated with Intercept™ pesticide soil drench (LBS Horticulture, Colne, U.K.) prior to sowing. Plants

were grown in a controlled environment under long day conditions (16 hours light at 23°C, 8 hours dark at 18°C) at a fixed fluence of 250µmol.m^{-2}.s^{-1}. Exogenous GA was applied to plants growing on soil via foliar spray and comprised either 100µM GA_3 (in 0.1% EtOH) or 1µM GA_4 (in $2x10^{-5}$% EtOH).

Seeds were germinated on either soil or sterile agar media (1x MS, 1% sucrose, 0.8% agar (pH5.8), see section 2.1.4), seedlings then transplanted to soil after germination (typically five to eight days after sowing). Seeds sown directly to soil were imbibed under non-sterile conditions, those plated on agar media were first surface-sterilised prior to imbibition using a three minute 70% EtOH treatment, a subsequent five minute incubation in a $^{1}/_{10}$ dilution of 1.24g-1.26g ml^{-1} sodium hypochlorite solution (BDH Lab Supplies, Poole, U.K.) containing 0.1% Tween detergent (Sigma-Aldrich, Dorset, U.K.), then six washes with sterile deionised H_2O (dH_2O, Milli-Q purification system, Millipore Corp., MA, U.S.A). Surface-sterilised seed was imbibed in either sterile dH_2O or 50µM GA_4 solution (in $2x10^{-3}$% EtOH) and stratified at 4°C for a minimum of three days prior to sowing. GA_4-imbibed seed stocks were washed 6 times with dH_2O immediately prior to sowing to reduce contamination in the surrounding soil/agar media during germination.

Seeds were sown by pipette, suspended in dH_2O when sowing onto agar plates or in sterile 0.12% agar solution when sowing onto soil to reduce clumping. After sowing with seed, MS-agar plates were sealed with micropore tape (3M Health Care, Neuss, Germany) and incubated under long day conditions (16 hours light at 180 µmol.m^{-2}.s^{-1}, 8 hours dark, at a constant temperature of 22°C). Soil trays were covered with propagator lids for at least three days after sowing to maintain humidity. Lids were then unsealed but left on the trays for 24 hours prior to their removal. Plants were grown on soil in 24-cell propagator trays with one corner cell removed and capillary matting in the base of each tray to aid watering. Multiple seeds were sown in each cell (typically 4-5), and were thinned to one per cell using scissors approximately a week after sowing. The only exception was plants grown for *Agrobacterium*-mediated transformation, which were grown on the same soil mix in circular 10.5cm diameter pots (7-10 plants per pot), to aid manipulation during transformation (see section 2.2.6).

2.1.4 Plant Growth Media

Unless specified otherwise, germination of *Arabidopsis* under sterile conditions in this project used a 1x concentration of Murashige and Skoog growth media (Duchefa Biochemie, Haarlem, The Netherlands), containing 1% sucrose (Fisher Scientific, Loughborough, U.K.), pH-buffered with MES free acid (Melford, Poole, U.K.) with the final pH adjusted to pH5.8 using 1M KOH solution (Fisher Scientific, Loughborough, U.K.). Growth media was either used in solution or including 0.8% agar (w/v; Agar Type A, Sigma-Aldrich, Dorset, U.K.). For plates incubated vertically during root growth assays, agar was replaced with 0.8% GelZan™ CM (Sigma-Aldrich Company Ltd., Dorset, U.K.). All media was sterilised prior to use by autoclaving and subsequently stored at 4°C. Where seedlings grown on plates required exogenous GA treatment or antibiotic selection (Table 2.2), the particular concentration of GA/antibiotic for that experiment was added to the molten sterile agar media before pouring. Media without sucrose was used for antibiotic resistance screening. All media was cooled to 55°C before any such additives were included.

2.2 MOLECULAR BIOLOGY

Unless stated otherwise, all chemicals used in the creation of solutions, buffers, media etc. were purchased from Sigma Aldrich U.K. (Sigma-Aldrich Company Ltd., Dorset, U.K.). Unless specified otherwise or bought commercially (as indicated), all buffers and reagents were prepared as according to Sambrook et al. (1989).

2.2.1 Nucleic Acid Extraction from Plant Tissues

Genomic DNA (gDNA) was extracted from tissues (generally single leaves) of individual *Arabidopsis* plants using a CTAB detergent-based method. Tissues were harvested in sterile microcentrifuge tubes and immediately frozen in liquid nitrogen ($N_{2(L)}$, -178°C). Tissues were homogenised whilst frozen using a QIAgen TissueLyser (QIAgen, Maryland, U.S.A.), using stainless steel ball-bearings to disrupt tissues. The homogenate was incubated in 200µl 2x CTAB extraction buffer (containing 50µgml^{-1} RNase A (Melford, U.K.)) at 65°C for 20 minutes, then mixed with 200µl Ready Red™ Chloroform:Isoamylalcohol mix (MP Biomedicals, U.K.). Aqueous and chloroform/isoamylalcohol phases were separated by

centrifugation (14,000rpm, 2 minutes at room temperature). DNA was precipitated from the recovered aqueous phase using 200µl propan-2-ol and subsequently pelleted by centrifugation (14,000rpm, 5 minutes at room temperature). Pelleted DNA was washed in 400µl 70% EtOH and then recollected by centrifugation (14,000rpm, 1 minute at room temperature). All solution was removed by pipetting and pellets were air-dried for two minutes to ensure the evaporation of all EtOH. Dried pellets were resuspended in 100µl dH_2O and stored at -20°C prior to use.

2x CTAB Extraction buffer:	100mM Tris pH9.0
	2% Hexadecyltrimethylammonium bromide ('CTAB': $C_{19}H_{42}NBr$; BDH laboratory supplies, Poole, U.K.)
	1.4M NaCl
	20mM EDTA pH8.0

Plasmid DNA was purified from bacterial cell cultures using the QIAprep miniprep kit (QIAgen, Maryland, U.S.A.), following the kit-supplied protocol.

RNA was extracted from whole seedling tissues using the RNeasy plant RNA extraction kit (QIAgen, Maryland, U.S.A.), following the supplied protocol. RNA was extracted from dissected floral organs using the Ambion RNAqeuous Micro micro-scale RNA extraction kit (Invitrogen Corporation, California, U.S.A.) including additional Ambion plant RNA isolation aid, following kit-supplied protocols. RNA purified by both methods was subsequently DNase-treated using Ambion Turbo DNase (Invitrogen Corporation, California, U.S.A.). DNase-treated RNA was quantified using a Nanodrop™ ND-1000 spectrophotometer (LabTech International Ltd., U.K.).

2.2.2 Polymerase Chain Reaction (PCR) Applications

PCR-based techniques were used during this project for the following purposes:

- Genotyping of mutant and transgenic plant lines.

- Amplification of target DNA sequences from genomic DNA (gDNA), complementary DNA (cDNA) and plasmid templates.
- Site-directed mutagenesis of plasmid DNA, using the Stratagene Quikchange II™ site-directed mutagenesis kit (Stratagene, California, U.S.A.), following kit protocols.
- Synthesis of cDNA from RNA, using the Invitrogen Superscript III First Strand cDNA synthesis system (Invitrogen Corporation, California, U.S.A.), following kit protocols.
- Semi-quantitative Real-Time PCR (qPCR).

Unless using kit-supplied enzymes, non-quantitative PCR reactions were performed using either GoTaq DNA Polymerase and buffers (Promega Corporation, Wisconsin, U.S.A.), or Phusion Taq DNA Polymerase and buffers (Finnzymes, Espoo, Finland) for high-fidelity amplifications, using the following typical reaction mixes and PCR programs:

GoTaq DNA Polymerase:

gDNA or cDNA (diluted $^1/_5$ with dH_2O) / plasmid	3.75µl / 50ng / bacterial colony
dNTP (10mM)	0.375µl
Primer 'F' (10µM)	0.375µl
Primer 'R' (10µM)	0.375µl
5x GoTaq Flexi buffer	3µl
$MgCl_2$ (25mM)	0.9µl
GoTaq DNA Polymerase (5U/µl)	0.075µl
dH_2O	6.15µl / to 15µl / to 15µl
Final Volume	15µl

94°C 3 minutes	(Initial denaturation)
[94°C 15 seconds; *a*°C 30 seconds; 72°C *b* seconds] x 35 cycles	(Thermocycling)
72°C 6 minutes	(Final extension)

Where *a* is determined by the primer pair specific to that reaction and where *b* is determined by the length of the target PCR product (see Appendix 2). GoTaq has an extension profile of approximately 1kilobase (kb) per minute.

Phusion Taq DNA Polymerase:

gDNA or cDNA / plasmid DNA	0.5µl / 50ng
dNTP (10mM)	1µl
Primer 'F' (10µM)	1.5µl
Primer 'R' (10µM)	1.5µl
5x Phusion Taq buffer HF	10µl
Phusion Taq Polymerase (5U/µl)	0.5µl
dH_2O	35µl / to 50µl
Final Volume	50µl

98°C 30 seconds	(Initial denaturation)
[98°C 10 seconds; *a*°C 20 seconds; 72°C *b* seconds] x 30-35 cycles	(Thermocycling)
72°C 6 minutes	(Final extension)

Where *a* is determined by the primer pair specific to that reaction and where *b* is determined by the length of the target PCR product. Phusion Taq has an extension profile of approximately 2kb per minute.

All PCR reactions were optimised for a final Mg^{2+} concentration of 1.5mM. Primers 'F' and 'R' are determined by the target PCR product (see Appendix 2). All primers were designed using the Vector NTI software package (Invitrogen Corporation, California, U.S.A.), taking %GC values and melting temperatures calculated therein, with standard primer specifications of a %GC value between 40 and 60% and a Tm of 55°C were possible. Terminal restriction sites were incorporated into amplified PCR products through addition to the primer sequence. Primers were synthesised by Sigma-Aldrich (Sigma-Aldrich Company Ltd., Dorset, U.K.) and purified by desalting unless stated otherwise. Primer stocks were resuspended in dH_2O at a

concentration of 100µM, with dilute working stocks prepared at a concentration of 10µM. . All PCR reactions were run on a DNA Engine Tetrad 2™ rapid thermocycler (Bio-Rad Life Sciences, Hemel Hempstead, U.K.) comprising four 96-well heat blocks with heated lids.

Discrimination of SNPs between genotyping PCR products (e.g. between *GA20ox3* and *ga20ox3-1*, Appendix 2) was achieved through use of Cleaved Amplified Polymorphic Sequence (CAPS) or derived CAPS (dCAPS) (Neff et al., 1998), based on the principle of differential digestion by restriction endonuclease using a recognition site unique to either wild-type or mutant DNA sequence. Primer design for CAPS and dCAPS reactions was performed using the dCAPS Finder 2.0 web-based design tool (http://helix.wustl.edu/dcaps/dcaps.html). Where PCR reactions had not been previously established (e.g. for genotyping of new mutant alleles), PCR products were cloned and sequenced to confirm the accuracy of the PCR reaction (see section 2.2.3).

All qPCR reactions were performed using Sigma SYBR Green Jumpstart™ Taq Readymix, using the following typical reaction mix and PCR program:

cDNA (diluted $^{1}/_{10}$ using dH_2O)	3.6µl
Primer 'F'	0.4µl
Primer 'R'	0.4µl
2x SYBR Green (+ ROX dye, $^{1}/_{500}$ dilution)	10µl
$MgCl_2$ (25mM)	5.6µl
Final Volume	20µl

95°C 2 minutes	(Initial denaturation)
[95°C 15 seconds; 60°C 1 minute] x 40 cycles	(Thermocycling)
95°C 15 seconds; 60°C 1 minute; 95°C 15 seconds; 60°C 15 seconds	(Dissociation Analysis)

qPCR reactions were run on the Applied Biosystems 7500 Real-Time PCR system (Life Technologies Corporation, California, U.S.A.). All primer pairs for target and reference genes

used have been developed and validated previously on this equipment (Czechowski et al., 2005; Rieu et al., 2008). Stable expression of the reference genes selected for these experiments (At2g23890, At4g05320 and At5g25760) was confirmed on cDNA samples used in these particular experiments. All qPCR experiments comprised three biological replicates run on 96 well plates, split either by tissue type or biological replicate, depending on the comparisons being made (see section 5.2.3). In all qPCR experiments the target and reference genes for each sample were included on the same plate to prevent the introduction of plate-to-plate variation, as were water and -RT controls for each PCR mix and RNA source, respectively. Two technical replicates of each reaction were included. A randomised plate design was followed, constrained by keeping gene-specific PCR reactions within fixed paired columns and cDNA samples in fixed rows across the plate to minimise set-up time and the risk of cross-contamination between wells.

2.2.3 DNA Cloning and Manipulation

The products of PCR amplification or restriction digestion were separated by size via electrophoresis, running through an agarose-TBE gel matrix against DNA ladder (1kb and 100bp ladder, Fermentas Inc., Maryland, U.S.A.; 25bp ladder, Promega Corporation, Wisconsin, U.S.A.), which was imaged through ethidium bromide fluorescence under UV light excitation using the Syngene GelDoc imaging system (Synoptics Ltd, Cambridge, U.K.). Extraction was achieved through the Promega Wizard SV Gel and PCR clean-up system (Promega Corporation, Wisconsin, U.S.A.) following the kit-supplied protocol. Purified DNA was quantified using a Nanodrop™ ND-1000 spectrophotometer (LabTech International Ltd., U.K.). Depending on whether the PCR products were amplified using proofreading (Phusion) or non-proofreading (GO) Taq, they were cloned into either the pGEM-T-Easy (Promega Corporation, Wisconsin, U.S.A.) or pSC-Blunt (Stratagene, California, U.S.A.) cloning vector systems following kit-supplied protocols. Sequencing of PCR products to confirm correct amplification was performed by the Eurofins MWG Operon sequencing company (Ebersberg, Germany). The returned sequencing data was then aligned against the expected sequence using the ContigExpress program within Vector NTI (Invitrogen Corporation, California, U.S.A.).

Transgenic constructs (see section 2.1.2) were designed from known sequences using Vector NTI (Invitrogen Corporation, California, U.S.A.), following a restriction digest and recombination approach in most cases. Restriction endonucleases were sourced from New England Biolabs UK (Hitchin, U.K.), Fermentas (Maryland, U.S.A.) and Promega (Wisconsin, U.S.A.), depending on availability, using the supplied buffers and following the recommended digest conditions. Where possible, two incompatible restriction sites were used at each cloning step to ensure ligation of DNA fragments in the correct orientation. Typical incubation for a cloning digest was 3-4 hours. To reduce recircularisation of vector DNA, such samples were incubated with 1µl Calf Intestinal Phosphatase (CIP; Promega Corporation, Wisconsin, U.S.A.) for an additional hour. Digested DNA fragments were purified following the method outlined above. With the exception of cloning into pGEM and pSC-Blunt vectors (which are supplied with specific ligases), ligations were performed using T4 DNA ligase (Fermentas Inc., Maryland, U.S.A.), using kit-supplied buffer and protocols. Typically three times the amount of insert DNA to vector DNA was included in a ligation, using the following formula:

(50ng vector DNA x *a* kb insert DNA)/ *b* kb vector DNA x (3 units insert/1 unit vector)

= *c* ng insert DNA

Where *a* and *b* are defined by the specific sizes of the DNA fragments in that ligation. Parallel vector-only and no-ligase controls were included as diagnostic tools. Unless specified otherwise, ligations were transformed into DH5α ultracompetent cells, with successful ligations being selected for by antibiotic resistance (see section 2.2.4). In situations where ligations may have occurred in more than one combination (e.g. possible insertion in more than one orientation) populations of colonies were screened using colony PCR (see section 2.2.2) to identify correct plasmid clones. The success of each cloning step was confirmed using diagnostic digestion of miniprep DNA (see above). Gateway recombination of pENTR11-RGA with either pGWB450-LTP12 or pGWB450-LAT52 was achieved using LR clonase (Invitrogen Corporation, California, U.S.A.), following kit-supplied recombination and transformation protocols (see section 2.2.4).

2.2.4 Bacterial Transformation and Culturing

Plasmids were introduced into competent *E. coli* strains using chemical transformation. Cell lines were propagated and made chemically-competent following the protocol described by Inoue et al. (1990), with competence further enhanced by culturing cells in SOB media at 19°C instead of LB media at 37°C.

SOB medium (pH6.7-7.0):	0.5% yeast extract (Formedium Ltd., Hunstanton, U.K.)
	2% tryptone
	10mM NaCl (Fisher Scientific, Loughborough, U.K.)
	2.5mM KCl (Fisher Scientific, Loughborough, U.K.)
	10mM $MgCl_2$
	10mM $MgSO_4$

50µl aliquots of DH5α ultracompetent cells (Invitrogen Corporation, California, U.S.A.) were transformed by heat shock at 42°C for 35 seconds after incubation with the plasmid (2µl for a ligation, 0.5µl for plasmid propagation) on ice for 30 minutes. Cells were allowed to recover on ice for 2 minutes before resuspending in 400µl SOC media and incubating at 37°C (agitating at 200rpm) for one hour. Typically 200µl and 50µl volumes of each transformation were spread on separate 2xYT agar media (Formedium, Hunstanton, U.K.) plates containing the appropriate antibiotic selection for that plasmid. These plates were incubated at 37°C overnight, by which time resistant bacterial colonies had grown. For certain cloning processes (e.g. into the pGEM or pSC-Blunt vectors, see section 2.2.3), kit-supplied competent cells were transformed using very similar protocols, adjusted according to the manufacturers' recommendations. Propagation of the pGWB vectors (which carry *ccd*B counter-selection) required transformation into Oneshot® *ccd*B survival™ 2 $T1^R$ chemically competent cells (Invitrogen Corporation, California, U.S.A.), following the manufacturer's protocol.

All *Arabidopsis* transformations were mediated through the *Agrobacterium tumefaciens* disarmed competent laboratory line GV3101. 50µl aliquots of competent *Agrobacterium* cells were transformed with 500ng of plasmid through snap-freezing in liquid nitrogen for 10

seconds after 5 minutes' incubation on ice, followed by a heat-shock at 37°C for 5 minutes. Cells were then resuspended in 1ml 2xYT liquid media (Formedium, Hunstanton, U.K.) and incubated at 28°C (200rpm) for 2-4 hours. The cultures were concentrated by pelleting and subsequently resuspending in 120µl 2xYT media before plating 100µl and 20µl volumes onto separate 2xYT agar plates containing rifampicin (50µg/ml) and gentamycin (25µg/ml) to select for ancilliary plasmids carried by GV3101, and a third antibiotic to select for the presence of the target transformed plasmid. Spread plates were incubated as 28°C for two days, after which time transformant colonies were visible.

Transformant bacteria were cultured from colonies in 2xYT media containing appropriate antibiotic selection, incubating at 37°C for *E. coli* and 28°C for *Agrobacterium*. Antibiotic stock and working concentrations are listed in Table 2.3. Culture volumes were typically 5ml for miniprep, though when miniprepping *Agrobacterium* a volume of up to 10ml was required. *E. coli* miniprep cultures were typically incubated overnight (shaking at 250rpm), whilst 500ml *Agrobacterium* cultures for plant transformation were started as a 5ml preculture inoculated from a single colony and incubated overnight, 100 µl of which subsequently inoculated a 50ml culture incubated over 24 hours or until visibly opaque and cloudy. After miniprepping and diagnostic digest to confirm the presence of the correct transgenic construct (see section 2.2.3), 5ml of the remaining culture was used to inoculate the final 500ml culture, incubated at 28°C (200rpm) until an optical density (O.D., $\lambda = 600$) reached a value of ≥ 2. The O.D. of $^{1}/_{10}$ dilute culture samples was measured using a Lightwave spectrophotometer (W.P.A., U.K.).

Transformed bacterial cell lines were preserved by storage at -80°C in 15% glycerol. Glycerol stocks were prepared by taking 750µl of the appropriate bacterial culture and mixing gently with 250µl 60% glycerol and immediately stored at -80°C. Bacterial lines were regenerated from glycerol stocks by streaking onto 2xYT agar media containing appropriate antibiotic selection and incubating overnight at 37°C, after which time individual colonies had developed. These colonies were then used to inoculate 2xYT cultures as described above.

Antibiotic	Solvent	Stock Concentration	Working Concentration	Organism Selection
Ampicillin	dH_2O	100 mg/ml	100 µg/ml	*E.coli*
Kanamycin	dH_2O	50 mg/ml	50 µg/ml	*E.coli, Agrobacterium, Arabidopsis*
Spectinomycin	dH_2O	100 mg/ml	100 µg/ml	*E.coli*
Rifampicin	DMSO	50 mg/ml	50 µg/ml	*Agrobacterium*
Gentamycin	dH_2O	25 mg/ml	25 µg/ml	*Agrobacterium*
PPT ('BASTA')	dH_2O	50 mM	50 µM	*Arabidopsis*

Table 2.3: Antibiotics used in molecular biology and *Arabidopsis* transformation.

2.2.5 *In Vitro* Protein Expression and Catalytic Activity Assay

To compare the effect of SNPs on GA20ox catalytic activity, full cDNA clones of target *AtGA20ox* paralogues were amplified and cloned into the pET-32a bacterial expression vector (Novagen, Merck Biosciences, Darmstadt, Germany; see Table 2.4 for restriction sites), which carries T7 IPTG-inducible promoter and terminator sequences. SNPs from mutant alleles were replicated in the appropriate cDNA clone using site-directed mutagenesis (see section 2.2.2) whilst the cDNA clone was in the pSC-Blunt cloning vector, the mutant clone subsequently ligated into pET32a following confirmation of the mutation by sequencing.

GA20ox-carrying pET32a constructs were transformed into the BL21-CodonPlus(DE3)-RIL *E. coli* competent cell line (Stratagene, California, U.S.A.) following the manufacturer's protocol. Having confirmed successful transformation by miniprep and diagnostic digest, 50ml 2xYT cultures were inoculated from the remaining miniprep culture and grown at 37°C until an $O.D._{600}$ of ≥ 0.5 was reached. Protein expression was then induced with 1µM IPTG for 6 hours at 25°C. Cells were pelleted and then lysed in buffer containing lysozyme. Lysates were DNase-treated at room temperature for 5 minutes and then centrifuged to pellet cellular debris. Supernatant containing heterologously-expressed GA20ox protein was then used for *in vitro* activity assays, as described below.

cDNA clone	Restriction Sites	Expression Vector
GA20ox1	*Sal*I-*Not*I	pET32a
GA20ox3	*Bam*HI-*Not*I	pET32a
GA20ox4	*Nco*I-*Xho*I	pET32a
GA20ox5	*Sal*I-*Not*I	pET32a

Table 2.4: Design of AtGA20ox-pET32a constructs for *in vitro* expression.

All cDNA clones were introduced into the pET32a polylinker site in the forward orientation between the T7 promoter and terminator. Clones included native start ATG and stop codons.

Lysis buffer: 100mM Tris-HCl pH7.5
5mM DTT
1mg/ml lysozyme

GA20ox protein activity was assayed by incubation with a radiolabelled substrate (^{14}C -GA_{12}) in the presence of cosubstrates and cofactors, after which all proteins in the lysate were denatured by addition of 5µl concentrated acetic acid. 2-ODDs require Fe^{2+} and ascorbate for optimal substrate conversion *in vitro*, with the further addition of catalase increasing substrate turnover (Prescott & John, 1996). Each assay had the following composition:

Lysate	90µl
^{14}C -GA_{12}	5µl (≈11,000 dpm)
Cofactor mix	5µl
Final Volume	100µl

Cofactor mix (pH7.0): 100mM Tris-HCl
80mM 2-oxoglutarate
80mM ascorbate
80mM DTT
10mM $FeSO_4$
40mg/ml BSA
20mg/ml catalase

Typically lysates were incubated at 30°C (with shaking at 220 rpm) for periods of 2, 24 or 48 hours, beyond which time it is likely that all enzymatic activity within the lysate has been lost. Radiolabelled products were separated on a reverse phase high performance liquid chromatography (HPLC) column (Shimadzu U.K. Ltd., Milton Keynes, U.K.) across a 60-70% aqueous methanol gradient (flow rate 1ml/minute), identifiable as distinct peaks of radioactivity measured with an on-line radioactivity monitor (Radioflow detector LB509, Berthold Technologies GmbH & Co KG, Bad Wildbad, Germany), released from the column in order of decreasing polarity. The identity of each peak was determined by comparison to known GA standards, namely GA_{12}, GA_{15}, GA_{24} and GA_9, run through the same gradient. Peak areas for each product were determined using the LC Solutions software package (Shimadzu U.K. Ltd., Milton Keynes, U.K.) to identify the relative composition of products in each assay. By 24 hours, in the majority of assays, wild-type GA20ox protein had typically converted all GA_{12} to GA_9.

2.2.6 *Arabidopsis* Transformation

Arabidopsis plants were transformed using the floral dip method. Large volume *Agrobacterium* cultures (see section 2.2.4) were pelleted by 10 minutes' centrifugation at 6,000rpm using a Beckman Coulter Avanti J-30I (Beckman Coulter Inc., California, U.S.A.). The concentration of *Agrobacterium* cells used across each transformation was standardised by the following formula:

$$a = 1/(O.D._{600} \times 10)$$

Where a represents the volume in litres of each *Agrobacterium* culture to be pelleted.

Agrobacterium cells were then resuspended in 1L of floral dipping solution (0.5x MS media (Duchefa Biochenie, Haarlem, The Netherlands), 5% sucrose, pH 5.7, 0.05% Silwet detergent (Lehle Seeds, Texas U.S.A.)), prior to transformation.

Arabidopsis plants for transformation by *Agrobacterium* were grown on soil in circular transformation pots with 7-10 plants grown in each pot. Once flowering had begun and the

primary inflorescence had begun to bolt, these were removed from each plant using scissors by cutting near the base of the elongated internodes to encourage the growth of secondary inflorescences. Plants were typically transformed when secondary inflorescences began to set siliques. The inflorescence tissues of *Arabidopsis* were submerged in *Agrobacterium* without vacuum infiltration for approximately 30 seconds, with care being taken not to wet the rosette leaves of the plants. The inflorescences were then partially dried on blue paper towel to remove excess solution/foam. Each pot was placed horizontally in a paper-lined propagator and incubated overnight before being stood upright.

2.2.7 *Arabidopsis* Histochemical Staining with X-Gluc

GUS staining was performed on *AtGA20ox::GUS* transgenic inflorescence tissues and germinating seed (see section 5.2.2). Whole floral clusters were harvested from primary inflorescences using forceps, synchronising inflorescence development between plants by harvesting at the 10th open flower. Seed for staining was imbibed in dH_2O and stratified at 4°C for three days, sown in sterile 1xMS 1% sucrose (pH5.8) liquid media and GUS stained 24 hours later. *Arabidopsis* tissues were incubated in ice-cold 90% acetone (Fisher Scientific, Loughborough, U.K.) for 10 minutes to fix GUS expression, and then rinsed once in ice-cold dH_2O before resuspending in GUS staining buffer containing 1mg/ml X-GlcA (Melford, Poole, U.K., dissolved in DMSO to $^1/_{10}$ final volume).

GUS staining buffer: 100mM Sodium Phosphate (pH 6.7)
10mM EDTA (pH 7.0)
0.005% Tween

Tissues were vacuum infiltrated to improve uptake of GUS staining buffer and incubated 37°C overnight, by which time GUS staining had developed. Other pigments were subsequently removed from GUS-stained tissues by incubating in 70% EtOH. The concentration of potassium ferricyanide (a chemical inhibitor of GUS activity) necessary in this assay was determined empirically, using 0.5µM when staining both inflorescence tissues and seeds. GUS staining of whole flower buds was visualised under a Leica MZ8 dissecting microscope

with a Leica DFC300 FX camera attachment (Leica Microsystems, Wetzlar, Germany). Images were recorded using the Leica Application Suite software package (Leica Microsystems, Wetzlar, Germany). Analysis of anther tissue GUS staining patterns was achieved through fixation and embedding of freshly GUS-stained inflorescences in Technovit 7100 histological resin prior to sectioning (see section 2.3.2).

2.3 MICROSCOPY

2.3.1 Pollen Viability Discrimination

Pollen was tested microscopically for viability using the Alexander protocol (Alexander, 1969), determined by the presence or absence of cytoplasm within the pollen grain. Aborted pollen containing no cytoplasm stains green due to staining of the pollen walls with Malachite green. Cytoplasmic contents in viable pollen are stained by a combination of acid Fuchsin (cytoplasm and mitochondria) and Orange G (nucleus), resulting in red to dark-red staining that masks green staining of the pollen walls. Viable pollen grains are therefore coloured dark red, whilst inviable pollen grains appear as pale green.

Fresh whole stamens were dissected from newly-opened flowers onto a microscope slide and covered with a drop of Alexander stain before lightly squashing beneath a glass coverslip. Slides were incubated at room temperature for 5 to 30 minutes before being viewed under Köhler brightfield microscopy using a Zeiss Axiophot light microscope (Carl Zeiss Ltd., Welwyn Garden City, U.K.) with attached Retiga EXi camera system (QImaging, Surrey, Canada). Images were captured using the Metamorph software package (MDS Analytical Technologies, Toronto, Canada).

Alexander stain:	0.05% Acid Fuchsin (w/v, dH_2O solvent)
	0.005% Orange G (w/v, dH_2O solvent)
	0.01% Malachite green (w/v, EtOH solvent)
	50mg/ml chloral hydrate
	50mg/ml phenol
	25% glycerol(v/v)

10% EtOH (v/v)

acidified with glacial ethanoic acid (1-4%, v/v)

2.3.2 Fluorescence Microscopy

Fluorescence microscopy was used in this project to stage pollen development by staining pollen nuclei with 4',6-diamidino-2-phenylindole (DAPI), and to locate fluorescence from C-terminal RGA::GFP fusion proteins in anther tissues. To stage pollen development whole anthers were dissected from flower buds onto a microscope slide and covered with a cover slip. Anther tissues were then infiltrated with 1µg/ml DAPI solution (dH_2O solvent) and visualised using fluorescence microscopy under ultraviolet illumination from a 100W mercury lamp. Anthers were visualised on a Zeiss axiophot upright microscope with attached monochrome camera (see section 2.3.1). Images were captured using the Metamorph software package (MDS Analytical Technologies, Toronto, Canada).

GFP fluorescence was screened in whole anthers, which were dissected from flower buds onto a drop of water on a microscope slide and lightly squashed beneath a cover slip. GFP fluorescence microscopy was performed on a Leica M205 FA dissecting microscope (Leica Microsystems, Wetzlar, Germany) using the Leica GFP1 filter set (excitation spectrum 425-460nm, emission spectrum 480nm). Fluorescence images were captured using the Leica Application Suite (LAS) AF software (Leica Microsystems, Wetzlar, Germany).

2.3.3 Tissue Embedding and Thick Sectioning

Inflorescences tissues were embedded in Technovit 7100 histological resin (Heraeus-Kulzer, via TAAB Laboratory Supplies, Aldermaston, U.K.) following the supplied protocol as follows. Samples were fixed in 4% paraformaldehyde (pH 7.5, 0.1% Triton-X-100, 0.1% Tween (Sigma-Aldrich, Dorset, U.K.)), using vacuum infiltration to aid uptake into tissues before incubating overnight at 4°C (rotating at 4rpm). All subsequent incubation steps were performed at room temperature. Samples were washed with phosphate buffered saline (PBS) solution (pH7.5) followed by dH_2O before undergoing dehydration in a stepped EtOH series (30%, 50%, 70%, 90%, 100%, 100%), with one hour's incubation in each solution.

Dehydrated samples were then pre-infiltrated with resin in a stepped series of Technovit resin:EtOH mixtures (1:2, 1:1, 2:1) for one hour per solution prior to infiltration with undiluted Technovit resin overnight, using vacuum infiltration to improve uptake. Samples were polymerised at room temperature in sealed BEEM capsules (TAAB Laboratory Supplies, Aldermaston, U.K.) with truncated pyramid tips to aid sectioning.

7 to 10µm-thick sections were cut on a Leica-Reichart Jung 2053 Biocut rotary microtome (Leica Microsystems, Wetzlar, Germany) and fixed to polylysine-coated glass microscope slides (VWR International, California, U.S.A.). Sections were stretched flat prior to fixing by placing a drop of dH_2O on the slide and floating the section on this, allowing surface tension to pull the section taut. The water drop was then withdrawn from underneath the section using a pipette followed by gentle warming of the slide to evaporate any remaining water and firmly affix the section. Where inflorescence tissues were not GUS stained the contrast between resin and embedded tissues was enhanced by staining with Toluidine blue (pH 9.0) (O'Brien et al., 1964). Each section was covered with dye and incubated at room temperature for 10-15 seconds before rinsing clean with dH_2O, affixing cover-slips using dH_2O. All thick sections were viewed under Köhler brightfield microscopy using a Zeiss Axiophot light microscope (Carl Zeiss Ltd., Welwyn Garden City, U.K.). Images were captured using the Metamorph software package (MDS Analytical Technologies, Toronto, Canada).

2.4 PHENOTYPIC CHARACTERISATION

Phenotypic analyses of mature plant phenotypes were performed to test for the effects of mutant genotypes on plant growth under control growth conditions and under chemical GA treatment. Phenotypic characterisation experiments were grown in a blocked, split-plot design (Gomez & Gomez, 1984) where GA treatments were applied across grouped blocks of soil trays (main plot) and the position of genotypes used within that particular experiment were randomised within each tray (split-plot). A maximum of twelve cells per tray were filled within a 6 x 4 cell grid such that no two directly adjacent cells both contained a plant (a 'checkerboard' design). All genotypes were sown directly to soil, sowing four seeds per cell with subsequent thinning to two seedlings per cell at 7 days, and one plant per cell at 14 days.

Aerial tissue phenotypes were measured according to protocols published in Rieu et al. (2008). Flowering time was scored by the first appearance of flower buds visible to the unaided eye. Silique-set at individual inflorescence positions was scored by eye, based on the degree of silique elongation. Mature plant phenotypic characters were measured when the majority of plants in the experiment had ceased opening new flowers on the primary inflorescence (the time in days specified for each experiment). Floral organ lengths were measured from plants grown in similar split-plot designs under the same growth conditions. Individual flowers were dissected using forceps to expose all floral organ types and recorded photographically (see section 2.2.7). Floral organ lengths were subsequently measured from these scaled images.

Germination and root growth experiments were performed on 1xMS 1% sucrose 0.8% agar media (see section 2.1.4), where chemical GA treatment was applied by supplementing the media. All seed was surface-sterilised before plating (see section 2.1.3). Seed used in germination assays was harvested from plant lines phenotypically rescued by chemical GA_4 treatment to reduce the risk of GA contamination of the assay from the preceding generation. Seed used in germination assays was after-ripened for a minimum of three months prior to use to break dormancy and imbibed in either dH_2O or 50μM GA_4 (see section 2.1.3). Seeds were geminated on media not supplemented with GA, with germination scored by radicle emergence after five days. Genotypes were sown onto separate plates (≈80 seeds per plate).

Root growth assays were performed as blocked, split-plot randomised designs, with GA treatment being applied at the level of whole plates (main plots), and the position of individual genotypes randomised within each plate. Each genotype was represented once per plate and seed was evenly spaced across a horizontal line. To ensure germination of severely GA-deficient mutants all seed lines were imbibed in 50μM GA_4, but rinsed repeatedly prior to sowing to minimise the effect on root growth under control conditions. After 5 immediate washes in sterile dH_2O imbibed seed was incubated at room temperature for 2 hours to allow absorbed exogenous GA to diffuse from the seed. The seed was then resuspended in fresh

sterile dH_2O and immediately sown out. Plates were grown vertically under continuous light ($250\mu mol.m^2.s^{-1}$) and primary root length was measured using callipers 7 days after sowing.

2.5 DATA ANALYSIS

All statistical analysis was performed using the GenStat statistical software package (VSN International Ltd., Hemel Hempstead, U.K.). A 3:1 segregation of antibiotic resistance whilst screening transgenic lines (see section 2.1.2) was determined using a χ^2 test against the null hypothesis of 3:1 segregation. Because of their balanced design, data from phenotypic characterisation experiments were compared using analysis of variance (ANOVA). Where the distribution of data for individual phenotypic characters did not meet the assumptions of homogeneity of variance comparisons were made on a transformed scale (as specified in the appropriate results section). Least significant differences were used to assess significance between pairs of genotypes or GA treatment conditions, using a significance threshold of either 5% or 1% (as specified for each analysis).

Models describing the growth of floral organs across development were calculated by taking measurements of floral organs from a fixed range of buds from individual primary inflorescences and performing regression analysis for each plant to obtain a mathematical relationship of growth for each individual plant. The significance of observed differences in growth between genotypes was then assessed at the population level using ANOVA for each parameter contained within the mathematical model describing floral organ growth. Because each parameter estimate is a single value arising from one individual plant within the experimental population, they are independent values and so avoid statistical problems relating to the non-independence of repeated measurements taken from the same plant. Most of the models used were non-linear, and were chosen to best describe the data within the chosen range of floral development for that experiment (Causton & Venus, 1981). These models are described in detail in the relevant results sections.

For analysis of qPCR data, expression values of target genes were normalised against the mean expression of three reference genes from within the same cDNA sample, using threshold

cycle (C_t) values obtained for each technical replicate using the Applied Biosystems 7500 software v2.01 (Life Technologies Corporation, California, U.S.A.) and individual PCR efficiencies calculated using the LinReg program (HFRC, Amsterdam, the Netherlands; Tuomi et al., 2010). A relative quantity (RQ) value was first calculated for each individual reaction using the following formula:

$$RQ = 1/(Efficiency\text{^}C_t)$$

where the PCR efficiency and C_t values are those obtained for that particular reaction. RQ values were then averaged between technical replicates, and a normalised expression (NE) value for each target gene was calculated by dividing the mean RQ value of the target gene by the geometric mean of the three reference gene RQ values obtained from that same cDNA. Three biological replicates of each experiment were performed, and the NE values thus calculated were used as the basis for statistical analysis where appropriate. Statistical analysis of qPCR data employed ANOVA, comparing expression of target genes between wild-type (Col-0) and *ga20ox1 ga20ox2* genotypes within the same floral tissue (see section 5.2.3) as described above.

CHAPTER 3: *ATGA20OX1*, *-2* AND *-3* ARE THE DOMINANT GA 20-OXIDASES THROUGHOUT *ARABIDOPSIS* DEVELOPMENT

3.1 INTRODUCTION

The GA 20-oxidase enzymes represent a potentially important rate-limiting step in GA biosynthesis, as evidenced by the increased concentrations of bioactive GA produced by (and GA-overdosed phenotypes of) transgenic *Arabidopsis* plants overexpressing *GA20ox* genes (Huang et al., 1998; Coles et al., 1999, see section 1.2.1). A family of five *GA20ox* genes have been identified in the *Arabidopsis* genome through sequence similarity (Figure 3.1a, Hedden et al., 2002). The importance of two of these paralogues (*AtGA20ox1* and *-2*) to vegetative growth and development has been directly demonstrated through knockout mutations in the Col-0 ecotype (Rieu et al., 2008). These two paralgoues, plus a third, *AtGA20ox3*, have been shown to have GA20ox activity *in vitro* (Phillips et al., 1995; Xu et al., 1995). GA20ox enzymes catalyse successive oxidative reactions at Carbon-20 of intermediate GA substrates (Hedden, 1997; Figure 3.1b), resulting in the eventual loss of C-20 and the production of C_{19}-GA species that can be recognised by GA3ox enzymes and processed into biologically active GA.

Loss of *AtGA20ox1* and *-2* results in a semi-dwarf phenotype, and tissues from these plants contain reduced levels of bioactive GA (Rieu et al., 2008), demonstrating the contribution of GA20ox activity to GA biosynthesis. However, the phenotype of the *ga20ox1 ga20ox2* mutant is far less severe than mutants such as *ga1-3*, in which GA biosynthesis is completely blocked (see section 1.2), suggesting that one or more of the remaining *AtGA20ox* genes has biological functions during *Arabidopsis* growth and development. Alternatively, the possibility must be borne in mind that other, unrelated enzymes may perform the same functions as the GA20ox family (or even that other GA biosynthesis pathways exist that circumvent GA20ox activity). There are no published accounts of mutations in known *GA20ox* genes causing a severe dwarf phenotype in any plant species. The most probable candidate for catalysing further GA20ox activity in *Arabidopsis* is AtGA20ox3.

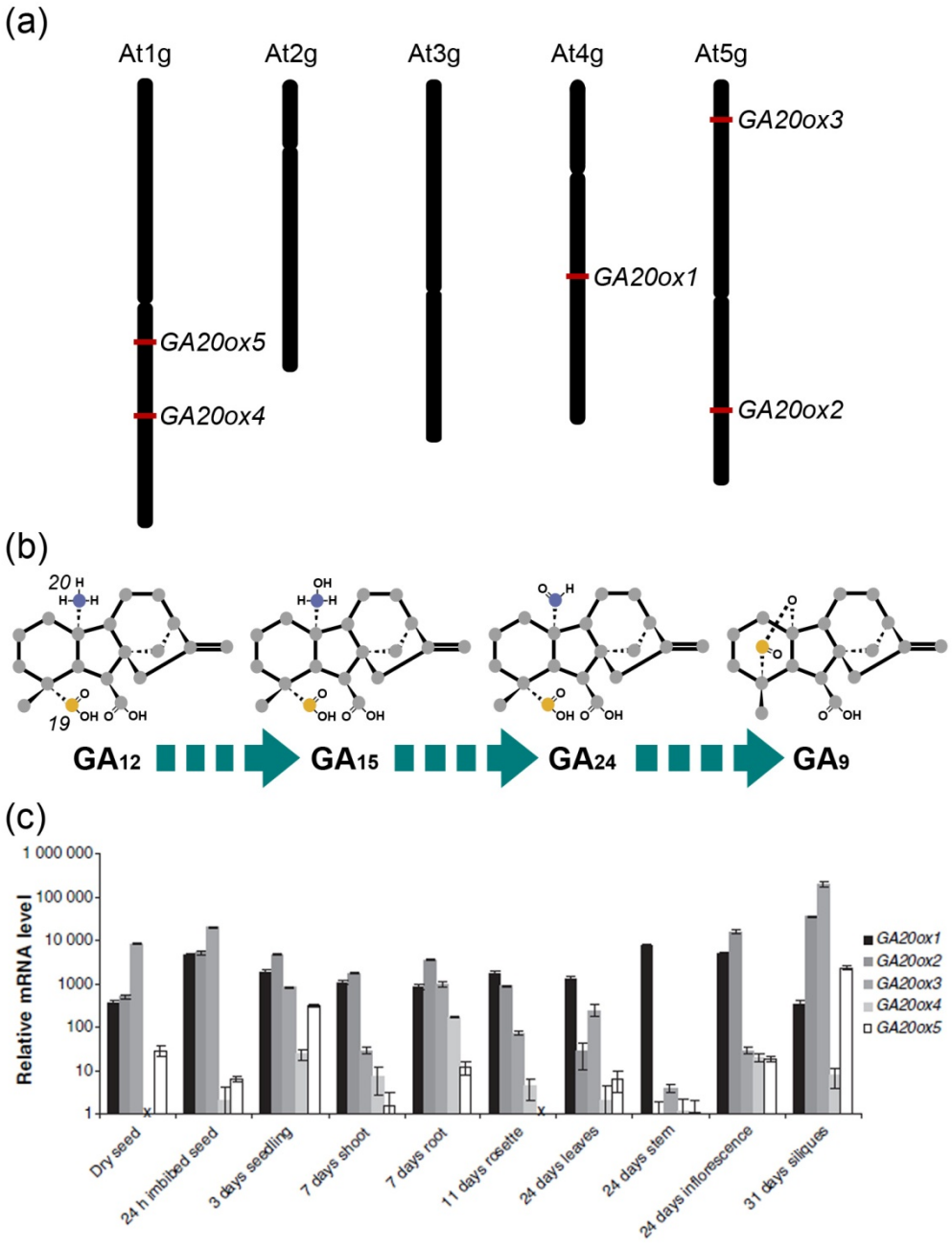

Figure 3.1: The *AtGA20ox* gene family.

(a) Genomic distribution of the AtGA20ox *gene family.*

(b) Schematic of GA 20-oxidase activity on non 13-hydroxylated substrates, converting GA_{12} *to* GA_9*. Numerals in italics denote carbon position. Sequential oxidative reactions at carbon position 20 (blue) eventually result in the loss of this carbon and its replacement by a lactone group derived from carbon 19 (yellow).*

(c) Expression profile of AtGA20ox *paralogues during* Arabidopsis *development.*

Reproduced with permission from Rieu et al. (2008).

The members of the *AtGA20ox* gene family demonstrate differential expression patterns during development, as shown through both quantitative Real-Time PCR (qPCR, Rieu et al., 2008) and Northern blot techniques (Phillips et al., 1995). Beyond this, detailed tissue-specific expression patterns of the individual *AtGA20ox* paralogues have not yet been published, with the exception of an *AtGA20ox1::GUS* translational fusion reporter gene expressed around the SAM during vegetative growth (Hay et al., 2002). A similar translational fusion reporter line has been established for *AtGA20ox2*, but attempts to replicate this approach for *AtGA20ox3*, *-4* and *-5* did not demonstrate any GUS staining (Phillips, A., unpublished data).

AtGA20ox1 and *-2* are the two most abundant and broadly-expressed *GA20ox* paralogues across *Arabidopsis* development, but expression data and mutant phenotypes suggest that functional specificity exists between them. *AtGA20ox1* is practically the only GA20ox paralogue expressed in stem tissues (Phillips et al., 1995; Rieu et al., 2008), a finding supported by the semi-dwarf phenotype of *ga20ox1* loss-of-function mutants (Xu et al., 1995; Rieu et al., 2008). However, despite the absence of AtGA20ox2 from wild-type stem tissue the *ga20ox1 ga20ox2* double mutant shows less stem elongation than *ga20ox1* (Rieu et al., 2008), demonstrating that functional redundancy also occurs between *AtGA20ox* paralogues. *AtGA20ox2* stem expression is in fact strongly up-regulated in the *ga20ox1* mutant (Rieu et al., 2008), presumably through homeostatic regulation of the GA biosynthesis pathway (see section 1.4). This highlights the potential for complex relationships between *AtGA20ox* paralogues. *AtGA20ox1*, *-2* and *-3* all show reduced expression under exogenous GA treatment (Phillips et al., 1995, Rieu et al., 2008), indicating that they are all responsive to feedback regulation. In contrast, expression of *AtGA20ox4* or *-5* did not respond to GA treatment (Rieu et al., 2008). *AtGA20ox3* expression has been shown to be significantly up-regulated in the *ga20ox1 ga20ox2* mutant background in all tissues tested (leaf, internode and inflorescence, Rieu et al., 2008), suggesting that expression of *AtGA20ox1*, *-2* and *-3* is governed by a complex relationship. In wild-type tissues *AtGA20ox3* is most strongly expressed in developing siliques and during germination.

In addition to plant stature, floral development also differs between *ga20ox1 ga20ox2* and *ga1-3*. *ga20ox1 ga20ox2* pistils, stamens and pistils reach a larger final size than those of *ga1-3* (Figure 1.8), the stamens producing viable pollen (Rieu et al., 2008), whilst *ga1-3* pollen development is arrested at the unicellular stage (Cheng et al., 2004). Similarly, *ga20ox1 ga20ox2* flowers are female fertile whilst *ga1-3* flowers are not (Koornneef & Van der Veen, 1980). However, successful silique-set is reduced across the first 10 flowers in *ga20ox1 ga20ox2* compared to wild type Col-0, apparently due to reduced stamen growth and delayed anther dehiscence (pollen release) creating a mechanical barrier to pollination (Figure 1.8, Rieu et al., 2008). Similar fertility phenotypes are also seen in *ga20ox1* (Rieu et al., 2008), and the *ga3ox1 ga3ox* mutant (Hu et al., 2008), though this is less severe in *ga20ox1*. Seed-set in these mutants subsequently recovers, which has been associated with restored growth of stamens relative to the pistil in the case of *ga3ox1 ga3ox3* (Hu et al., 2008). The mechanism regulating this process is unknown.

Genetic evidence presented in this chapter details the characterisation of *AtGA20ox3* function during plant development through the creation and phenotypic analysis of new *ga20ox* combinatorial mutant lines. The results indicate that *AtGA20ox1*, *-2* and *-3* are the three dominant *GA20ox* paralogues throughout *Arabidopsis* development, with loss of all three producing a severely dwarfed, infertile phenotype very similar to *ga1-3*. This is the first instance in which the *GA20ox* paralogues responsible for the majority of GA biosynthesis have been identified in any plant species, and confirms that the GA20ox pathway comprises the primary route through GA biosynthesis. *AtGA20ox3* functions almost entirely redundantly with either *AtGA20ox1*, *-2* or both at all stages of development, dependent on the phenotypic character examined. Loss of *AtGA20ox1*, *-2* and *-3* induces an apparent block in stamen development, exhibited by the failure of the tapetum cell layer to degrade in a timely fashion. However, evidence is also presented describing a previously undiscovered mechanism that enhances floral organ growth and development in later flowers of GA-deficient mutants in a manner that is apparently independent of GA biosynthesis.

3.2 RESULTS AND DISCUSSION

3.2.1 Identification of *AtGA20ox3* Loss-of-Function Mutant Alleles

Three strong candidates for *AtGA20ox3* loss-of-function alleles were identified from searches of mutant allele databases (Figure 3.2a). Two exonic SNPs were identified from TILLING lines (Till et al., 2003), one predicting a premature stop codon in exon one (TILLING line CS86016, Col-0 ecotype, herein referred to as *ga20ox3-1*) and the second predicting the mutation of a conserved leucine residue to phenylalanine (TILLING line CS87002, herein referred to as *ga20ox3-2*). The third, carrying an exonic 6.8kb T-DNA insertion 128bp 3' of the start codon, was identified from the Cold Spring Harbor Lab enhancer trap collection (Sundaresan et al., 1995; Martienssen, 1998, line ET10670, L*er* ecotype, herein referred to as *ga20ox3-3*).

The effect of the two separate SNP mutations on AtGA20ox3 catalytic activity was analysed *in vitro* using bacterially-expressed cDNA clones of *AtGA20ox3* mutagenised via site-directed mutagenesis to replicate the two alleles. Bacterial lysates expressing these proteins were incubated with radiolabelled substrate (^{14}C-GA$_{12}$) for 24 hours, the identity of the resulting radiolabelled GA products established using high performance liquid chromatography (HPLC; see section 2.2.5). Lysates expressing wild-type AtGA20ox3 protein showed almost complete conversion of ^{14}C-GA$_{12}$ to ^{14}C-GA$_9$ (96.89%, Figure 3.2b). The *ga20ox3-1* SNP (predicted to result in a truncated protein) completely abolished GA20ox activity, with only ^{14}C-GA$_{12}$ being recovered from the assay. In contrast, mutation of the conserved leucine in *ga20ox3-2* reduced but did not completely inhibit conversion of ^{14}C-GA$_{12}$ to ^{14}C-GA$_9$. It was concluded that the *ga20ox3*-1 allele confers a complete loss of function, whilst *ga20ox3-2* represents a knockdown allele. Given the potential for other *AtGA20ox* paralogues (including *AtGA20ox4* and -*5*) to contribute to GA20ox activity *in planta* and thereby mask mutant phenotypes, and the availability of complete loss-of-function alleles, *ga20ox3-2* was discounted as an analytical tool for this project. The effect of the *ga20ox3-3* T-DNA insertion on *AtGA20ox3* transcription was tested using non-quantitative reverse transcription PCR (RT-PCR) against cDNA derived from three day-old seedlings. No wild-type *AtGA20ox3* transcript was found

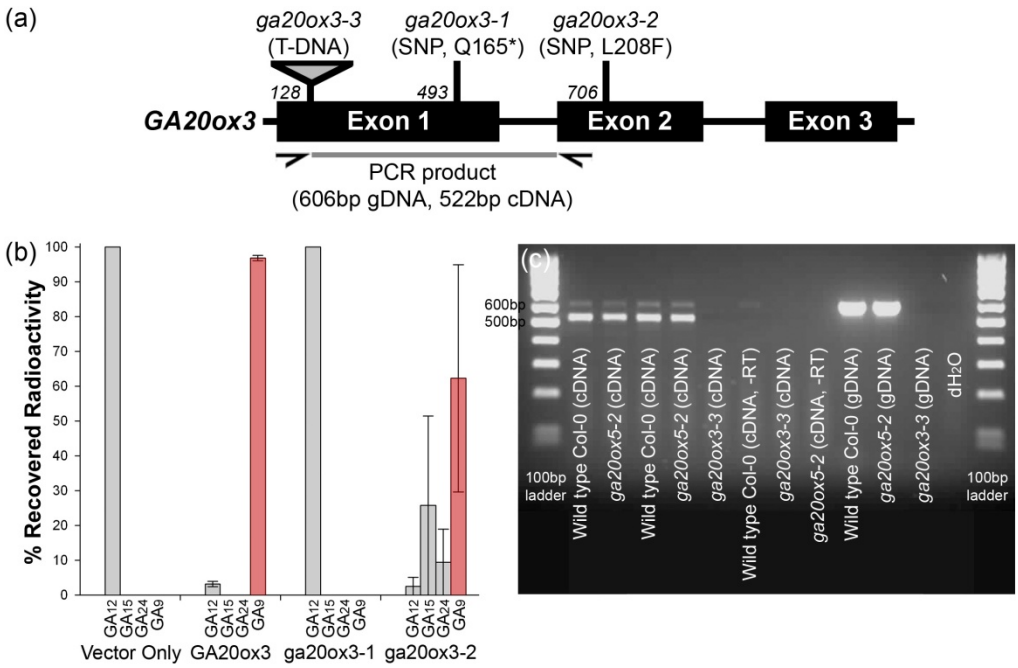

Figure 3.2: Characterisation of *AtGA20ox3* loss-of-function mutant alleles.

(a) AtGA20ox3 *gene model, showing the position and nature of the* ga20ox3-1*,* ga20ox3-2 *and* ga20ox3-3 *mutant alleles. Numerals in italics denote positions of mutations in bp relative to GA20ox3 ATG. Primer binding sites used in RT-PCR (c) are marked by half arrows, with the size of the respective PCR products listed beneath.*

(b) HPLC analysis of wild-type and mutant AtGA20ox3 activity in vitro*. Results shown are the mean of two technical replicates after 24 hours incubation with radiolabelled GA_{12}, error bars represent one S.E. Where present, ^{14}C-GA_9 is highlighted in red.*

(c) RT-PCR analysis of the effect of ga20ox3-3 *on* GA20ox3 *expression. The presence of the* ga20ox3-3 *T-DNA insertion prevents transcription from both RNA-derived and genomic template DNA (cDNA product 522bp, gDNA product 606bp), but not in wild type (*Ler*) or* ga20ox5-2 *(*Ler*, homozygous WT for* AtGA20ox3*, see section 4.2.1). RNA extracted from three day old whole seedlings.*

in *ga20ox3-3* samples (Figure 3.2c), indicating that production of functional GA20ox3 protein was disrupted by the *ga20ox3-3* T-DNA insertion. *ga20ox3-3* was therefore assigned as a second, independent loss-of-function allele.

The existence of the *ga20ox3-1* allele was confirmed *in planta* prior to the start of this project, and had previously been crossed to the *ga20ox1 ga20ox2* double mutant discussed in section 3.1 (Fernandez-Garcia, N., unpublished data). The position of the *ga20ox3-3* T-DNA insertion was confirmed by sequencing of PCR products amplified from the 5' and 3' T-DNA-genomic junctions (data not shown). The *ga20ox3-3* allele was introgressed into the Col-0 ecotype by 6 successive back-crosses before crossing to *ga20ox1 ga20ox2*. Combinatorial homozygous mutants were identified in the subsequent progeny of these crosses by genotyping PCR reactions specific to each allele (see section 2.2.2 and Appendix 2), and pure-breeding mutant lines established from these plants were subjected to phenotypic characterisation. Both possible triple loss-of-function mutants were created using these alleles, but detailed analysis of single and double combinatorial mutant phenotypes was restricted to *ga20ox3-1*.

3.2.2 Loss of *AtGA20ox1*, *-2* and *-3* Causes a Failure of Germination and Severe Vegetative Dwarfism

Both *ga20ox1 ga20ox2 ga20ox3* triple mutant combinations were first identified from segregating populations through a non-germinating seed phenotype. Embryos from non-germinating seeds were manually dissected out and subsequently developed into dwarf plants, their identity as triple mutants confirmed by genotyping. This non-germinating phenotype was subsequently confirmed by germination assay, using after-ripened homozygous seed stocks produced by chemical GA_4 treatment of the parent plants to ensure the set of viable seed. Rescue by GA_4 was used to reduce the risk of contamination from one generation to the next, as GA_4 is inactivated by native *Arabidopsis* GA 2-oxidases (see section 1.2.1). The requirement of bioactive GA for successful germination is well established, with GA-deficient mutants such as *ga1-3* unable to germinate without exogenous GA treatment (Koornneef & Van der Veen, 1980). In the absence of chemical GA treatment all single and double mutant genotypes showed close to 100% germination, similar to wild type, whilst *ga20ox1 ga20ox2 ga20ox3-1* and *ga1-3* seed failed to germinate (Table 3.1a). Germination was entirely rescued by imbibitions of the seed with bioactive GA, indicating that the failure of *ga20ox1 ga20ox2 ga20ox3-1* to germinate is due to GA-deficiency and that *AtGA20ox1*, *-2* and *-3* act

redundantly to promote germination. These results are consistent with the findings of previous expression analyses (Ogawa et al., 2003; Rieu et al., 2008), which independently identified these three paralogues as being highly expressed during germination. They also support the *in vitro* evidence that the *ga20ox3-1* and *ga20ox3-3* mutant alleles each represent a complete loss of function of AtGA20ox3 *in planta*.

Once the block in germination is overcome, both *ga20ox1 ga20ox2 ga20ox3* mutant combinations exhibit severely-dwarfed vegetative phenotypes (Figure 3.3a). This suggests that *AtGA20ox1*, *-2* and *-3* are the dominant paralogues promoting vegetative growth in *Arabidopsis*, and supports the hypothesis that the GA 20-oxidase enzymes are the primary route through which bioactive GA is synthesised *in planta*. No single or double mutant combination carrying *ga20ox3-1* displayed a similar degree of dwarfism (Figure 3.3b), indicating at least some functional redundancy between all three paralogues to promote vegetative growth. The close phenotypic similarity of *ga20ox1 ga20ox3-1* to *ga20ox1* and of *ga20ox2 ga20ox3-1* to *ga20ox2* suggest that *AtGA20ox3* does not possess specific functions of its own, acting instead in conjunction with either *AtGA20ox1* or *-2*. This was largely confirmed by quantitative phenotypic analysis of a range of vegetative characters from both seedlings (hypocotyl growth, n = 324; root growth, n = 288) and 49 day-old plants (by which time all genotypes except *ga20ox1 ga20ox2 ga20ox3-1* and *ga1-3* were senescent, n = 216; summarised in Table 3.1). A number of exceptions were identified, however, in which additional loss of *AtGA20ox3* in the absence of either *AtGA20ox1* or *-2* had a significant effect on phenotype. For example, in 7 day-old seedlings the mean root length of *ga20ox2 ga20ox3-1* is significantly different from *ga20ox2* ($p < 0.01$), the double mutant displaying reduced root growth, whilst mean hypocotyl length of *ga20ox1 ga20ox3-1* is significantly different from *ga20ox1* ($p < 0.01$), the additional loss of *AtGA20ox3* again causing reduced growth. These results very likely reflect more on the relative contribution of *AtGA20ox1* and -2 to the growth of these tissues than on the importance of *AtGA20ox3*- the only instance in which the *ga20ox3-1* single mutant is significantly different from wild type is in the elongation of particular vegetative internodes on the primary inflorescence (discussed below).

Figure 3.3: *AtGA20ox* mutant vegetative phenotypes.

(a) Comparison of mature ga20ox1 ga20ox2 ga20ox3-1 *and* ga20ox1 ga20ox2 ga20ox3-3 *triple mutant phenotypes against* ga1-3 *at 44 days old.*

(b) Comparison of mature phenotypes of all combinations of ga20ox1*,* ga20ox2 *and* ga20ox3-1 *mutant alleles against wild type and* ga1-3 *at 41 days old.*

In all vegetative phenotypes measured, the *ga20ox1 ga20ox2 ga20ox3-1* triple mutant is significantly different from that of *ga20ox1 ga20ox2* ($p < 0.01$), indicating that *AtGA20ox3* contributes to GA20ox activity across a broad range of tissues during plant development. In most vegetative characters measured, *ga20ox1 ga20ox2 ga20ox3-1* is not significantly different from *ga1-3*, which suggests that loss of these three paralogues is sufficient to account for all GA20ox activity in those tissues. Two exceptions were 7-day root length ($p < 0.01$), by which time the roots of the triple mutant were longer than *ga1-3*, and mature rosette diameter ($p < 0.01$), with again *ga20ox1 ga20ox2 ga20ox3-1* demonstrating enhanced growth compared to *ga1-3*. Seven day-old roots are also the tissue in which Rieu et al. (2008) found the highest expression of *AtGA20ox4* out of any tissue sampled (Figure3.1c). All vegetative phenotypes

(a)

Genotype	Germination Frequency (%)		7 Day Hypocotyl Length (mm)		7 Day Root Length (mm)	
	-GA	+GA	-GA	+GA	-GA	+GA
Wild type (Col-0)	98.88	100.00	1.14 [0.0530]	2.89* [0.4367]	37.86	44.83*
ga20ox1	98.17	99.14	1.04 [0.0115]	2.85* [0.4396]	35.82	36.44[d]
ga20ox2	99.47	99.46	0.89[a] [-0.0556]	2.30[d]* [0.3454]	33.78	42.91*
ga20ox3-1	99.44	98.91	1.04 [0.0037]	2.63* [0.3932]	35.98	41.67
ga20ox1 ga20ox2	98.65	97.89	0.85[a] [-0.0768]	2.25[d]* [0.3422]	35.05	41.33*
ga20ox1 ga20ox3-1	99.45	99.74	0.91[a] [-0.0471]	2.36* [0.3621]	32.60	42.05*
ga20ox2 ga20ox3-1	99.21	99.19	0.80[a] [-0.1048]	2.08[d]* [0.2982]	28.29[a]	43.29*
ga20ox1 ga20ox2 ga20ox3-1	0.00	98.33	0.67[b] [-0.1816]	2.21[d]* [0.3224]	20.08[b]	38.10[d]*
***ga1-3* (Col-0)**	0.00	98.89	0.63[b] [-0.2044]	3.68[e]* [0.5646]	11.14[c]	33.19[d]*
1% LSD	-		***[0.08374]*** *([0.08497])*		***5.445*** *(6.056)*	

(b)

Genotype	Rosette Diameter (mm)		Primary Inflorescence Height (mm)		Number of Vegetative Internodes (V.I.)	
	-GA	+GA	-GA	+GA	-GA	+GA
Wild type (Col-0)	120.80 [10.968]	141.40* [11.884]	548.30 [23.363]	657.30* [25.624]	2.917	4.500*
ga20ox1	126.10 [11.223]	134.10 [11.595]	246.60[a] [15.581]	575.30[d]* [24.025]	2.962	4.713*
ga20ox2	134.70 [11.574]	134.20 [11.525]	555.40 [23.486]	643.9* [25.352]	1.476[a]	4.417*
ga20ox3-1	132.60 [11.468]	144.50 [11.975]	527.50 [23.036]	613.20* [24.676]	2.344	3.667*
ga20ox1 ga20ox2	135.50 [11.602]	146.50 [12.090]	135.60[b] [11.509]	615.50* [24.754]	0.918[a]	6.196[d]*
ga20ox1 ga20ox3-1	116.40 [10.854]	136.50* [11.681]	249.30[a] [15.834]	606.00* [24.614]	2.404	4.417*
ga20ox2 ga20ox3-1	132.80 [11.522]	132.80 [11.502]	511.70 [22.439]	638.80* [25.256]	1.307[a]	4.167*
ga20ox1 ga20ox2 ga20ox3-1	65.20[a] [8.070]	125.70[d]* [11.175]	13.80[c] [2.067]	591.90* [24.366]	0.167[b]	4.488*
***ga1-3* (Col-0)**	53.50[b] [7.197]	148.20* [12.079]	9.30[c] [1.873]	612.40* [24.723]	0.645[b]	5.393[d]*
1% LSD	***[0.6873]*** *([0.7644])*		***[1.3926]*** *([1.4304])*		***0.7069*** *(0.7014)*	

(c)

Genotype	Length V.I. 1 (mm)		Length V.I. 2 (mm)		Length V.I. 3 (mm)	
	-GA	+GA	-GA	+GA	-GA	+GA
Wild type (Col-0)	38.92 [6.190]	30.75 [5.381]	43.17 [6.545]	47.42 [6.823]	23.50 [4.438]	43.50* [6.566]
ga20ox1	9.00[a] [3.027]	24.73* [4.851]	13.40[a] [3.574]	40.00* [6.356]	6.90[a] [2.348]	44.64* [6.656]
ga20ox2	33.90 [5.784]	29.50 [5.360]	11.90[a] [2.399]	33.25[d]* [5.578]	0.00[b] [0.204]	44.33* [6.437]
ga20ox3-1	35.45 [5.831]	33.36 [5.787]	32.64 [5.548]	39.27 [6.200]	4.45[a] [1.442]	53.09* [7.260]
ga20ox1 ga20ox2	9.36[a] [2.590]	17.18* [4.076]	0.73[b] [0.573]	31.55* [5.379]	0.00[b] [0.306]	34.91* [5.818]
ga20ox1 ga20ox3-1	11.18[a] [3.290]	27.33* [5.184]	11.00[a] [3.250]	39.58* [6.283]	2.00[b] [1.027]	42.08* [6.464]
ga20ox2 ga20ox3-1	16.56[a] [3.583]	28.17* [5.265]	2.00[b] [0.699]	37.08* [5.974]	0.00[b] [0.290]	39.58* [6.170]
ga20ox1 ga20ox2 ga20ox3-1	0.33[b] [0.459]	23.00* [4.683]	0.42[b] [0.478]	31.70[d]* [5.527]	0.00[b] [0.316]	39.20* [6.110]
ga1-3 **(Col-0)**	0.08[b] [0.394]	19.67[d]* [4.220]	0.12[b] [0.372]	36.78* [6.033]	0.36[b] [0.462]	35.11* [5.800]
1% LSD	***[1.1519]****([1.1609])*		***[1.2153]****([1.2110])*		***[1.2166]****([1.2281])*	

Table 3.1: Phenotypic analysis of *ga20ox* mutant vegetative characters.

Values given are means of 18 (hypocotyl), 16 (root) and 12 independent measurements (all other characters), respectively. Measurements of elongated vegetative internodes (V.I) were taken from the primary inflorescence. Where statistical analysis was performed on a transformed scale to meet the assumptions of the statistical model (hypocotyl, log; all others, √(x + 1), transformed values are supplied (denoted by square brackets). Pairwise comparisons were made within each character using Least Significant Differences (LSDs) with a significance threshold of 1%. LSDs for comparing between genotypes within a GA treatment are in bold type, those for comparing between GA treatments within a genotype are in rounded brackets. Superscript letters denote significant difference of a genotype from wild type ($p < 0.01$) within that GA treatment. Different letters indicate genotypes significantly different from one another. Asterisks denote a significant difference between GA treatments within the same genotype. Comparisons were not made between genotypes in different GA treatments. Germination frequency was not subject to statistical analysis.

were rescued to wild-type growth or greater by chemical GA treatment (Table 3.1).

In their analysis of the functions of *AtGA20ox1* and *-2*, Rieu et al. (2008) identified partially separable roles between these two paralogues in determining the architecture of the primary inflorescence, which comprises both elongated vegetative internodes (separating cauline leaves and/or secondary inflorescences), established prior to the floral transition, and inflorescence internodes (separating developing flowers/siliques), established afterwards. They found that *AtGA20ox1* primarily promotes internode elongation whilst *AtGA20ox2* regulates the number of vegetative internodes that elongate, and the analysis performed as part of this project identified the same relationship (Table 3.1b and c). In an extension to this analysis, the lengths of three vegetative internodes were compared between genotypes (defined by their position relative to the point of floral transition, with the uppermost vegetative internode labelled 'V.I. 1', the next down 'V.I. 2' etc.). At all three V.I. positions the lengths of *ga20ox1* internodes differed significantly from wild type ($p < 0.01$), being shorter at all three positions. V.I. length was only significantly different between *ga20ox2* and wild type for V.I. 2 and 3 ($p < 0.01$), although this can be explained by the *ga20ox2* primary inflorescence elongating fewer vegetative internodes (1.476 compared to 2.917). Similarly, the length of V.I. 1 is not significantly different between *ga20ox1 ga20ox2* and *ga20ox1*. However, loss of both *AtGA20ox2* and *-3* reduces the length of V.I. 1, causing it to become significantly different from wild type ($p < 0.01$) and similar to *ga20ox1* ($p > 0.01$). This indicates that *AtGA20ox3* has a partially-redundant function in internode elongation, which correlates with the finding of Rieu et al. (2008) that *AtGA20ox3* is the second-most highly expressed *AtGA20ox* in stem tissue (Figure 3.1c). Analysis of the length of V.I. 3 shows a significant difference between *ga20ox3-1* and wild type ($p < 0.01$), both of which elongate a similar number of vegetative internodes, indicating both that *AtGA20ox3* has a direct (if minor) role in promoting internode elongation and that its relative importance varies depending on the internode position being examined.

The clear conclusions from phenotypic analysis of these mutants is that *AtGA20ox1*, *-2* and *-3* are the dominant contributors to GA20ox activity in most *Arabidopsis* vegetative tissues,

promoting both germination and vegetative growth. However, the evidence presented here regarding seedling root growth and rosette diameter indicates that there is still potentially room for minor contributions by the two remaining *AtGA20ox* paralogues, *AtGA20ox4* and *-5*, during plant development. Unlike *AtGA20ox1* and *-2*, *AtGA20ox3* does not appear to possess functional specificity/dominance over particular aspects of vegetative growth because loss of this gene whilst *AtGA20ox1* or *-2* remains functional does not generally result in additional phenotypes. Instead, *AtGA20ox3* apparently acts to support the function of one or both of the two more dominant paralogues. Future expression analyses of individual vegetative tissues may identify more subtle and complex relationships between these three paralogues.

3.2.3 *AtGA20ox3* Acts Redundantly with *AtGA20ox1* and *-2 to* Promote Flowering and Both Male and Female Fertility

As discussed in section 1.5.1, GA promotes the transition of *Arabidopsis* from vegetative growth to the reproductive phase of development under both long day (LD) and short day (SD) conditions. Loss of *AtGA20ox1* and *-2* significantly delays the transition to flowering under permissive long day conditions (Rieu et al., 2008), but as with other aspects of development the delay is not as severe as that exhibited by *ga1-3*. In order to establish whether AtGA20ox3 activity is sufficient to explain the difference between these two phenotypes, the point of floral transition (as marked by the appearance of visible flower buds) under LD was scored for each combination of mutants carrying *ga20ox1*, *ga20ox2* and *ga20ox3-1* ($n = 216$) using both a chronological measure (days from sowing) and a developmental measure (total number of leaves at the time of flowering).

The Col-0 wild type displayed a mean flowering time of 17.83 days and 13.42 leaves, neither of which was affected by GA treatment (Figure 3.4). As observed by Rieu et al. (2008), flowering of *ga20ox1 ga20ox2* is delayed ($p < 0.01$, 22.50 days and 18.83 leaves), whilst flowering of *ga20ox1 ga20ox2 ga20ox3-1* differs significantly from *ga20ox1 ga20ox2* on both measures ($p < 0.01$), displaying a further delay in flowering (31.16 days and 21.21 leaves).

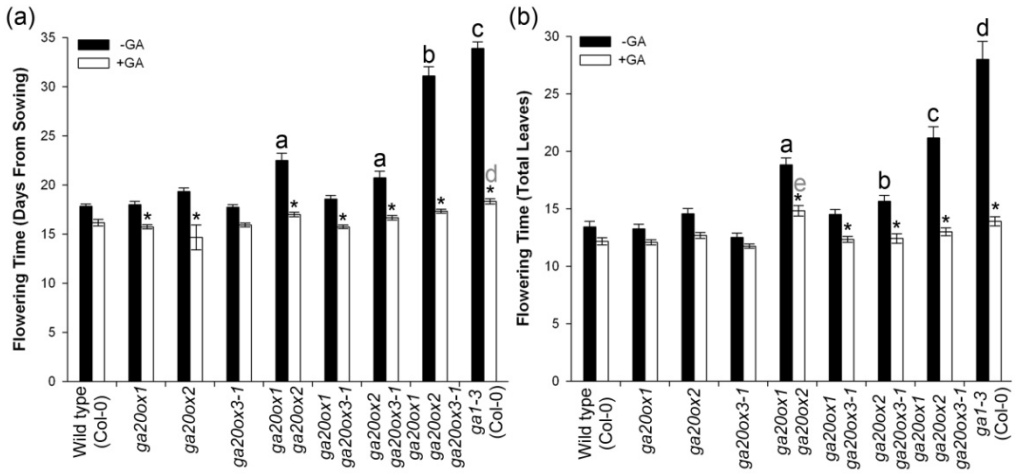

Figure 3.4: Effect of the loss of *AtGA20ox3* on floral transition under long days (LD). *Graphs show mean time to flowering as measured by chronological time from sowing (a) and total number of leaves at flowering (b). Values are means of 12 independent measurements. Error bars represent one S.E. Pairwise comparisons were made using 1% LSDs between genotypes within the same GA treatment (Days = 1.818; Leaves = 1.987) and between GA treatments within the same genotype (Days = 1.860; Leaves = 2.003). Letters denote a significant difference from -GA wild type (black) or +GA wild type (grey), respectively. Genotypes marked with different letters are significantly different from one another. Asterisks denote a significant difference between GA treatments within the same genotype. Comparisons were not made between genotypes in different GA treatments.*

However, flowering time of *ga20ox1 ga20ox2 ga20ox3-1* is also significantly different from *ga1-3* on both measures ($p < 0.01$; 33.87 days and 27.93 leaves for *ga1-3*). These results imply that, whilst *AtGA20ox3* contributes significantly to the promotion of flowering time under long days, the loss of these three paralogues is not sufficient to explain the delay observed in the GA-deficient control. The flowering times of all single mutants and *ga20ox1 ga20ox3-1* are not significantly different from wild type on either scale, but *ga20ox2 ga20ox3-1* is ($p < 0.01$). This indicates that, whilst *AtGA20ox3* once again acts redundantly with *AtGA20ox1* and *-2*, *AtGA20ox1* alone cannot compensate for the absence of *AtGA20ox2* and *-3*, whilst *AtGA20ox2* alone compensate for the loss of *AtGA20ox1* and *-3*. This might be due to homeostatic up-regulation (as with stem elongation, see section 3.1), or could reflect

differential tissue expression patterns of the three paralogues, as the GA signal associated with floral transition is perceived at the SAM (see section 1.5.1).

Flowering of *ga20ox2 ga20ox3-1* is not significantly different from *ga20ox1 ga20ox2* when measured chronologically ($p > 0.01$) but, interestingly, they are significantly different when measured by leaf number ($p < 0.01$). Similarly, the gap between *ga20ox1 ga20ox2 ga20ox3-1* and *ga1-3* is far greater in developmental time than chronological time. One possible explanation is that the rate of organogenesis is altered by GA-deficiency in some mutants, compatible with the role of GA at the SAM (see section 1.5.1). Chemical GA treatment rescued flowering time in all mutants to that of wild type, with the exception of *ga1-3* (measured chronologically) and *ga20ox1 ga20ox2* (measured developmentally), flowering of which are both accelerated under GA treatment but remain significantly different from the GA-treated wild type.

The concentration of bioactive GA_4 across whole plants was quantified in these genotypes (data courtesy of Peter Hedden, Terezie Linhartova and Yuji Kamiya), using the floral transition as a marker to synchronise plant development. All mutant genotypes contained significantly different concentrations of GA_4 from wild type at flowering ($p < 0.05$, Table 3.2). All mutants showed reduced GA_4 concentrations, suggesting that loss of any of these genes is sufficient to impair GA biosynthesis. The concentration of GA_4 in each *ga20ox* single mutant is significantly different from the other two ($p < 0.05$), with *ga20ox1* showing the greatest reduction in comparison to wild type, then *ga20ox2* and least of all *ga20ox3-1*, consistent with their respective phenotypes. The concentration of GA_4 was not significantly different between *ga20ox1 ga20ox2 ga20ox3-1* and *ga1-3* ($p > 0.05$), supporting the hypothesis that *AtGA20ox1*, *-2* and *-3* perform the vast majority of GA biosynthesis during vegetative growth. However, this contrasts with the results of the analysis of flowering time (see above), where *ga20ox1 ga20ox2 ga20ox3-1* and *ga1-3* are significantly different. The GA measurements presented in this study are taken from whole plants, so tissue-specific variations cannot be accounted for, and it may well be that localised GA biosynthesis catalysed by *AtGA20ox4* or *-5* is masked by the inclusion of other, GA-deficient tissues. Even

Genotype	GA_4 Concentration (ng/g dry weight)				
	Mean	**Rep. 1**	**Rep. 2**	**Rep. 3**	**Rep. 4**
Wild type (Col-0)	**2.210**	2.346	2.222	2.063	-
ga20ox1	**1.080**[a]	1.320	1.014	0.991	0.993
ga20ox2	**1.360**[b]	1.375	1.408	1.290	1.369
ga20ox3-1	**1.969**[c]	2.036	1.988	2.151	1.702
ga20ox1 ga20ox2	**0.628**[d]	0.647	0.767	0.613	0.484
ga20ox1 ga20ox3-1	**0.553**[d]	0.483	0.622	-	-
ga20ox2 ga20ox3-1	**1.378**[b]	1.337	1.492	1.297	1.385
ga20ox1 ga20ox2 ga20ox3-1	**0.154**[e]	0.188	0.133	0.133	0.161
***ga1-3* (Col-0)**	**0.244**[e]	0.202	0.306	0.225	-
5% LSD	***0.0171***	**-**	**-**	**-**	**-**

Table 3.2: Concentrations of bioactive GA_4 in *ga20ox* mutants at flowering.
GA_4 concentrations were obtained from two to four replicates per genotype (as shown), each replicate pooling tissue from approximately 24 individual plants. Pairwise comparisons were made between genotypes using 5% LSD, as shown. Superscript letters denote values significantly different from wild type ($p < 0.05$). Different letters denote values that are significantly different from one another.

a very low level of GA biosynthesis at the SAM might be sufficient to accelerate flowering in *ga20ox1 ga20ox2 ga20ox3-1*.

All double mutants are significantly different from *ga20ox1 ga20ox2 ga20ox3-1* and *ga1-3* ($p < 0.05$), the two most GA-deficient genotypes of those examined, supporting the hypothesis that each of these three *AtGA20ox* paralogues contributes to GA biosynthesis during vegetative development. GA_4 concentrations in *ga20ox2* and *ga20ox2 ga20ox3-1* tissues are not significantly different, suggesting that *AtGA20ox3* function is redundant with *AtGA20ox1*. Loss of *AtGA20ox3* on top of *AtGA20ox1* apparently causes a significant difference in GA_4 concentration ($p < 0.05$), reducing the concentration of GA_4 to that similar to *ga20ox1 ga20ox2*. These results supports the hypothesis that *AtGA20ox1* and *-3* have redundant functions in vegetative tissues, and highlights the surprisingly mild vegetative phenotype observed in *ga20ox1 ga20ox3-1* (see section 3.2.2), which again may emphasise the

importance of localised GA20ox activity in plant tissues. However, it must be borne in mind that this result is a mean of only two replicates, and so should be treated with some caution.

Beyond the floral transition, flowers develop and open sequentially on the primary inflorescence in place of leaves, resulting in multiple siliques being set by the end of flowering. During the characterisation experiment described above (49 days in length), *ga20ox1 ga20ox2 ga20ox3-1* and *ga1-3* did not set seed, although a small number of infertile flowers were produced by each genotype (Figure 3.5a). The number of siliques produced by single and double mutant combinations carrying *ga20ox1* was significantly different from wild type in all cases ($p < 0.01$, setting fewer siliques before flowering terminated) but not significantly different from one another. Loss of *AtGA20ox2* or *-3* individually did not affect the number of siliques produced, but loss of both paralogues produced a phenotype similar to the absence of *AtGA20ox1*. These results indicate that, whilst *AtGA20ox1* is more important to promoting flower number, *AtGA20ox2* and *-3* also function in this process.

As observed by Rieu et al., 2008, early flowers of *ga20ox1 ga20ox2* did not set seed (see further discussion in section 3.2.5), but after approximately the 10th inflorescence position all genotypes except *ga20ox1 ga20ox2 ga20ox3-1* and *ga1-3* reliably set siliques. The silique phenotypes of the different *ga20ox* mutants were analysed as a measure of fertility, taking siliques beyond the early phase to separate out the two effects. Three mature siliques were examined from each plant ($n = 216$), taken from between inflorescence positions 20-30, approximately the mid-point of flowering, scoring infertile *ga20ox1 ga20ox2 ga20ox3-1* and *ga1-3* flowers as zero values. The mean lengths of mature siliques from all single and double mutant combinations carrying *ga20ox2* were significantly different from wild type ($p < 0.01$, Figure 3.5b), displaying reduced growth. Loss of both *AtGA20ox1* and *-2* exacerbated this effect compared to loss of *AtGA20ox2* alone, but loss of both *AtGA20ox2* and *-3* did not have additional effects on silique length. These results concur with the findings of Rieu et al. (2008) that *AtGA20ox2* promotes silique outgrowth, with *AtGA20ox1* being partially redundant with *AtGA20ox2*. Loss of *AtGA20ox3* has no effect on silique outgrowth in the presence of either *AtGA20ox1* or *-2*. In contrast to these results, loss of individual *AtGA20ox*

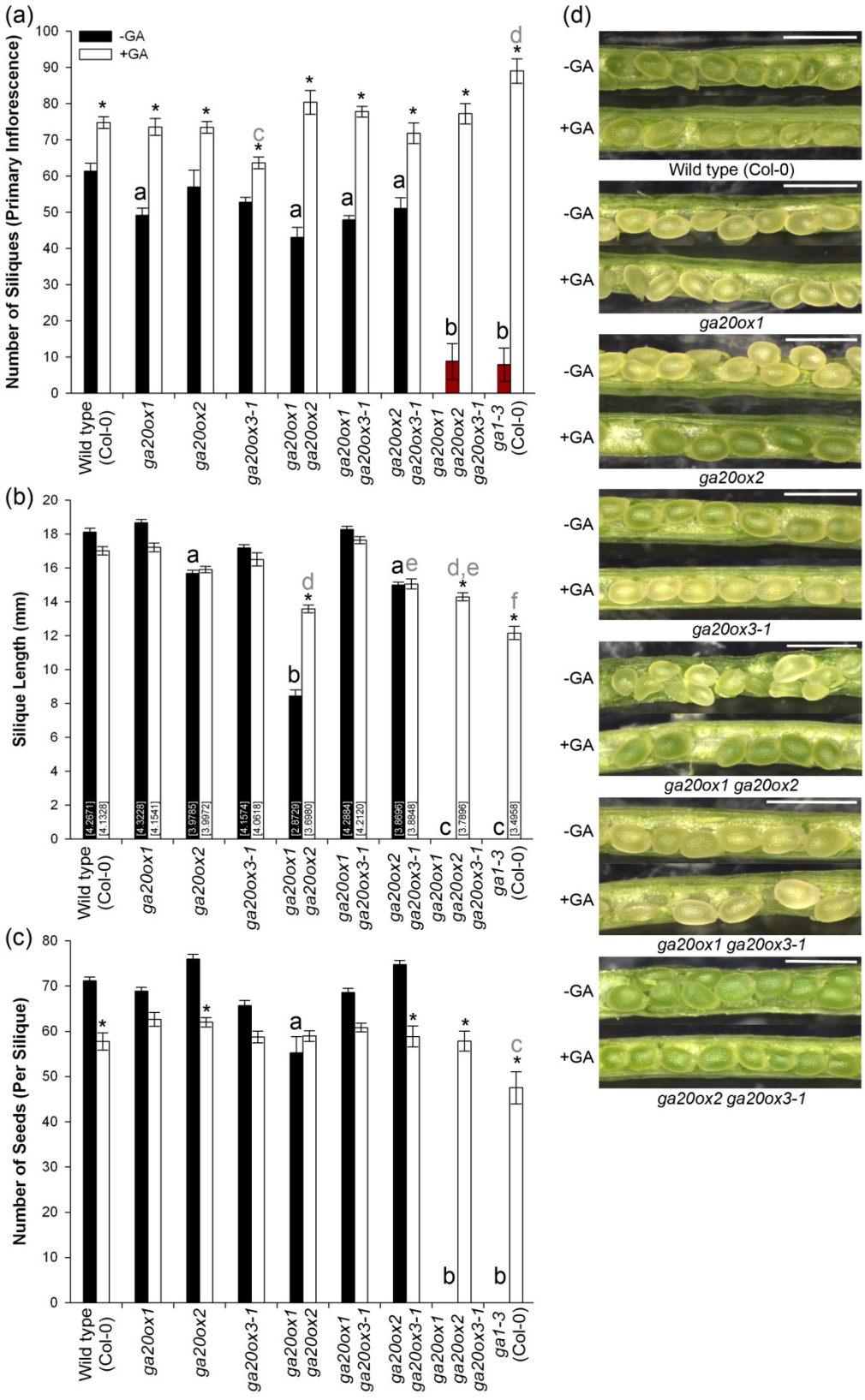

Figure 3.5: Effect of the loss of *AtGA20ox3* function on silique development.

(a) Mean number of siliques set on the primary inflorescence during flowering. ga20ox1 ga20ox2 ga20ox3-1 *and* ga1-3 *only produced infertile flowers which did not set seed (highlighted in red).*

(b) Mean silique length at maturity. Siliques taken from the mid-point of flowering. Pairwise comparisons calculated on a transformed scale. Transformed mean values marked on the appropriate bar.

(c) Mean number of seeds per silique, measured from the siliques in (b).

(d) Photographs of developing seeds within siliques, demonstrating altered seed packing in ga20ox2*,* ga20ox1 ga20ox2 *and* ga20ox2 ga20ox3-1 *mutants in the absence of chemical GA treatment.*

Each bar represents the mean of 12 (silique number) and 36 measurements (silique length and seed number) respectively: three siliques per plant were measured. Error bars represent one S.E. Pairwise comparisons were made using a 1% LSD between genotypes within the same GA treatment ((a) 9.832; (b) 0.16952; (c) 9.138) and between GA treatments within the same genotype ((a) 9.877; (b) 0.17387; (c) 9.117). Letters denote a significant difference from -GA wild type (black) or +GA wild type (grey), respectively. Genotypes marked with different letters are significantly different from one another. Asterisks denote a significant difference between GA treatments within the same genotype. Comparisons were not made between genotypes in different GA treatments.

paralogues had far less impact on the number of seeds within these siliques, with only *ga20ox1 ga20ox2* being significantly different from wild type ($p < 0.01$, Figure 3.5c). This differential result between silique length and seed number manifests as an altered seed packing phenotype (Figure 3.5d), in which siliques from genotypes lacking *AtGA20ox2* present a double row of seeds in each valve rather than the single row observed in wild type. This can be explained through reduced elongation of silique tissues during silique development. The high expression of *AtGA20ox3* found by Rieu et al. (2008) in developing wild-type siliques (see Figure 3.1c) strongly suggests that this paralogue contributes to silique growth and development, but the infertility of *ga20ox1 ga20ox2 ga20ox3-1* and *ga1-3* precludes further interpretation of *AtGA20ox3* function from this dataset.

Chemical GA treatment restores seed set in both *ga20ox1 ga20ox2 ga20ox3-1* and *ga1-3* (Figure 3.5c). Interestingly, whilst GA treatment increases silique growth in more severely GA-deficient mutants (Figure 3.5b), it also significantly affects the number of seeds per silique in a number of otherwise fully-fertile genotypes ($p < 0.01$, Figure 3.5c), reducing seed numbers to values similar to that of untreated *ga20ox1*. As such, chemical GA treatment has a significant negative impact on seed set, a conclusion also reached by previous studies (Jacobsen & Olszewski, 1993; Rieu et al., 2008). It has been shown that *in vitro* pollen tube growth is reduced in the presence of high concentrations of GA (Singh et al., 2002), which could plausibly explain this phenomenon. Another possibility is that chemical GA treatment alters the relative growth of male and female reproductive organs, resulting in a mechanical barrier that reduces pollen transfer to the stigma.

The relatively minor effect of loss of *AtGA20ox1* and *-2* on seed number (a conclusion supported by Rieu et al., 2008) suggests that *AtGA20ox1*, *-2* and *-3* could all act redundantly in promoting fertility, with no one paralogue demonstrating dominance over the others. Seed number is determined by two factors (discounting seed abortion, which was not observed during seed counting): the number of ovules developing within the carpel and the success of pollen in fertilising ovules during the time that they are receptive, a factor governed by pollen germination and pollen tube growth. To directly test these two effects *in planta*, reciprocal crosses were made between wild-type and *ga20ox* mutant flowers, subsequently counting the number of seeds set (Figure 3.6). Wild-type pistils manually pollinated with pollen from single or double *ga20ox* mutants all produced similar numbers of seeds, suggesting that loss of one or two *AtGA20ox* paralogues out of the three does not impair post-anthesis pollen development *in vivo*. Crosses using *ga20ox1 ga20ox2 ga20ox3-1* or *ga1-3* pollen set practically no seed. However, whilst is was possible to visually confirm transfer of large quantities of pollen in most of the crosses performed for this experiment, pollen proved very difficult to release from anthers of the latter two genotypes. The few seeds that were set may have been the result of contamination of the emasculated pistils by airborne pollen. *ga1-3* is published as a male-sterile mutant with a block in pollen development (Koornneef & Van der Veen, 1980; Cheng et al., 2004). Whilst this result cannot be used to directly infer the

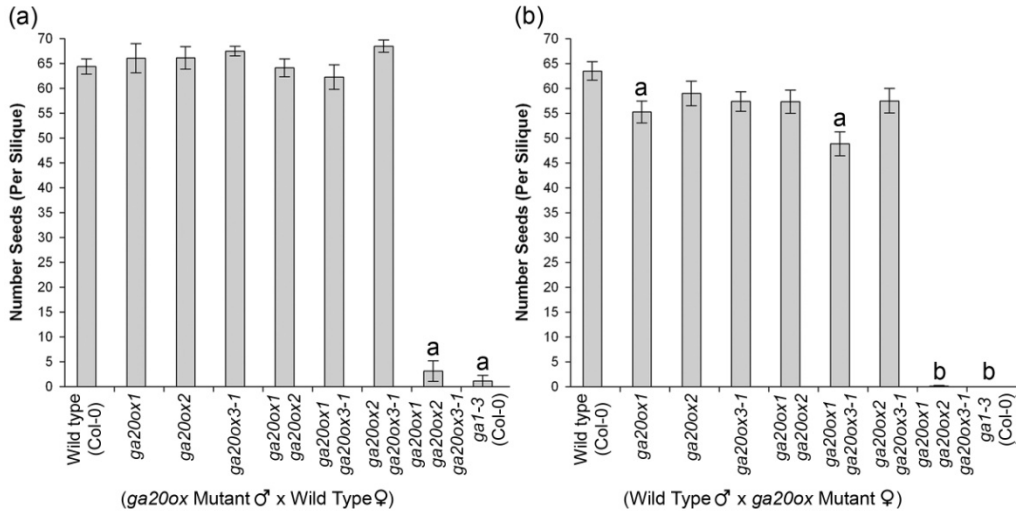

Figure 3.6: Effect of the loss of *AtGA20ox3* on male and female fertility.

Graphs show mean number of seeds developed in wild type pistils when pollinated with ga20ox mutant pollen (a) and in ga20ox mutant pistils when pollinated with wild-type pollen (b). Error bars represent one S.E. Pairwise comparisons were made between genotypes using a 5% LSD ((a) 6.286; (b) 6.448). Letters denote means that are significantly different from wild type, with different letters indicating means that are significantly different from each other.

performance of *ga20ox1 ga20ox2 ga20ox3-1* pollen, this genotype also appears to be functionally male-sterile.

In the reciprocal experiment, wild-type pollen was crossed to *ga20ox* mutant pistils (Figure 3.6b). *ga20ox1* and *ga20ox1 ga20ox3-1* mutant siliques contained a significantly different number of seed from wild type ($p < 0.05$), though only slightly fewer (means of 55.26 and 48.87, respectively, against 63.50 in wild type), suggesting that loss of *AtGA20ox1* may marginally reduce the number of ovules developing in the silique. The *ga20ox1* and *ga20ox1 ga20ox3-1* mutants do not differ significantly from each other. However, this result contrasts with that seen in natural self-pollination (Figure 3.5c), in which *ga20ox1* and *ga20ox1 ga20ox3-1* are not significantly different from wild type. Any effect on ovule number is therefore likely to be very slight. Also, the number of seeds produced when a *ga20ox1 ga20ox2* pistil is pollinated with wild-type pollen is not significantly different from the wild-

type control, contrasting both with the results of *ga20ox1* and *ga20ox1 ga20ox3-1* in this experiment and the situation seen in self-pollination of *ga20ox1 ga20ox2* (Figure 3.5c). This result suggests that *ga20ox1 ga20ox2* pistils carry a similar number of ovules as wild type. The reduction in seed-set during *ga20ox1 ga20ox2* self-pollination may be due either to impaired *ga20ox1 ga20ox2* pollen development *per se*, or to other factors such as floral organ growth restricting access of pollen to the stigma (see section 3.2.5). *ga20ox1 ga20ox2 ga20ox3-1* and *ga1-3* pistils pollinated with wild-type pollen did not set seed, indicating that loss of *AtGA20ox1*, *-2* and *-3* causes female sterility.

The effects of *AtGA20ox1*, *-2* and *-3* on pollen performance post-anthesis were further tested via the segregation of the three mutant alleles in the progeny of a self-pollinating *GA20ox1*/*ga20ox1 GA20ox2*/*ga20ox2 GA20ox3*/*ga20ox3-1* plant (n = 368). This experimental approach has the additional advantage that the performance of *ga20ox1 ga20ox2 ga20ox3-1* pollen can also be assessed. Previous expression studies in rice indicate that GA biosynthesis in developing pollen grains begins after the separation of haploid microspores (Chhun et al., 2007), and as such pollen phenotypes should reflect the haploid genotype. A statistically significant deviation from the expected frequencies of offspring genotypes was observed ($p = 0.008$, Table 3.3a), indicating that loss of *AtGA20ox* paralogues has an impact on gametophyte fitness. Surprisingly, when the results are categorised by phenotype (grouping the population by homozygous mutant loci), the mutant genotype demonstrating the greatest fitness penalty is incurred by *ga20ox3-1* (67.63% of the expected frequency, Table 3.3b), whilst the *ga20ox1 ga20ox3-1* and *ga20ox2 ga20ox3-1* double mutants are less affected (98.55% and 86.96%, respectively). The mutant genotype demonstrating the next greatest fitness penalty is *ga20ox1 ga20ox2* (75.36% of the expected frequency), suggesting that loss of these two paralogues may reduce pollen growth post-anthesis and thus explain the reduced numbers of seed seen in *ga20ox1 ga20ox2* self-pollination. However, unexpectedly, the fitness penalty incurred by *ga20ox1 ga20ox2 ga20ox3-1* pollen was found to be less than that incurred by *ga20ox1 ga20ox2* (86.96% of the expected frequency), suggesting that the effect of the loss of *AtGA20ox1*, *-2* and *-3* on pollen performance is negligible.

(a)

Genotype	Expected Freq. (E)	Observed Freq. (O)	O-E	$(O-E)^2$	$(O-E)^2/E$
GA20ox1; GA20ox2; GA20ox3	5.75	12	6.25	39.06	6.793
GA20ox1/ga20ox1; GA20ox2; GA20ox3	11.5	16	4.50	20.25	1.761
ga20ox1; GA20ox2 ;GA20ox3	5.75	5	-0.75	0.56	0.098
GA20ox1; GA20ox2/ga20ox2; GA20ox3	11.5	13	1.50	2.25	0.196
GA20ox1; ga20ox2; GA20ox3	5.75	1	-4.75	22.56	3.924
GA20ox1; GA20ox2; GA20ox3/ga20ox3-1	11.5	17	5.50	30.25	2.630
GA20ox1; GA20ox2; ga20ox3-1	5.75	1	-4.75	22.56	3.924
GA20ox1/ga20ox1; GA20ox2/ga20ox2; GA20ox3	23	21	-2.00	4.00	0.174
GA20ox1/ga20ox1; ga20ox2; GA20ox3	11.5	14	2.50	6.25	0.543
GA20ox1/ga20ox1; GA20ox2; GA20ox3/ga20ox3-1	23	31	8.00	64.00	2.783
GA20ox1/ga20ox1; GA20ox2; ga20ox3-1	11.5	6	-5.50	30.25	2.630
ga20ox1; GA20ox2/ga20ox2; GA20ox3	11.5	17	5.50	30.25	2.630
ga20ox1; ga20ox2; GA20ox3	5.75	4	-1.75	3.06	0.533
ga20ox1; GA20ox2; GA20ox3/ga20ox3-1	11.5	8	-3.50	12.25	1.065
ga20ox1; GA20ox2; ga20ox3-1	5.75	7	1.25	1.56	0.272
GA20ox1; GA20ox2/ga20ox2; GA20ox3/ga20ox3-1	23	36	13.00	169.00	7.348
GA20ox1; GA20ox2/ga20ox2; ga20ox3-1	11.5	9	-2.50	6.25	0.543
GA20ox1; ga20ox2: GA20ox3/ga20ox3-1	11.5	16	4.50	20.25	1.761
GA20ox1; ga20ox2; ga20ox3-1	5.75	3	-2.75	7.56	1.315
GA20ox1/ga20ox1; GA20ox2/ga20ox2; GA20ox3/ga20ox3-1	46	43	-3.00	9.00	0.196
GA20ox1/ga20ox1; GA20ox2/ga20ox2; ga20ox3-1	23	19	-4.00	16.00	0.696
GA20ox1/ga20ox1; ga20ox2; GA20ox3/ga20ox3-1	23	16	-7.00	49.00	2.130
GA20ox1/ga20ox1; ga20ox2; ga20ox3-1	11.5	12	0.50	0.25	0.022
ga20ox1; GA20ox2/ga20ox2; GA20ox3/ga20ox3-1	23	17	-6.00	36.00	1.565
ga20ox1; GA20ox2/ga20ox2; ga20ox3-1	11.5	10	-1.50	2.25	0.196
ga20ox1; ga20ox2; GA20ox3/ga20ox3-1	11.5	9	-2.50	6.25	0.543
ga20ox1; ga20ox2; ga20ox3-1	5.75	5	-0.75	0.56	0.098
				X^2 = 46.370	
				(D.f. = 26)	
				p = 0.008	

(b)

Phenotype	Expected Freq.	Observed Freq.	Proportion of Expected (%)
Wild type (Col-0)	155.25	189.00	121.74
ga20ox1	51.75	47.00	90.82
ga20ox2	51.75	47.00	90.82
ga20ox3-1	51.75	35.00	67.63
ga20ox1 ga20ox2	17.25	13.00	75.36
ga20ox1 ga20ox3-1	17.25	17.00	98.55
ga20ox2 ga20ox3-1	17.25	15.00	86.96
ga20ox1 ga20ox2 ga20ox3-1	5.75	5.00	86.96

Table 3.3: Segregation distortion analysis of *ga20ox* loss-of-function alleles.

(a) Chi-squared statistical analysis of the segregation of progeny of a single GA20ox1/ga20ox1 GA20ox2/ga20ox2 GA20ox3/ga20ox3-1 *parent, against the null hypothesis of no fitness penalty (1:2:1 segregation) for each allele. Experimental population size = 368.*

(b) Summary of population structure, according to the presence of homozygous mutant loci. Genotypes that are wild type or heterozygous at the remaining loci are included in each category.

There are a number of limitations to this experimental technique. Firstly, the distortion in segregation cannot be directly linked to either male or female-dependent inheritance: ascribing fitness penalties to male function in this instance is based on the absence of any observed seed abortion in self-fertilised mutant siliques during phenotyping (see above), and the similarity in ovule numbers between wild type and *ga20ox* single and double mutants (based on seed counts, Figure 3.6b). Secondly, developing pollen is in contact with parental (diploid) stylar tissue within the pistil, which carries functional copies of all *AtGA20ox* paralogues. It has been demonstrated in rice that pollen requires bioactive GA for germination and subsequent pollen tube elongation (Chhun et al., 2007), and GA-deficiency in *Arabidopsis* similarly reduces pollen tube elongation (Singh et al., 2002). However, in this instance the presence of bioactive GA in the wild-type female tissues may mask genotype-specific defects in pollen tube growth, and as such important functions for *AtGA20ox1*, *-2* or *-3* in post-anthesis pollen development cannot be ruled out on the basis of these results.

From these experiments the conclusion can be drawn that *AtGA20ox1*, *-2* and *-3* all promote both male and female fertility in *Arabidopsis*. The infertility of the *ga20ox1 ga20ox2 ga20ox3-1* mutant further suggests that these are the dominant three *GA20ox* paralogues in these processes. Whilst *AtGA20ox2* demonstrates some functional specialisation in promoting silique growth, all three paralogues seem almost completely functionally redundant in promoting successful seed set. Reduced seed set in self-pollinated *ga20ox1 ga20ox2* siliques during the main phase of flowering may be due to reduced pollen tube growth. Whilst direct functions in pollen germination and pollen tube growth cannot be ascribed with certainty from the results presented here, the combined evidence from these experiments indicates that in the presence of functional copies of any of these three paralogues, loss of other *AtGA20ox* paralogues is liable to only have minor effects on fertility *in planta*.

3.2.4 Loss of *AtGA20ox1*, *-2* and *-3* Results in a Failure of Tapetal Programmed Cell Death (PCD)

Observations of the male sterile phenotype of *ga20ox1 ga20ox2 ga20ox3-1* during manual crossing (see section 3.2.3) suggest that this is not solely due to a mechanical block in pollination, as exhibited by early *ga20ox1 ga20ox2* flowers (Rieu et al., 2008). In order to better understand the effect of the loss of *AtGA20ox1*, *-2* and *-3* on male fertility, anther development in early flowers of the *ga20ox1 ga20ox2 ga20ox3-1* triple mutant was subjected to microscopic phenotypic analysis. A defect in anther development was observed in this mutant, with the tapetum cell layer (Figure 3.7, marked 'T') persisting in all developing buds examined. As discussed in section 1.5.3, during wild-type development the tapetum undergoes programmed cell death (PCD) during anther stages 10-11 (Sanders et al., 1999) as a necessary step in pollen development, and by the end of anther stage 11 it has completely degenerated. Successful tapetum PCD was observed in both wild-type (Figure 3.7, a-d) and *ga20ox1 ga20ox2* inflorescences (e-f) of a similar age to those of the triple mutant, both genotypes showing complete progression through to successful anther dehiscence (d and h). In contrast, whilst the tapetal cells in *ga20ox1 ga20ox2 ga20ox3-1* show morphological signs of entry into PCD (j and k), degeneration of this layer is not completed and a visible remnant

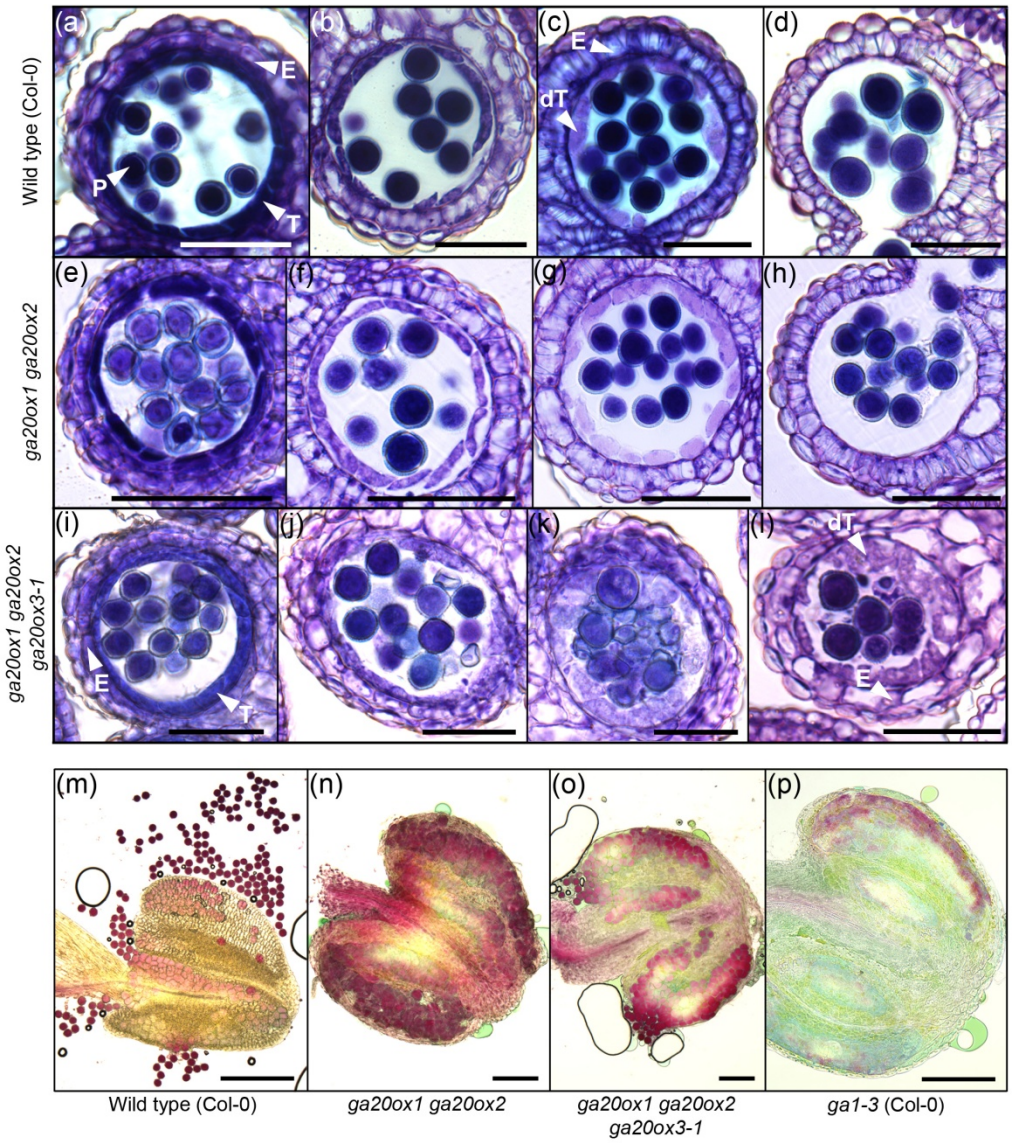

Figure 3.7: Effect of the loss of *AtGA20ox3* on anther and pollen development.

(a)-(d) Wild type (Col-0) anther development, anther stages 9-13.

(e)-(h) ga20ox1 ga20ox2 *anther development, anther stages 9-13*

(i)-(l) ga20ox1 ga20ox2 ga20ox3-1 *anther development, demonstrating developmental arrest. Wild type and ga20ox1 ga20ox2 inflorescence tissues were harvested for sectioning after the opening of the first flower, with the equivalent ga20ox1 ga20ox2 ga20ox3-1 stage also being taken. Scale bars = 50µm. T, tapetum; dT, degenerating tapetum; P, microspore/pollen; E, endothecium.*

(m)-(p) Comparative pollen viability staining of selected ga20ox *mutants. Dark red staining indicates viable pollen; pale green staining indicates pollen that does not contain cytoplasm. Scale bars = 100µm*

remains within the locule (l). *ga20ox1 ga20ox2 ga20ox3-1* locules contain free microspores (i-l), indicating that the tapetum may well function normally in this mutant up to the advent of PCD. During anther stage 11 another layer within the anther wall, the endothecium (Figure 3.7, marked 'E'), expands and undergoes secondary thickening, visible in cross-section as striations across the cell. This developmental change is observed in both wild-type and *ga20ox1ga20ox2* anthers (a-d; e-h) but is not apparent in *ga20ox1 ga20ox2 ga20ox3-1*, suggestive of a more comprehensive arrest in anther development around anther stage 10.

Recent experimental work in rice has demonstrated a direct link between GA signalling and tapetum function, including entry into PCD (Aya et al., 2009, see 1.5.3). Anthers of GA-deficient mutants in both rice (*oscps1-1*, Aya et al., 2009) and *Arabidopsis* (*ga1-1*, Goto & Pharis, 1999; *ga1-3*, Cheng et al., 2004) have been shown to exhibit developmental arrest once meiosis is completed. The tapetum has also been shown to behave abnormally in *ga1-3* (L*er* ecotype) and not undergo PCD (Cheng et al., 2004). The results presented here are entirely consistent with these previous findings, and indicate that *AtGA20ox1*, *-2* and *-3* are the dominant *GA20ox* paralogues in promoting anther development. The lack of a developmental block in any other *ga20ox* mutant studied in this project indicates that *AtGA20ox1*, *-2* and *-3* all act redundantly to promote anther development, though given the complex homeostatic relationships that exist between these paralogues it is not necessarily the case that all three are highly expressed in the wild-type background. Similarly, because GA20ox enzymes do not directly catalyse the production of bioactive GA, and because the GA biosynthesis pathway is known to be spatially distributed between tissues in other organs (see section 1.2), *AtGA20ox1*, *-2* and *-3* need not necessarily be expressed in the tapetum itself. *GA20ox* gene expression in the tapetum has been reported in both rice (Kaneko et al., 2003) and tobacco (Itoh et al., 1999), but the expression patterns of the *AtGA20ox* gene family have not yet been described in reproductive tissues.

Pollen development is dependent on the timely degeneration of the tapetum for release and deposition of key components of the pollen coat that are synthesised by tapetum cells (see section 1.5.3). Pollen development within *ga20ox1 ga20ox2 ga20ox3-1* anthers was assessed

using Alexander pollen viability discrimination staining (Alexander, 1969), a cytoplasmic stain that determines whether pollen has aborted. Wild-type and *ga20ox1 ga20ox2* pollen both stained as viable (dark red, Figure 3.7 m and n). *ga20ox1 ga20ox2 ga20ox3-1* pollen also stained as viable (o), whilst in contrast, the majority of pollen in *ga1-3* anthers stained as inviable (pale green, p). This might represent a difference in pollen development between *ga20ox1 ga20ox2 ga20ox3-1* and *ga1-3*, which could be explained by the additional function of either *AtGA20ox4* or *-5*.

3.2.5 Fertility Defects in the Early Phase of Flowering in *ga20ox* Mutants can be Attributed to Floral Organ Growth

In order to more closely characterise the infertility phenotypes previously described in early flowers of *ga20ox1* and *ga20ox1 ga20ox2* mutants (Rieu et al., 2008), silique-set was scored across the first 10 positions of the primary inflorescence for all mutant combinations of *ga20ox1*, *ga20ox2* and *ga20ox3-1*, under both control growth conditions and chemical GA treatment (n = 216). Silique-set was found to vary between inflorescence positions, with reversions to infertility frequently observed before stable silique-set was achieved (Figure 3.8). Interestingly, defects in inflorescence patterning were also observed both in some *ga20ox* mutants and under chemical GA treatment in all genotypes, with the normal alternating arrangement of siliques on either side of the primary inflorescence being disrupted (Figure 3.8). Although not investigated further as part of this project, this phenotype presumably relates to the function of GA in organogenesis, as previously noted in vegetative development at the SAM. Interestingly, Bartrina et al. (2011) also identified disrupted inflorescence phyllotaxy in mutants impaired in cytokinin degradation. As discussed in section 1.5.1, GA and CK have opposing functions in meristem maintenance/organogenesis during vegetative development, and these findings could indicate that the same regulatory mechanism exists in the inflorescence meristem.

Statistical analysis of this data identified significant interactions between genotype and GA treatment ($p < 0.001$) and also between inflorescence position and GA treatment ($p < 0.001$), but not between inflorescence position and genotype ($p = 0.222$). This indicates that the

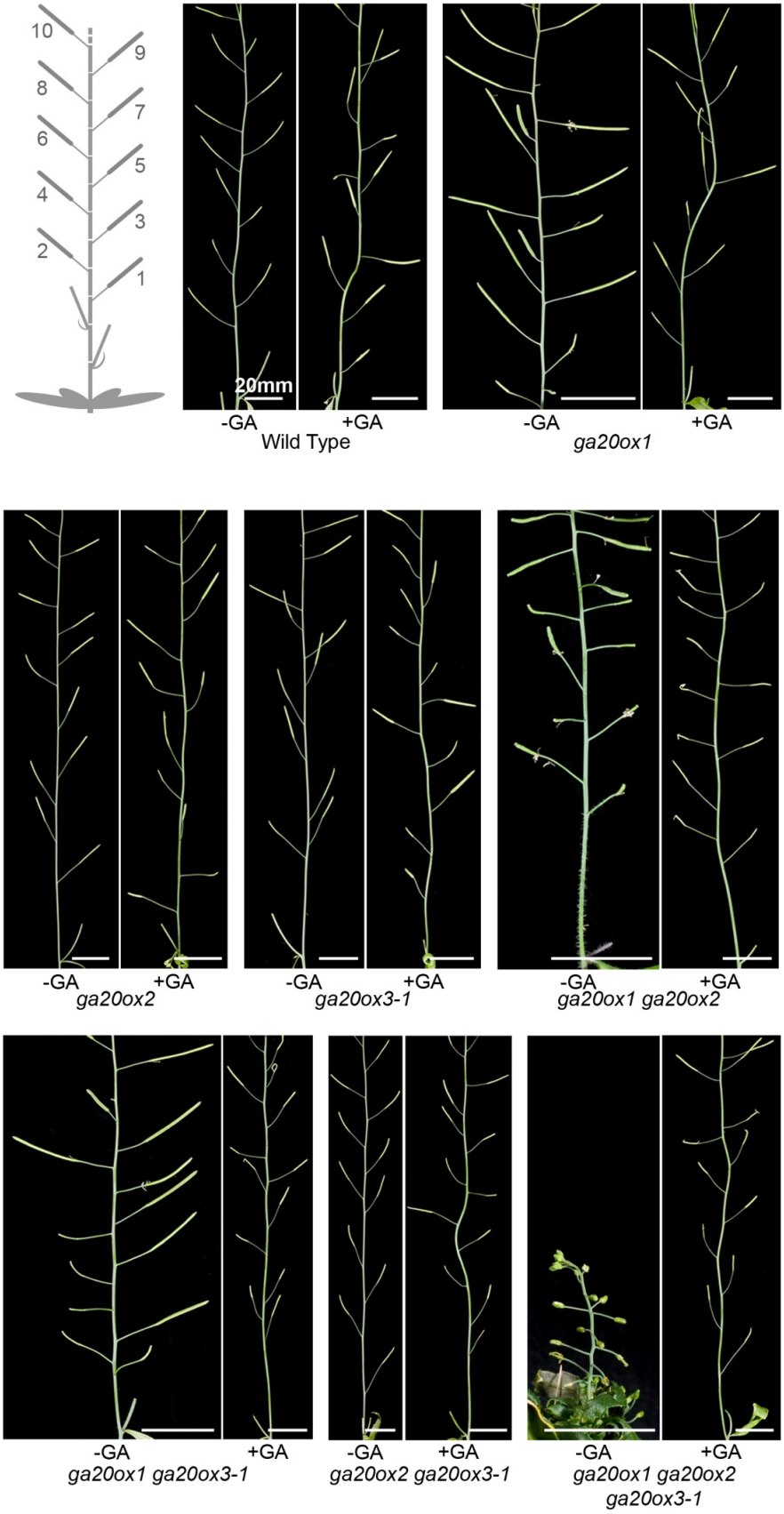

Figure 3.8: Early fertility phenotypes of *ga20ox* mutants (inflorescence positions 1-10).

Siliques in which seed set did not occur fail to elongate. All scale bars = 1mm.

relationship between silique-set and inflorescence position is the same across all genotypes within each GA treatment. The proportion of siliques successfully set in the first 10 inflorescence positions by the *ga20ox1* and *ga20ox1 ga20ox3-1* mutants is significantly different from wild type in the absence of GA treatment ($p < 0.01$, Figure 3.9a), falling to 0.5217 and 0.4710, respectively, compared to 0.9249. These two mutant genotypes are not significantly different from one another, whilst *ga20ox1 ga20ox2* is significantly different from these and wild type ($p < 0.01$), the loss of both *AtGA20ox1* and *-2* exacerbating the phenotype seen in *ga20ox1*. This agrees with the previous findings of Rieu et al. (2008) that *AtGA20ox1* and *-2* have overlapping functions in promoting successful seed set at early inflorescence positions, and that *AtGA20ox1* predominates. The severe infertility of *ga20ox1 ga20ox2 ga20ox3-1* observed here indicates that *AtGA20ox1, -2* and *-3* act together as the dominant *AtGA20ox* paralogues to promote successful early silique-set. The relationship between the double mutants described above demonstrates that *AtGA20ox3* function is again wholly redundant with *AtGA20ox1* and *-2*, and also that its contribution to silique-set is likely to be minor.

In an effect similar to that seen on seed number, chemical GA treatment significantly enhances early silique-set in more severely GA-deficient mutants (*ga20ox1 ga20ox2*, *ga20ox1 ga20ox2 ga20ox3-1* and *ga1-3*, $p < 0.01$) but also significantly affects silique-set in wild type and less-severe mutants ($p < 0.01$), causing a reduction in early fertility. Under GA-treated conditions all genotypes show a similar proportion of silique-set, with the exception of *ga1-3* which remains significantly different from the rest of the population ($p < 0.01$). When the relationship between GA treatment and inflorescence position is considered across all genotypes (Figure 3.9b) GA treatment is seen to have a uniformly repressive effect on silique-set across the first 10 inflorescence positions ($p < 0.01$), with the sole exception of inflorescence position 8. Importantly, a clear trend of increasing fertility with increasing inflorescence position also exists, irrespective of chemical GA treatment. This trend is statistically significant, with the proportion of siliques set at later inflorescence positions significantly different from that at earlier positions ($p < 0.01$, not shown). The appearance of this trend under both growth conditions suggests that this phenomenon is not GA-dependent.

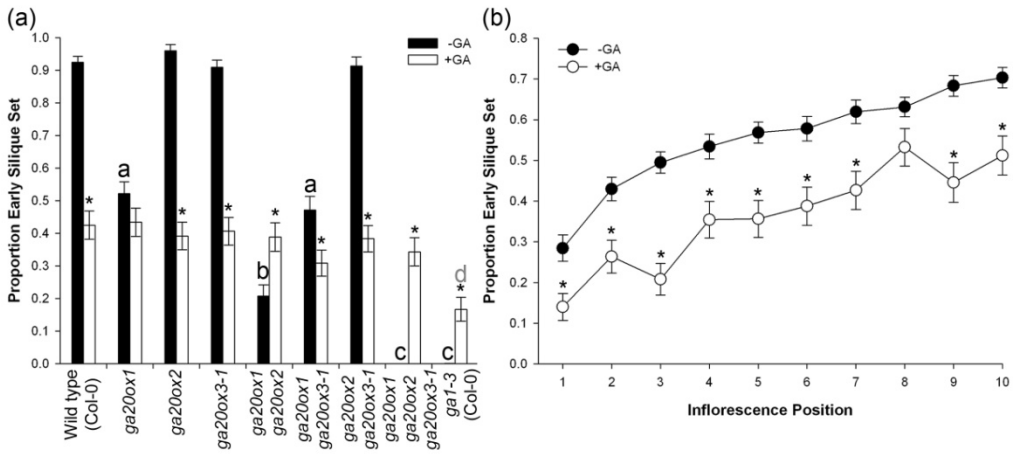

Figure 3.9: Early silique-set in *ga20ox* paralogues (primary inflorescence positions 1-10).

(a) Proportion of siliques set in the first 10 positions on the primary inflorescence. Each bar represents the mean of 12 measurements, error bars represent one S.E. Pairwise comparisons were made using a 1% LSD between genotypes within the same GA treatment (individual LSDs for each comparison, not shown) and between GA treatments within the same genotype (individual LSDs for each comparison, not shown). Letters denote a significant difference from -GA wild type (black) or +GA wild type (grey), respectively. Genotypes marked with different letters are significantly different from one another. Asterisks denote a significant difference between GA treatments within the same genotype. Comparisons were not made between genotypes in different GA treatments.

(b) Proportion of siliques set across all genotypes for each inflorescence position. Each point represents the mean of 108 measurements, error bars represent one S.E. Pairwise comparisons were made using a 1% LSD between -GA and +GA conditions within the same inflorescence position (individual LSD's for each comparison, not shown). Asterisks denote a significant difference between GA treatments within the same inflorescence position.

Past research has concluded that the reduced silique-set phenotype of the *ga20ox1 ga20ox2* double mutant is caused by reduced stamen length in relation to pistil length at flower opening (Rieu et al., 2008). Two conditions need to be fulfilled for successful silique-set: pollination whilst the stigma is still receptive (dependent on co-ordinated floral organ growth) and fertilisation of ovules within the pistil (dependent on successful pollen germination and pollen tube growth post-pollination). The results presented in section 3.2.4 support the conclusion of

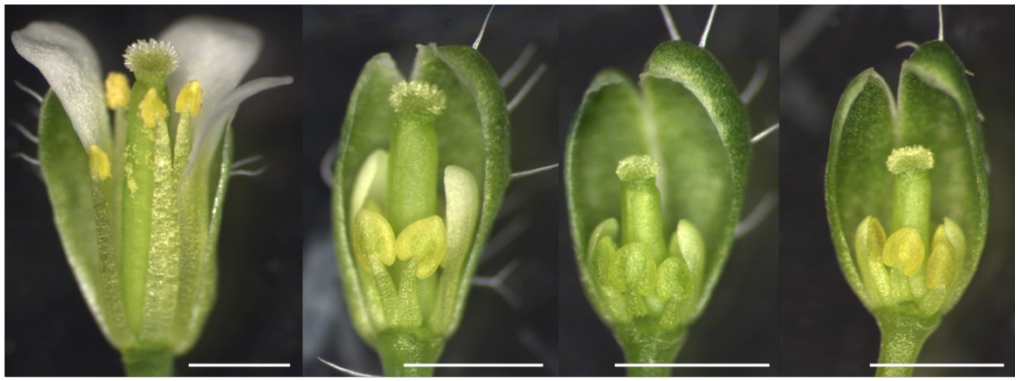

Figure 3.10: Effect of the loss of *AtGA20ox* expression on floral phenotype. *Photographs show the phenotype of the first flower to develop on the primary inflorescence of each respective genotype, as listed. All scale bars = 1mm.*

Rieu et al. (2008) that abnormal post-pollination pollen development is unlikely to account for the observed reduction in fertility during early flowering, unless dramatic differences in pollen performance occur between early and mid-range flowering. As previously found by Rieu et al. (2008), the phenotype of early *ga20ox1 ga20ox2* flowers (Figure 3.10) supports the hypothesis that the major cause of early infertility is retarded stamen growth. Concomitantly, the observed rescue in fertility is hypothesised as being due to increasing in stamen growth with increasing inflorescence position, as observed in the *ga3ox1 ga3ox3* mutant (Hu et al., 2008, see section 3.1). The first flowers to develop on *ga20ox1 ga20ox2 ga20ox3-1* show an even greater reduction in floral organ growth (Figure 3.10), and closely resemble those of *ga1-3*. This similarity strongly suggests that *AtGA20ox1*, *-2* and *-3* are the dominant *AtGA20ox* paralogues underpinning GA biosynthesis during floral development, and that the differences in floral phenotype between *ga20ox1 ga20ox2* and *ga1-3* are due to the activity of *AtGA20ox3*.

To more closely investigate the relationship between *AtGA20ox1*, *-2* and *-3*, floral organ growth and early fertility, the lengths of floral organs at flower opening were compared between genotypes across the early inflorescence (inflorescence positions 1-10, position 15 also included as representative of later flowering). Inflorescence positions were harvested independently, with only one flower taken per plant to avoid affecting subsequent flower

development (n = 704). Whilst the *ga20ox1 ga20ox2 ga20ox3-1* inflorescence elongates sufficiently during early flowering to allow accurate positioning of flowers on the inflorescence, it was not technically feasible to analyse *ga1-3* using this methodology. Early *ga20ox1 ga20ox2* and *ga20ox1 ga20ox2 ga20ox3-1* flowers do not open, and so maturity of unopened floral buds was determined by internode elongation against that seen in wild-type inflorescences. Pistil length was measured from its base to the underside of the stigma, (the organ to which pollen adheres and germinates), whilst stamen length (taking long stamens only, see section 1.5.2) was recorded from the base of the filament to the apical tip of the anther, so that a stamen length equal to or greater than 100% of its corresponding pistil permits pollen to be successfully delivered to the stigma upon anther dehiscence.

Stamen length of wild-type flowers was 100% of pistil length or greater at all inflorescence positions measured (Figure 3.11a). Significant differences were found between the relative lengths of stamens to pistils between a number of *ga20ox* mutants and wild type at some early inflorescence positions ($p < 0.05$, Figure 3.11a). Specifically, the *ga20ox1* and *ga20ox1 ga20ox2* mutants exhibit reduced stamen growth relative to the pistil compared to wild type at inflorescence positions 2, 4 and 10, and 1-5, respectively, both genotypes demonstrating stamen lengths of less than 100% of pistil length until inflorescence position 4-5. In contrast, *ga20ox2* and *ga20ox2 ga20ox3-1* both exhibit greater stamen growth relative to pistil length than observed in wild type at inflorescence positions 2, 3, 5 and 9, and 1, 2, 3 and 5, respectively. Interestingly, these results suggest that loss of *AtGA20ox2* whilst *AtGA20ox1* is still present enhances relative stamen growth, and that loss of *AtGA20ox1* function decreases relative stamen growth, a phenotype that is exacerbated at very early inflorescence positions by the loss of *AtGA20ox2*. These results correlate very well with those obtained regarding early fertility (see above), including parallels between an increased probability of silique-set with increasing inflorescence position and increasing relative stamen growth in flowers across the same range. *ga20ox1 ga20ox2 ga20ox3-1* stamen growth remains significantly different from wild type across all inflorescence positions recorded, exhibiting relative stamen lengths of between 50-60% of the corresponding pistil. Chemical GA treatment restores relative stamen growth in all genotypes to that seen in GA-treated wild type (Figure 3.11b), the only

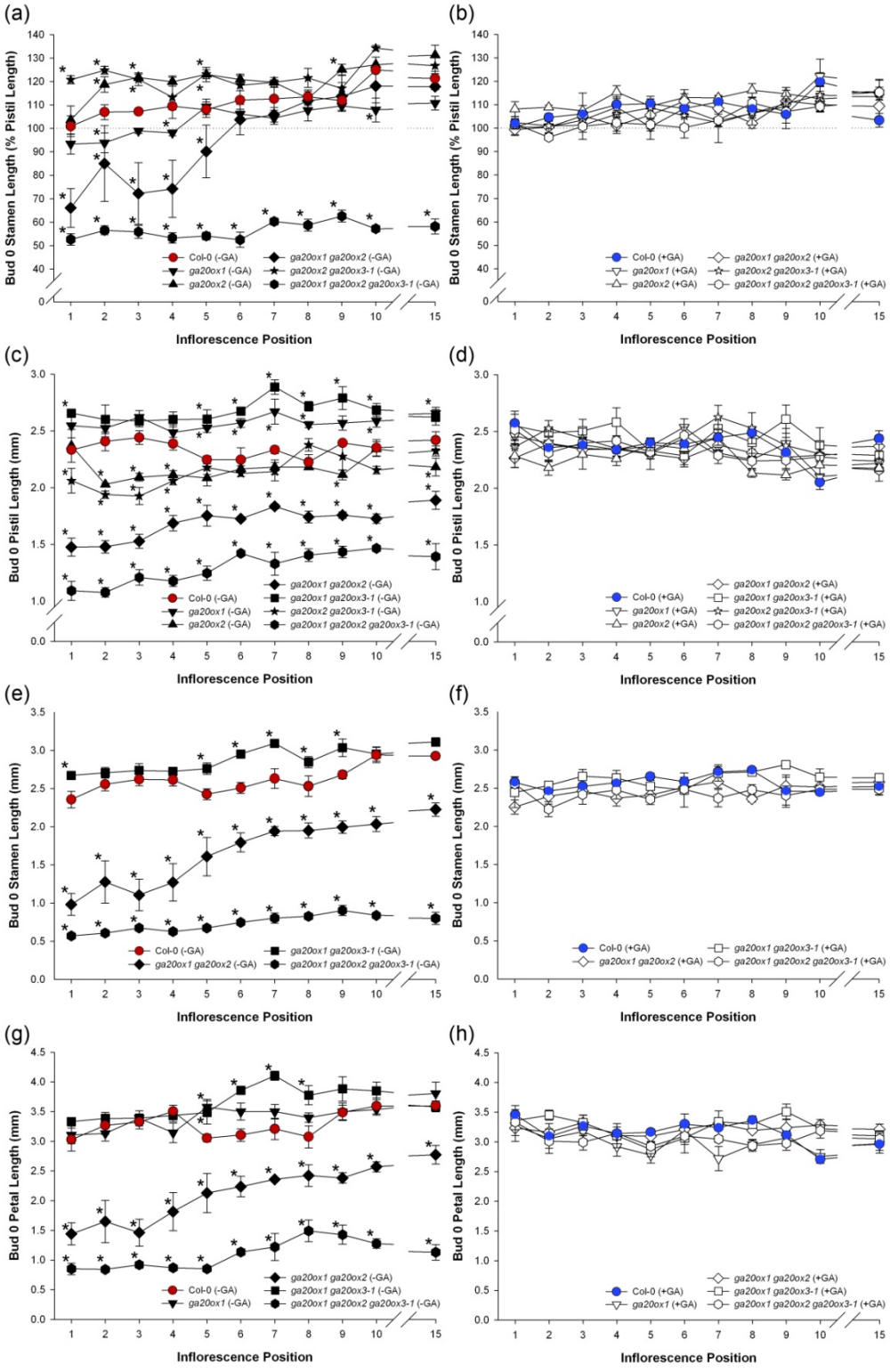

Figure 3.11: Floral organ size of *ga20ox* mutants at flower opening across early inflorescence positions.

Graphs show the length of stamens relative to pistils at flower opening (a, b) and also comparisons between absolute lengths of pistils (c, d), stamens (e, f) and petals (g, h), under control growth conditions (a, c, e, g) and chemical GA treatment (b, d, f, h). Only genotypes

demonstrating significant differences in length from wild type at at least one inflorescence position are shown. All other genotypes showed no difference from wild type.
Values shown represent the means of four measurements from independent flowers at each inflorescence position. Error bars represent one S.E. Pairwise comparisons were made between wild type and mutant genotypes within the same inflorescence position under control growth conditions using a 5% LSD ((a, b) 11.199; (c, d) 0.07157; (e, f) 0.09344; (g, h) 0.3975). Comparisons of absolute lengths of pistils and stamens were made on transformed data (square root) to meet the assumptions of the statistical model. Asterisks denote significant difference from wild type ($p < 0.05$) at that inflorescence position. Comparisons between GA treatments within the same genotype and inflorescence position, and between genotypes within the same inflorescence position under chemical GA treatment, are not shown.

significant differences occurring at inflorescence position 15 ($p < 0.05$, not shown), where relative stamen length is reduced but remains above 100%.

Relative stamen growth can be altered through the changing growth of either the pistil or the stamen, so the absolute lengths of reproductive organs from this experiment were analysed to determine the causes underlying the changed relationships observed between pistils and stamens. Consistent with reduced growth of *ga20ox2* mutant siliques (see section 3.2.4), loss of *AtGA20ox2* results in reduced pistil growth relative to wild type across some early inflorescence positions in *ga20ox2* and *ga20ox2 ga20ox3* ($p < 0.05$; positions 2, 3, 4, 9 and 15, and positions 1, 2, 3 and 4, respectively, Figure 3.11c), and across all recorded inflorescence positions in *ga20ox1 ga20ox2* and *ga20ox1 ga20ox2 ga20ox3-1* ($p < 0.05$). In contrast, stamen growth is not significantly affected in *ga20ox2* and *ga20ox2 ga20ox3* mutants (Figure 3.11c). As such, the relative increase in stamen growth observed in very early inflorescence positions in these genotypes is due to reduced pistil growth, strongly indicating that *AtGA20ox2* has a dominant function in promoting pistil growth.

In contrast, loss of *AtGA20ox1* whilst functional *AtGA20ox2* remains apparently causes *increased* pistil growth relative to the wild type, with *ga20ox1* and *ga20ox1 ga20ox3-1* pistils being significantly different from wild type at numerous inflorescence positions ($p < 0.05$; positions 5, 6, 7, 8 and 10, and positions 1, 5, 6, 7, 8, 9, 10 and 15, respectively). Increased stamen and petal growth relative to wild type is seen in similar positions in *ga20ox1 ga20ox3-1* ($p < 0.05$; positions 1, 5, 6, 7, 8 and 9, and positions 5, 6, 7, and 8, respectively, Figures 3.11c and e), but stamen growth in *ga20ox1* flowers is not significantly different from wild type. The two most obvious explanations for this counter-intuitive result relate either to the experimental design or to homeostatic changes in expression. In this experiment, floral development was synchronised between independent flowers using the morphological marker of flower opening, which occurs when the growing petals push apart the enclosing sepals. As such, staging of development is dependent on floral organ growth, and reduced or delayed petal growth might therefore delay flower opening. Petal growth is a GA-dependent process (e.g. Figure 3.10), and it is hypothesised that petals rely on stamens as a source of bioactive GA (see section 1.2), and thus growth of these two organs is linked. If the effect of removing *AtGA20ox1* (and, to a lesser extent, *AtGA20ox3*) was to reduce the rate of stamen/petal growth, flower opening could well be delayed. Assuming that *AtGA20ox2* activity maintains pistil growth in the absence of *AtGA20ox1* and *-3* (supported by the results presented above), the increased pistil length observed in *ga20ox1* and *ga20ox1 ga20ox3* could be explained by delayed flower opening affecting flower staging, with the pistils in these genotypes having developed further than in the wild type. If this is the case, then co-ordinated floral organ growth could be modelled as competition between *AtGA20ox2* primarily promoting pistil growth and *AtGA20ox1* and *-3* primarily promoting stamen growth.

An alternative explanation is that these experimental results accurately reflect accelerated pistil growth in the absence of *AtGA20ox1*, and are instead due to altered floral expression of other *AtGA20ox* paralogues through homeostatic regulation. *AtGA20ox2* is the most obvious candidate, and it has been previously shown that *AtGA20ox2* expression is up-regulated in some *ga20ox1* tissues (Rieu et al., 2008). However, analysis of *AtGA20ox* expression at the level of whole floral clusters did not see a significant change in expression of either

AtGA20ox2 or *-3* in *ga20ox1* tissues (Rieu et al., 2008), though it could be that localised changes in expression were masked by inclusion of so many other tissues. Furthermore, this hypothesis is dependent on *AtGA20ox* up-regulation as a consequence of homeostatic feedback regulation causing overgrowth of floral organs, presumably through *AtGA20ox* over-expression, whilst still under homeostatic regulation. Evidence presented in this project suggests that chemical GA treatment of wild-type Col-0 does not cause an increase in pistil elongation (Figure 3.11a and b, also see section 6.2.2), making it unlikely that hyperexpression of a GA20ox enzyme would increase pistil length above that of wild type. These hypotheses are both speculative, but can be tested by localising the tissue expression patterns of the *AtGA20ox* paralogues within floral tissues (see section 5.2.3).

The two most severely GA-deficient mutant phenotypes in this population, *ga20ox1 ga20ox2* and *ga20ox1 ga20ox2 ga20ox3-1*, demonstrate reduced growth of pistils, stamens and petals, floral organ lengths being significantly different from wild type across all inflorescence positions in this study ($p < 0.05$, Figure 3.11c, e and g). *ga20ox1 ga20ox2 ga20ox3-1* floral organ lengths are significantly different from *ga20ox1 ga20ox2* ($p < 0.05$), with loss of *AtGA20ox3* exacerbating the phenotype of *ga20ox1 ga20ox2*. These results demonstrate that *AtGA20ox1* and *-2* are the dominant paralogues in promoting floral organ growth, but with a significant (if minor) contribution by *AtGA20ox3*. *ga20ox1 ga20ox2* pistil length remains relatively uniform across early inflorescence positions (Figure 3.11c), whilst *ga20ox1 ga20ox2* stamens display a clear trend of increasing stamen length with increasing inflorescence position (Figure 3.11e). This trend is statistically significant, with stamen lengths of later inflorescence positions being significantly different from those observed at the first positions ($p < 0.05$, data not shown). Intriguingly, a very similar situation is observed regarding petal growth (Figure 3.11g), supporting the hypothesis mentioned above that stamen and petal growth are linked. From these results, it can be concluded that the increase in relative stamen growth observed in later *ga20ox1 ga20ox2* flowers (and the consequent increase in the frequency of silique-set at these positions), is primarily due to an increase in stamen growth. In contrast, stamen growth in *ga20ox1 ga20ox2 ga30ox3-1* does not increase with increasing inflorescence position (Figure 3.11e), and so we can speculatively attribute the

phenotypic rescue observed in *ga20ox1 ga20ox2* stamens to the action of *AtGA20ox3*. Chemical GA treatment substantially restores growth of floral organs in all mutants to that of GA-treated wild type (Figure 3.11d, f and h), with only sporadic inflorescence positions being significantly different from wild type for some mutants (data not shown). This indicates that the mutant phenotypes observed under control growth conditions are GA-dependent, and due to defects in GA biosynthesis caused by the loss of AtGA20ox activity.

As mentioned above, many of the genotypes (including wild type) display an apparent trend of increasing floral organ length with increasing inflorescence position, a phenotype that might potentially explain the trend in increasing fertility observed across this same range (Figure 3.9b). To test the effect of genotype on these growth relationships, this dataset was re-analysed (excluding position 15) using a linear regression approach. Both pistil and stamen length demonstrated a complex, non-linear relationship with inflorescence position, requiring transformation of these two datasets (natural logarithm) to meet the criteria of this analytical method. A high percentage of the variation within each dataset was explained by linear modelling (R^2 = 86.0, 92.0 and 81.7 for ln(pistil length), ln(stamen length) and petal length, respectively) and all model terms (interactions between genotype, GA treatment and inflorescence position) were required to predict the length of each floral organ type ($p \leq 0.05$). This indicates that changes in floral organ growth across inflorescence positions are dependent on all three of these factors.

From the model parameters thus obtained, both the intercept (i.e. floral organ length at 'inflorescence position 0') and coefficient (the slope/gradient of the relationship) were compared using 95% confidence intervals to determine the effects of genotype and GA treatment (Table 3.4). Significant differences were found in the coefficients between wild type and *ga20ox1 ga20ox2* (pistils, stamens and petals), *ga20ox1 ga20ox2 ga20ox3-1* (pistils and stamens) and *ga20ox2 ga20ox3-1* (pistils). This indicates that in the absence of *AtGA20ox1*, *-2* and *-3* changes the relationship between floral organ length and inflorescence position. Under chemical GA treatment changes in floral organ length between inflorescence positions within these mutants are not significantly different from wild type, further indicating

(a)

Genotype	Ln(Pistil) Intercept			
	-GA		+GA	
	Mean	95% C.I.	Mean	95% C.I.
Wild Type (Col-0)	[0.8639]	[0.8158; 0.9120]	[0.9233]	[0.8752; 0.9714]
ga20ox1	[0.9282]	[0.8801; 0.9763]	[0.9070]	[0.8589; 0.9551]
ga20ox2	[0.7523]	[0.7042, 0.8004][a]	[0.8356]	[0.7871; 0.8841]
ga20ox3-1	[0.8589]	[0.8108; 0.9070]	[0.8380]	[0.7899; 0.8861]
ga20ox1 ga20ox2	[0.3903]	[0.3422; 0.4384][b]	[0.8460]	[0.7979; 0.8941]*
ga20ox1 ga20ox3-1	[0.9540]	[0.9059; 1.0021]	[0.9196]	[0.8715; 0.9677]
ga20ox2 ga20ox3-1	[0.6606]	[0.6125; 0.7087][a]	[0.8875]	[0.8394; 0.9356]*
ga20ox1 ga20ox2 ga20ox3-1	[0.0436]	[-0.0045; 0.0917][c]	[0.9033]	[0.8552; 0.9514]*

(b)

Genotype	Ln(Pistil) Coefficient			
	-GA		+GA	
	Mean	95% C.I.	Mean	95% C.I.
Wild Type (Col-0)	[-0.0030]	[-0.0108; 0.0047]	[-0.0111]	[-0.0189; -0.0034]
ga20ox1	[0.0024]	[-0.0054; 0.0101]	[-0.0099]	[-0.0176; -0.0021]
ga20ox2	[0.0034]	[-0.0043; 0.0112]	[-0.0034]	[-0.0113; 0.0046]
ga20ox3-1	[-0.0064]	[-0.0142; 0.0014]	[0.0045]	[-0.0032, 0.0123][b]
ga20ox1 ga20ox2	[0.0216]	[0.0139; 0.0294][a]	[-0.0015]	[-0.0092; 0.0062]*
ga20ox1 ga20ox3-1	[0.0071]	[-0.0006; 0.0149]	[-0.0038]	[-0.0115; 0.0040]
ga20ox2 ga20ox3-1	[0.0162]	[0.0085; 0.0240][a]	[-0.0008]	[-0.0085; 0.0070]*
ga20ox1 ga20ox2 ga20ox3-1	[0.0362]	[0.0284; 0.0439][a]	[-0.0093]	[-0.0171; -0.0016]*

Table 3.4: Linear regression model parameters of floral organ length against inflorescence position.

Tables show mean and 95% confidence intervals of the intercept (a, c, e) and slope (b, d, f) of the regressed relationship for each genotype with and without chemical GA treatment for pistils, stamens and petals (as specified). Transformed data presented in square brackets.

(c)

Genotype	Ln(Stamen) Intercept			
	-GA		+GA	
	Mean	95% C.I.	Mean	95% C.I.
Wild Type	[0.8730]	[0.8058; 0.9402]	[0.9440]	[0.8766; 1.0114]
ga20ox1	[0.8546]	[0.7874; 0.9218]	[0.88530]	[0.8173; 0.9533]
ga20ox2	[0.5890]	[0.5218; 0.6562]^{a}	[0.9107]	[0.8435; 0.9779]*
ga20ox3-1	[0.9044]	[0.8372; 0.9716]	[0.9210]	[0.8534; 0.9886]
ga20ox1 ga20ox2	[-0.0945]	[-0.1617; -0.0273]^{b}	[0.8396]	[0.7724; 0.9068]*
ga20ox1 ga20ox3-1	[0.9670]	[0.8998; 1.0342]	[0.9019]	[0.8347; 0.9691]
ga20ox2 ga20ox3-1	[0.8296]	[0.7624; 0.8968]	[0.8852]	[0.8180; 0.9524]
ga20ox1 ga20ox2 ga20ox3-1	[-0.6024]	[-0.6696; -0.5352]^{c}	[0.8711]	[0.8037; 0.9385]*

(d)

Genotype	Ln(Stamen) Coefficient			
	-GA		+GA	
	Mean	95% C.I.	Mean	95% C.I.
Wild Type	[0.0133]	[0.0025; 0.0242]	[-0.0005]	[-0.0114; 0.0105]
ga20ox1	[0.0204]	[0.0095; 0.0312]	[0.0044]	[-0.0068; 0.0156]
ga20ox2	[0.0172]	[0.0063; 0.0280]	[0.0286]	[0.0178; 0.0394]^{c}
ga20ox3-1	[0.0097]	[-0.0012; 0.0205]	[0.0052]	[-0.0057; 0.0160]
ga20ox1 ga20ox2	[0.0914]	[0.0805; 0.1022]^{a}	[0.0091]	[-0.0018; 0.0199]*
ga20ox1 ga20ox3-1	[0.0141]	[0.0032; 0.0249]	[0.0100]	[-0.0009; 0.0208]
ga20ox2 ga20ox3-1	[0.0202]	[0.0094; 0.0311]	[0.0095]	[-0.0014; 0.0203]
ga20ox1 ga20ox2 ga20ox3-1	[0.0487]	[0.0379; 0.0596]^{b}	[0.0021]	[-0.0087; 0.0130]*

Comparisons were made between 95% confidence intervals (95% C.I.), with non-overlapping ranges indicating significant difference between treatments. Letters denote significant difference of a genotype from wild type within a GA treatment, with different letters denoting genotypes that are significantly different from each other. Asterisks denote significant difference between control growth conditions and chemical GA treatment within a genotype.

(e)

Genotype	Petal Intercept			
	-GA		+GA	
	Mean	95% C.I.	Mean	95% C.I.
Wild Type (Col-0)	3.1144	(2.9202; 3.3086)	3.3775	(3.1831; 3.5719)
ga20ox1	3.1296	(2.9353; 3.3238)	3.1862	(2.9920; 3.3804)
ga20ox2	3.0995	(2.9053; 3.2937)	3.1416	(2.9474; 3.3358)
ga20ox3-1	3.1680	(2.9738; 3.3622)	3.2390	(3.0448; 3.4332)
ga20ox1 ga20ox2	1.3181	(1.1239; 1.5123)[a]	3.1806	(2.9864; 3.3748)*
ga20ox1 ga20ox3-1	3.2349	(3.0407; 3.4291)	3.2915	(3.0973; 3.4857)
ga20ox2 ga20ox3-1	2.9798	(2.7856; 3.1740)	3.2821	(3.0879; 3.4763)
ga20ox1 ga20ox2 ga20ox3-1	0.6830	(0.4888; 0.8772)[b]	3.1326	(2.9383; 3.3268)*

(f)

Genotype	Petal Coefficient			
	-GA		+GA	
	Mean	95% C.I.	Mean	95% C.I.
Wild Type (Col-0)	0.0275	(-0.0037; 0.0587)	-0.0362	(-0.0678; -0.0046)*
ga20ox1	0.0452	(0.0140; 0.0764)	-0.0358	(-0.0670; -0.0046)*
ga20ox2	0.0300	(-0.0012; 0.0612)	-0.0049	(-0.0361; 0.0263)
ga20ox3-1	0.0213	(-0.0099; 0.0525)	-0.0017	(-0.0329; 0.0295)
ga20ox1 ga20ox2	0.1325	(0.1013; 0.1637)[a]	0.0064	(-0.0248; 0.0376)*
ga20ox1 ga20ox3-1	0.0753	(0.0441; 0.1065)	-0.0040	(-0.0352; 0.0272)*
ga20ox2 ga20ox3-1	0.0527	(0.0215; 0.0839)	-0.0051	(-0.0363; 0.0261)
ga20ox1 ga20ox2 ga20ox3-1	0.0737	(0.0425; 0.1049)	-0.0118	(-0.0430; 0.0194)*

that there is a GA-dependent component governing this relationship. Significant differences were also found between the intercepts of *ga20ox2* (pistil), *ga20ox2 ga20ox3-1* (pistil), *ga20ox1 ga20ox2* (pistil, stamen, petal) and *ga20ox1 ga20ox2 ga20ox3-1*(pistil, stamen, petal) compared against wild type (Table 3.4), suggesting that floral organ length is starting from a reduced size in these genotypes. Furthermore, these results support the conclusion that loss of

AtGA20ox2 alone is sufficient to reduce pistil growth, whilst the underlying relationship between pistil length and inflorescence position remains mostly unchanged.

The coefficient of the relationship between pistil length and inflorescence position is not significantly different between *ga20ox1 ga20ox2* and *ga20ox1 ga20ox2 ga20ox3-1*, but does differ significantly for both stamens and petals. However, inspection of raw stamen lengths across inflorescence position for *ga20ox1 ga20ox2* shows that, instead of a gradual restoration in stamen length across inflorescence positions, a binomial distribution is apparent, with a number of stamen lengths between inflorescence positions 1 and 5 belonging to a distinct sub-population of much shorter stamens (Figure 3.12a). Marking other floral organs from these specific plants identified a similar phenomenon in relation to petal length (Figure 3.12b), but not in pistil nor sepal length (Figure 3.12c and d). During their examination of a very similar phenotype in the GA-deficient double mutant *ga3ox1 ga3ox3*, Hu et al. (2008) observed a late-stage developmental arrest in anthers coinciding with a very short stamen phenotype. The binomial distribution of stamen lengths seen in *ga20ox1 ga20ox2* argues that a similar developmental arrest could occur in early flowers of *ga20ox1 ga20ox2*. Excluding this sub-population from the linear regression analysis of stamens and petals (necessitating ln transformation of the petal data) results in the coefficients of *ga20ox1 ga20ox2* stamens and petals now overlapping with wild type (Table 3.5b and d), although in both cases the intercepts remain significantly different (Table 3.5a and c). Once the effect of a putative developmental arrest is removed from the dataset, the changes in stamen and petal lengths with increasing inflorescence position do not differ significantly between wild type and *ga20ox1 ga20ox2*, although the initial starting length is reduced. It can be argued that this result supports the hypothesis of a late-stage checkpoint in stamen development that is overcome by bioactive GA, in addition to the previously identified checkpoints during meiosis and prior to tapetum PCD. Another inference from this analysis is that stamen and petal growth are linked, with arrest in one causing reduced growth in the other. Stamens and petal lengths in the *ga20ox1 ga20ox2* arrested sub-population fall outside the 95% confidence region of *ga20ox1 ga20ox2 ga20ox3-1* (Figure 3.12e and f), suggesting that *AtGA20ox3* still contributes to growth in these very early *ga20ox1 ga20ox2* flowers.

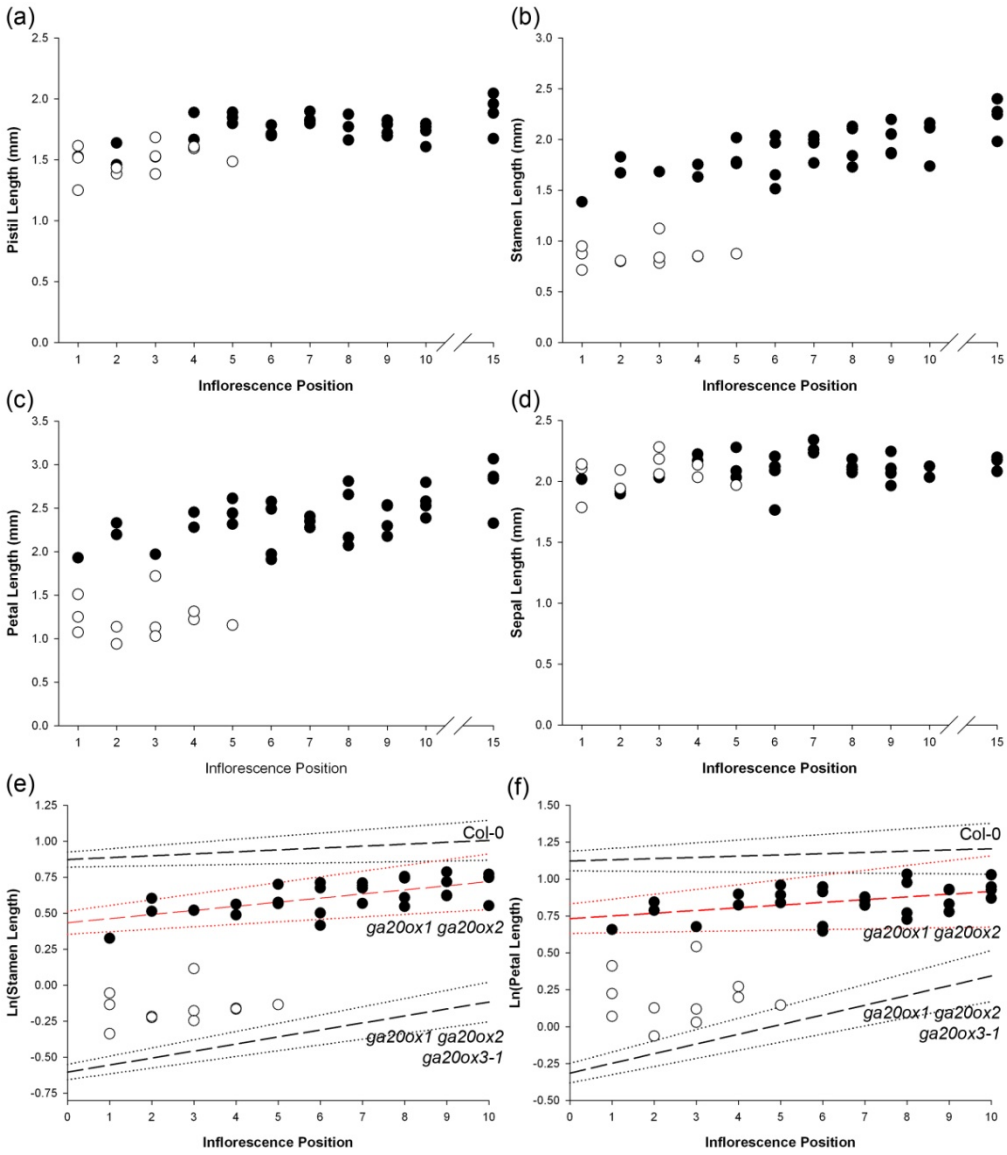

Figure 3.12: Floral organ lengths of *ga20ox1 ga20ox2*.

Plots of raw floral organ length data across inflorescence position by floral organ type, showing pistil (a), stamen (b), petal (c) and sepal (d) lengths. White circles denote floral organ length measurements from plants exhibiting very short stamens (see b). Black circles denote measurements from the remaining population. Distinct sub-populations are observed in stamens and petals, but not pistils or sepals.

Transformed population data for stamens (e) and petals (f) were plotted against the modelled relationships of floral organ lengths against inflorescence position for key genotypes, as shown. Regression values calculated excluding flowers exhibiting very short stamens (Table 3.4).

(a)

Genotype	Ln(Stamen) Constant			
	-GA		+GA	
	Mean	95% C.I.	Mean	95% C.I.
Wild Type (Col-0)	[0.8730]	[0.8202; 0.9258]	[0.9440]	[0.8910; 0.9970]
ga20ox1	[0.8546]	[0.8018; 0.9074]	[0.8853]	[0.8317; 0.9389]
ga20ox2	[0.5890]	[0.5362; 0.6418][a]	[0.9107]	[0.8579; 0.9635]*
ga20ox3-1	[0.9044]	[0.8516; 0.9572]	[0.9210]	[0.8678; 0.9742]
ga20ox1 ga20ox2	[0.4345]	[0.3546; 0.5144][b]	[0.8396]	[0.7868; 0.8924]*
ga20ox1 ga20ox3-1	[0.967]	[0.9142; 1.0198]	[0.9019]	[0.8491; 0.9547]
ga20ox2 ga20ox3-1	[0.8296]	[0.7768; 0.8824]	[0.8852]	[0.8324; 0.9380]
ga20ox1 ga20ox2 ga20ox3-1	[-0.6024]	[-0.6552; -0.5496][c]	[0.8711]	[0.8171; 0.9241]*

(b)

Genotype	Ln(Stamen) Coefficient			
	-GA		+GA	
	Mean	95% C.I.	Mean	95% C.I.
Wild Type (Col-0)	[0.0133]	[0.0048; 0.0219]	[-0.0005]	[-0.0091; 0.0081]
ga20ox1	[0.0204]	[0.0119; 0.0289]	[0.0044]	[-0.0044; 0.0132]
ga20ox2	[0.0172]	[0.0087; 0.0257]	[0.0286]	[0.0201; 0.0371][b]
ga20ox3-1	[0.0097]	[0.0012; 0.0182]	[0.0052]	[-0.0034; 0.0137]
ga20ox1 ga20ox2	[0.0285]	[0.0172; 0.0398]	[0.0091]	[0.0005; 0.0176]
ga20ox1 ga20ox3-1	[0.0141]	[0.0055; 0.0226]	[0.0100]	[0.0014; 0.0185]
ga20ox2 ga20ox3-1	[0.0202]	[0.0117; 0.0287]	[0.0095]	[0.0010; 0.0180]
ga20ox1 ga20ox2 ga20ox3-1	[0.0487]	[0.0402; 0.0572][a]	[0.0021]	[-0.0064; 0.0106]*

Table 3.5: Revised linear regression model parameters for *ga20ox1 ga20ox2*.

Tables show mean and 95% confidence intervals of the intercept (a, c) and slope (b, d) of the regressed relationship for each genotype with and without chemical GA treatment for stamens and petals (as specified). Transformed data presented in square brackets. Altered results for ga20ox1 ga20ox2 *highlighted in red. Statistical analysis as specified for Table 3.3.*

(c)

Genotype	Ln(Petal) Constant			
	-GA		+GA	
	Mean	95% C.I.	Mean	95% C.I.
Wild Type (Col-0)	[1.1221]	[1.0561; 1.1881]	[1.2191]	[1.1529; 1.2853]
ga20ox1	[1.1379]	[1.0719; 1.2089]	[1.1565]	[1.0905; 1.2225]
ga20ox2	[1.1309]	[1.0649; 1.1969]	[1.1423]	[1.0759; 1.2087]
ga20ox3-1	[1.1469]	[1.0809; 1.2129]	[1.1727]	[1.1067; 1.2387]
ga20ox1 ga20ox2	[0.7316]	[0.6318; 0.8314][a]	[1.1509]	[1.0849; 1.2169]*
ga20ox1 ga20ox3-1	[1.1770]	[1.1110; 1.2430]	[1.1849]	[1.1189; 1.2509]
ga20ox2 ga20ox3-1	[1.0914]	[1.0254; 1.1574]	[1.1864]	[1.1204; 1.2524]
ga20ox1 ga20ox2 ga20ox3-1	[-0.3146]	[-0.3806; -0.2486][b]	[1.1364]	[1.0704; 1.2024]*

(d)

Genotype	Ln(Petal) Coefficient			
	-GA		+GA	
	Mean	95% C.I.	Mean	95% C.I.
Wild Type (Col-0)	[0.00831]	[-0.0023; 0.0190]	[-0.0120]	[-0.0227; -0.0013]
ga20ox1	[0.01381]	[0.0032; 0.0245]	[-0.0120]	[-0.0027; -0.0014]*
ga20ox2	[0.00885]	[-0.0018; 0.0195]	[-0.0015]	[-0.0124; 0.0093]
ga20ox3-1	[0.00671]	[-0.0039; 0.0174]	[-0.001]	[-0.0113; 0.0099]
ga20ox1 ga20ox2	[0.01843]	[0.0043; 0.0326]	[0.0025]	[-0.0082; 0.0131]
ga20ox1 ga20ox3-1	[0.02055]	[0.0099; 0.0312]	[-0.0009]	[-0.0116; 0.0097]*
ga20ox2 ga20ox3-1	[0.01589]	[0.0052; 0.0265]	[-0.0018]	[-0.0124; 0.0089]
ga20ox1 ga20ox2 ga20ox3-1	[0.06575]	[0.0551; 0.0764][a]	[-0.0034]	[-0.0140; 0.0073]*

The effect of genotype and GA treatment on anther size was also analysed from this dataset, using anther length as a proxy measurement. ANOVA found two significant two-way interactions, between genotype and inflorescence position ($p < 0.001$) and between inflorescence position and GA treatment ($p = 0.024$), but a three-way interaction was not significant ($p = 0.129$). This indicates that (with no significant interaction between genotype

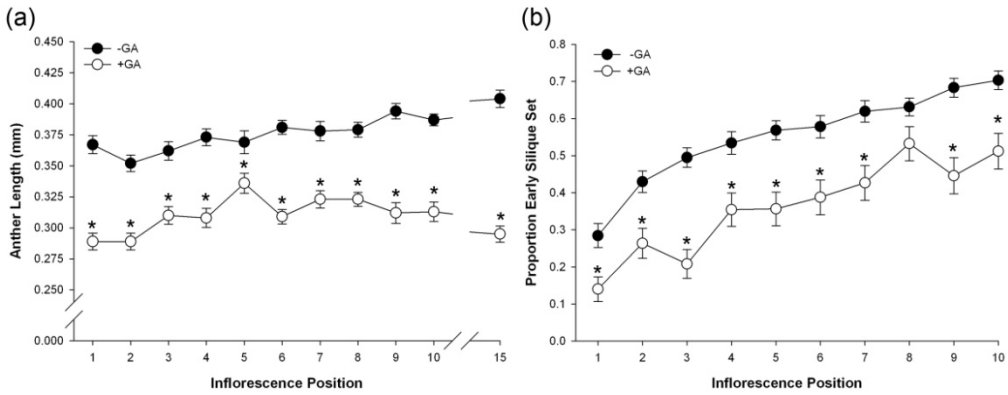

Figure 3.13: Effect of chemical GA treatment on anther size and early fertility.

(a) Anther length (averaged across all genotypes) plotted against inflorescence position, separating control growth conditions (-GA) and chemical GA treatment (+GA). Data points represent means of 32 measurements. Error bars represent one S.E.. Pairwise comparisons were made on a transformed scale (log) between GA treatments within the same inflorescence position using a 5% LSD (0.0671). Asterisks denote significant difference between GA treatments within an inflorescence position.

(b) Proportion of siliques set plotted against inflorescence position, separating control growth conditions (-GA) and chemical GA treatment (+GA). Reproduced from Figure 3.9b.

and GA treatment) anther size in all genotypes responds to GA treatment in a similar manner. No clear effect of different genotypes on anther size was discernable (data not shown), but a clear negative effect of GA treatment on anther size across all inflorescence positions was observed (Figure 3.13a). This uniform effect of GA treatment on anther size has an intriguing similarity to the effect of GA treatment seen on the probability of silique-set (Figure 3.13b). Importantly, the effects of chemical GA treatment on relative floral organ lengths (see above) do not provide an obvious cause for the observed reduction in pollination success, whilst the similarity of the effect of GA treatment on anther size could indicate that this is the proximal cause. Anther size *per se* is unlikely to have such a dramatic effect, but it may reflect other developmental changes within the anther, potentially either pollen development or anther dehiscence.

The conclusions that can be drawn from these results are that reduced fertility during early flowering in GA-deficient mutants is strongly correlated with changes to the relative growth of pistils and stamens, whilst reduced fertility observed under chemical GA treatment (representing a GA-overdosed state) does not correlate well with floral organ length, and may instead be explained by other factors relating to anther development. *AtGA20ox2* plays a dominant role in promoting pistil growth, and the results presented here can be interpreted to support the hypothesis that *AtGA20ox1* has a competing role in promoting stamen growth. *AtGA20ox3* has a significant but minor role, with loss of *AtGA20ox1* and *-2* resulting in reduced growth of all reproductive organs. The rescue of silique-set observed by Rieu et al. (2008) in the *ga20ox1 ga20ox2* mutant can be explained by increased growth of stamens in later flowers due to the direct or indirect action of *AtGA20ox3*. Phenotypic rescue of *ga20ox1 ga20ox2* is not gradual, indicative of stamen development overcoming a possible late-stage GA-dependent developmental block.

3.2.6 Floral Organisation and Floral Organ Identity are Perturbed in *ga20ox* Mutants

During floral phenotypic characterisation, it became apparent that *ga20ox* mutants present abnormal floral phenotypes more frequently than wild type, including missing or extra floral organs and floral organs with developmental abnormalities. A census of floral organs was conducted using the population from which floral organ lengths were measured (n = 704), recording the occurrence of floral abnormalities across early inflorescence positions under control growth conditions and GA treatment. Three significant two-way interactions were found, between GA treatment and inflorescence position ($p < 0.001$), inflorescence position and genotype ($p = 0.033$) and between genotype and GA treatment ($p = 0.024$), though no three-way interaction was observed ($p = 0.807$). No clear differences between genotypes were observed regarding the relationship of floral abnormalities to inflorescence position (data not shown), but comparing the mean occurrence of floral abnormalities across early all inflorescence positions found that occurrence in *ga20ox1 ga20ox3* is significantly different from wild type ($p < 0.05$), with more abnormalities present (Figure 3.14a). *ga20ox1* was also significantly different from wild type ($p < 0.05$) but displayed a reduced occurrence.

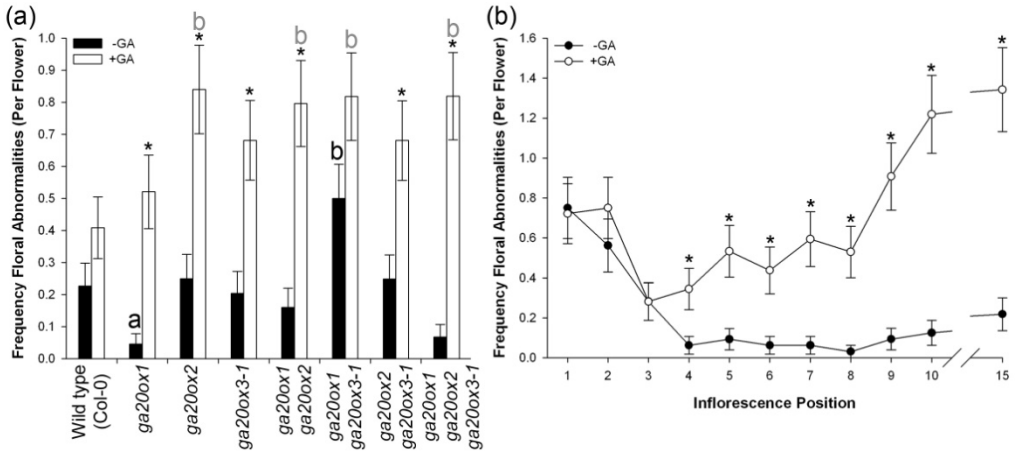

Figure 3.14: Occurrence of floral developmental abnormalities in *ga20ox* mutants.

(a) Frequency of floral abnormalities in flowers across early inflorescence positions by genotype, grown under control growth conditions (-GA) and under chemical GA treatment (+GA). Bars represent the mean value of 44 measurements.

(b) Frequency of floral abnormalities across all genotypes by inflorescence position, grown under control growth conditions (-GA) and under chemical GA treatment (+GA). Data points represent the mean value of 32 measurements.

Error bars represent one S.E. Data were analysed against an underlying Poisson distribution using Generalised Linear Modelling. Pairwise comparisons were made using a 5% LSD (individual LSD's calculated for each comparison, not shown). Letters denote a significant difference from -GA wild type (black) or +GA wild type (grey), respectively. Genotypes marked with different letters are significantly different from one another. Asterisks denote significant difference between GA treatments within an inflorescence position. Comparisons were not made between GA treatments of different inflorescence positions (b).

Unexpectedly, the occurrence of floral abnormalities in *ga20ox1 ga20ox2* and *ga20ox1 ga20ox2 ga20ox3-1* were not significantly different from wild type. Chemical GA treatment had a significant effect ($p < 0.05$) of increasing the frequency of floral abnormalities in all genotypes except wild type (which retained a relatively low frequency) and *ga20ox1 ga20ox3-1* (in which the frequency of floral abnormalities under control growth conditions was not significantly different from most *ga20ox* mutants under GA treatment). Similarly, GA treatment was found to increase the frequency of floral abnormalities at most inflorescence

positions studied (Figure 3.14b). Under control growth conditions, a higher frequency of abnormalities was identified at very early inflorescence positions, dropping to a very low level by inflorescence position 4. Given the lack of phenotype in the more severely GA-deficient mutants, one explanation may be that these abnormalities arise due to an imbalance in, or mis-placement of, bioactive GA across the floral meristem, a hypothesis which also fits with the observed effect of chemical GA treatment.

Having established that there is a GA-dependent effect on the occurrence of floral abnormalities, they were further sub-divided into two phenotypic categories: those relating to floral organ number (i.e. disruption to the floral plan) and those relating to floral organ development. Comparing the number of floral organs of each flower by genotype against the expected number of floral organs in each whorl (Figure 3.15a and b), it becomes clear that the greatest effect is on stamen number (whorl 3). Flowers demonstrated a tendency to present fewer short (lateral) stamens than expected (Figure 3.15a), an effect seen most clearly in *ga20ox1 ga20ox3-1* (which showed a significant increase in floral abnormalities). Chemical GA treatment has the effect of reducing further the mean number of short stamens present across most genotypes (Figure3.15b). Floral organs arise from concentric whorls of identity within the floral meristem which are established by the interactions between MADS-box proteins (see section 1.5.2), but the number of individual floral organs within those whorls is determined downstream of these events through the establishment of distinct cellular boundaries between the nascent organ primordia (Aida & Tasaka, 2006). Observations made during this experiment suggest that the GA-dependent defects are related to primordium outgrowth rather than to boundary establishment, as the absence of floral organs manifested as discrete gaps whilst the surrounding floral pattern remained intact. Lateral ('short') stamens occupy a specific position within whorl three (Figure 3.15c), their primordia arising from the floral meristem slightly later than medial ('long') stamens (Smyth et al., 1990). The reason for their apparent susceptibility to GA is not readily apparent. Whilst some occurrences of supernumerary stamens were also noted (Figure 3.15a and b), it is unclear whether their frequency is significantly increased in a GA-dependent manner.

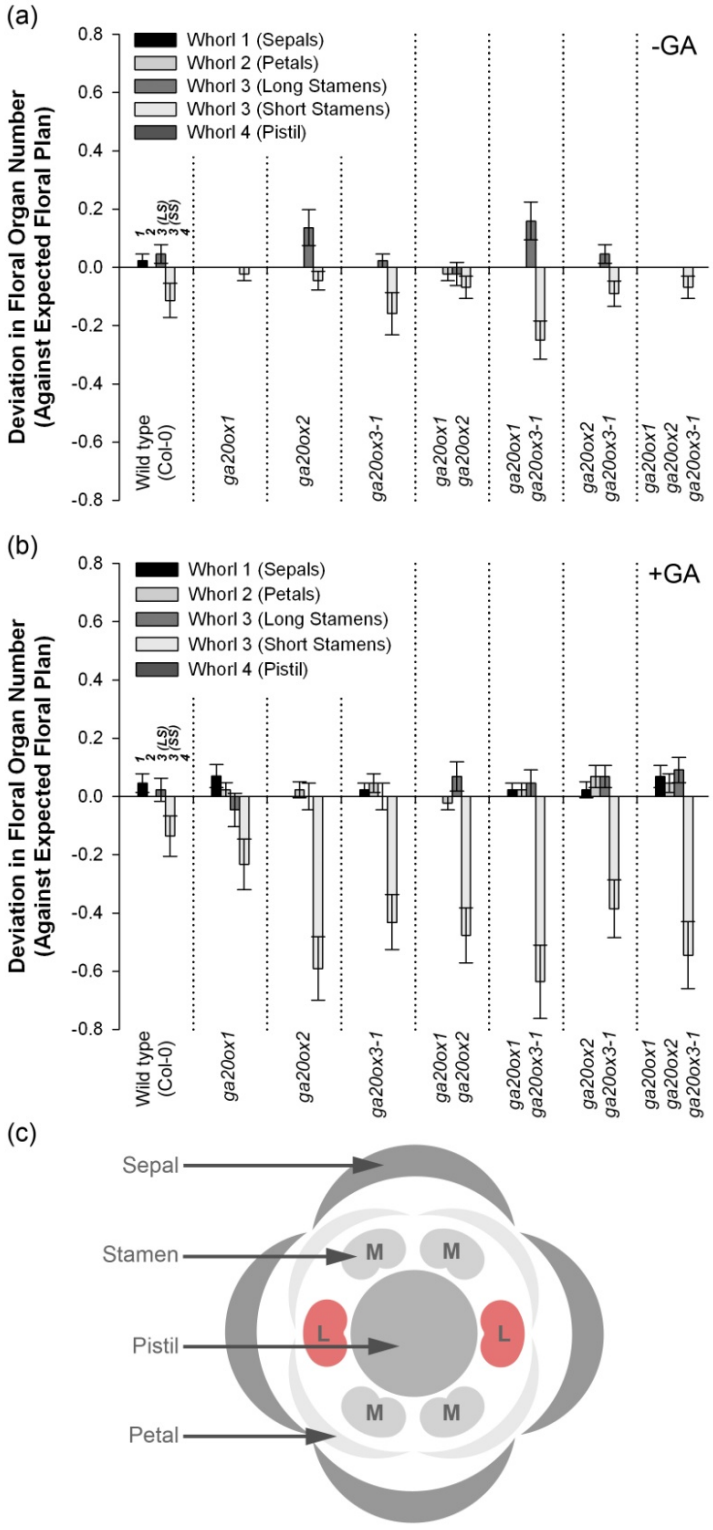

Figure 3.15: The effect of GA on floral organ number.

Graphs summarise the mean deviation in number of each type of floral organ from the expected floral plan by genotype under control growth conditions (a) and under chemical GA treatment (b). The effect of GA on the floral plan (c) is most pronounced on the lateral ('short') stamens (highlighted in red).

Stamens also demonstrate the greatest incidence of subsequent abnormal floral organ development under both control growth conditions and chemical GA treatment (Figure 3.16a and b). Under GA treatment, most genotypes demonstrate an increased frequency of stamen developmental abnormalities (Figure 3.16b), the effect being most pronounced in long stamens. Under control growth conditions by far the most common phenotype was the partial homeosis of short stamens to petalloid stamens (Figure 3.16c). Intriguingly, although the extent of homeosis was variable (as shown), apparently it was restricted to one side of the stamen (full homeosis was not observed). Similar phenotypes were observed under chemical GA treatment in both short and long stamens (Figure 3.16d), but under GA treatment a second class of developmental abnormality was more prevalent in long stamens, in which 'split' or 'branched' stamens arose from the same floral organ position (Figure 3.16e). The extent of this phenotype was also variable, as demonstrated by the examples shown.

Interactions between GA signalling and the floral homeotic gene *AGAMOUS* (*AG*) during floral development have been previously established (see section 1.5.2), but this the first instance in which such a phenotype has been recorded in GA-related mutants. AG acts with other MADS-box proteins to establish stamen identity in whorl three, and the loss of *AG* function results in the homeotic conversion of stamens to petals (Bowman et al., 1991). As such, it is highly probable that the stamen identity defects identified here occur either at the level of AG or in the downstream signalling cascade. The double-stamen phenotype is more difficult to reconcile with known roles of GA, but might conceivably be caused by ectopic formation of floral organ boundaries across previously-established stamen primordia. These results demonstrate novel phenotypes not previously associated with the effects of GA-deficiency and GA overdose in early floral development of *Arabidopsis*. Normal floral development is destabilised both by loss of *AtGA20ox1* and *-3* (but not in more severely GA-deficient mutants) and by chemical GA treatment, possibly suggesting that the phenotypes arise due to inappropriate GA signalling in the floral meristem. Whorl 3 is the most severely affected region of the developing flower, demonstrating altered stamen number and stamen developmental defects. One of these phenotypes can be associated with a known mechanism linking GA to the homeotic gene *AG*, but others are more obscure but may be related to the

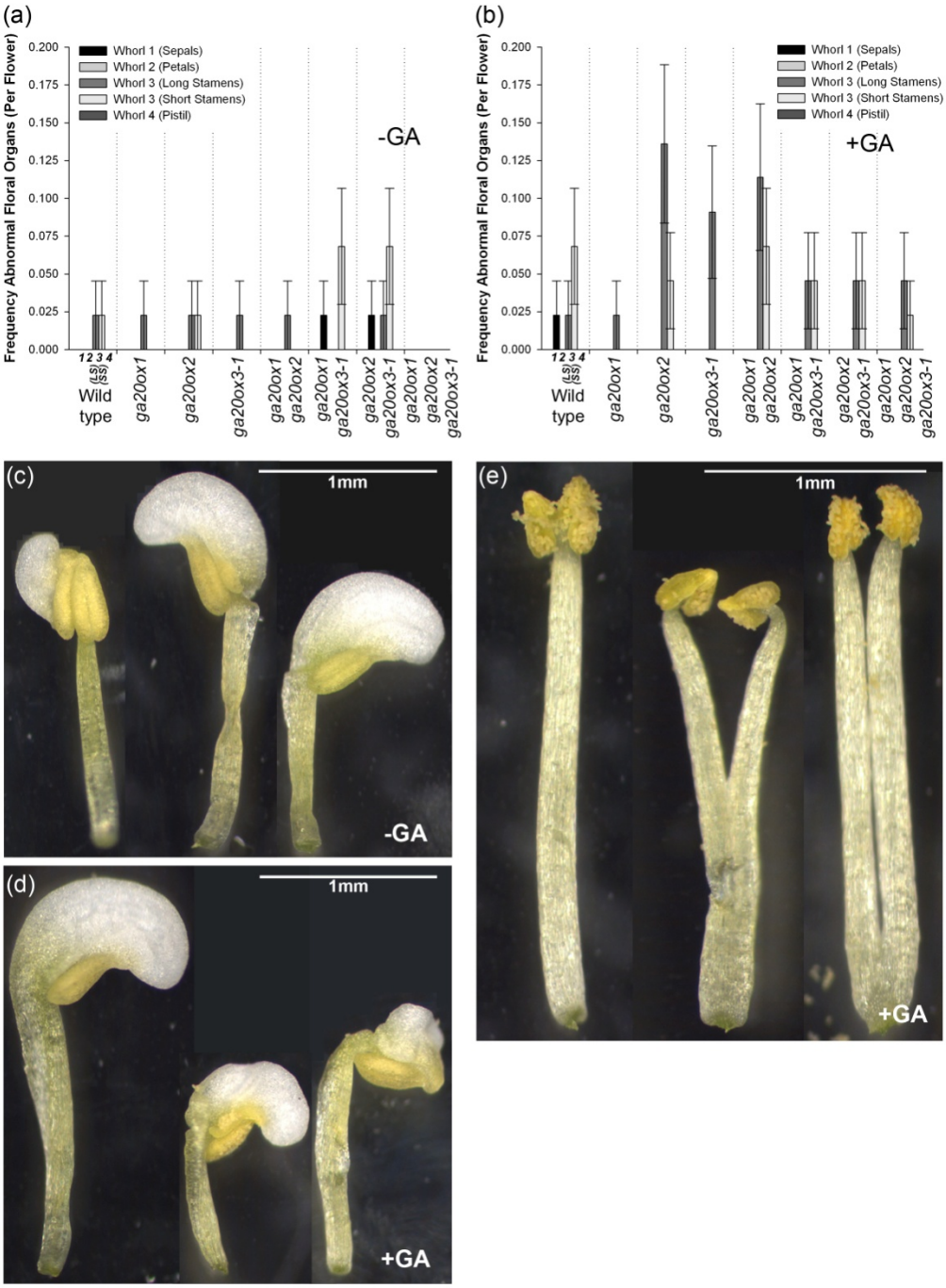

Figure 3.16: The effect of GA on floral organ development.

Graphs summarise the mean frequency of developmental abnormalities in different floral organ types by genotype, under control growth conditions (a) and under chemical GA treatment (b). Floral organs in whorl 3 (stamens) are the most dramatically affected. Two different stamen phenotypes were observed across all genotypes: partial conversion of identity to petals under both control growth conditions (c) and under GA treatment (d), and the appearance of 'double stamens' under GA treatment (e).

positioning and formation of boundaries between organ primordia during floral development.

3.2.7 Floral Growth Phenotypes Eventually Recover in GA-Deficient Backgrounds, Even in the Absence of Chemical GA Treatment

The phenotypic analyses of *ga20ox* mutant described so far in this chapter were all performed on plants up to 50 days old, by which time all genotypes except *ga20ox1 ga20ox2 ga20ox3-1* and *ga1-3* had finished development and were entering senescence. However, these latter two mutants demonstrated greater longevity than the other, less GA-deficient genotypes, potentially due to a far slower rate of growth, reduced fertility and/or arguably increased stress tolerance conferred by their severely-dwarfed vegetative phenotypes. By 50 days these two genotypes had developed far fewer flowers than even *ga20ox1 ga20ox2* (Figure 3.5a), so in order to observe later phases of reproductive development these two genotypes were subsequently grown until senescence (90-100 days). Very surprisingly, it was found that substantial rescue of floral organ growth reliably occurred in later flowers on the primary inflorescence (from approximately floral position 20-25) in both genotypes (Figure 3.17), though all floral organs remained far smaller than those exhibited by wild type flowers. This phenotype was observed on several different occasions, including when special precautions were taken to isolate the population to prevent contamination with bioactive GA.

Restoration of stamen growth relative to the pistil was observed in these later flowers, developmental recovery in both *ga20ox1 ga20ox2 ga20ox3-1* and *ga1-3* proceeding to the point of successful anther dehiscence on some occasions. Some seeds were recovered from *ga20ox1 ga20ox2 ga20ox3-1* plants (Figure 3.17b), and genotyping of the subsequent progeny confirmed them as homozygous *ga20ox1 ga20ox2 ga20ox3-1* mutants (data not shown), indicating that successful self-fertilisation occurred. Despite several attempts, it was not possible to recover seed from *ga1-3* plants under circumstances in which there was no possibility of contamination with bioactive GA. On the basis of this evidence, self-fertilisation of *ga1-3* cannot be confirmed or refuted. These results are unexpected because published evidence on the floral development of *ga1-3* demonstrates developmental arrest at

Figure 3.17: Phenotypic rescue of flowers in GA-deficient mutants.

(a) Comparison of floral phenotypes between early and late ga20ox1 ga20ox2 ga20ox3-1 *flowers. Late* ga20ox1 ga20ox2 ga20ox3-1 *flowers demonstrate anther dehiscence, with released pollen grains visible.*

(b) Self-fertilised ga20ox1 ga20ox2 ga20ox3-1 *silique, containing mature seed from a 95 day-old plant.*

(c) Comparison of floral phenotypes between early and late ga1-3 *flowers.*

floral stage 10 (Koornneef & Van der Veen, 1980; Cheng et al., 2004), and in none of the published work using this genotype as a GA-deficient control are the phenotypes described above reported. Furthermore, under our growth conditions individual *ga1-3* plants often displayed bolting, particularly of secondary inflorescences (data not shown), whilst the published phenotype of *ga1-3* is that no internode elongation occurs (Koornneef & Van der

Veen, 1980). These differences can potentially be reconciled either by the age of the plants characterised in this experiment (not specified in previously published phenotypic characterisations), or through the fact that the *ga1-3* (Col-0) line used in these experiments differs phenotypically from the original *ga1-3* line in the L*er* ecotype. Further investigation is required to establish the precise cause for the phenotypes observed here.

The above observations raise interesting implications for the role of GA in floral development. Firstly, given that a trend of increasing fertility and relative stamen growth was identified in early flowers irrespective of GA treatment, it could be hypothesised that the late recovery seen in *ga20ox1 ga20ox2 ga20ox3-1* and *ga1-3* could be caused by that same underlying trend. If this is the case, then the results presented here suggest the existence of a pathway independent of GA biosynthesis that can partially restore GA-deficient floral phenotypes. Whilst attempts were made during this experiment to prevent contamination by bioactive GA, the possibility still exists that the phenotype of *ga1-3* was influenced by contamination by the GA intermediate *ent*-kaurene, which lies downstream of CPS in the GA biosynthesis pathway (Figure 1.3) and which has been shown to transmit between plants as an airborne volatile (Otsuka et al., 2004). Previous GA analyses have identified very small quantities of bioactive GA in *ga1-3* tissues (King et al., 2001; Silverstone et al., 2001), though whether due to contamination or residual endogenous CPS function remains undetermined. *ga20ox1 ga20ox2 ga20ox3-1*, however, is blocked in GA biosynthesis downstream of *ent*-kaurene, and so this precursor cannot be responsible for alterations in the phenotype of this mutant. Grafting experiments performed in pea between GA-deficient mutants demonstrated that at least one GA precursor beyond GA_{12} is transmissible between plant tissues, further radiolabelling experiments suggesting that the mobile precursor is the product of GA20ox activity (in the case of pea, GA_{20}; Proebsting et al., 1992). However, there is no published evidence of C_{19}-GAs transmitting between individual plants.

The recovery of self-fertilised seed from *ga20ox1 ga20ox2 ga20ox3-1* plants is very interesting, because it indicates that both male and female fertility have been restored in later flowers. This is reminiscent of the effect seen in the stamens of early flowers of *ga20ox1*

ga20ox2 but at a much later stage of flowering, the simplest hypothesis being that the same mechanism underpins both. The evidence from the *ga20ox1 ga20ox2* phenotype suggests that the rescue of stamen development in this genotype is due to AtGA20ox3 activity. One possible explanation is that AtGA20ox4 or -5 accumulates in the *ga20ox1 ga20ox2 ga20ox3-1* floral tissues, eventually producing sufficient bioactive GA to restore pollen development. This hypothesis is partially supported by the lack of observed fertility in equivalent *ga1-3* plants, but cannot explain the recovery of floral development observed in this mutant. In the case of stamen development, this includes overcoming a developmental block imposed by the absence of GA, presumably by DELLA repression, during pollen development and also potentially during stamen maturation (see section 3.2.5).

As discussed in sections 1.3.2 and 1.5.4, DELLA proteins are a point of integration between GA and other hormone signalling pathways, including auxin (Fu & Harberd, 2003), ABA (Achard et al., 2006), ethylene (Achard et al., 2003; Achard et al., 2007) and jasmonate (JA; Hou et al.. 2010). Of these, both auxin and JA act to promote GA downstream responses. JA signalling in particular is associated with floral development, and has recently been shown to transmit part of the GA signal that triggers GA-dependent growth responses during stamen maturation (Cheng et al., 2009). However, stamen development in JA biosynthetic and signalling mutants proceeds further than those of GA-deficient or insensitive mutants (Stintzi & Browse, 2001, Feys et al., 1994), and chemical JA treatment cannot rescue GA-deficient stamen development (Cheng et al., 2009), suggesting that JA signalling alone is not sufficient to rescue stamen development to the extent observed in *ga20ox1 ga20ox2 ga20ox3-1* and *ga1-3*. However, it might comprise a significant component, in conjunction with other mechanisms such as auxin signalling. The role of auxin in stamen development is not well understood, with evidence for both early and late functions in promoting stamen outgrowth and development (Cheng et al., 2006; Cecchetti et al., 2008), and potential interactions with the JA signalling pathway via AUXIN RESPONSE FACTOR 6 (ARF6) and ARF8 (Nagpal et al., 2005) in a relationship similar to that between GA and JA. However, the hierarchy between these three signalling pathways during stamen development has not yet been clearly

defined, and the question of whether combined auxin and JA signalling can overcome a block imposed by the absence of GA has not been addressed.

3.3 CONCLUSIONS

Through analysis of new combinatorial mutants created during this project, the conclusion from the genetic evidence presented in this chapter is that *AtGA20ox1*, *-2* and *-3* act to mediate the vast majority of GA biosynthesis in nearly all developmental processes during the *Arabidopsis* lifecycle, although one or two exceptions indicate the possibility of very minor roles for *AtGA20ox4* and/or *-5*. The severity of the *ga20ox1 ga20ox2 ga20ox3-1* mutant phenotype also serves to confirm that the *AtGA20ox* gene family catalyse the predominant pathway through which bioactive GA is synthesised *in planta*. In almost all phenotypic characters studied, *AtGA20ox1* and *-2* were the dominant paralogues to influence phenotype, with the presence of either masking the contribution of *AtGA20ox3*. Detailed analysis of floral phenotypes has generated hypotheses regarding functional specialisation of *AtGA20ox1* and *-2* in promoting stamen and pistil growth, respectively, provided supporting evidence for an additional GA-dependent checkpoint late in stamen development, and identified novel effects of GA during early floral developmental. In contrast, the negative effect of GA treatment on fertility is not closely associated with alterations in floral organ growth, and may instead be due to effects on anther development. In anther tissues it requires the loss of *AtGA20ox1*, *-2* and *-3* to block normal degeneration of the tapetum, demonstrating the redundant action of all three paralogues in anther development. This research has also uncovered circumstantial evidence of a pathway either downstream or independent of GA biosynthesis that results in a gradual increase in floral organ size as flowering progresses.

CHAPTER 4: *ATGA20OX4* MIGHT HAVE MINOR FUNCTIONS DURING *ARABIDOPSIS* DEVELOPMENT, BUT *ATGA20OX5* LACKS FULL GA20OX ACTIVITY

4.1 INTRODUCTION

The results obtained in chapter 3 clearly indicate that *AtGA20ox1*, *-2* and *-3* are the predominant GA 20-oxidase enzymes across the whole of *Arabidopsis* development. However, significant differences were identified between the severely-dwarfed triple mutant, *ga20ox1 ga20ox2 ga20ox3-1*, and the GA-deficient mutant *ga1-3* in a number of phenotypic characters, the most pronounced being in flowering time. One hypothesis to explain these discrepancies is that one or both of the remaining *AtGA20ox* paralogues in this background, *AtGA20ox4* and *-5*, promote growth in the absence of *AtGA20ox1*, *-2* and *-3*, although there is no published evidence of their possessing GA20ox activity (see section 3.1). The *ga20ox1 ga20ox2 ga20ox3-1* phenotype represents a useful tool for uncovering the biological functions of these two minor *AtGA20ox* paralogues. Previous expression mapping experiments found that *AtGA20ox4* and *-5* are expressed in inflorescence tissue at levels similar to *AtGA20ox3* (Rieu et al., 2008; Figure 3.1c), and data from transcriptomic analysis (Kilian et al., 2007) suggests that the tissue in which *AtGA20ox4* is most highly expressed is mature pollen (Phillips, A., personal communication). *AtGA20ox5* shows the greatest phylogenetic divergence within the *Arabidopsis GA20ox* gene family (Figure 4.1a, Hedden et al., 2002), and phylogenetic analysis including *GA20ox* gene families from other plant species whose genomes have been sequenced identifies *AtGA20ox5* as an outlier that falls into an entirely separate clade from all other *AtGA20ox* paralogues (Figure 4.1b, Phillips, A., unpublished data). Previous unpublished attempts to characterise AtGA20ox5 function *in vitro* have failed to identify full conversion of GA_{12} to GA_9 (see section 4.2.4 for further discussion).

Genetic evidence presented in this chapter characterising quadruple *ga20ox* combinatorial mutants, utilising new loss-of-function alleles for *AtGA20ox4* and *-5,* only partially supports the existence of significant differences between the *ga20ox1 ga20ox2 ga20ox3* and *ga1-3* phenotypes, suggesting little or no function for *AtGA20ox4* or *-5*. *AtGA20ox4* may have a

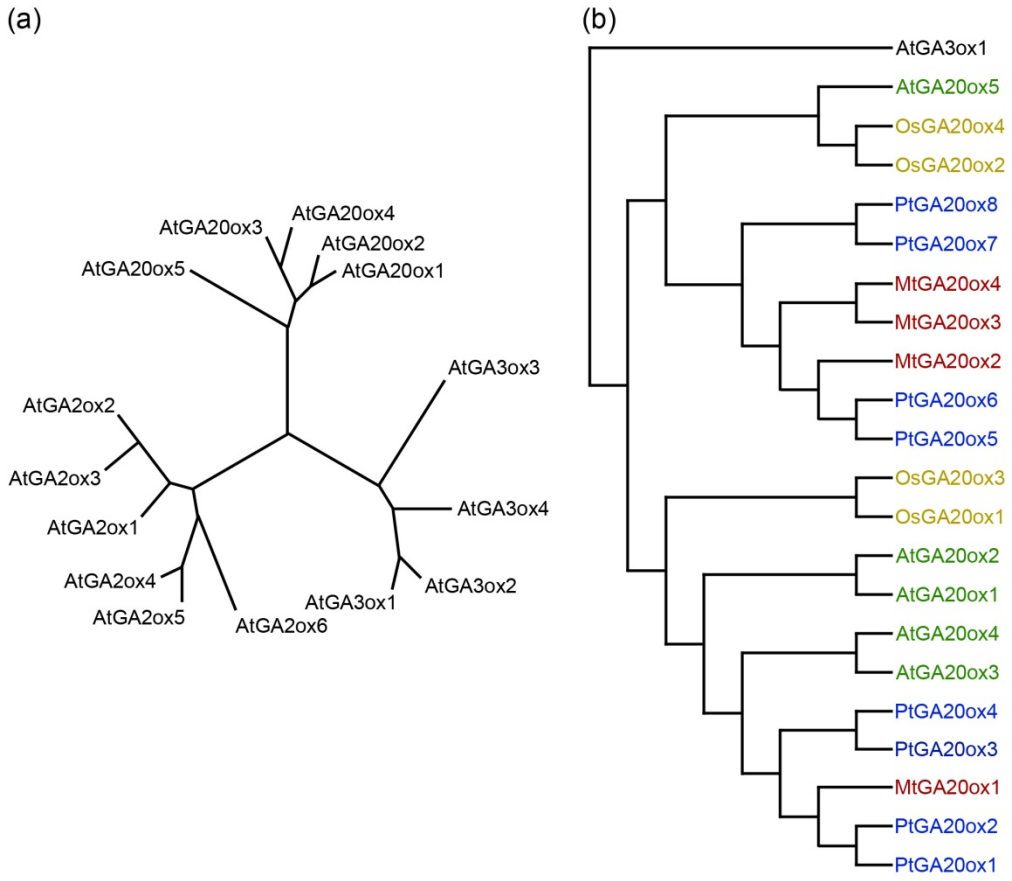

Figure 4.1: Phylogenetic analysis of the *AtGA20ox* gene family.

(a) Unrooted cladogram demonstrating the relationships between AtGA20ox *paralogues and other Arabidopsis GA biosynthetic gene families (*AtGA3ox *and* AtGA2ox*). Reproduced with permission from Hedden et al., 2002.*

(b) Rooted cladogram comparing GA20ox *paralogues from different sequenced plant species;* Arabidopsis *(At), rice (Os), poplar (Pt) and medicago (Mt). Paralogues from each species are separately coloured to aid distinction. (Phillips, A., unpublished data).*

specific minor role in promoting the transition to flowering. Whilst AtGA20ox4 displays full GA20ox catalytic activity *in vitro*, AtGA20ox5 cannot perform full GA20ox activity. However, constitutive expression of *AtGA20ox5 in planta* partially complements the *ga20ox1 ga20ox2 ga20ox3-1* phenotype, and similar phenotypic rescue is seen even with the additional loss of *AtGA20ox4*. This suggests that in the absence of full GA20ox activity, bioactive GA could be synthesised through an alternative pathway, driven by AtGA20ox5.

4.2 RESULTS AND DISCUSSION

4.2.1 Identification of *AtGA20ox4* and *-5* Loss-of-Function Mutant Alleles

Two candidate mutant alleles were identified from database searches for both *AtGA20ox4* and *AtGA20ox5*. Two separate SNPs were found in the *AtGA20ox4* locus (Figure 4.2a), the first (TILLING line CS87368, Col-0 ecotype, herein referred to as *ga20ox4-1*) representing the mutation of a proline residue otherwise conserved across known GA20ox enzymes (data not shown), the second (herein referred to as *ga20ox4-2*) representing a natural sequence variation identified in the *Arabidopsis* accession Burren-0 (Ossowski et al., 2008), in which a one base-pair deletion occurs within exon one. The existence of both SNPs was confirmed *in planta* by sequencing PCR products amplified from the *ga20ox4-1* and *ga20ox4-2* loci (data not shown). Two independent mutant lines carrying T-DNA insertions were identified within the *AtGA20ox5* locus. The first insertion (SALK_094959, Alonso et al., 2003) was published as falling within the second intron (data not shown), but proved impossible to verify *in planta*. A second insertion in exon 3 (6.6kb, herein referred to as *ga20ox5-2*, Figure 4.2a) was identified from the from the Cold Spring Harbor Lab 'genetrap' collection (GT9248, L*er* ecotype, Sundaresan et al., 1995; Martienssen, 1998). The presence of this T-DNA insertion in exon 3 of *AtGA20ox5* was confirmed through sequencing of PCR products amplified from the 5' and 3' T-DNA-genomic junctions (data not shown).

The effect of the two separate SNPs on AtGA20ox4 catalytic activity was examined *in vitro* using bacterially-expressed, mutagenised cDNA clones of *AtGA20ox4*. After 2 hours incubation, wild-type GA20ox4 protein had catalysed the conversion of ^{14}C-labelled GA_{12} to ^{14}C-GA_9 (Figure 4.2b). In contrast, over the same incubation neither ga20ox4-1 nor ga20ox4-2 protein catalysed ^{14}C-GA_{12} to ^{14}C-GA_9: ga20ox4-1 only catalysed partial conversion of ^{14}C-GA^{12} to ^{14}C-GA_{15} and ga20ox4-2 demonstrated no measurable catalytic activity (Figure 4.2b). As well as confirming the full GA20ox activity of wild-type GA20ox4 protein *in vitro*, these results indicate that both mutation decrease GA20ox catalytic activity. Incubation of lysates over a longer period (48 hours) found that *ga20ox4-1* partially converted ^{14}C-GA_{12} through to ^{14}C-GA_9, whilst ga20ox4-2 still showed no evidence of catalytic activity (Figure 4.2c),

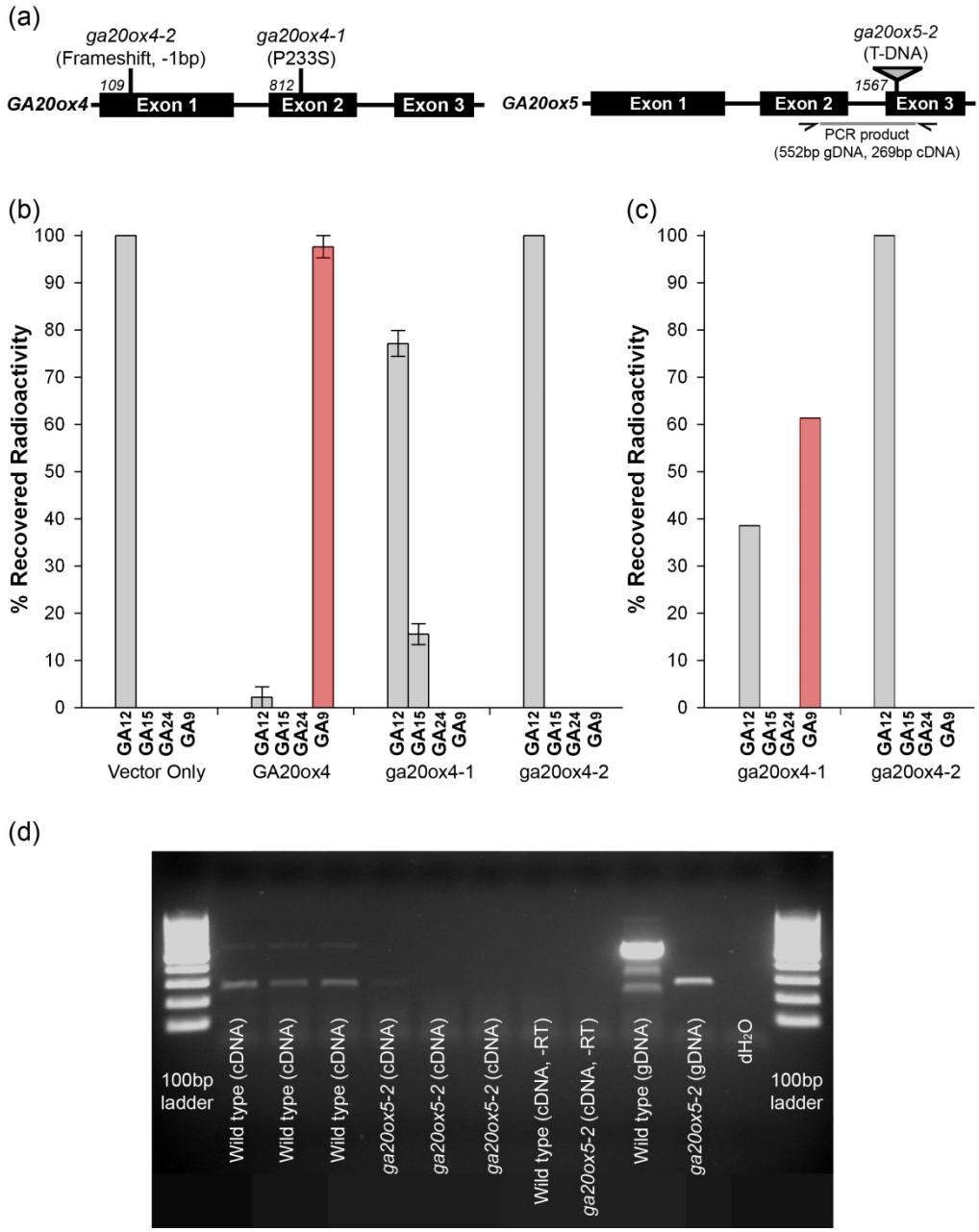

Figure 4.2: Characterisation of mutant alleles of *AtGA20ox4* and *-5*.

(a) Gene models of AtGA20ox4 *and* -5*, showing the positions (numbers in italics) and nature of the* ga20ox *mutant alleles under investigation. Primers and PCR product shown beneath* AtGA20ox5 *were used to discriminate wild-type transcript in (d).*

(b,c) HPLC analysis of wild-type and mutant AtGA20ox4 activity in vitro. Results shown were obtained after 2 hours (b) and 48 hours (b) incubation with radiolabelled GA_{12}, respectively. Bars in (b) represent the mean of two technical replicates. Error bars represent one S.E. Bars in (c) represent the results from individual lysates. Where present, the final product of GA20ox activity (GA_9) is highlighted in red.

(d) RT-PCR analysis of ga20ox5-2 *transcription from three day-old seedling tissue. cDNA product 269bp, gDNA product 606bp (see (a)). The presence of the* ga20ox5-2 *T-DNA insertion prevents transcription from both RNA-derived and genomic template DNA (L*er*), but not in wild type (L*er*)*

suggesting that the *ga20ox4-2* allele represents a complete loss-of-function. The effect of the ga20ox4-2 deletion is to cause a shift in the downstream translational reading frame. Analysis of this altered reading frame predicts the creation of numerous premature stop codons along the sequence, resulting in a truncated protein (data not shown). *ga20ox4-1*, however, though reducing GA20ox catalytic activity by approximately half, still has the potential for full GA20ox function *in planta*, and as such represents a knock-down allele rather than a complete loss-of-function. In consequence, subsequent phenotypic analyses were restricted to the *ga20ox4-2* allele. The effect of the *ga20ox5-2* T-DNA insertion on the transcription of *AtGA20ox5* was tested via non-quantitative RT-PCR, using template RNA derived from 3 day-old whole seedlings (which have been previously shown to express *AtGA20ox5*, Rieu et al., 2008, Figure 3.1c). It was found that *AtGA20ox5* transcript was detectable in wild-type seedlings but not in homozygous *ga20ox5-2* seedlings (Figure 4.2d), suggesting that transcription is interrupted in the *ga20ox5-2* allele. On the basis of these results, *ga20ox5-2* was assigned as a loss-of-function allele.

4.2.2 *AtGA20ox4* Promotes Floral Transition in the *ga20ox1 ga20ox2 ga20ox3-1* Background

To test for significant contributions of *AtGA20ox4* and *-5* towards promoting growth and development *in planta*, the two quadruple mutant combinations *ga20ox1 ga20ox2 ga20ox3-1 ga20ox4-2* and *ga20ox1 ga20ox2 ga20ox3-1 ga20ox5-2* were created and characterised. Both the *ga20ox4-2* and *ga20ox5-2* alleles (coming from the Bur-0 and L*er* ecotypes, respectively) were introgressed into the Col-0 ecotype by six sequential back-crosses prior to establishing these combinatorial mutant lines. The *ga20ox1 ga20ox2 ga20ox3-1 ga20ox4-2* and *ga20ox1 ga20ox2 ga20ox3-1 ga20ox5-2* quadruple mutants both display severely-dwarfed phenotypes similar to the *ga20ox1 ga20ox2 ga20ox3* and *ga1-3* mutants (Figure 4.3). Phenotypic analysis

Figure 4.3: Mature rosette phenotypes of *ga20ox* combinatorial mutants (55 day old plants).

of these new mutant combinations was targeted to characters where differences between *ga20ox1 ga20ox2 ga20ox3-1* and *ga1-3* had been previously identified (7-day root length, n = 192; mature rosette diameter and flowering time, n = 48, see section 3.2.2), which might be caused by the continuing presence of *AtGA20ox4* or *-5*. The *ga20ox1 ga20ox2 ga20ox3-3* triple mutant was included in these experiments to verify the phenotypic results obtained previously from *ga20ox1 ga20ox2 ga20ox3-1*.

As previously found (see section 3.2.3), the difference in flowering times between *ga20ox1 ga20ox2 ga20ox3-1* and *ga1-3* was significant ($p < 0.01$), as measured both chronologically (days from sowing, Figure 4.4a) and developmentally (total leaves present at flowering, Figure 4.4b). Flowering time of *ga20ox1 ga20ox2 ga20ox3-1 ga20ox4-2* was significantly different from *ga20ox1 ga20ox2 ga20ox3-1* ($p < 0.01$) but not significantly different from *ga1-3* when measured by days, and was significantly different from both of these genotypes ($p < 0.01$) when measured by leaf number. In contrast, flowering time of *ga20ox1 ga20ox2 ga20ox3-1 ga20ox5-2* was not significantly different from *ga20ox1 ga20ox2 ga20ox3-1* on either scale of measurement, and was significantly different from *ga1-3* ($p < 0.01$) both chronologically and developmentally. This specific result suggests that *AtGA20ox4* has some function in promoting the transition to flowering in the absence of *AtGA20ox1*, *-2* and *-3*. However, the *ga20ox1 ga20ox2 ga20ox3-3* phenotype contradicts this conclusion, its chronological flowering time not differing significantly from *ga1-3* ($p > 0.01$). However, when measured on the developmental scale, *ga20ox1 ga20ox2 ga20ox3-3* is not significantly different from either *ga20ox1 ga20ox2 ga20ox3-1* or *ga20ox1 ga20ox2 ga20ox3-1 ga20ox4-2*, and like them is significantly different from *ga1-3* ($p < 0.01$). This apparent contradiction

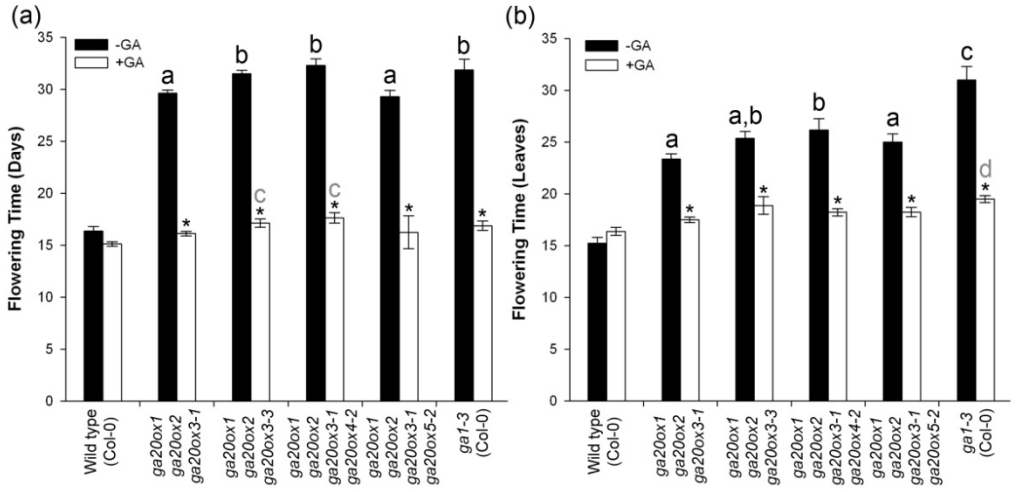

Figure 4.4: The effect of loss of *AtGA20ox4* or *-5* on *Arabidopsis* flowering.

Comparison of flowering time between genotypes, grown under control growth conditions or under GA treatment, as measured by the number of days from sowing (a) and total number of leaves (b) at the first appearance of flower buds.

Bars represent the mean of 8 independent measurements, error bars represent one S.E. Pairwise comparisons were made using a 1% LSD with a significance threshold of 1% between genotypes within the same GA treatment (Days = 1.793; Leaves = 2.610) and between GA treatments within the same genotype (Days = 1.937; Leaves = 2.527). Letters denote a significant difference from -GA wild type (black) or +GA wild type (grey), respectively. Genotypes marked with different letters are significantly different from one another. Asterisks denote a significant difference between GA treatments within the same genotype. Comparisons were not made between genotypes under different GA treatments.

between the phenotypes of the two *ga20ox 1 ga20ox2 ga20ox3* triple mutants might be explained by ecotypic differences, the *ga20ox3-3* allele having been derived from the L*er* background (see section 3.2.1). The growth phenotypes of Col-0 and L*er* are quite distinct (see chapter 6), and as such the difference in flowering time between the two triple mutant genotypes may represent pleiotropic effects due to the incorporation of other, L*er* ecotype-specific alleles in addition to *ga20ox3-3*. Both the *ga20ox4-2* and *ga20ox5-2* alleles were also introduced from other ecotypes (as was the *ga1-3* allele), and as such the validity of the results obtained from direct phenotypic comparisons between these 'hybrid' mutant genotypes can be questioned. GA treatment caused a significant acceleration in flowering time under both

scales of measurement for all mutants, although some remain significantly different from GA-treated wild type (Figure 4.4a and b). Ecotypic differences may also explain why flowering of *ga1-3* remains significantly different from both *ga20ox1 ga20ox2 ga20ox3-3* and *ga20ox1 ga20ox2 ga20ox3-1 ga20ox4-2* ($p < 0.01$) when measured developmentally (Figure 4.4b). Alternatively, these two genotypes might retain residual GA20ox activity, either from a known paralogue or potentially an unrelated gene. Despite these reservations, loss of *AtGA20ox4* activity from the *ga20ox1 ga20ox2 ga30ox3-1* background does apparently cause a significant further delay on flowering time, although a definite role for *AtGA20ox4* in this process has not been demonstrated conclusively.

Whilst the experimental results regarding flowering time of *ga20ox1 ga20ox2 ga20ox3-1* agree with those of earlier characterisation experiments, the phenotypic results obtained for both rosette size and root growth differ from previous findings, in that there were no significant differences observed between *ga20ox1 ga20ox2 ga20ox3-1* (or *ga20ox1 ga20ox2 ga20ox3-3*) and *ga1-3* (Table 4.1), indicating that loss of *AtGA20ox1*, *-2* and *-3* is sufficient to replicate the GA-deficient phenotype of *ga1-3* and thus excluding further functions for either *AtGA20ox4* or *-5*. Under control growth conditions all mutant genotypes were significantly different from wild type for both characters ($p < 0.01$), but not significantly different from one another. The effect of GA treatment on rosette growth of these mutants corresponds with previous experiments, but the effect of GA treatment on root growth does not (see section 3.2.2), instead causing a reduction in wild-type root growth on this occasion. The different results between these two experiments are therefore likely to be due to technical reasons, potentially through differences in growth conditions. Similar reasons could apply to differences in rosette diameter, or might be due to alterations in the experimental population affecting the statistical analysis.

It can be seen that an additional qualitative rosette phenotype is associated with these *ga20ox* mutants, in that their rosette leaves routinely exhibit strong curling, a phenotype far less evident in *ga1-3* plants (Figure 4.3). Both *ga20ox1 ga20ox2 ga20ox3-1 ga20ox4-2* and *ga20ox1 ga20ox2 ga20ox3-1 ga20ox5-2* exhibit leaf curling, so this phenotype cannot be

Genotype	7 Day Root Length (mm)		Rosette Diameter (mm)	
	-GA	+GA	-GA	+GA
Wild type (Col-0)	23.83	19.98*	113.80 [10.6630]	134.40* [11.5890]
ga20ox1 ga20ox2 ga20ox3-1	14.50[a]	17.47	75.38[a] [8.6690]	135.90* [11.6500]
ga20ox1 ga20ox2 ga20ox3-3	16.84[a]	20.78*	66.00[a] [8.1280]	169.40[b]* [12.9920]
ga20ox1 ga20ox2 ga20ox3-1 ga20ox4-2	14.22[a]	16.83	66.25[a] [8.4560]	163.90[b,c]* [12.8170]
ga20ox2 ga20ox2 ga20ox3-1 ga20ox5-1	17.06[a]	18.79	71.62[a] [8.4560]	145.50* [12.0530]
***ga1-3* (Col-0)**	13.98[a]	16.97	74.88[a] [8.6320]	151.60[c]* [12.3060]
1% LSD	***3.599*** *(3.673)*		***[0.6197]*** *([0.6967])*	

Table 4.1: Phenotypic analysis of *ga20ox* quadruple mutant vegetative characters.

Values given are means of 16 (roots) and 8 (rosettes) measurements, respectively. Rosette diameter data were analysed on a transformed scale (square root, denoted by square brackets) to meet the assumptions of the statistical model. Pairwise comparisons were made within each character using 1% LSDs, given in bold type for comparing between genotypes within a GA treatment and in rounded brackets for comparing between GA treatments within a genotype. Superscript letters denote significant difference of a genotype from wild type ($p < 0.01$) within that GA treatment. Different letters indicate genotypes significantly different from one another. Asterisks denote a significant difference between GA treatments within the same genotype. Comparisons were not made between genotypes in different GA treatments.

ascribed to the presence or absence of a particular paralogue. The phenotypic differences between these and *ga1-3* could be due either to residual activity of the single remaining *AtGA20ox* paralogue in each case, or potentially to hybrid ecotypic phenotypes in *ga1-3*.

The floral phenotypes of these mutants were all very similar (Figure 4.5), but also dependent on the inflorescence position examined, as was found previously for *ga20ox* mutants and *ga1-3* (see sections 3.2.5 and 3.2.7). Comparing floral phenotypes at approximately the 10th flower position (Figure 4.5a) suggests that differences in floral organ size exist between *ga20ox1ga20ox2 ga20ox3* mutants and *ga1-3*. Additional loss of *AtGA20ox4* might further

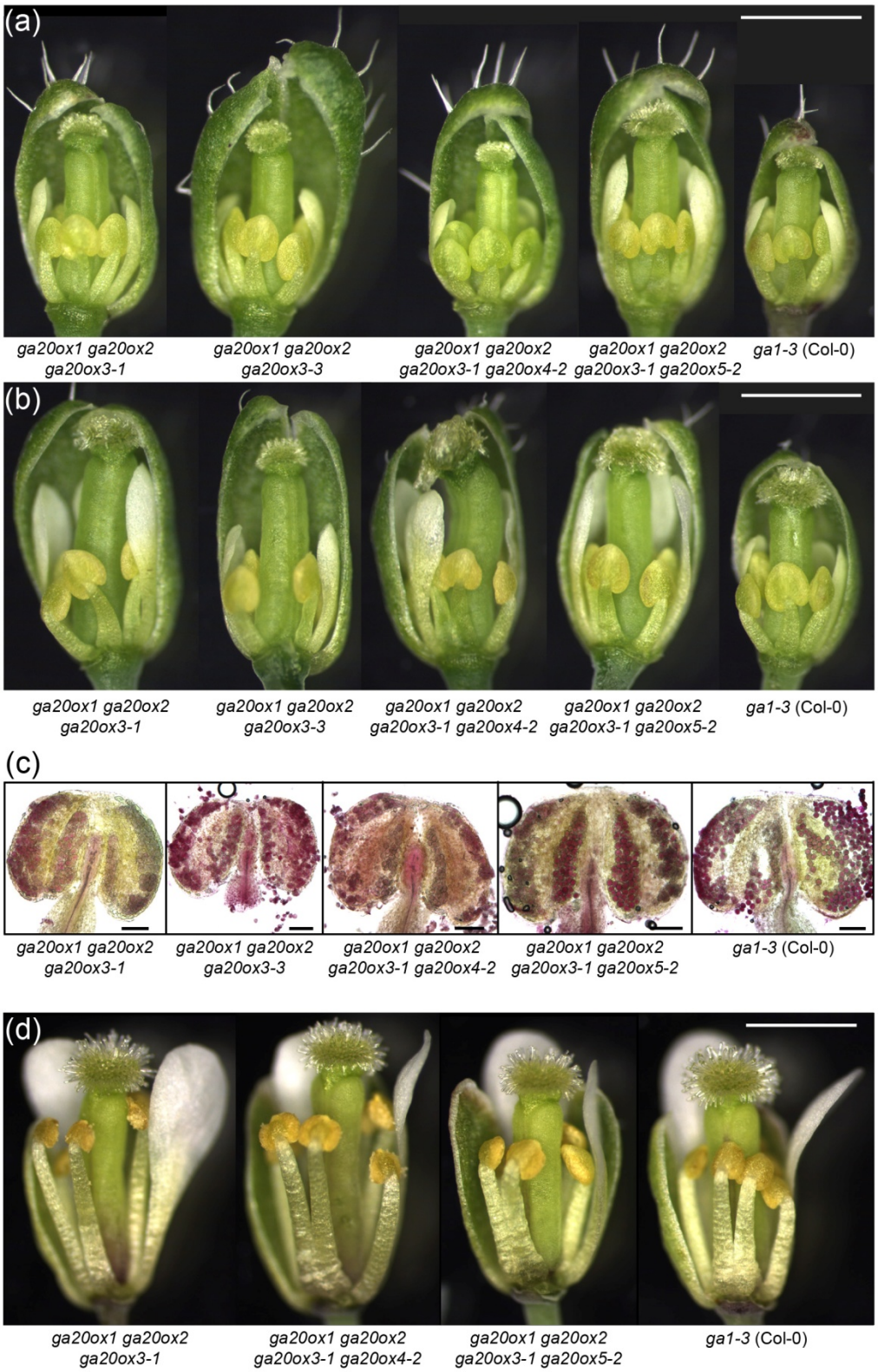

Figure 4.5: The effect of loss of *AtGA20ox4* or *-5* function on floral development. *Comparison between floral phenotypes of* ga20ox *combinatorial mutants (as shown) and* ga1-3*, with mature flower buds taken from approximately the 10th (a) and 15th (b) primary inflorescence positions, respectively. Scale bars = 1mm.*

(c) Comparative pollen viability staining of ga20ox *mutant anthers, harvested from flowers similar to those described in (b). Dark red staining indicates viable pollen; pale green staining indicates pollen that does not contain cytoplasm. Scale bars = 100µm.*
(d) Phenotypic rescue of late ga20ox *combinatorial mutant and* ga1-3 *flowers, taken from between inflorescence positions 20-25. Scale bar = 1mm.*

reduce floral organ growth, whilst loss of *AtGA20ox5* had no apparent effect at this stage. However, the closed nature of these GA-deficient flowers makes it difficult to synchronise development, and the possibility that the *ga20ox1 ga20ox2 ga20ox3-1 ga20ox4-2* buds observed may not have been fully developed cannot be completely discounted. Floral buds examined at approximately inflorescence position 15 (Figure 4.5b) did not show these differences, with all *ga20ox* combinatorial mutant flowers appearing very similar whilst *ga1-3* flowers were still apparently smaller. However, in all genotypes studied floral organ growth had increased between these two inflorescence positions, most notably the pistil and petals. Furthermore, pollen from *ga1-3* anthers taken from flowers at inflorescence 15 stained as viable (Figure 4.5c), in contrast to similar experiments comparing flowers from earlier inflorescence positions (see section 3.2.4). These results suggest that floral development progresses further in later flowers of *ga1-3*, consistent with the floral phenotypes presented in section 3.2.7. A more detailed analysis of pollen development in these flowers (Figure 4.6) found tricellular pollen present in all *ga20ox* combinatorial mutants examined and also in *ga1-3*. It should be noted that in the case of *ga20ox1 ga20ox2 ga20ox3-1 ga20ox4-2*, tricellular pollen was far rarer than in other genotypes. These results apparently contradict previously published results in which *ga1-3* pollen development arrested at the unicellular stage, prior to pollen mitosis I (Cheng et al., 2004). This might be accounted for by ecotypic differences, as the previous study was conducted in the L*er* background, or potentially technical differences between experiments such as growth conditions. However, even then, the block on pollen development previously recorded was not absolute, with approximately 6% of microspores containing two or more nuclei, and the stage of flowering from which these results were obtained is not specified. These observations are therefore not incompatible with previously published findings, and suggest that the block on pollen development is relaxed in later

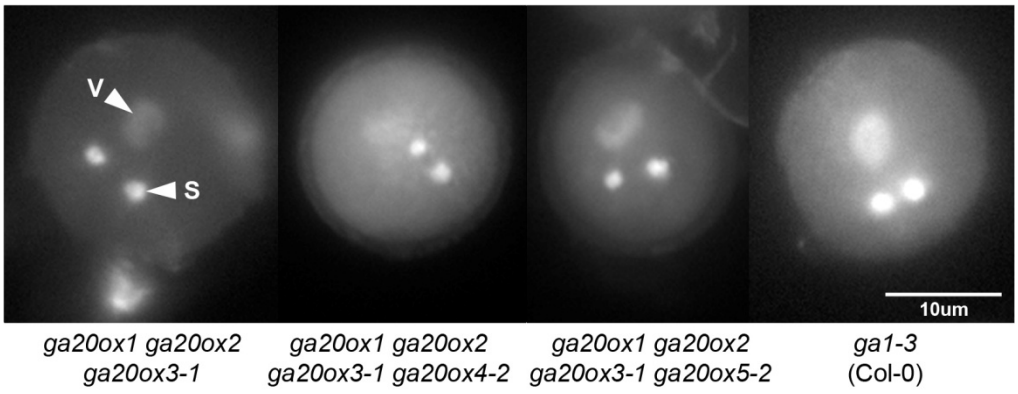

Figure 4.6: Pollen development in GA-deficient flowers.

Pollen nuclei imaged by DAPI fluorescent stain (Ruzin, 1999). Pollen shown is tricellular in each case, with the nuclei of the vegetative cell (V) and the two sperm cells (S) visible.

flowers even in the absence of bioactive GA. They also provide further evidence for a gradual rescue of floral organ growth independent of GA biosynthesis. Flowers taken from these mutants even later in flowering (inflorescence positions 20-25) were indistinguishable from one another, including those of *ga1-3*. Flowers by this point developed sufficiently to open, and demonstrated a significant improvement in stamen growth (Figure 4.5d). Fertility of these flowers was not tested experimentally.

The inheritance of the *ga20ox4-2* allele between generations was analysed to test whether loss of *AtGA20ox4* has any impact on post-anthesis pollen development and fitness. Previous analysis testing the inheritance of *AtGA20ox1*, *-2* and *-3* raised the possibility that development of GA-deficient pollen is rescued by GA synthesised by maternal tissues carrying functional copies of all three of these paralogues (see section 3.2.3). In an attempt to unmask any mutant phenotypes in post-anthesis pollen development, this experiment was performed in the *ga20ox1 ga20ox2* background, in which GA biosynthesis is reduced whilst fertility remains relatively unaffected (Rieu et al., 2008). The inheritance of both *ga20ox3-1* and *ga20ox4-2* was scored in the F_2 progeny of a self-pollinating *ga20ox1 ga20ox2 GA20ox3*/*ga20ox3-1 GA20ox4*/*ga20ox4-2* plant (n = 91) grown without chemical GA treatment. No significant distortion from Mendelian segregation ratios was observed (p = 0.1837, Table 4.2), including the frequency of severely GA-deficient genotypes

Genotype	Expected Freq. (E)	Observed Freq. (O)	O-E	$(O-E)^2$	$(O-E)^2/E$
GA20ox3; GA20ox4	5.6875	4	-1.6875	2.848	0.50069
GA20ox3/ga20ox3-1; GA20ox4	11.375	4	-7.3750	54.390	4.78159
ga20ox3-1; GA20ox4	5.6875	5	-0.6875	0.473	0.08310
GA20ox3; GA20ox4/ga20ox4-2	11.375	16	4.6250	21.390	1.88049
GA20ox3; ga20ox4-2	5.6875	6	0.3125	0.098	0.01717
GA20ox3/ga20ox3-1; GA20ox4/ga20ox4-2	22.75	24	1.2500	1.563	0.06868
ga20ox3-1; GA20ox4/ga20ox4-2	11.375	9	-2.375	5.641	0.49588
GA20ox3/ga20ox3-1; ga20ox4-2	11.375	13	1.6250	2.641	0.23214
ga20ox3-1; ga20ox4-2	5.6875	10	4.3125	18.600	3.26992
				$X^2 = 11.3297$	
				(D.f. = 8)	
				p = 0.1837	

Table 4.2: Segregation distortion analysis of the *ga20ox3-1* and *ga20ox4-2* loss-of-function alleles.

Chi-squared statistical analysis of the segregation of ga20ox3-1 *and* ga20ox4-2 *alleles in the* ga20ox1 ga20ox2 *background against the null hypothesis of no fitness penalty for either allele. Experimental population size = 91.*

(*ga20ox1 ga20ox2 ga20ox3-1* and *ga20ox1 ga20ox2 ga20ox3-1 ga20ox4-2*). This result could be taken to indicate that neither *AtGA20ox3* nor *AtGA20ox4* has a function in post-anthesis pollen development. However, pollen in this experiment was developing on and through maternal tissues carrying functional copies of both of these genes, and as such mutant pollen phenotypes could still be being masked by GA biosynthesis in maternal tissues. The female infertility demonstrated by *ga20ox1 ga20ox2 ga20ox3-1* and *ga1-3* (see section 3.2.3) prevents this hypothesis from being tested *in planta* through this methodology.

Despite some evidence of *AtGA20ox4* promoting flowering in *ga20ox1 ga20ox2 ga20ox3-1*, no definite role for either *AtGA20ox4* or *-5* in promoting plant growth has been conclusively demonstrated in the developmental contexts included in these analyses, characterisation experiments having failed to validate phenotypic differences between *ga20ox1 ga20ox2*

ga20ox3-1 and *ga1-3*. That said, functions for *AtGA20ox4* and *-5* in other aspects of plant development cannot be conclusively ruled out. In particular, broad-scale expression mapping identified the highest expression of *AtGA20ox5* in developing siliques, a stage of development not covered in this project. Also, plants for all characterisation experiments in this project were grown under controlled, optimal environmental conditions. In future, AtGA20ox4 or -5 might be found to make significant contributions to growth under sub-optimal conditions.

Together with the observations of section 3.2.7, these results also suggest that stamen developmental arrest seen in severely GA-deficient mutants can be overridden by other factors. The mechanism underlying this is unknown, but seems to be a gradual process that acts across flowering, causing quantitative phenotypic recovery with increasing inflorescence position. The fact that the same phenotypic changes are observed in all *ga20ox* combinatorial genotypes and *ga1-3* argues that this process is independent or downstream of GA biosynthesis. Expression of *AtGID1* has been shown to be feedback-regulated (Griffiths et al., 2006), and *AtGID1B* expression is significantly up-regulated in *ga20ox1 ga20ox2* plant tissues (Rieu et al., 2008). Whether such changes in expression occur in inflorescence tissues during flowering has not been previously addressed.

4.2.3 AtGA20ox5 Does Not Possess Full GA 20-Oxidase Activity

Having established that AtGA20ox4 possesses full GA20ox activity during characterisation of the *ga20ox4* mutant alleles (see section 4.2.1), catalytic activity of the *AtGA20ox5* paralogue was similarly tested *in vitro* via bacterial expression of wild-type protein. Activity of AtGA20ox5 was compared against AtGA20ox1, which demonstrates full GA20ox catalytic activity (Phillips et al., 1995). After 24 hours incubation, lysates expressing AtGA20ox1 showed partial conversion of radiolabelled GA_{12} to GA_9, whereas no GA_9 was detected in lysates expressing AtGA20ox5 (Figure 4.7a), which instead showed an accumulation of GA_{24}, the immediate precursor to GA_9. Samples from the same lysates were also incubated with radiolabelled GA_{24} for 24 hours to directly test catalytic activity of the final oxidation step. AtGA20ox1 catalysed full conversion of GA_{24} to GA_9, whilst no GA_9 was recovered from lysates containing AtGA20ox5 (Figure 4.7b).

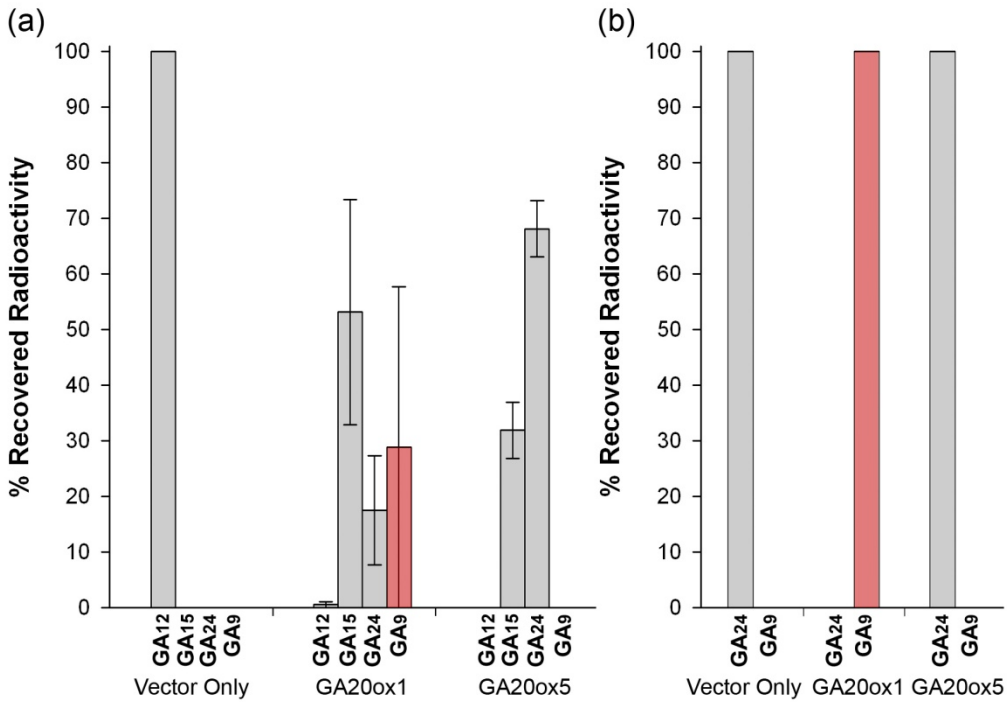

Figure 4.7: *In vitro* analysis of AtGA20ox5 catalytic activity.

Bacterially-expressed AtGA20ox1and AtGA20ox5 were incubated with radiolabelled substrate for 24 hours, either GA_{12} (a) or GA_{24} (b), the products subsequently identified by HPLC. Graphs represent the mean of two technical replicates, error bars represent one S.E. Where produced, the final product of GA20ox activity (GA_9) is highlighted in red.

These results demonstrate that AtGA20ox5 can catalyse GA_{12} to GA_{24} *in vitro*, but cannot perform the final oxidative step associated with canonical GA20ox activity. No unidentified peaks of radioactivity were present in these assays, indicating that no alternative GA products were produced by AtGA20ox5. As such, AtGA20ox5 represents a paralogue with only partial GA20ox function, and therefore probably requires the presence of another, fully functional GA20ox to allow synthesis of bioactive GA.

4.2.4 Overexpression of *AtGA20ox5* Partially Rescues Growth in *ga20ox1 ga20ox2 ga20ox3-1*

To test the hypothesis that AtGA20ox5 lacks full GA20ox activity *in planta*, a cDNA clone of this paralogue was constitutively expressed, driven by the 35S promoter (Figure 4.8a) in the *ga20ox1 ga20ox2 ga20ox3-1* mutant background. As a positive control, a cDNA clone of

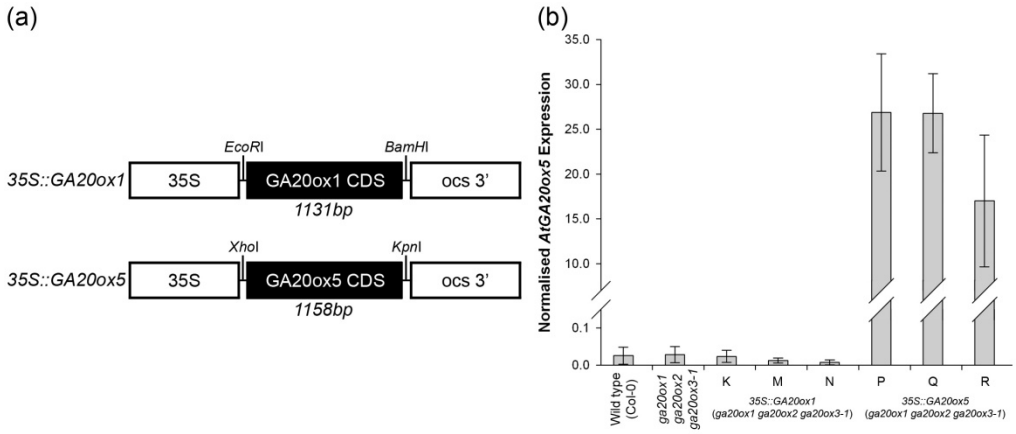

Figure 4.8: Transgenic overexpression of *AtGA20ox1* and *-5* in the *ga20ox1 ga20ox2 ga20ox3-1* background.

(a) Schematic of transgenic overexpression constructs. Black boxes indicate a complete coding sequence (CDS) for each gene derived from cDNA clones, white boxes indicate regulatory elements from the pMS37 vector (see section 2.1.2).

(b) AtGA20ox5 *expression in control and transgenic 5-day old seedlings (as shown). K, M and N and P, Q and R each represent lines from separate transformation events for their respective transgene. Bars are means of three biological replicates, error bars represent one S.E. Each biological replicate represents RNA pooled from 15 seedlings.*

AtGA20ox1 was similarly expressed. Three homozygous lines of each transgene, each representing a separate transformation event, were selected for analysis at the T_3 generation. Overexpression of *AtGA20ox5* in the *35S::GA20ox5* lines was confirmed in 5-day old seedlings by qPCR (Figure 4.8b), by which stage transgenic lines were already demonstrating enhanced growth phenotypes (data not shown). Expression levels of *AtGA20ox5* were found to be unaffected in the *ga20ox1 ga20ox2 ga20ox3-1* background compared to wild type, and in *ga20ox1 ga20ox2 ga20ox3-1* plants expressing *35S::GA20ox1*. The level of *AtGA20ox5* expression in *35S::GA20ox5* (*ga20ox1 ga20ox2 ga20ox3-1*) lines was up to three orders of magnitude higher than that seen in wild type. These results clearly demonstrate that the *35S::GA20ox5* (*ga20ox1 ga20ox2 ga20ox3-1*) transgenic lines are specifically overexpressing *AtGA20ox5*, and that any observed phenotypes in these lines can be ascribed to the action of this paralogue.

The phenotypes of these transgenic lines were compared with those of wild type and *ga20ox1 ga20ox2 ga20ox3-1*, and an additional transgenic line expressing *35S::GA20ox1* in the wild-type background (n = 144), to determine to what extent AtGA20ox5 activity complements the GA-deficient phenotypes of *ga20ox1 ga20ox2 ga20ox3-1*. By maturity (33 days), *ga20ox1 ga20ox2 ga20ox3-1* plants constitutively expressing *AtGA20ox1* demonstrated complete rescue of their vegetative phenotype, similar to that of *35S::AtGA20ox1* in wild type (Figure 4.9a). Constitutive expression of *AtGA20ox5*, in contrast, caused a significant rescue of vegetative growth but not to the extent seen in wild type. In terms of fertility, constitutive expression of *AtGA20ox1* in *ga20ox1 ga20ox2 ga20ox3-1* restored silique-set throughout the primary inflorescence (Figure 4.9b), whilst *ga20ox1 ga20ox2 ga20ox3-1* plants constitutively expressing *AtGA20ox5* failed to set siliques at early inflorescence positions, with fertility only being restored during later flowering (Figure 4.9c). This phenotype can be attributed to reduced stamen growth in early *35S::GA20ox5* (*ga20ox1 ga20ox2 ga20ox3-1*) flowers (Figure 4.9d), with later flowers demonstrating full length stamens (relative to the pistil) at flower opening (Figure 4.9e). In contrast, early flowers from *35S::GA20ox1* (*ga20ox1 ga20ox2 ga20ox3-1*) demonstrate full length stamens at flower opening (Figure 4.9d), and subsequently exhibit stamen overgrowth in later flowers (Figure4.8e). This effect is also visible in wild type and *35S::GA20ox1* (Col-0) flowers, as is substantial rescue of stamen growth in *ga20ox1 ga20ox2 ga20ox3-1*. The changes in stamen length therefore probably reflect the same underlying changes in stamen length observed elsewhere in this project (see sections 3.2.5, 3.2.7 and 4.2.2).

Statistical analysis of flowering time found that constitutive expression of *GA20ox1* in *ga20ox1 ga20ox2 ga20ox3-1* completely rescues flowering under long day growth conditions, whilst the *ga20ox1 ga20ox2 ga20ox3-1* control plants exhibit a significant delay relative to wild type ($p < 0.01$). When measured by days from sowing (Figure 4.10a) all three transgenic lines exhibit a GA-overdosed phenotype significantly different from wild type ($p < 0.01$), flowering earlier than wild type. When measured developmentally (in terms of number of leaves at flowering, Figure 4.10b), flowering in these lines is either not significantly different from wild type (lines K and M) or accelerated ($p < 0.01$; line N), demonstrating a phenotype

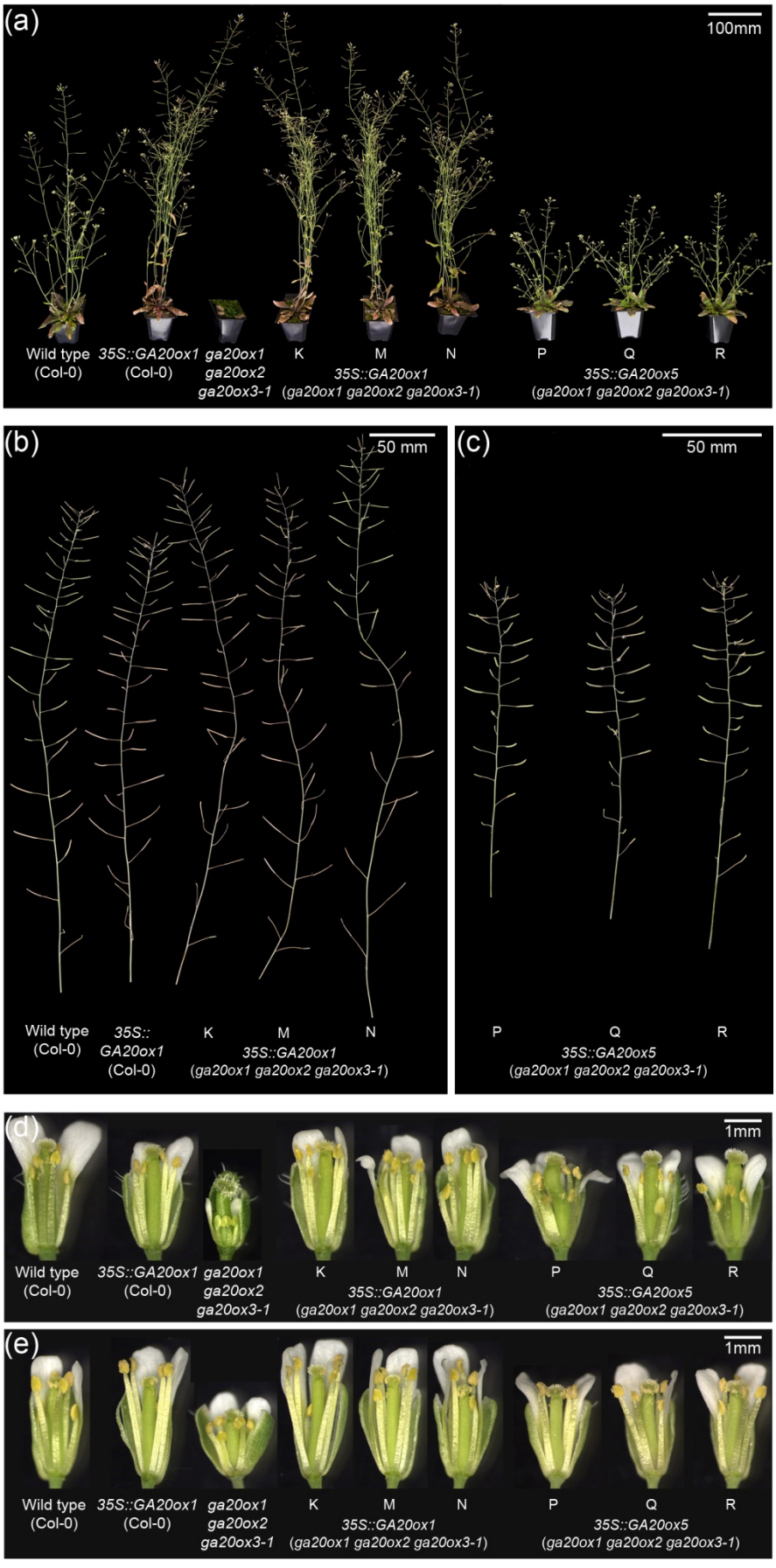

Figure 4.9: Phenotypic effects of constitutive *AtGA20ox5* expression.

Three independent homozygous lines are shown for each transgene, labelled K, M and N for 35S::GA20ox1 *(*ga20ox1 ga20ox2 ga20ox3-1*) and P, Q, and R for* 35S::GA20ox5 *(*ga20ox1 ga20ox2 ga20ox3-1*). Whole plant phenotypes (a) are shown at 33 days. Primary inflorescences from control and transgenic lines (b and c) were isolated and photographed once flowering had stopped (40 days). By this time* ga20ox1 ga20ox2 ga20ox3-1 *had not begun to bolt. Flowers were taken and photographed as they opened during two phases of flowering, between inflorescence positions 1-5 (d) and positions 20-25 (e). Plants grown under chemical GA treatment not shown.*

similar to *35S::GA20ox1* (Col-0). Similar to its effects on vegetative phenotype, constitutive expression of *GA20ox5* in *ga20ox1 ga20ox2 ga20ox3-1* caused a partial rescue in flowering time in all three transgenic lines across both measurements of flowering time ($p < 0.01$), though they remain significantly different from wild type ($p < 0.01$) and still exhibit delayed flowering. Flowering time was completely rescued by chemical GA treatment. These results indicate that ectopic expression of *AtGA20ox5* can partially complement GA-deficient phenotypes during both vegetative and reproductive development, indicating that GA biosynthesis has been increased. This result is somewhat unexpected in light of the *in vitro* evidence that AtGA20ox5 lacks full GA20ox activity (see section 4.2.3), but can be explained by the continued activity of AtGA20ox4 (a fully functional GA20ox enzyme) in these transgenic lines. AtGA20ox5 could conceivably enhance GA biosynthesis through its capacity to catalyse the first two oxidation reactions of GA20ox activity, increasing the flux of GA intermediates through the GA20ox reaction series and thus the concentration of GA_{24} available to AtGA20ox4, increasing the quantity of GA_9 produced.

To test the dependence of AtGA20ox5 on AtGA20ox4 to rescue growth in *ga20ox1 ga20ox2 ga20ox3-1*, the *35S::GA20ox5* expression cassette was crossed into the *ga20ox1 ga20ox2 ga20ox3-1 ga20ox4-2* background, and the phenotypes compared in the F_2 generation. Substantial rescue of the *ga20ox1 ga20ox2 ga20ox3-1 ga20ox4-2* dwarf phenotype still occurred in these transgenic lines, which demonstrated close similarity to *35S::GA20ox5* (*ga20ox1 ga20ox2 ga20ox3-1*) sibling plants (Figure 4.11a). From this result, it must be

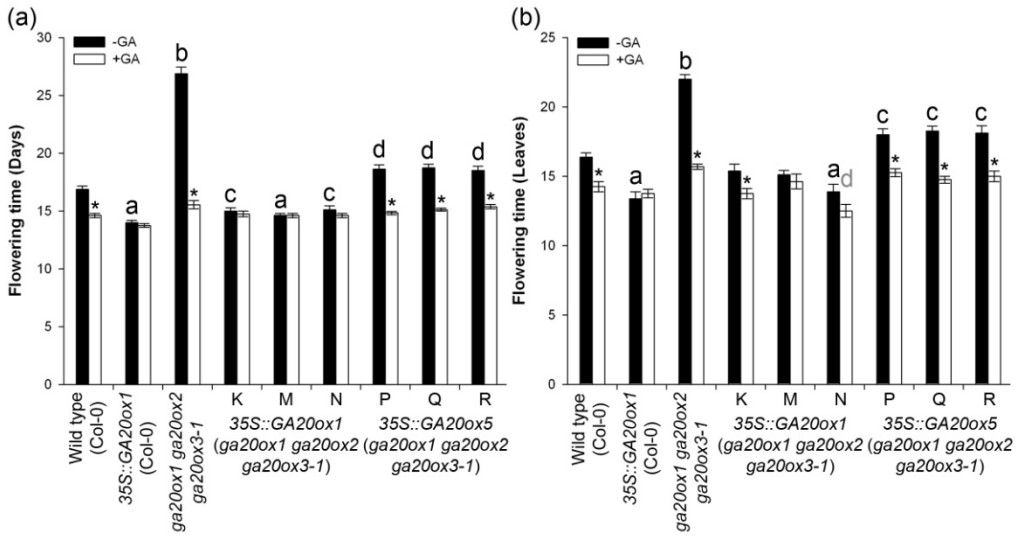

Figure 4.10: The effect of constitutive *AtGA20ox5* expression on flowering time. *Comparison of flowering time between control genotypes and transgenic lines under control growth conditions and chemical GA treatment, as measured by the number of days from sowing (a) and the total number of leaves at flowering (b). Graphs represent the mean of 16 measurements for each combination of genotype and GA treatment, error bars represent one S.E. Pairwise comparisons were made using 1% LSDs between genotypes within the same GA treatment (Days = 0.9977; Leaves = 1.4947) and between GA treatments within the same genotype (Days = 1.0214; Leaves = 1.4709). Letters denote a significant difference from -GA wild type (black) or +GA wild type (grey), respectively. Genotypes marked with different letters are significantly different from one another. Asterisks denote a significant difference between GA treatments within the same genotype. Comparisons were not made between genotypes in different GA treatments.*

concluded that phenotypic rescue from overexpression of *AtGA20ox5* is not likely due to the supporting activity of another GA20ox enzyme, on the assumption that no other 2-ODD apart from the *GA20ox* gene family possesses GA20ox activity. A number of possible explanations present themselves. Firstly, although not supported by *in vitro* results (Figure 4.7b), AtGA20ox5 might convert some GA_{24} into GA_9 *in planta*, thus allowing GA biosynthesis to continue. Another possibility is that an alternative pathway exists within these plants through which a bioactive form of GA is being synthesised. Given its dependence on AtGA20ox5, this pathway cannot be entirely independent of GA20ox activity. However, it must be borne

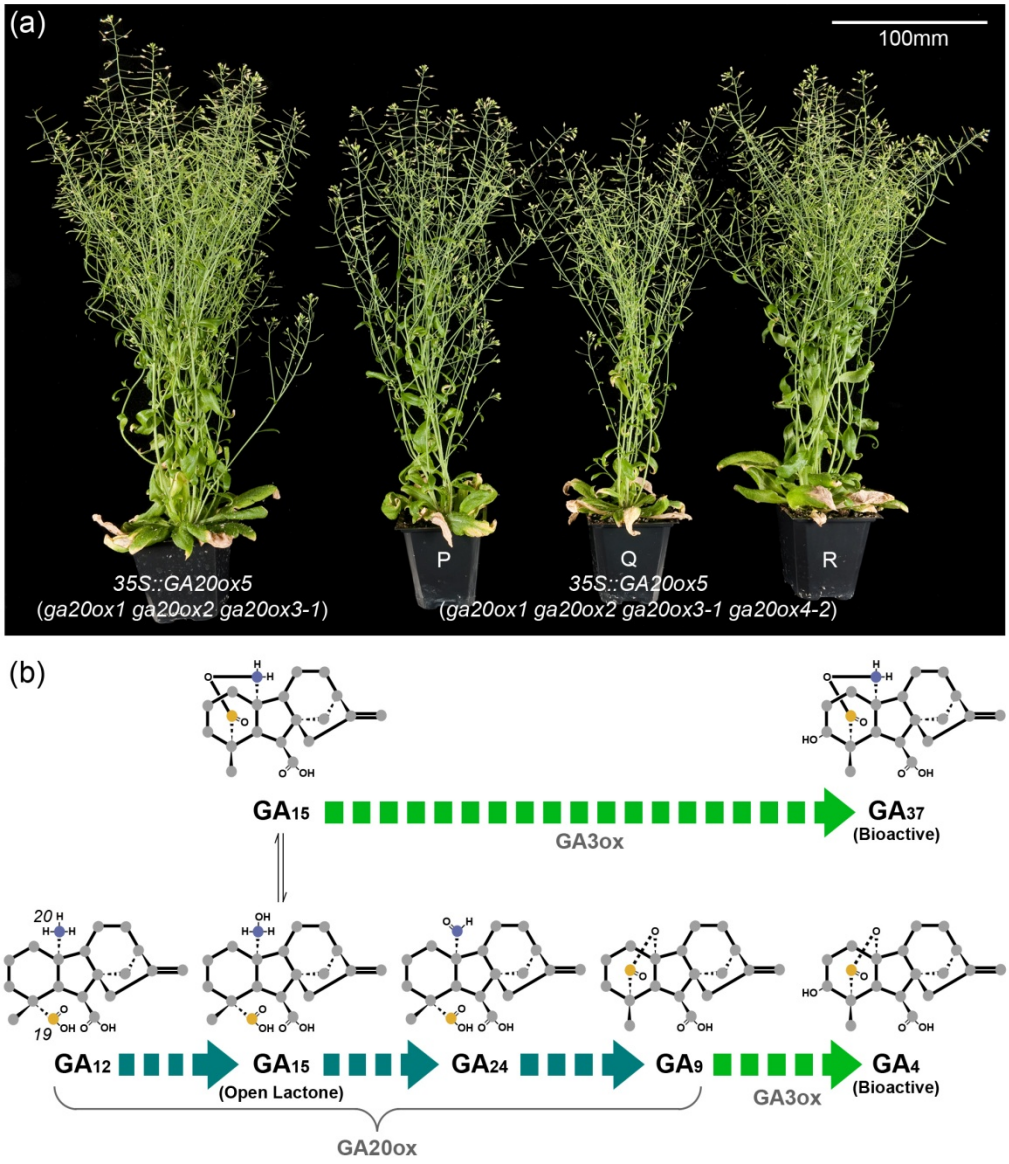

Figure 4.11: The effect of constitutive *AtGA20ox5* expression in the absence of other *AtGA20ox* paralogues.

(a) Phenotypic comparison of 43-day old plants constitutively expressing AtGA20ox5 *in the* ga20ox1 ga20ox2 ga20ox3-1 *and* ga20ox1 ga20ox2 ga20ox3-1 ga20ox4-2 *GA-deficient backgrounds. The quadruple mutant transgenic plants shown are derived from three independent crosses, each from an independent* ga20ox1 ga20ox2 ga20ox3-1 *transgenic line (see Figure 4.7). The 35S::GA20ox5 (ga20ox1 ga20ox2 ga20ox3-1) plant shown is an* F_2 *sibling from line P.*

(b) Schematic diagram of GA biosynthesis, summarising a potential alternative pathway to the synthesis of bioactive GA in the absence of the canonical GA20ox biosynthesis pathway.

in mind that HPLC-based identification of the products of GA20ox activity relies on comparison of retention times against known GA species, thus the identity of the products of AtGA20ox5 activity from these *in vitro* experiments remains subject to doubt. No other peaks of radiation were observed, but the possibility exists, albeit small, that other GA species with similar retention times are produced by this enzyme. Products from previous, similar experiments testing the catalytic activity of wild-type AtGA20ox5 were analysed by GC-MS and identified as GA_{15} and GA_{24}, with the biologically-inactive C_{20}-GA species GA_{25} also present within the GA_{24} peak (Hedden, P., personal communication). A GA20ox enzyme expressed in pumpkin endosperm, CmGA20ox1, has been previously found to display unusual catalytic activity, converting only a small proportion of C_{20}-GA substrate to C_{19}-GAs *in vitro* and preferentially producing GA_{25} (Radi et al., 2006).

There is evidence for at least one alternative GA biosynthesis pathway through the intermediate GA_{15}, which, according to a model whereby AtGA20ox5 activity stops with the production of GA_{24}, would be expected to accumulate in plants overexpressing *AtGA20ox5* in the absence of other, fully functional GA20ox paralogues. GA_{15} lactonises at low pH (Figure 4.11b), and is formed as an artefact following acidification when GAs are extracted for analysis (Hedden, P., personal communication). Results from a cell-free assay in pea and *in vitro* analysis of a recombinant *Arabidopsis* GA20ox clone demonstrate that GA_{15} open-lactone is the actual substrate for GA20ox activity in these species, whilst the lactonised form is not recognised (Kamiya & Graebe, 1983; Ward et al., 1997). However, analysis of recombinant AtGA3ox1 activity in cell-free systems found that the lactonised form of GA_{15} is converted to GA_{37} by this enzyme (Williams et al., 1998), suggesting that its structure sufficiently mimics that of GA_9 to be accepted as a substrate. Other C_{20}-GAs were 3β-hydroxylated by AtGA3ox1 in the same study, and GA analysis has isolated 3β-hydroxylated C_{20}-GAs, including GA_{37}, from *Arabidopsis* shoot tissues (Talon et al., 1990). Bioassays in numerous species demonstrate that application of GA_{37} elicits some growth response, indicative of bioactivity (Graebe & Ropers, 1978). As such, an accumulation of GA_{15} open-lactone in the *35S::GA20ox5* lines described above could encourage accumulation of the lactonised GA_{15}, and thus lead to accumulation of GA_{37}. This hypothesis remains to be tested

by GA analysis of tissues from these transgenic lines. Whilst the severity of the dwarfism exhibited by the two *ga20ox1 ga20ox2 ga20ox3-1 ga20ox4-2* described in section 4.2.2 indicates that under less artificial circumstances the activity of AtGA20ox5 is not sufficient for this pathway to have significant phenotypic effects, this result nevertheless suggests that, although the canonical GA20ox pathway is the predominant route to the synthesis of bioactive GA in higher plants, the GA biosynthesis pathway has the capacity for flexibility.

4.3 CONCLUSIONS

The *in vitro* protein activity results presented in this chapter demonstrate that AtGA20ox4 possesses full canonical GA20ox activity, whilst AtGA20ox5 displays only partial GA20ox activity, catalysing the conversion of GA_{12} through to GA_{24}, but not GA_9. Despite the evidence from previous experiments presented in chapter 3, phenotypic analysis of higher order *ga20ox* loss-of-function mutants created during this project only partially supports a function for *AtGA20ox* paralogues outside of *AtGA20ox1*, *-2* and *-3*, with the triple mutant in many cases not being significantly different from *ga1-3* in these repeat experiments. Comparison between the *ga20ox1 ga20ox2ga20ox3-1* and *ga20ox1 ga20ox2 ga20ox3-1 ga20ox4-2* mutants suggests a minor role for *AtGA20ox4* in promoting flowering. These results also demonstrate variations in phenotype between the *ga20ox1 ga20ox2 ga20ox3-1* and *ga20ox1 ga20ox2 ga20ox3-3* mutants, which might be due to ecotypic variations introduced from the different mutant backgrounds during breeding of these combinatorial mutants.

Despite the failure of AtGA20ox5 to convert GA_{24} to GA_9 *in vitro*, constitutive expression of AtGA20ox5 in both the *ga20ox1 ga20ox2 ga20ox3-1* and *ga20ox1 ga20ox2 ga20ox3-1 ga20ox4-2* mutant backgrounds causes substantial phenotypic rescue. With the absence of other fully functional GA20ox paralogues in these lines, synthesis of bioactive GA might occur through an alternative pathway. Evidence from past literature raises the possibility of a bioactive C_{20}-GA (GA_{37}) being produced via accumulation of GA_{15} in these lines, subsequently converted to GA_{37} by AtGA3ox1. Whilst having little biological relevance during wild-type plant growth, if validated by GA analysis this result highlights the inherent flexibility of the GA biosynthesis pathway that might prove a useful tool for future research.

CHAPTER 5: PROFILING *ATGA20OX* GENE EXPRESSION DURING FLORAL DEVELOPMENT

5.1 INTRODUCTION

Previous analysis of floral organ lengths in this project (see section 3.2.5) has raised the hypothesis that individual *AtGA20ox* paralogues have complementary functions in promoting the growth of stamens (*AtGA20ox1*) and pistils (*AtGA20ox2*). The simplest mechanism to explain this is differential expression of the *AtGA20ox* genes in reproductive tissues during floral development. Little is currently known about the expression patterns of the *AtGA20ox* genes, although expression analysis based on whole inflorescences indicates that *AtGA20ox1* and *-2* are the most highly expressed (Rieu et al., 2008; Figure 3.1c). The floral phenotypes of *ga20ox* mutants earlier in this project suggest a relatively minor role for at least *AtGA20ox3*, though contributions of *AtGA20ox4* and *-5* have not been specifically tested.

Reported expression patterns of *AtGA3ox* genes indicate that the sites of GA biosynthesis during *Arabidopsis* floral development include the stamen, receptacle and (to a lesser extent) the pistil and sepal (Mitchum et al., 2006, Hu et al., 2008; Figure 1.10). Within the *AtGA3ox* gene family expression is not divided by floral organ. *AtGA3ox1* demonstrates a broad expression pattern encompassing the stamen filament, pistil tissues and receptacle, whilst *AtGA3ox2*, *-3* and *-4* are restricted to the anther (see section 1.5.3). GA3ox enzymes are dependent upon GA20ox activity for a supply of substrate (GA_9 in *Arabidopsis*, Talon et al., 1990) to synthesise bioactive GA, and as such loss of GA20ox activity affects growth of particular floral organs by restricting the availability of GA_9. In pea, the mobility of an alternative GA20ox product, GA_{20}, between tissues has been demonstrated through radiolabelling (Proebsting et al., 1992), suggesting that GA20ox activity in remote floral tissues might be able to partially compensate for its absence from other floral organs. This may explain the functional redundancy between *AtGA20ox1* and *-2*, as demonstrated by the *ga20ox1 ga20ox2* floral phenotype, and also how *AtGA20ox3* promotes floral organ growth of *ga20ox1 ga20ox2* in comparison with *ga1-3* (Figure 3.10). Alternatively, *AtGA20ox3* expression has been shown to be up-regulated in *ga20ox1 ga20ox2* inflorescence tissues (Rieu

et al., 2008), and it could be that expression of *AtGA20ox3* coincides with *AtGA20ox1* and/or -*2* and thus maintains GA20ox activity in their absence.

A further hypothesis arising from earlier work in this project is that *AtGA20ox1*, -*2* and -*3* all act to promote programmed cell death (PCD) in the tapetum cell layer (see section 3.2.4). The requirement for GA signalling to promote entry of the tapetum into PCD has been demonstrated in rice (Aya et al., 2009, see section 1.5.3), and *AtGA3ox* expression has been reported in tapetal cells immediately prior to PCD (Hu et al., 2008; Figure 1.10). Tapetal expression of *AtGA20ox* paralogues has not been previously demonstrated, though tapetal *GA20ox* expression has been localised in rice (Kaneko et al., 2003; Hirano et al., 2008) and tomato (Rebers et al., 1999).

This chapter presents expression evidence from semi-quantitative real-time PCR (qPCR) and *AtGA20ox::GUS* transgenic reporter lines created during this project indicating that *AtGA20ox* paralogues display individual expression patterns during floral development. *AtGA20ox* expression in the pistil is dominated by *AtGA20ox2*, whilst both *AtGA20ox1* and -*2* are expressed in developing stamens. *AtGA20ox3* expression is negligible in wild-type floral tissues in comparison to *AtGA20ox1* and -*2* (as are *AtGA20ox4* and -*5*), but is up-regulated in reproductive organs in the *ga20ox1 ga20ox2* mutant. GUS staining indicates that the tissue expression patterns of *AtGA20ox* and *AtGA3ox* partially overlap, but that anther expression of *AtGA20ox* may slightly precede *AtGA3ox*. Microscopic analysis of GUS-stained anther tissues indicates that *AtGA20ox1*, -*2*, -*3* and -*4* are each expressed specifically in tapetal cells prior to PCD.

5.2 RESULTS AND DISCUSSION

5.2.1 Differences in Stamen Growth Between *AtGA20ox* Loss-of-Function Mutants Manifests During Late Floral Development

In order to identify the stages of floral development in which *AtGA20ox* expression has the greatest effect on floral organ growth, floral organ lengths during development were measured

in *ga20ox* combinatorial loss-of-function mutants (n = 70), analysing a window of development on the primary inflorescence centred on the point of flower opening (denoted as 'floral bud 0'), encompassing floral organ growth prior to flower opening (to bud -8) and post-anthesis (to bud +4, Figure 5.1a). To compensate for changes in floral organ lengths that occur with increasing inflorescence position (see section 3.2.5), all inflorescences were synchronised by harvesting at the opening of flower 10. It was not technically feasible to analyse either *ga20ox1 ga20ox2 ga20ox3-1* or *ga1-3* by this method as neither genotype produces open flowers during this phase of flowering and so development could not be rigorously compared. Floral organ lengths were compared between genotypes within the same bud positions using ANOVA.

Analysis of each floral organ type found a significant interaction between genotype and bud position ($p < 0.001$ for each). However, the only significant differences in length compared to wild type were found in *ga20ox1 ga20ox2* ($p < 0.01$, all floral organs, Figure 5.1b-d), the only exceptions being petals of *ga20ox1* and *ga20ox1 ga20ox3-1*, which were significantly different from wild type at bud position -8 only ($p < 0.01$, not shown), and sepals of both *ga20ox1* (buds -7 and -8) and *ga20ox1 ga20ox3-1* (buds 1, 2 and 3, $p < 0.01$). Differences in length between wild type and *ga20ox1 ga20ox2* pistils are significant only after flower opening (buds 2 to 4, Figure 5.1b), whilst significant differences first occur between stamens just prior to flower opening (bud -1 to 4, Figure 5.1c). After flower opening, pistil growth increases dramatically in the wild type and most mutants due to successful pollination and the beginning of silique development (Figure 5.1a and b). The reduced pistil/silique growth observed in *ga20ox1 ga20ox2*, also observed by Rieu et al. (2008), can in part be ascribed reduced pollination success (see section 3.2.5) as well direct effects on pistil tissue growth.

Stamen growth is gradual across most of the developing flower buds sampled (Figure 5.1c), but exhibits a dramatic increase during flower opening (bud -1 to 1), correlated to floral stages 12 and 13 (Smyth et al., 1990). *ga20ox1 ga20ox2* still demonstrates an acceleration of stamen growth at this stage, but the magnitude and final stamen length are both significantly reduced compared to wild type. These results support the earlier conclusions of this project that

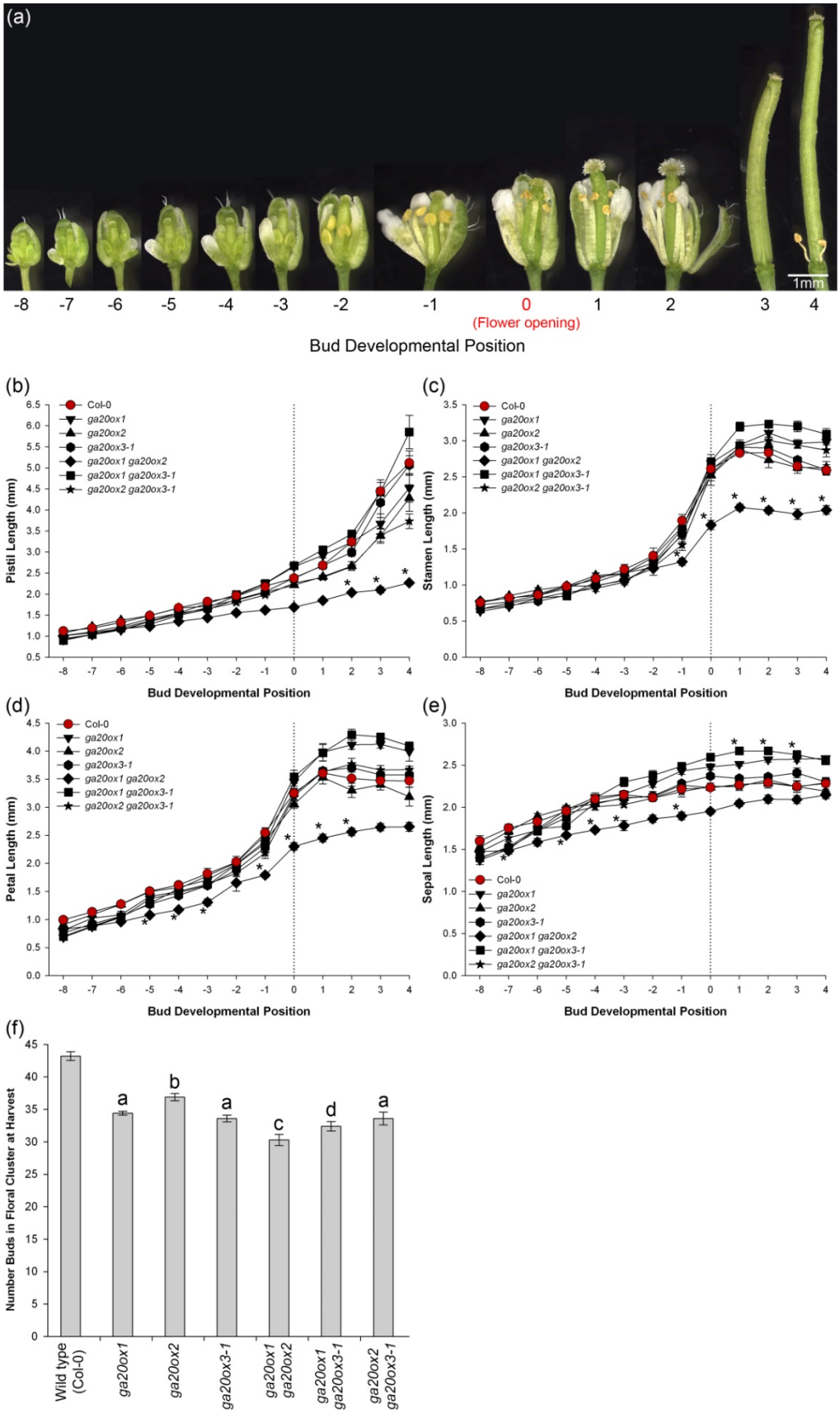

Figure 5.1: Floral organ growth in *ga20ox* single and double mutants.

Comparison of floral organ lengths during floral development, measuring a series of developing flowers harvested from the same primary inflorescence, based on bud position relative to flower opening (represented graphically in (a)). Development between inflorescences was synchronised by harvesting buds on the day that the 10th flower opened (denoted as 'Bud 0'). Lengths of pistils (b), long stamens (c), petals (d) and sepals (e) were recorded for each bud position. The number of unopened buds in each floral cluster at the point of harvesting was also recorded (f). Graphs represent means of 10 independent inflorescences, error bars represent one S.E. Statistical analysis of floral organ lengths was performed on a transformed scale (log), with pairwise comparisons were made between mutant genotypes and wild type within individual bud positions using a 1% LSD for floral organ lengths ((d), 0.4069; (c), 0.2148; (d), 0.2859; (e), 0.1499) and a 5% LSD for numbers of floral buds (1.933). Asterisks denote significant difference from wild type ($p < 0.01$) at that bud position. Comparisons were not made between bud positions. Letters denote significant difference from wild type, genotypes marked with different letters are significantly different from each other.

AtGA20ox1 and *-2* both act to promote stamen growth (see section 3.2.5), and further indicate that late stamen development is the stage most affected by the loss of these genes. A similar phenotype is observed during petal growth (Figure 5.1d), though differences between wild type and *ga20ox1 ga20ox2* petal lengths become significant at a far earlier stage (bud -5, $p < 0.01$). A similar link between stamen and petal growth in *ga20ox1 ga20ox2* was observed in previous experiments (see section 3.2.5). Interestingly, growth of *ga20ox1 ga20ox2* sepals differs significantly from wild type during the development of unopened flower buds ($p < 0.01$, buds -7, -5, -4, -3 and -1, Figure 5.1e), but not later in development, suggesting that whilst the rate of growth of sepals is reduced in *ga20ox1 ga20ox2*, final sepal size is not affected. A similar phenotype was found in rosette leaves of this genotype (Rieu et al., 2008).

These results indicate that loss of *AtGA20ox1* and *-2* has a significant effect on the growth and development of all floral organs. Furthermore, the conclusion of this experiment must be that these two paralogues are functionally redundant in promoting floral organ growth due to the

similarity of *ga20ox1* and *ga20ox2* floral organs to wild type, in contrast with the *ga20ox1* and *ga20ox2* single mutant phenotypes described previously in section 3.2.5. However, whilst earlier experiments focussed on a particular stage of floral development (bud 0) and examined changes in floral organ length across the primary inflorescence at that stage, this experiment examines a far broader range of floral development at a fixed point on the primary inflorescence (position 10). Hence the loss of replication for that particular floral stage in this dataset may make the analysis less sensitive to small differences. Furthermore, the greatest disparity in floral organ lengths at flower opening was observed at earlier inflorescence positions, becoming less marked by position 10.

As part of this experiment the number of developing (unopened) buds in the floral cluster of each inflorescence harvested was recorded, and genotype was found to be a significant factor in explaining variations in bud number ($p < 0.001$). From this it can be inferred that loss of *AtGA20ox* activity alters the rate at which floral meristems arise from the inflorescence meristem, a hypothesis which correlates well with the previously observed disruption to inflorescence patterning in these mutants (see section 3.2.5). All *ga20ox* mutants included are significantly different from wild type ($p < 0.05$, Figure 5.1f), with reduced numbers of buds in their floral clusters at harvest. All three single mutants are significantly different from wild type, with the *ga20ox1* and *ga20ox3-1* mutant phenotypes being more severe than *ga20ox2*, suggesting that *AtGA20ox3* has enhanced functions in controlling this phenotypic character. GA acts to promote organogenesis during vegetative development (Hay et al., 2002), and these results are consistent with a similar function during reproductive development. The effect of the individual paralogues is likely to be due to their effect on the availability of GA at the IM, but their precise expression patterns in this tissue are unknown. However, because of these differences, buds at equivalent positions in the floral cluster may not necessarily be at the same developmental stage. Comparisons made close to flower opening (the reference point for harvesting) will not be strongly affected by these differences (and so can still be generally considered as valid), but differences between genotypes will be exaggerated with increasing distance from the reference point. In this dataset few significant differences were

observed in this more distant region, but the limitations of this approach must still be borne in mind.

A further experiment was performed to compare the growth of floral organs during floral development in three GA-deficient mutant genotypes in which floral development is known to be affected (*ga20ox1 ga20ox2*, *ga20ox1 ga20ox2 ga20ox3-1* and *ga1-3*) against wild type (n = 48). To ameliorate the effects of different numbers of developing floral buds between genotypes, the maximum possible developmental sequence was recorded from each inflorescence (between flower opening and the smallest bud that it was possible to dissect), and floral organ lengths were placed on a relative developmental scale according to the number of buds present in that particular inflorescence, with the start of floral development represented by '0' and flower opening by '1' (Figure 5.2). As before, development was synchronised by harvesting when the 10th flower opened. In the cases of *ga20ox1 ga20ox2 ga20ox3-1* and *ga1-3* (where development is arrested prior to flower opening at this phase of flowering), mutant buds were judged to have reached full development based both on whether maximum bud size had been reached in comparison to neighbouring buds, and on their position relative to the start of internode elongation within the floral cluster, which begins at approximately bud -4 in wild-type floral development (see Figure 6.1). Internode elongation was observed in most *ga20ox1 ga20ox2 ga20ox3-1* and some *ga1-3* plants in this experiment. Regression analysis was performed on the data from each individual inflorescence to obtain a mathematical model describing the growth of each floral organ type, and the population of model parameters thus obtained was analysed by ANOVA (see sections 2.4 and 2.5).

Within each of the four floral organ types, genotype was found to have a significant effect on the model parameters ($p < 0.001$). With the exception of sepals, the models describing floral organ growth are non-linear (Table 5.1), making their explanation in a biological context more complex. Pistil growth of each mutant genotype is significantly different from wild type ($p < 0.05$, Table 5.1), and significantly different between each mutant genotype ($p < 0.05$). These results indicate that loss of *AtGA20ox1* and *-2* together has a significant effect on pistil growth compared to wild type, that the further loss of *AtGA20ox3* has a significant additional effect

(a)

Genotype	Pistil ($y=Ax^B$)		Stamen ($y = \exp(C + Dx + Ex^2)$)		
	A	**B**	**C**	**D**	**E**
Wild type (Col-0)	2.211	1.594	-1.303	-0.540	2.722
ga20ox1 ga20ox2	1.594^{a}	1.153^{a}	-1.710^{a}	1.820^{a}	0.341^{a}
ga20ox1 ga20ox2 ga20ox3-1	1.383^{b}	1.164^{a}	-2.436^{b}	4.660^{b}	-2.561^{b}
***ga1-3* (Col-0)**	1.260^{c}	1.121^{a}	-2.305^{b}	4.060^{c}	-2.185^{b}
5% LSD	***0.1124***	***0.1100***	***0.1679***	***0.5940***	***0.5078***

(b)

Genotype	Petal ($y = Fx^G$)		Sepal ($y = H + Jx$)	
	F	**G**	**H**	**J**
Wild type (Col-0)	3.037	3.204	0.001	2.404
ga20ox1 ga20ox2	1.914^{a}	2.178^{a}	0.156^{a}	1.949^{a}
ga20ox1 ga20ox2 ga20ox3-1	1.053^{b}	1.408^{b}	0.088	2.177^{b}
***ga1-3* (Col-0)**	0.841^{c}	1.187^{c}	0.174^{a}	1.848^{a}
5% LSD	***0.1534***	***0.2161***	***0.0576***	***0.1282***

Table 5.1: Models of floral organ growth between *ga20ox* mutants.

Values given in the tables are the mean parameters governing the growth of each genotype according to the equation given for each type of floral organ listed: pistil (a), (long) stamen (a), petal (b) and sepal (b). Individual growth models were calculated for each inflorescence harvested (12 of each genotype) using regression analysis, and parameters were subsequently compared using ANOVA. Comparisons were made between genotypes within each parameter using a 5% LSD, as listed. Superscript letters denote genotypes that are significantly different from the wild type ($p < 0.05$), genotypes with different letters are significantly different from each other. No comparisons were made between parameters.

but that significant differences in pistil growth still exist between *ga20ox1 ga20ox2 ga20ox3-1* and *ga1-3*. Pistil growth was modelled using the allometric relationship:

$$y = Ax^B$$

which can be expressed on the logarithmic scale as:

$$\ln(y) = A + B(\ln(x))$$

where y = pistil length, x = position on the common developmental scale, parameter A is the estimate of pistil length at position 0 on the developmental scale and B is the logarithmic rate of pistil growth during development. On the untransformed scale 'A' and 'B' can be considered loosely as a linear rate of growth and a non-linear (or acceleration) component, respectively. Interestingly, parameter B was not significantly different between the three mutant genotypes (though all three were significantly different from wild type, Table 5.1), suggesting that changes in pistil growth rate through development dependent on GA biosynthesis are governed primarily through expression of *AtGA20ox1* and *-2*. For these three genotypes the value of B was close to one, indicating an almost linear growth rate during pistil development. Significant differences between all three mutant genotypes were observed in parameter A ($p < 0.05$), indicating that the underlying linear rate of pistil growth is influenced by *AtGA20ox1*, *-2* and *-3*, and potentially other *AtGA20ox* paralogues. The data from this experiment suggests that, whilst pistil growth is significantly reduced in the *ga20ox1 ga20ox2 ga20ox3-1* and *ga1-3* mutants, growth is not fully arrested (Figure 5.2a), though it may well be that growth becomes arrested beyond the range of development recorded here. The effect of AtGA20ox activity on wild-type pistil growth is most pronounced in the second half of floral development (Figure 5.2a, beginning at approximately bud developmental position -11), with wild-type and *ga20ox1 ga20ox2* pistil growth gradually diverging from this point. At this time it is not known whether this is linked to a specific developmental stage.

As with pistils, stamen growth differs significantly between wild type and all mutant genotypes ($p < 0.05$) and also between all three mutant genotypes ($p < 0.05$, Table 5.1a). Whilst wild type and *ga20ox1 ga20ox2* both exhibit a rapid increase in stamen growth late in development, growth of stamens in *ga20ox1 ga20ox2 ga20ox3-1* and *ga1-3* is asymptotic and plateaus prior to flower opening (Figure 5.2b), with no evidence of accelerated growth occurring. These results indicate that growth becomes arrested in both of these genotypes at a

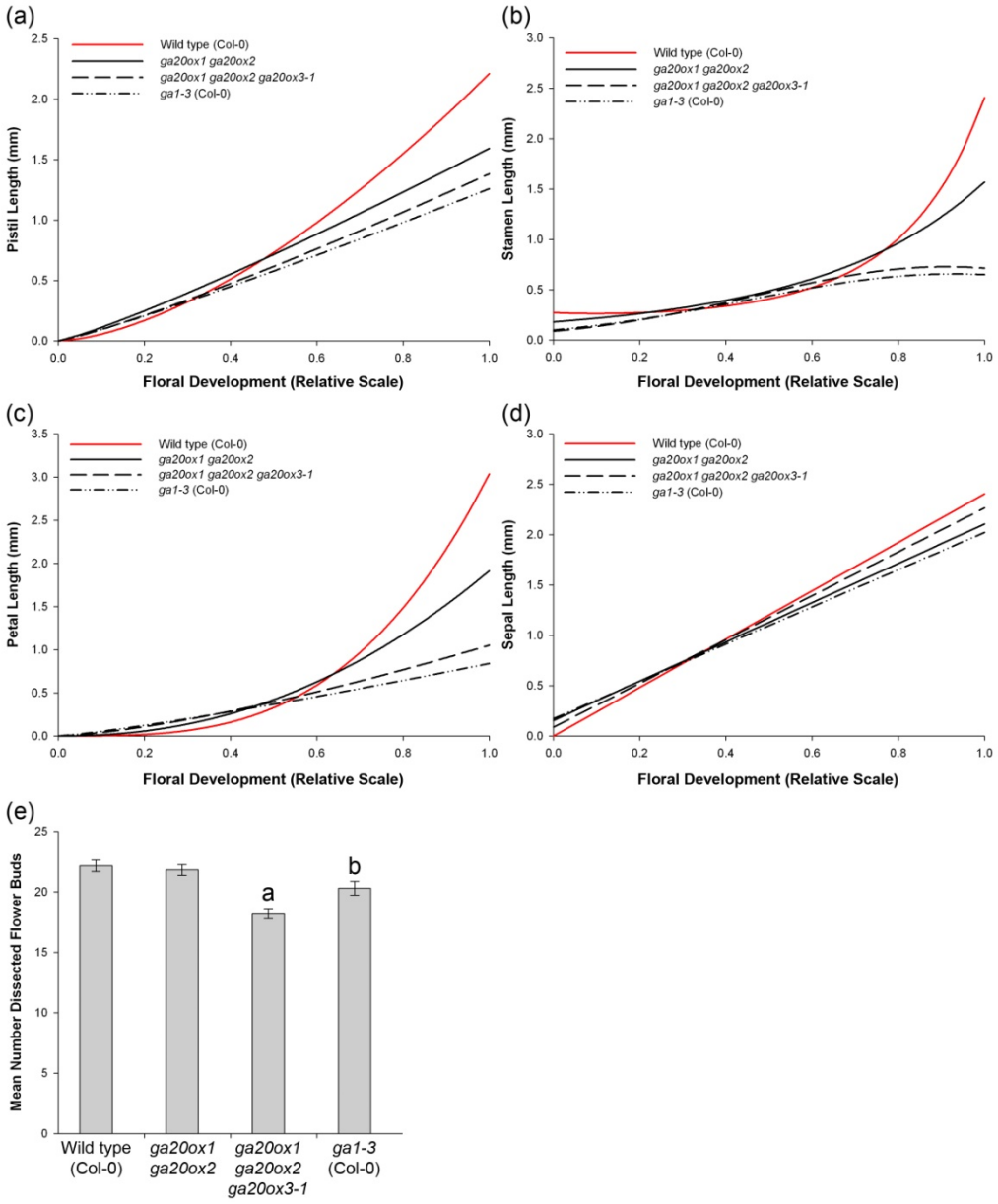

Figure 5.2: Floral organ growth of *ga20ox* mutants across floral development.

A comparison of floral organ growth between selected genotypes (as listed) across the full range of floral development up to flower opening, comparing pistils (a), (long) stamens (b), petals (c) and sepals (d). Organ lengths were obtained by sequential dissection of developing buds on individual primary inflorescences on which flower 10 had most recently opened, and set against a relative developmental scale by dividing the relative bud position by the number of buds on that particular inflorescence. 0 represents the approximate start of floral organ development and 1 represents flower opening. The growth relationships displayed are derived from model formulae calculated by regression analysis of floral organ lengths on each individual inflorescence (12 per genotype), with the mean values of the growth

parameters for each genotype (given in Table 5.1) subsequently calculated. The mean number of buds per genotype is summarised in (e), error bars represent one S.E. Pairwise comparisons were made between genotypes using a 5% LSD (1.325). Letters indicate significant difference from wild type ($p < 0.05$). Genotypes denoted by different letters are significantly different from each other.

similar developmental stage, although the final length differs between the two genotypes. Whilst growth of these two genotypes is very similar, the significant difference between them suggests that there is an additional (if minor) role in promoting floral organ growth for one of the remaining *AtGA20ox* paralogues, although the possibility of ecotype-related differences cannot be completely discounted. Stamen growth across this particular developmental range is described by the model:

$$y = \exp\hat{}(C + Dx + Ex^2)$$

which can be expressed on the logarithmic scale as:

$$\ln(y) = C + Dx + Ex^2$$

where parameter C is the estimate of stamen length at developmental position 0, D estimates the linear rate of stamen growth and E the quadratic rate of growth. The only parameter to differ significantly between *ga20ox1 ga20ox2 ga20ox3-1* and *ga1-3* is D ($p < 0.05$), resulting in an increase in the final length attained whilst other growth kinetics (such as the position of the asymptote) remain the same. This might indicate that whilst stamen growth is more pronounced in the *ga20ox1 ga20ox2 ga20ox3-1* mutant, stamen development reaches the same point in both genotypes. However, it should be noted that, whilst still significant, this difference is marginal (Table 5.1a) and so the importance of *AtGA20ox4* or *-5* to stamen growth remains questionable. Growth characteristics between wild-type and *ga20ox1 ga20ox2* stamens are significantly different for all parameters ($p < 0.05$), though no major divergence in length occurs until late in development (beginning at approximately bud -4, on the back-translated scale, not shown), where stamen length increases far more rapidly and by a

greater extent in the wild type than *ga20ox1 ga20ox2* (Figure 5.2b), as was observed previously (Figure 5.1c).

Petal growth was also found to be significantly different between all genotypes analysed ($p < 0.05$). Interestingly, petal growth was not arrested in either *ga20ox1 ga20ox2 ga20ox3-1* or *ga1-3* (Figure 5.2c), and in fact can be described by an equation similar to that used for pistils (Table 5.1b). Furthermore, both the linear growth parameter (F) and acceleration parameter (G) differ significantly between these two genotypes ($p < 0.05$), suggesting that the relationship between these two genotypes differs more for petal growth than for stamens. Together these results cast doubt on the stamens being the exclusive source of GA underpinning petal growth: if this were the case, one might expect the same differences in petal and stamen growth to be seen in both genotypes. As such, petal growth may be less dependent on contributions by the stamen than was previously thought, and could be influenced by GA originating from other sources such as the sepal or receptacle. The lack of complete growth arrest in *ga1-3* also suggests that petal growth is generally less dependent on GA than are stamens. The differences between wild-type and *ga20ox1 ga20ox2* petal growth manifest slightly earlier in development than during stamen development (Figure 5.2b and c). This difference in timing could be explained by petal growth being influenced by GA biosynthesis in tissues other than the stamens where *AtGA20ox1* and *-2* are expressed.

In contrast to the other floral organs, sepal growth could be described by a linear relationship (Table 5.1b). Surprisingly, whilst all three mutant genotypes showed significantly different sepal growth compared to wild type ($p < 0.05$), *ga20ox1 ga20ox2* and *ga1-3* do not differ significantly, but *ga20ox1 ga20ox2 ga20ox3-1* differs from both ($p < 0.05$). Growth of *ga20ox1 ga20ox2 ga20ox3-1* sepals was found to be closer to that of wild type than *ga20ox1 ga20ox2* (Figure 5.2d), although the rate of growth (parameter J) is significantly different from wild type ($p < 0.05$, Table 5.1b). These relationships do not make intuitive sense, and may reflect experimental artefacts created by the significantly different number of developing floral buds between each mutant genotype ($p < 0.05$, Figure 5.2e). Although each inflorescence was dissected to the smallest possible bud (and thus hopefully a similar

developmental stage), minor variations in the developmental range captured between genotypes could have been incorporated in this analysis despite these precautions. Alternatively, the differences might be explained by ecotype-derived variations at other loci.

From these experiments it can be concluded that loss of *AtGA20ox1* and *-2* affects the growth of different floral organ types at different stages of development, with stamen growth being most severely affected in the final stages before anthesis. This might reflect a direct contribution to GA biosynthesis in stamen tissues by these genes. Stamen growth appears to be blocked in *ga20ox1 ga20ox2 ga20ox3-1* before this final elongation phase is reached, which might be an indirect consequence of the developmental arrest previously observed (see section 3.2.4). As such, no firm conclusions can be drawn as to whether *AtGA20ox3* is also expressed during late stamen development. A similar caveat applies to other floral organs, though it is not known whether the developmental block observed in anthers extends to more distant floral tissues. The effect of loss of *AtGA20ox1* and *-2* on pistil growth becomes apparent far earlier in development, suggesting that *AtGA20ox* expression in this organ may begin (or, at least, become limiting on growth) at an earlier developmental stage. Importantly, evidence from this study suggests that petals might be obtaining GA from multiple sources within the flower, rather than being exclusively dependent on GA biosynthesis in stamens (although these appear to be a major contributor). Dependent on the mobility of GA_9, it must be borne in mind that the effect of each *AtGA20ox* paralogue on floral phenotype is not necessarily limited to its particular tissue expression domain.

5.2.2 *AtGA20ox* Paralogues Demonstrate Individual Expression Patterns in Floral Tissues

AtGA20ox::GUS transgenic reporter lines were constructed as part of this project to directly map *AtGA20ox* expression in developing floral tissues. Previous attempts had successfully produced *AtGA20ox::GUS* translational fusion constructs (carrying in-frame exonic and intronic sequence up to the start of exon 3, Figure 5.3a) for *AtGA20ox1* (Hay et al., 2002) and *AtGA20ox2* (unpublished data), but similar attempts to create reporter lines for the remaining *AtGA20ox* paralogues failed to show any GUS staining (Phillips, A., personal

Transgenic Line	T_0 Transformation Pot	Number T_3 lines GUS Stained
pGA20ox1-TC-GUS	A	8
pGA20ox1-TC-GUS	B	7
pGA20ox1-TC-GUS	C	7
pGA20ox2-TC-GUS	D	8
pGA20ox2-TC-GUS	E	8
pGA20ox2-TC-GUS	F	3
pGA20ox3-TC-GUS	G	12
pGA20ox3-TC-GUS	H	14
pGA20ox3-TC-GUS	I	11
pGA20ox4-TC-GUS	J	2
pGA20ox4-TC-GUS	K	7
pGA20ox4-TC-GUS	L	3

Table 5.2: GUS staining statistics for pGA20ox-TC-GUS transgenic reporter lines. *Each transformation pot represents a separate* Agrobacterium *transformation, with each pot having contained multiple T_0 plants (see section 2.1.2).*

communication). To circumvent this technical obstacle the reporter lines generated during this project contained transcriptional fusion constructs, in which 5' promoter sequence from individual *AtGA20ox* paralogues directly drives expression of the GUS coding sequence (Figure 5.3a, see section 2.1.2). In order to encompass the maximum possible number of regulatory elements in the absence of intronic sequence, which may contain some regulatory elements, as evidenced by *CPS::GUS* expression studies (Silverstone et al., 1997), a large fragment of each promoter was taken from each paralogue.

Homozygous transgenic lines reporting expression of *AtGA20ox1*, *-2*, *-3* and *-4* in the wild type (Col-0) background were successfully established, but there was not sufficient time to establish similar lines reporting *AtGA20ox5*, which remain at the T_2 generation (data not shown). Preliminary GUS staining of *AtGA20ox5::GUS* T_2 plant tissues did not identify GUS expression in floral tissues, but some GUS staining was observed in developing seeds (data not shown). Populations of homozygous T_3 lines were GUS-stained and their floral expression patterns compared. The numbers of lines screened for each reporter are given in Table 5.2. For some lines, particularly pGA20ox4-TC-GUS, the number of lines screened was limited by availability, despite repeated transformations and screening of T_1 seed. From

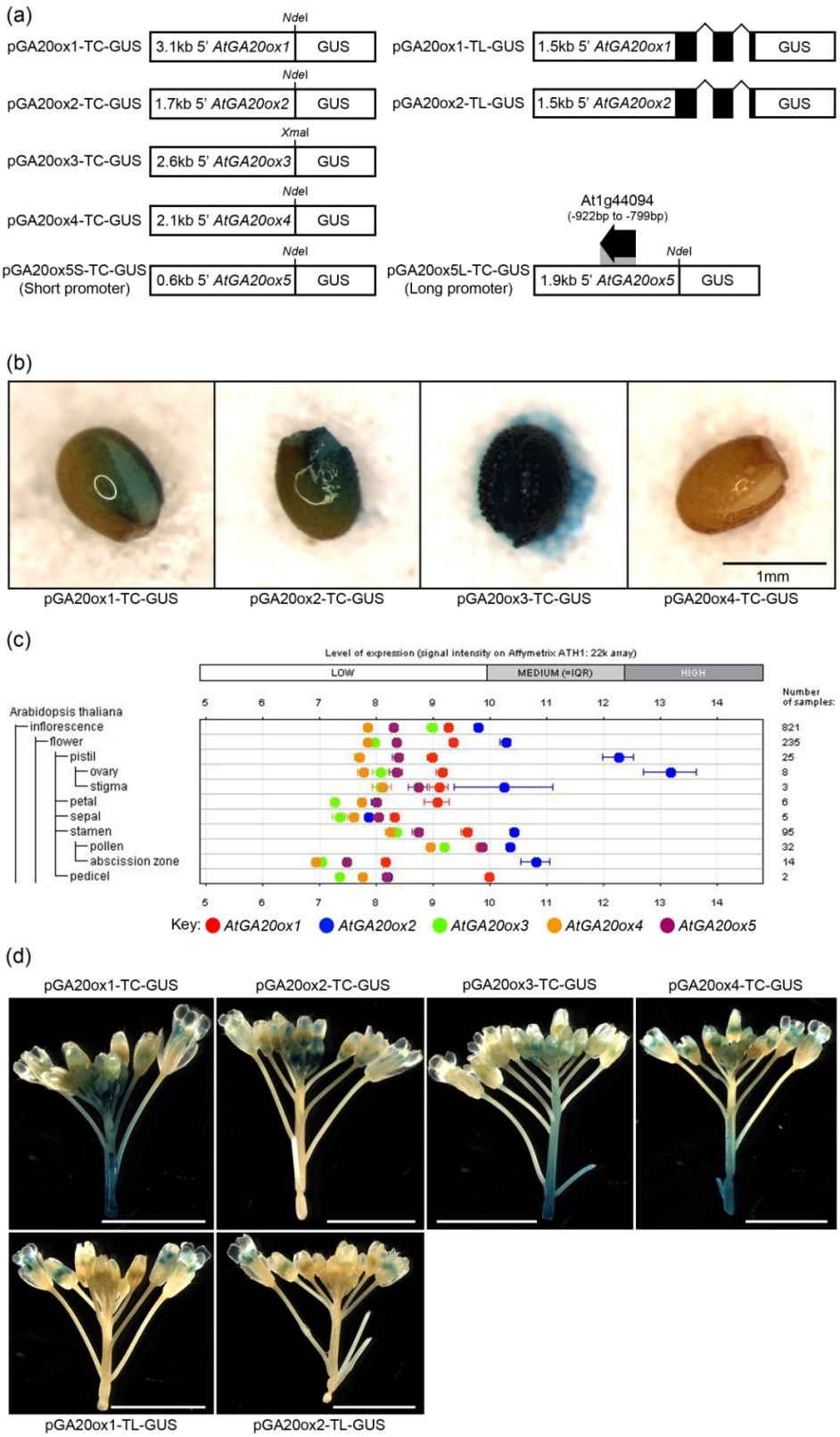

Figure 5.3: *AtGA20ox::GUS* expression in germinating seed and floral tissues.

(a) Schematic of AtGA20ox::GUS reporter constructs, including transcriptional fusions created during this project (linking 5' AtGA20ox *promoter sequence to a* GUS *cDNA clone via an* Nde*I or* Xma*I restriction site, see section 2.1.2) and existing translational fusions*

(linking AtGA20ox *promoter and coding sequence in-frame with* GUS*). Lengths of the* AtGA20ox *promoter sequences 5' of the ATG are as listed.*
(b) GUS-stained 24hr germinating seed from homozygous transcriptional fusion reporter lines.
(c) AtGA20ox *floral expression as reported by the Genevestigator microarray analysis web tool. Figure is edited from Genevestigator output. Expression scale given is* log_2.
(d) GUS-stained primary inflorescence tissue from homozygous transcriptional and translational fusion reporter lines. All inflorescences were harvested at the opening of the 10^{th} *flower.*
All GUS staining occurred in the presence of 0.5µM potassium ferricyanide (see section 2.2.7). All scale bars = 1mm.

each reporter construct, one transgenic line displaying a representative GUS expression pattern from across all three transformation pots was selected for comparative analysis. In the case of pGA20ox4-TC-GUS, only one homozygous T_3 line demonstrated floral GUS staining.

GUS expression in representative T_3 homozygous lines was assessed in germinating seed (Figure 5.3b), in which *AtGA20ox* expression has been independently investigated (Ogawa et al., 2003; Rieu et al., 2008), and in developing floral tissues (Figure 5.3d). In 24hr-germinating seed, GUS expression was observed for *AtGA20ox1, -2* and *-3*, all of which are expressed during germination (Ogawa et al., 2003, Rieu et al., 2008). GUS staining in pGA20ox3-TC-GUS seeds was far more intense than in either pGA20ox1-TC-GUS or pGA20ox2-TC-GUS. This corresponds to the published expression of *AtGA20ox3* in germinating seed, which has been independently found to be far higher than either *AtGA20ox1* or *-2* (Ogawa et al., 2003, Rieu et al., 2008). In contrast, previous pGA20ox3-TL-GUS lines displayed no GUS staining in seeds (Phillips, A., personal communication). No GUS staining was visible in germinating pGA20ox4-TC-GUS seeds, and similarly no *AtGA20ox4* transcript was detected in expression analysis of germinating seeds (Rieu et al., 2008). In the absence of more detailed expression data, in the context of germination GUS staining in these reporter lines is consistent with the published expression of these four paralogues.

The available data regarding floral expression of the *AtGA20ox* gene family is currently limited. Expression analysis by Rieu et al. (2008) found that *AtGA20ox1* and *-2* were the most highly expressed paralogues in inflorescence tissues, with *AtGA20ox2* expression being slightly greater (Figure 3.1c). Analysis of publicly available microarray data via the Genevestigator web tool (Hruz et al., 2008; https://www.genevestigator.com/gv/) predicts that *AtGA20ox2* expression is highest in the pistil, and that *AtGA20ox2* is also the most highly expressed *AtGA20ox* in whole stamens (Figure 5.3c). In contrast, *AtGA20ox1* is most highly expressed in the flower pedicel (the subtending stalk), and then in the stamen. Expression of *AtGA20ox3* is less than either *AtGA20ox1* or *-2* in all tissues specified, being most highly expressed in pollen (as are *AtGA20ox4* and *-5*). However, it is unclear to which stage of floral developmental this data refers, and there is no indication as to how gene expression changes during development.

GUS staining of whole inflorescence tissues (synchronised at the opening of flower 10) found GUS expression in all four transcriptional fusion reporter lines, as well as in the two previously-established translational fusion lines (Figure 5.3d). A clear distinction between the GUS staining of pGA20ox1-TC-GUS and pGA20ox1-TL-GUS in inflorescence stem tissues is visible, with GUS staining in the stem of the TC fusion but not the TL (Figure 5.3d). Loss of *AtGA20ox1* confers a semi-dwarf phenotype (Rieu et al., 2008), and the same study also identified high *AtGA20ox1* expression in stem tissues (specified as 'vegetative stem', Griffiths et al., 2006), supporting the pGA20ox1-TC-GUS expression pattern. Furthermore, GUS staining is present in the pedicels of pGA20ox1-TC-GUS flowers, as predicted by the Genevestigator dataset (Figure 5.3c). These results suggest that the expression pattern reported by pGA20ox1-TC-GUS is more representative than pGA20ox1-TL-GUS. No GUS staining is visible in inflorescence stems of either pGA20ox2-TC-GUS or pGA20ox2-TL-GUS, a result supported by both expression data and the *ga20ox2* mutant phenotype (Rieu et al., 2008). Low *AtGA20ox3* expression was detected in wild-type vegetative stem tissue (Rieu et al., 2008, Figure 3.1c), and GUS staining is visible in the inflorescence stem of pGA20ox3-TC-GUS. pGA20ox4-TC-GUS also displays GUS staining in the inflorescence stem, although previous analysis of stem tissues did not find *AtGA20ox4* expression (Rieu et al.,

2008). The same study identified expression of *AtGA20ox1*, *2*, *-3* and *-4* across whole floral clusters, and clear GUS staining is visible in the floral tissues of each reporter line, suggesting that each of these paralogues is involved in floral development.

AtGA20ox reporters each displayed individual GUS staining patterns in floral tissues, with changes in expression pattern occurring during floral development (Figures 5.4 and 5.5). Staining patterns differ both spatially and temporally between the transcriptional and translational fusion forms of both *AtGA20ox1* and *-2*: pGA20ox1-TC-GUS reported expression in the anther, stamen filament, pistil and receptacle (Figure 5.4a), whilst GUS staining in pGA20ox1-TL-GUS was restricted to the anther (Figure 5.4b). The same difference was observed between the TC and TL GUS fusions reporting *AtGA20ox2* expression (Figures 5.4c and d). These results clearly demonstrate that the form of GUS fusion used has a significant effect on the patterns of GUS expression (see section 5.2.3 for further discussion). GUS staining occurs in sepal, anther, pistil and receptacle tissues of pGA20ox3-TC-GUS flowers (Figure 5.4e), and in sepal, anther and filament tissues of pGA20ox4-TC-GUS (Figure 5.4f). These results indicate that the different *AtGA20ox* paralogues are expressed in individual, partially-overlapping patterns within floral tissues. It should be noted that the expression patterns of the transcriptional fusions, particularly the stamen and pistil expression of *AtGA20ox1* and *-2*, closely match the phenotypic evidence generated previously from *ga20ox* combinatorial mutant lines (see sections 3.2.5 and 5.2.1). These results also suggest that the floral expression patterns of *AtGA20ox1* and *-2* are more similar to each other than to *AtGA20ox3* and *-4*, and *vice versa*. Previous phylogenetic analyses have found a similar relationship, with *AtGA20ox1* and *-2* forming a separate clade from *AtGA20ox3* and *-4* (Figure 4.1a, Hedden et al., 2002).

Using intensity/extent of GUS staining as an approximate quantitative measure, the level of *AtGA20ox* expression within floral organs was found to change during floral development. Floral staining patterns were examined in detail across a range of developing buds, from bud -11 to bud 0 (flower opening). Side-by-side analysis of the previously published *AtGA3ox* reporter line pGA3ox3-TL-GUS (Hu et al., 2008) indicates that this range includes

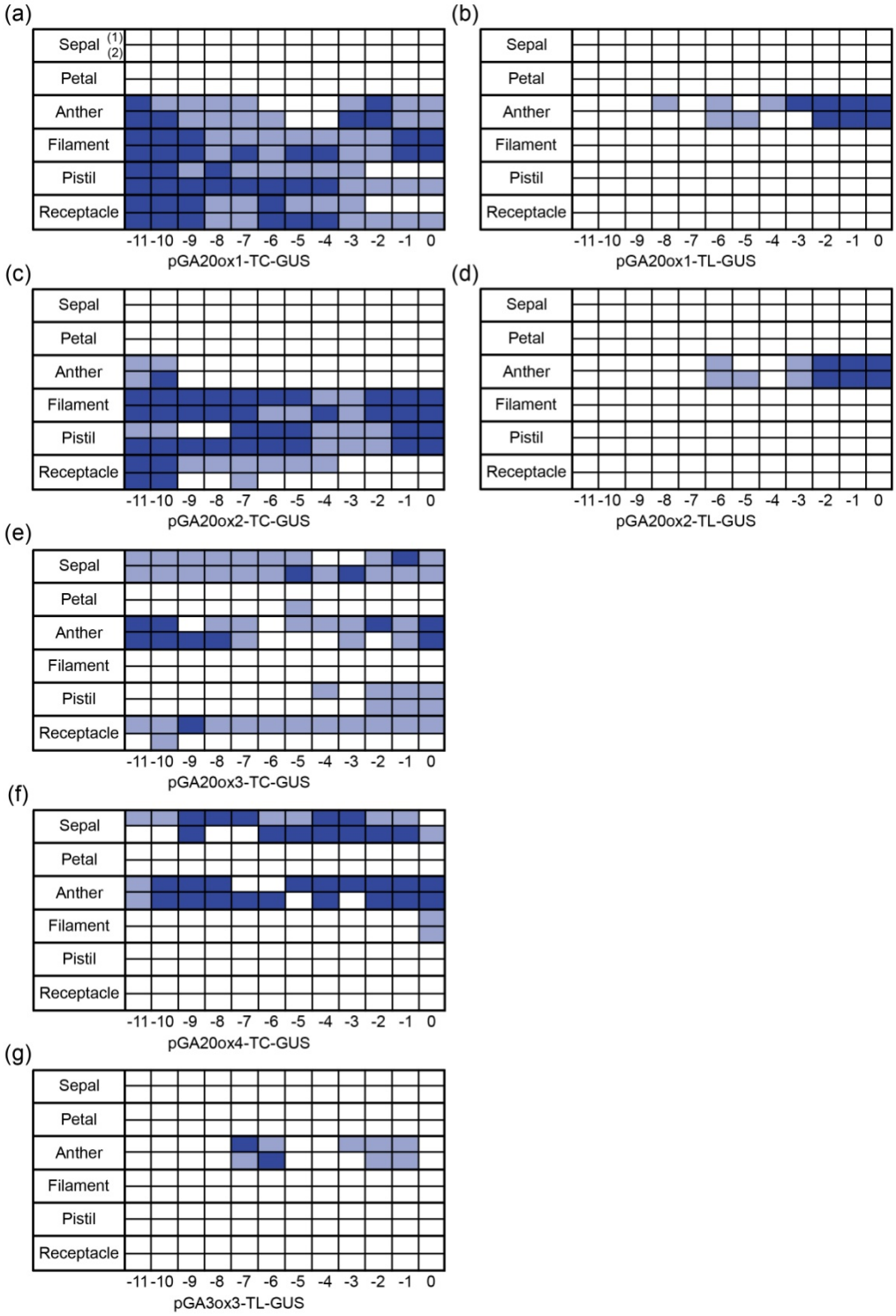

Figure 5.4: Floral expression patterns of *AtGA20ox::GUS* transgenic reporter lines. *Comparison of floral organ GUS staining patterns across a fixed period of floral development (bud -11 to bud 0 (flower opening)) between transcriptional fusion (a, c, e, f) and (where available) translational fusion reporter lines (b, d). The published GUS reporter line pGA3ox3-TL-GUS (g, Hu et al., 2008) was included to comparing the timing of* AtGA20ox *and* AtGA3ox *anther expression. GUS staining is represented by heat maps. Dark blue*

represents strong or extensive GUS staining, pale blue represents weak or spatially-restricted GUS staining within the organ in question. Primary inflorescence development was synchronised by GUS staining when the 10th flower opened. Two technical replicates of each line are shown, numbered (1) and (2) in (a).

events leading up to tapetum PCD (anther stages 9-10, Sanders et al., 1999), where GUS staining is strongest in this line (bud -7 to -6, Figure 5.4g), and probably also includes earlier stamen developmental events such as meiosis. Within this range, pistil GUS staining is initially strong in pGA20ox1-TC-GUS, but gradually declines through development, and staining is weak or absent by flower opening (Figure 5.4a). GUS staining of pGA20ox2-TC-GUS pistils is more constant through development (Figure 5.4c), whilst GUS staining occurs in pGA20ox3-TC-GUS pistils only in later buds (bud -4 to 0, Figure 5.4e). In consequence, pistil growth in *ga20ox1 ga20ox2* would be expected to be affected from early in development, which is consistent with the observed growth phenotype observed (Figure 5.2a). The relative dominance of *AtGA20ox2* in promoting pistil growth (see section 3.2.5) can be explained both through its prolonged expression during pistil development and also the tissue expression patterns within the pistil exhibited by the three different reporters. pGA20ox2-TC-GUS expression occurs in a linear stripe along the length of the pistil throughout development (Figure 5.5b), whilst pGA20ox1-TC-GUS, initially widespread, becomes restricted in later developmental stages to the apical tip, directly beneath the stigma (Figure 5.5a) and pGA20ox3-TC-GUS expression occurs only weakly in the pistil vasculature (Figure 5.5c). As such, *AtGA20ox2* expression appears to be the most widespread in pistil tissues, and its loss would therefore be expected to have the greatest impact on pistil growth.

In some respects, stamen growth represents a more complex system, as the majority of growth is due to elongation of the filament whilst bioactive GA is synthesised both directly in filament tissues and in the adjacent anther, based on *AtGA3ox* expression (Figure 1.10). GUS staining was observed in the stamen filament throughout the selected developmental period for both pGA20ox1-TC-GUS and pGA20ox2-TC-GUS, though both show a changing pattern of expression of strong GUS staining in the filaments of early buds, weaker staining in mid-

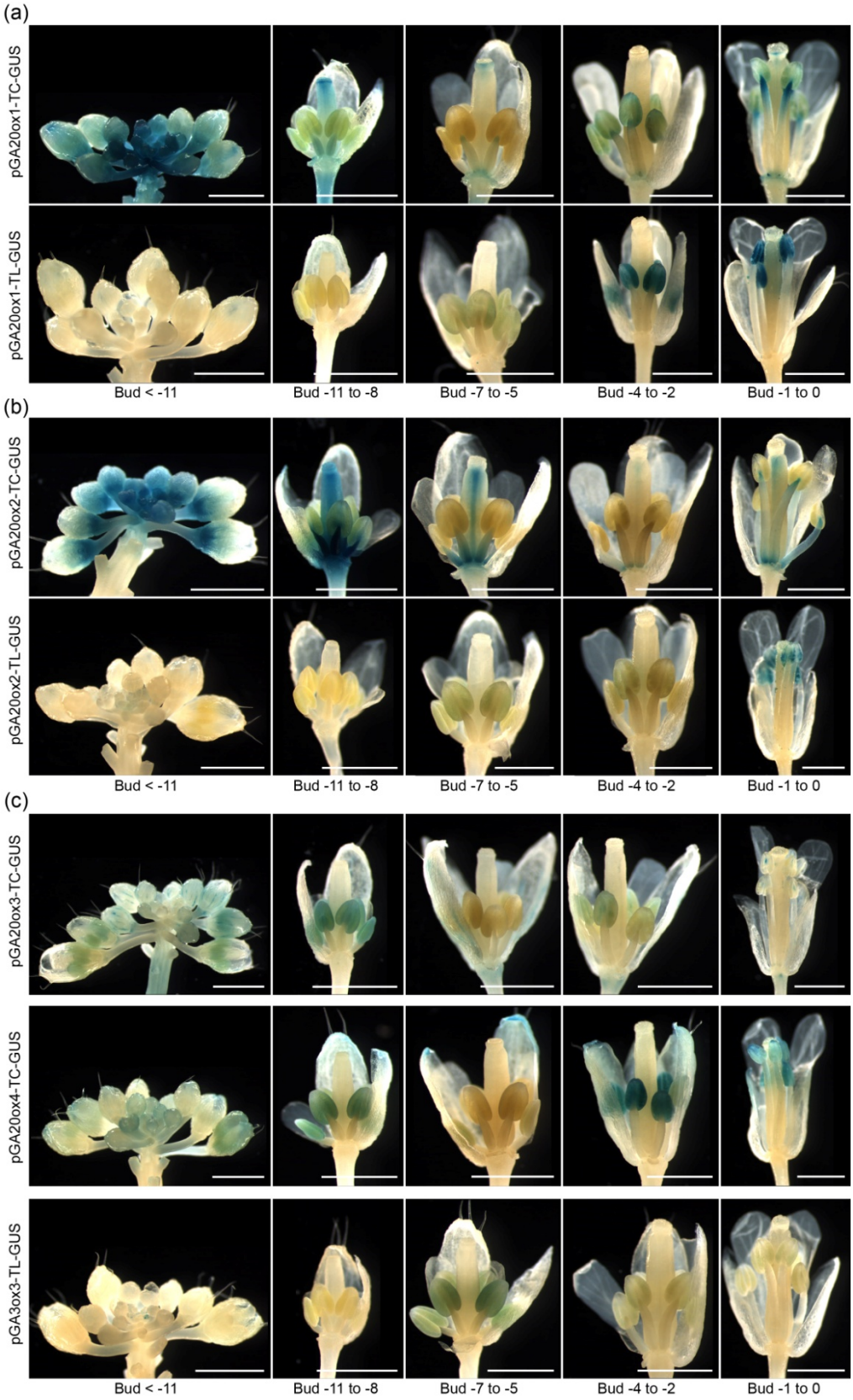

Figure 5.5: Floral tissue expression patterns of *AtGA20ox::GUS* transgenic reporter lines. *Photographs are representative of the data presented in Figure 5.4., comparing expression patterns between transcriptional and translational fusions reporting the expression of*

AtGA20ox1 *(a) and* AtGA20ox2 *(b), and between reporter lines for* AtGA20ox3*,* -4 *and* AtGA3ox3 *(c). The different stages shown broadly reflect the changes in tissue expression patterns observed during floral development. All scale bars = 1mm.*

range buds and then an increase shortly prior to flower opening (approximately buds -2 to 0, Figure 5.4a and c). Whilst GUS staining is visible throughout the filament of both reporter lines in early buds, expression of pGA20ox1-TC-GUS becomes restricted to the base and apical tip of the filament later in development (Figure 5.5a), whilst pGA20ox2-TC-GUS expression remains broad (Figure 5.5b). Filament GUS staining in pGA20ox4-TC-GUS is only observed in open flowers (bud 0, Figure 5.4f), restricted to the apical region of the filament (Figure 5.5c).

The precise contribution to filament growth by GA synthesised in the anther is not yet known. The GUS staining evidence presented above indicates that *AtGA20ox1*, *-2*, *-3* and *-4* are all expressed in the anther at various stages of development. Both pGA20ox1-TC-GUS and pGA20ox3-TC-GUS display an episodic expression pattern, with strong GUS staining in early buds that then declines, only to be re-elevated prior to flower opening (buds -3 to 0, Figure 5.4a and e). A similar pattern may occur in pGA20ox4-TC-GUS (Figure 5.4f), but is less clearly distinguishable. pGA20ox2-TC-GUS expression was only observed in anthers of early buds (buds -11 to -10, Figure 5.4c). In contrast, anther GUS staining in early buds is not observed in either pGA20ox1-TL-GUS or pGA20ox2-TL-GUS, in which GUS staining gradually increases in later buds until flower opening (bud -5 to bud 0, Figures 5.4b and d). The changes in GUS staining in pGA20ox1-TC-GUS anthers are stronger than the changes observed in filament tissues, with the late peak in anther staining coinciding with the start of late filament elongation (buds -3 to -2, Figure 5.4a). It could be that the greatest influence of *AtGA20ox1* on filament elongation late in stamen development is via expression in the anther. Interestingly, the decline in anther expression in pGA20ox1-TC-GUS and pGA20ox3-TC-GUS mid-range buds occurs when staining in pGA3ox3-TL-GUS anthers is strongest (buds -7 and -6, Figure 5.4g). Both *AtGA20ox1* and *-3* are feedback regulated via the GA signalling

pathway (see section 1.4), and thus the expression of *AtGA3ox* at this stage of development may indirectly cause the down-regulation of *AtGA20ox* expression in anther tissues.

Comparing anther GUS staining patterns of *AtGA20ox::GUS* transcriptional fusion reporter lines demonstrates that tissue expression patterns differ, both between reporter constructs and between the early and late peaks of GUS staining. Late expression of both pGA20ox1-TC-GUS and pGA20ox4-TC-GUS apparently occurs throughout mature anther tissues (Figure 5.5a, c). Intriguingly, pGA20ox3-TC-GUS expression during late anther development is more complex, with weak staining throughout the anther in a narrow window prior to flower opening (bud -4 to -2), becoming restricted to the filament-anther junction (bud -1 to 0, Figure 5.5.c). GUS staining tissue patterns in pGA20ox1-TL-GUS and pGA20ox2-TL-GUS anthers again vary from their transcriptional equivalents, in both cases the anther staining due to GUS expression in the pollen (Figure 5.5a and b). During the early peak of GUS staining observed in transcriptional fusion lines, the staining pattern seen in anthers is noticeably different, in all cases strongly reminiscent of expression in pGA3ox3-TL-GUS anthers, which has been previously shown to be tapetum-specific (Hu et al., 2008). Evidence from mutant analysis has implicated *AtGA20ox1*, *-2* and *-3* in promoting tapetum PCD (see section 3.2.4), and the evidence from this experiment suggests that these paralogues might be expressed specifically in the tapetum.

AtGA20ox expression is reported in the receptacle by pGA20ox1-TC-GUS, pGA20ox2-TC-GUS and pGA20ox3-TC-GUS (Figure 5.4a, c and e). Both pGA20ox1-TC-GUS and pGA20ox2-TC-GUS are strongly expressed in the receptacles of early buds, but declines as development progresses. pGA20ox3-TC-GUS staining of the receptacle is weak but remains constant throughout the developmental period specified. At the base of the flower, AtGA20ox activity in the receptacle has the potential to affect growth of other floral organs. Interestingly, GUS staining of petals was not consistently observed for any GUS reporter construct. Similarly, no sepal GUS staining was observed in pGA20ox1-TC-GUS or pGA20ox2-TC-GUS flowers, despite sepal growth being affected in the *ga20ox1 ga20ox2* mutant (Table 5.1b, Figure 5.2d). Sepal growth might therefore be indirectly affected through

expression of *AtGA20ox1* and *-2* in adjacent floral organs. Similar to pistil tissues, sepal GUS staining by pGA20ox3-TC-GUS is restricted to the vasculature (Figure 5.5c), suggesting that the effect of AtGA20ox3 activity on growth might not be restricted to its site of expression due to movement of substrates/products through the vasculature. No other *AtGA20ox::GUS* reporter demonstrated vascular-specific expression in floral tissues, and (paradoxically) may hint at a specialised 'generalist' function for *AtGA20ox3* that could help explain the lack of specific phenotypes in the absence of this paralogue.

5.2.3 Expression of *AtGA20ox1* and *-2* Dominates Late Floral Development

An attempt was made to validate the floral tissue GUS staining patterns described in section 5.2.2 via qPCR, mapping *AtGA20ox* expression immediately prior to flower opening (at approximately floral stage 12, Smyth et al., 1990, Figure 5.6a), during which period stamen filament elongation is affected by loss of *AtGA20ox1* and *-2* (see section 5.2.1). To achieve this, stage 12 flowers from primary inflorescences were dissected into their component organs (sepals, petals, anthers, filaments, pistil and receptacle, Figure 5.6b) and RNA extracted from each type. Inflorescence development was synchronised with the previous GUS-staining analysis at the 10th open flower. As was expected from the *ga20ox1 ga20ox2* mutant phenotype, *AtGA20ox1* and *-2* were found to be the most highly expressed *AtGA20ox* paralogues at this stage of development (Figure 5.6b). Expression was found to be organ-specific, with *AtGA20ox1* most highly expressed in the stamen filament and receptacle and *AtGA20ox2* most highly expressed in the pistil. Interestingly, overlapping expression of these two paralogues was not observed.

Comparing these results to the previously-established GUS staining patterns (Figure 5.6c and d), it can be seen that the qPCR results for *AtGA20ox1* match GUS staining of pGA20ox1-TC-GUS more closely than pGA20ox1-TL-GUS. Similarly, the pistil GUS staining of pGA20ox2-TC-GUS is supported by the expression analysis results, whilst no GUS staining is observed in pGA20ox2-TL-GUS. However, the filament-specific expression predicted by pGA20ox2-TC-GUS is not supported by the expression data. Instead, a low level of

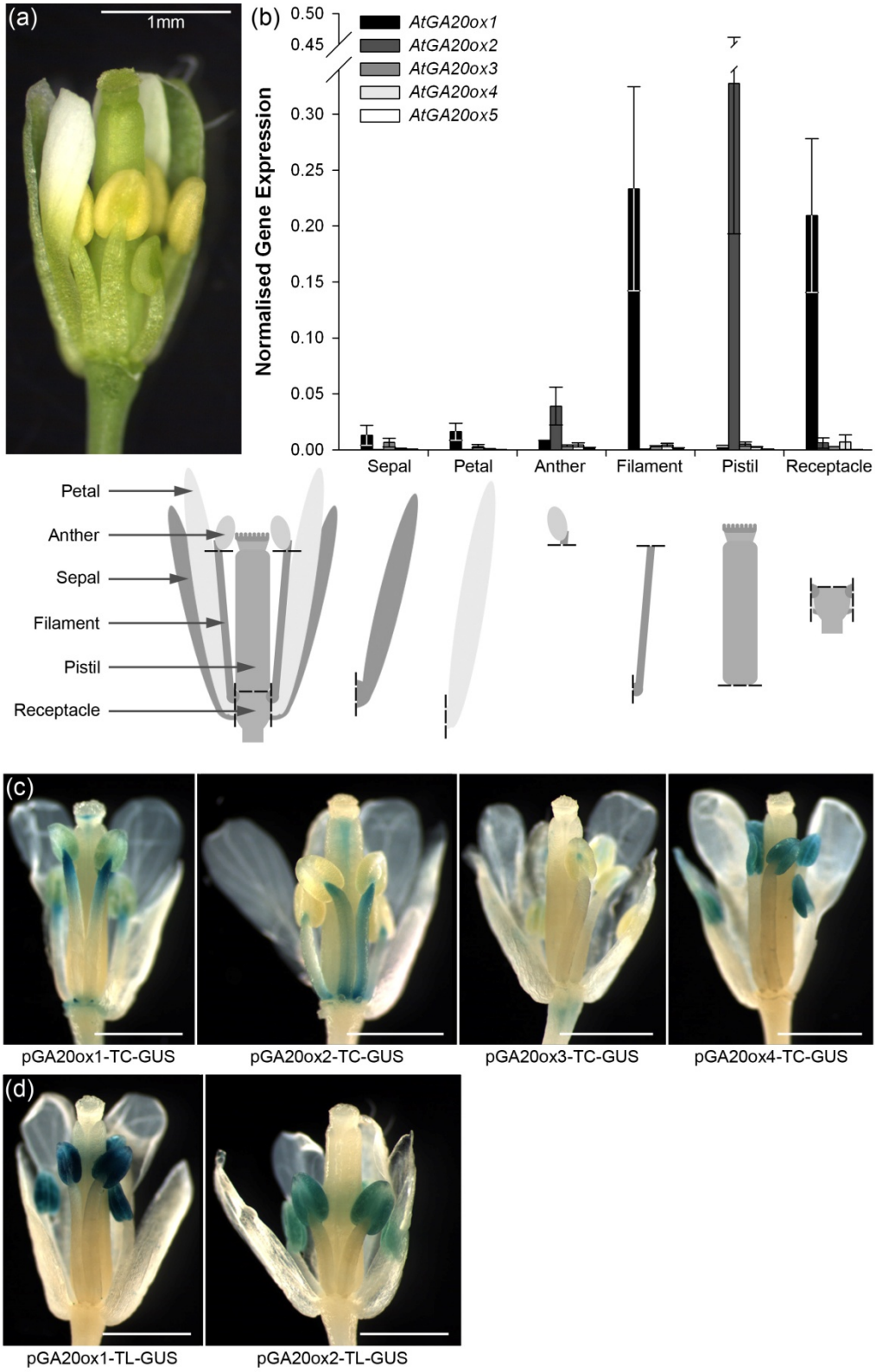

Figure 5.6: Expression profiling of the *AtGA20ox* gene family in late floral development. *(a) Dissected* Arabidopsis *flower bud, floral stage 12, representative of the floral tissues harvested for expression profiling.*

(b) Expression profiling of individual floral organs from stage 12 wild type (Col-0) flowers. Flowers were dissected into component organs (as shown), with stamens sub-divided into anthers and filaments. Tissue was harvested from long stamens only. Floral organ tissue was pooled from 35-40 flowers from independent primary inflorescences. Inflorescence development was synchronised at the 10th flower to open. Graph shows the expression of each AtGA20ox *paralogue (normalised against three reference genes, see materials and methods) within each floral organ type. Bars represent the mean of three biological replicates, error bars represent one S.E.*

(c) AtGA20ox *floral tissue expression patterns as predicted by* AtGA20ox::GUS *transcriptional fusion reporter transgenic lines (see Figure 5.3-5.5).*

(d) Floral tissue expression patterns of AtGA20ox1 *and* -2 *as predicted by translational fusion reporter transgenic lines (see Figure 5.3-5.5).*

All scale bars = 1mm.

AtGA20ox2 expression is detected in anthers at this stage (Figure 5.6b), which does not correlate with expression of pGA20ox2-TC-GUS (Figure 5.6c) but does with pGA20ox2-TL-GUS (Figure 5.6d). From these results and others discussed above, it can be argued that pGA20ox1-TC-GUS is a more accurate reporter of *AtGA20ox1* expression than the existing translational fusion. pGA20ox2-TC-GUS provides a more accurate record of *AtGA20ox2* expression as far as the pistil is concerned, but its stamen expression pattern cannot be validated from these results. Similarly, some differences are observed between the *AtGA20ox1::GUS* reporter lines and the expression analysis data. A small amount of *AtGA20ox1* expression is detected in both sepals and petals (Figure 5.6b), at a level equal to or greater than other *AtGA20ox* genes in these tissues, which is not reflected by either *AtGA20ox1::GUS* reporter line. Conversely, the limited pistil expression predicted by pGA20ox1-TC-GUS (Figure 5.6c) is not supported by the expression analysis.

Compared to *AtGA20ox1* and *-2*, expression of *AtGA20ox3*, *-4* and *-5* was found to be very low in all stage 12 floral tissues (Figure 5.6b). As such, it is difficult to reconcile this data with the GUS expression patterns reported for *AtGA20ox3* and *-4*. That said, *AtGA20ox3*

expression was found to be highest in sepal and pistil tissues, both of which displayed GUS staining. *AtGA20ox4* expression was highest in the receptacle, the anther and the filament. However, the biological importance of the expression of these genes is questionable in light of the expression of *AtGA20ox1* and *-2* in the same organs.

The discrepancies between the results of expression analysis and GUS staining (and between transcriptional and translational reporters for the same paralogue) might be explained through homeostatic regulation between the *AtGA20ox* paralogues. *AtGA20ox1*, *-2* and *-3* are all transcriptionally down-regulated in response to bioactive GA (Rieu et al., 2008). The same study also demonstrated that expression of *AtGA20ox2* is de-repressed in *ga20ox1* internode tissues. Expression of *AtGA20ox1* in filament tissues could potentially repress *AtGA20ox2*, which is predicted in filaments by pGA20ox2-TC-GUS. The most obvious difference between the transcriptional and translational forms of reporter is the inclusion of paralogue-specific exonic and intronic sequences. In tobacco, there is some evidence that *NtGA20ox* expression is suppressed at the post-transcriptional level by the binding of proteins to intronic sequences (Sakamoto et al., 2001). Similarly, inclusion of intronic sequences was shown to alter the expression patterns reported for the *AtGA3ox* paralogues, (Mitchum et al., 2006; Hu et al., 2008), though whether this is connected to GA homeostasis is unknown. A similar phenomenon was observed with GUS reporting of *AtCPS*, which is not regulated by GA homeostasis (Silverstone et al., 1997). The responsiveness of the transcriptional *AtGA20ox::GUS* reporters to bioactive GA has not been tested. Lacking intronic regulatory sequences, the transcriptional fusion GUS reporter constructs created during this project may not be fully subject to feedback regulation, and thus might represent *AtGA20ox* paralogue expression in the absence of homeostatic regulation. Whilst feedback regulation has been reported at the transcriptional level (Rieu et al., 2008), at present it is unknown if regulation also occurs at the translational or protein level. Differences in the lengths of promoter sequence used between transcriptional and translational fusions might also contribute to differences in expression (Figure 5.3a).

The near-absence of *AtGA20ox3* expression in late-stage wild-type floral tissues is surprising, given the difference in floral phenotype observed between *ga20ox1 ga20ox2* and *ga20ox1 ga20ox2 ga20ox3-1* (Figure 3.10). Two explanations present themselves. Firstly, evidence suggests that *ga20ox1 ga20ox2 ga20ox3-1* flowers represent a developmentally-arrested state (for stamens at least, see section 3.2.4), and that the phenotypic differences between it and *ga20ox1 ga20ox2* are due to this developmental arrest. If this arrest were to be overcome, *ga20ox1 ga20ox2 ga20ox3-1* flowers might develop to a similar extent as *ga20ox1 ga20ox2*, thus demonstrating no requirement for AtGA20ox3. However, this does not explain the discrepancies between *AtGA20ox3* GUS staining and expression analysis in wild-type floral tissues (Figure 5.6). Alternatively, *AtGA20ox3* expression is known to be repressed in the presence of functional *AtGA20ox1* and *AtGA20ox2* as *AtGA20ox3* expression is significantly up-regulated in *ga20ox1 ga20ox2* tissues, including inflorescence tissues (Rieu et al., 2008). Therefore, *AtGA20ox3* expression may normally be repressed in wild-type floral tissues through feedback regulation, but becomes up-regulated in the *ga20ox1 ga20ox2* mutant and thus causes partial phenotypic rescue. In this situation the discrepancies between GUS staining and expression data would be explained by the absence of homeostatic regulation of the *AtGA20ox::GUS* transcriptional fusions hypothesised above.

To test this second hypothesis, expression levels of *AtGA20ox3*, *-4* and *-5* were compared between wild-type and *ga20ox1 ga20ox2* stage 12 floral tissues (Figure 5.7b). *AtGA20ox3* expression was found to be significantly different between wild type and *ga20ox1 ga20ox2* in sepals, stamen filaments and the pistil ($p < 0.05$, Figure 5.7c, f and g), *AtGA20ox3* being up-regulated in *ga20ox1 ga20ox2* in each case. In contrast, there was no significant difference in *AtGA20ox3* expression between wild type and *ga20ox1 ga20ox2* petals, anthers or the receptacle (Figure 5.7b, e and h). No significant difference was found between wild-type and *ga20ox1 ga20ox2* floral tissues for either *AtGA20ox4* or *AtGA20ox5* ($p > 0.05$), with the exception of *AtGA20ox5* in sepals ($p < 0.05$, Figure 5.7c), which is apparently up-regulated.

These results suggest that, in the *ga20ox1 ga20ox2* background, *AtGA20ox3* expression is up-regulated in specific floral tissues, and that up-regulation of *AtGA20ox3* could account for the

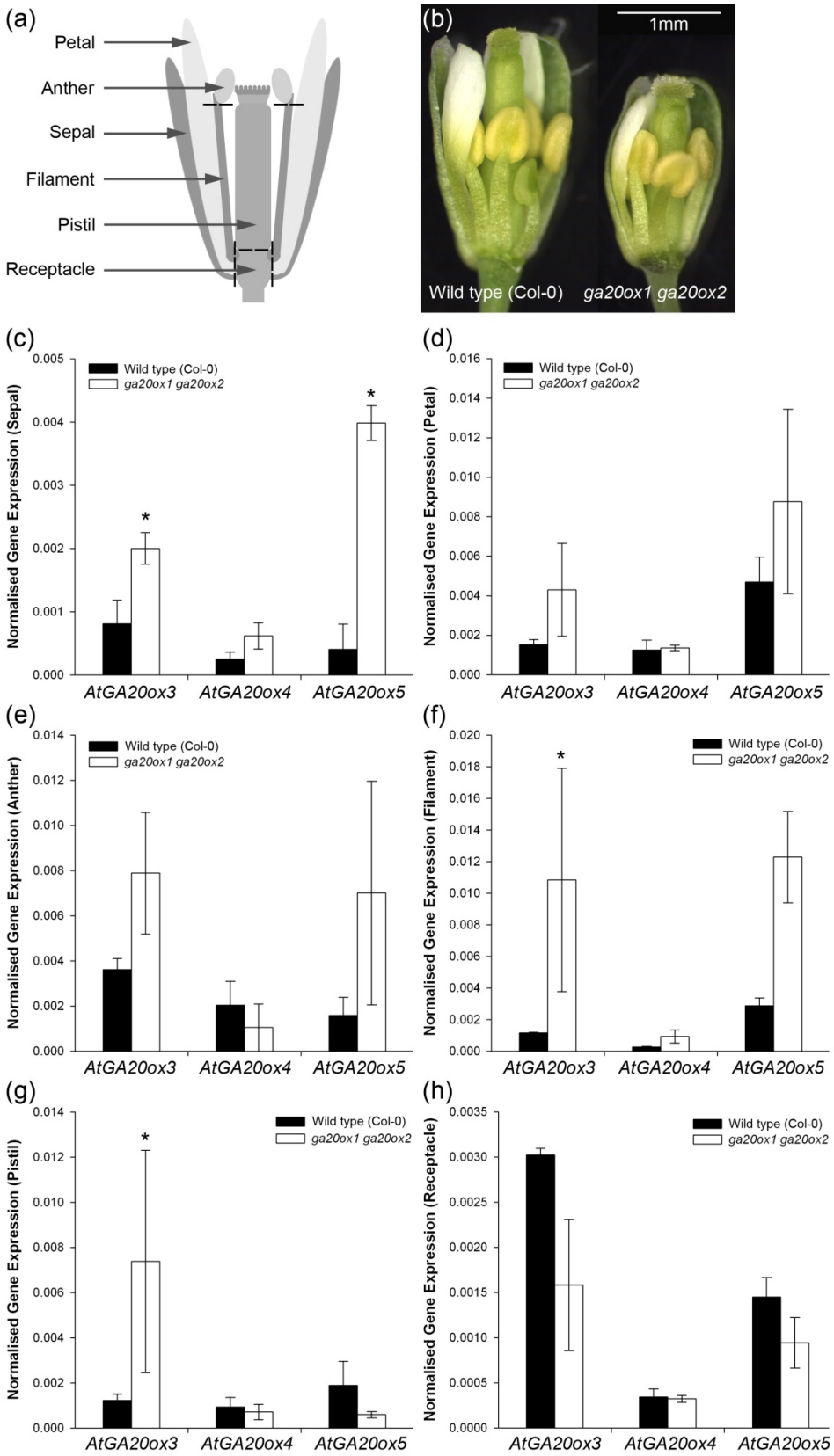

Figure 5.7: Floral expression of *AtGA20ox3*, *-4* and *-5* in the absence of *AtGA20ox1* and *-2*. *Expression levels were compared within individual floral organs (specified in (a)) of wild type and* ga20ox1 ga20ox2 *stage 12 flowers (b). Tissue was pooled from 35-40 independent*

flowers. Inflorescence development was synchronised at the 10th flower to open. Tissue was harvested from long stamens only. Gene expression was compared independently in sepal (c), petal (d), anther (e), filament (f), pistil (g) and receptacle (h) tissues using ANOVA. Bars represent the mean of three biological replicates, error bars represent one S.E. Petal, anther and pistil data required square root transformation, and filament data required log transformation, to meet the assumptions of statistical modelling. Genotype was not found to be a significant factor in partitioning variation in petal (p = 0.085), anther (p = 0.184) or receptacle tissue (p = 0.052). Pairwise comparisons were made in the remaining tissues between wild type and ga20ox1 ga20ox2 *genotypes within the same gene using a 5% LSD ((c), 0.000842; (f), 1.509; (g), 0.03237). Asterisks denote significant difference between wild-type and* ga20ox1 ga20ox2 *gene expression. Comparisons were not made between genes within the same genotype.*

relatively mild floral phenotype of *ga20ox1 ga20ox2* in light of wild-type *AtGA20ox* expression patterns. Whether this applies throughout floral development cannot be answered by this particular study, as only one developmental stage has been assessed. Two of these tissues (pistil and sepal) are predicted sites of *AtGA20ox3* expression based on GUS staining (Figure 5.5e and 5.6c), and loss of *AtGA20ox3* from the *ga20ox1 ga20ox2* background results in a further significant reduction in pistil and stamen length (see section 3.2.5). Petal growth is also enhanced by the presence of *AtGA20ox3*, but no up-regulation was found in this tissue. However, it must be borne in mind that both mutant and expression analysis suggests that petal growth is dependent on GA contributed by stamens and other floral tissues rather than themselves acting as a site for GA biosynthesis. Genetic evidence regarding the recovery of anther development in the *ga20ox1 ga20ox2* mutant compared to *ga20ox1 ga20ox2 ga20ox3-1* indicates a further role for *AtGA20ox3*, but no corresponding increase in anther expression was detected (Figure 5.7e). However, the developmental block associated with GA-deficiency occurs at an earlier stage of development which was not included in this experiment (see section 1.5.3), and *AtGA20ox3* expression independent of *AtGA20ox1* or *-2* might occur at that stage. Alternatively, given the potential mobility of bioactive and intermediate GAs (Proebsting et al., 1992), an increase in AtGA20ox activity in the filament

(Figure 5.7e) might be sufficient to indirectly increase the concentration of bioactive GA in the adjacent anther.

The absence of up-regulation of *AtGA20ox4* correlates with previous evidence that *AtGA20ox4* expression does not respond to GA treatment (Rieu et al., 2008) and is therefore thought not to be regulated through GA homeostasis. The increase of *AtGA20ox5* expression in sepal tissues is surprising, however, because this too is reported by the same study to not respond significantly to GA treatment. In a number of other floral tissues (anther and filament) mean *AtGA20ox5* expression was increased in *ga20ox1 ga20ox2* compared to wild type, but not by a significant amount. This result suggests that *AtGA20ox5* expression might be partially regulated by GA signalling, or this could potentially be the indirect result of some other change brought about by the absence of *AtGA20ox1* and *-2*.

The results from these experiments suggest that *AtGA20ox1* and *-2* are the most highly-expressed *AtGA20ox* genes in floral tissues late in development, although the expression levels presented here are relative, not absolute. They are expressed in non-overlapping, organ-specific patterns (*AtGA20ox1* in the filament and receptacle, *AtGA20ox2* in the pistil and, to a far lesser extent, the anther) and the greatest effects on floral phenotype by loss-of-function mutants correlates with these sites of expression. *AtGA20ox1* and *-2* apparently act to repress expression of *AtGA20ox3* in wild-type tissues, this paralogue becoming up-regulated in specific reproductively tissues in the *ga20ox1 ga20ox2* background. In contrast, *AtGA20ox4* and *-5* are not up-regulated in either the pistil or stamen. Comparisons between expression profiling of floral tissues and *AtGA20ox::GUS* reporter lines highlights the possibility of homeostatic regulation reinforcing organ-specific expression domains for *AtGA20ox1* and *-2*.

5.2.4 Expression of *AtGA20ox1*, *-2*, *-3* and *-4* is Reported in Tapetum Cells Prior to Tapetum Degeneration

To corroborate the GUS-staining results that implied tapetum-specific expression of *AtGA20ox* paralogues (see section 5.2.2), an attempt was made to quantify the expression of each individual *AtGA20ox* paralogue across a broader range of floral development, taking

advantage of an existing RNA developmental series of paired whole floral buds (Griffiths, J., unpublished data) between bud -12 and bud -3 (Figure 5.8). The large error bars associated with these results (Figure 5.8a and b) are caused by large variations between biological replicates (Figure 5.8c). For most target genes two biological replicates show similar expression whilst the third forms an outlier, although the identity of this outlier changes depending on the gene under investigation. Although the variability of this dataset means that it should be interpreted with caution, *AtGA20ox1* was found to be the most highly-expressed *AtGA20ox* paralogue in all stages sampled (Figure 5.8a) in two out of three replicates. A peak in *AtGA20ox1* expression is observed between bud sample -11/-12 and bud sample -7/-8 in these same two replicates, which correlates with the phase in which pGA20ox1-TC-GUS expression is observed in the tissues of early floral buds (Figure 5.4a). In contrast, *AtGA20ox2* expression (far less than that observed for *AtGA20ox1*) increases later in development in two replicates, from bud sample -5/-6, (Figure 5.8a and c). However, these expression levels are averaged across whole bud tissues: changes in *AtGA20ox2* stamen expression could be masked by relatively high expression in the pistil of the same buds, as evidenced by GUS staining (Figure 5.5) and mutant analysis (see sections 3.2.5 and 5.2.1).

As was found late in floral development (see section 5.2.3), expression of *AtGA20ox3*, *-4* and *-5* in developing floral tissues is very low in comparison to *AtGA20ox1* and *-2* (Figure 5.8a), which suggests only minor contributions to floral development. However, pooling RNA from whole buds might have masked localised expression in specific floral tissues. Two biological replicates demonstrate a peak in *AtGA20ox3* expression across bud samples -11/-12 and -9/-10 (Figure 5.8b), overlapping with the peak seen in *AtGA20ox1*. GUS staining indicates that the focus of expression of these two paralogues during floral development is stamen tissues (Figure 5.4a and e) as opposed to the broader expression of *AtGA20ox2* in both stamens and the pistil (Figure 5.4c), and this correlation of expression peaks might reflect this. The variability of expression of *AtGA20ox4* and *-5* from replicate to replicate (Figure 5.8c) makes interpretation unreliable. Similarly, the timing and extent of expression of *AtGA3ox3*, included as a marker for tapetum degeneration (Hu et al., 2008), proved to be highly variable between biological replicates.

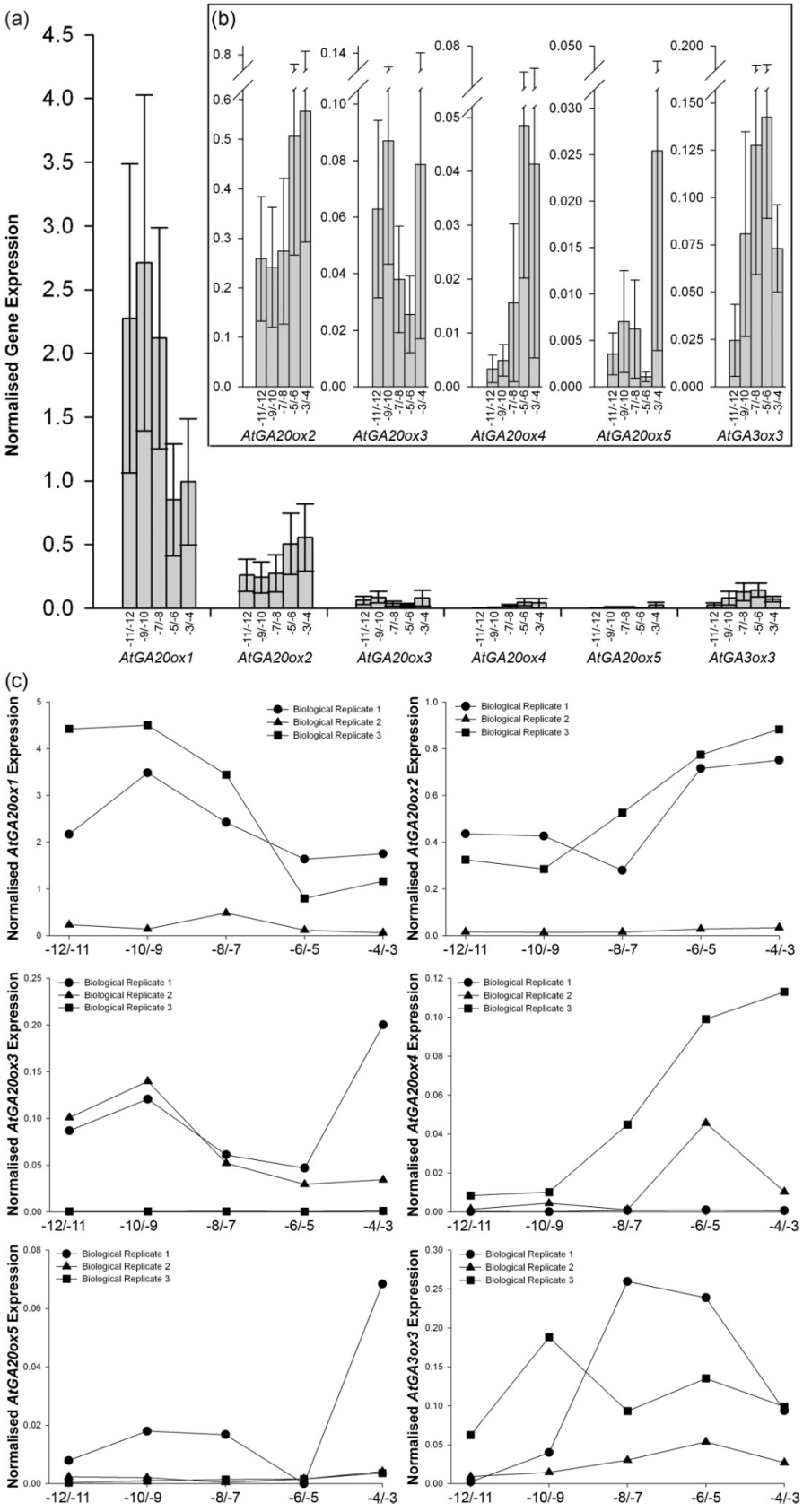

Figure 5.8: *AtGA20ox* expression during wild-type floral development.

Comparison between AtGA20ox *expression levels in whole floral buds across a fixed period of floral development, normalised against expression of reference gene At2g28390, scaled*

against expression of AtGA20ox1 *(a) and individually (b). Developing buds were harvested in sequential pairs from the primary inflorescence from bud -3 relative to flower opening. Bars represent the mean of three biological replicates, error bars represent one S.E. Normalised expression levels of target genes from each biological replicate are detailed in (c).*

A number of technical problems are associated with this dataset. Firstly, these three replicates were harvested at different points in time during one day. *AtGA20ox1* expression has been previously shown to oscillate in a circadian-dependent manner in petiole tissues (Hisamatsu et al., 2005), and so time of harvesting may have had a significant effect on *AtGA20ox1* expression levels. Furthermore, expression of *AtGA20ox1*, *-2* and -3 is linked through feedback regulation, so changes in the expression of *AtGA20ox1* are likely to affect the expression of these other two paralogues. In addition, the buds sampled within each biological replicate are not truly independent of one another, by virtue of the fact that they were harvested from the same inflorescences. Flower opening is not an instant process and so requires personal judgements to be made regarding its position, which will subsequently affect all bud samples collected from that inflorescence. Also, floral development is a continuous process, so will have continued whilst harvesting progressed, causing further shifts of gene expression between biological replicates. Whilst these results provide some supporting evidence for the GUS expression patterns seen during floral development, they are not by any means conclusive.

To investigate the tissue expression patterns of *AtGA20ox* paralogues during anther development in more detail, a microscopic analysis of the pGA20ox-TC-GUS transgenic reporter lines was undertaken. GUS staining of tapetum cells was observed in stage 9/10 anthers for all reporter lines (Figure 5.9a), prior to tapetum degeneration. No GUS staining was observed in degenerating tapetum cells. This is consistent with reports of *AtGA3ox* expression, which also occurs in the tapetum at this stage of development (Hu et al., 2008, see section 1.5.3). Similarly, *AtGA20ox* expression is reported in anther tissues during meiosis and anther dehiscence, again matching the cumulative expression pattern of the *AtGA3ox* gene

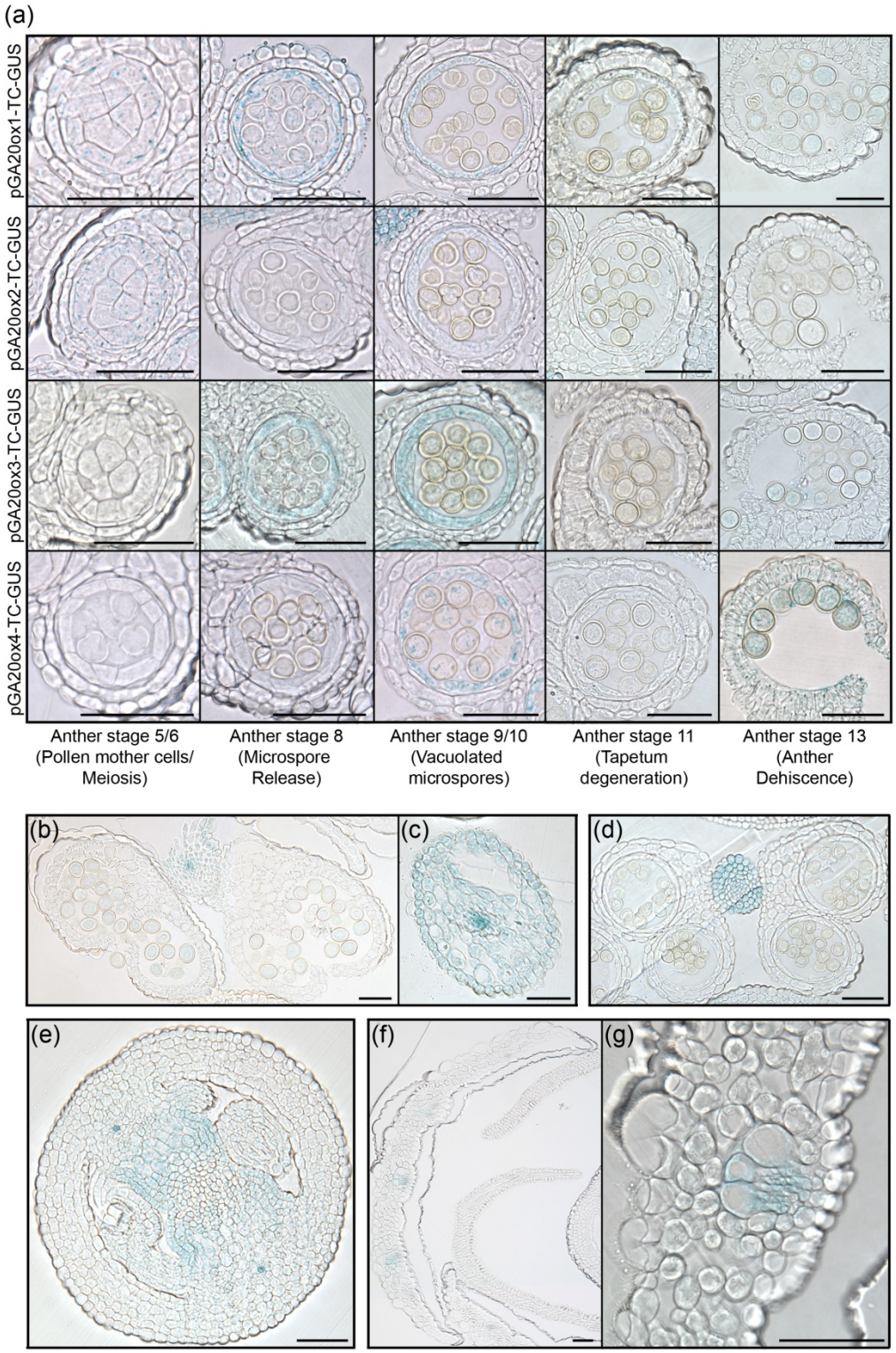

Figure 5.9: Floral tissue expression patterns of *AtGA20ox* paralogues.

Individual GUS staining patterns were observed in wild-type anther tissues during pollen development for AtGA20ox1, -2, -3 and -4 TC reporter lines (a). GUS staining reported in filament tissues for pGA20ox1-TC-GUS (b, c) filament and pistil tissues for pGA20ox2-TC-GUS (d, e) and sepal vasculature for pGA20ox3-TC-GUS (f, g). All scale bars = 50µm.

family, suggesting that these two steps of GA biosynthesis are co-expressed during anther development. However, the *AtGA20ox* paralogues do not follow the divisions seen in the *AtGA3ox* gene family, where *AtGA3ox1* contributes almost all GA3ox activity to floral tissues but is excluded from the anther, whilst *AtGA3ox2*, *-3* and *-4* are localised exclusively to anther tissues (see section 1.5.3). In comparison, expression of the *AtGA20ox* paralogues is divided more equally, as demonstrated by their individual expression anther patterns (Figure 5.9a).

Both pGA20ox1-TC-GUS and pGA20ox2-TC-GUS were weakly expressed in PMCs and the tapetum at anther stage 5, but whilst pGA20ox1-TC-GUS expression continued in anther tissues though to stage 10, becoming restricted to the tapetum by this stage, pGA20ox2-TC-GUS expression declined after meiosis but reappeared in the tapetum prior to PCD. pGA20ox2-TC-GUS expression was not reported in subsequent anther development, but pGA20ox1-TC-GUS expression was later found in mature pollen at anther dehiscence. In contrast, pGA20ox3-TC-GUS and pGA20ox4-TC-GUS were only expressed post-meiotically, with GUS staining restricted to the tapetum and, in the case of pGA20ox4-TC-GUS, weakly in developing microspores, up to anther stage 10. Expression of both of these paralogues was reported in mature anthers, pGA20ox3-TC-GUS weakly across both pollen and anther wall tissues, and pGA20ox4-TC-GUS in mature pollen. In other floral tissues, pGA20ox1-TC-GUS and pGA20ox2-TC-GUS were expressed throughout the filament cross-section, though *AtGA20ox1* was focussed in the filament vasculature (Figure 5.9b and c) with *AtGA20ox2* more uniformly expressed (Figure 5.9d). Pistil expression of pGA20ox2-TC-GUS is localised to the transmission tract, and is also visible in vasculature (Figure 5.9e). Sepal expression of pGA20ox3-TC-GUS was also localised to vascular tissues (Figure 5.9f and g). These results suggest that *AtGA20ox* expression occurs directly in the tapetum cell layer prior to its entry into PCD. Expression of *AtGA20ox3* and *-4* in this tissue explains the continuation of anther development in the *ga20ox1 ga20ox2* mutant. Unlike the GUS analysis of whole flowers these results suggest that *AtGA20ox* expression overlaps with *AtGA3ox*, both in the tapetum and at other points in pollen development. This discrepancy can be reconciled by slight differences in the timing of expression between *AtGA20ox* and *AtGA3ox* genes within anther stages 9-10.

Together with the *AtGA3ox* expression patterns, these results strongly suggest that the tapetum is the main site of GA biosynthesis within the developing anther, and thus could potentially act to co-ordinate the anther and pollen developmental programmes. Whilst no tapetum-specific expression profile is available yet for *Arabidopsis* as is the case in rice (Hirano et al., 2008), a partial validation of these results can be performed by comparing the post-meiotic GUS staining of developing pollen against an existing high-resolution gametophyte-specific microarray experiment (Honys and Twell, 2004). Expression of *AtGA20ox1*, *-2* and *-4* was found during pollen development, all of which show some GUS staining in their respective reporter lines, whereas expression of *AtGA20ox3* and *-5* was not, when GUS staining reported some expression of *AtGA20ox3* in developing microspores. However, similar analysis of the *AtGA3ox* gene family in the pollen transcriptome finds only *AtGA3ox3* is represented, whereas previous GUS analysis of that family had identified pollen-specific expression of *AtGA3ox2*, *-3* and *-4*. These discrepancies between GUS reporters and microarray analysis in both families could be due either to over-sensitivity of the GUS reporters, or the level of expression of some paralogues falling below the detection threshold of the microarray. Interestingly, a division of *AtGA20ox* expression is visible across pollen development in the transcriptome data, with *AtGA20ox1* and *-4* expressed in unicellular and bicellular pollen only, whilst *AtGA20ox2* is expressed in late pollen development from the bicellular stage through to mature pollen. This division was not detected by GUS analysis, although *AtGA20ox1* and *-4* were reported in microspores prior to tapetum degeneration/pollen mitosis. As might be expected from all other experimental results from this project, expression levels of *AtGA20ox1* and *-2* are far greater than *AtGA20ox4* in developing pollen.

The transcriptome data of Honys and Twell (2004) indicates that, cumulatively, *AtGA20ox* and *AtGA3ox* are both expressed in all post-meiotic stages of *Arabidopsis* pollen development, with a peak in expression of both families overlapping with entry of the microspores into pollen mitosis and of the tapetum into PCD. Previous GUS analysis did not find *AtCPS* expression in the tapetum prior to its degeneration, but did identify it in developing pollen from the bicellular stage onwards (Silverstone et al., 1997). However, no *AtCPS* expression was identified in the transcriptome post-meiotic pollen (although both *AtKO* and *AtKAO* are

represented in the unicellular and bicellular stages), suggesting a potential bottleneck in the early stages of GA biosynthesis. However, the stamen filament must be considered as a potential remote source of both intermediate and bioactive GAs for anther tissues. The relationship between anther and filament in terms of GA flux has yet to be investigated, and the degree of interdependency between these two organs is currently unknown.

5.3 CONCLUSIONS

From the experiments detailed in this chapter it can be concluded that the *AtGA20ox* paralogues exist in a series of hierarchical relationships during floral development, with *AtGA20ox1* and -*2* dominating. The expression patterns of these two paralogues are focussed predominantly on separate reproductive organs, *AtGA20ox2* in the pistil and *AtGA20ox1* in the stamen filament. However, both are expressed in the tapetum during a critical phase of pollen development. GA deficiency affects the growth of these two reproductive organs at different developmental stages, with the greatest impact on stamen development occurring during late filament elongation. *AtGA20ox3* potentially acts prior to this stage to promote entry of the tapetum into PCD in conjunction with *AtGA20ox1* and -*2*, but is nevertheless expressed at a very low level in comparison with *AtGA20ox1* and -*2*, which apparently act to repress its expression through homeostatic regulation in wild-type floral tissues. Any direct role for *AtGA20ox3* in later floral developmental events remains unclear. The expression patterns of the *AtGA20ox* paralogues in floral tissues change during floral development, producing two synchronised peaks of expression, one prior to tapetum degeneration and a second immediately prior to flower opening. Despite demonstrating individual expression patterns, multiple *AtGA20ox* paralogues are expressed simultaneously in the tapetum after meiosis, overlapping with *AtGA3ox* paralogues, suggesting that the tapetum is an important source of late GA-biosynthetic activity in the anther at this stage of development.

CHAPTER 6: THE EFFECT OF CHEMICAL AND GENETIC GA OVERDOSE ON *ARABIDOPSIS* REPRODUCTIVE DEVELOPMENT

6.1 INTRODUCTION

Previous research has demonstrated that chemical treatment of *Arabidopsis* with bioactive GA has a negative effect on fertility (Jacobsen & Olszewski, 1993) a conclusion supported by earlier experiments within this project (see section 3.2.3). These utilised GA_3 (Figure 1.2), a species of biologically active GA that is resistant to deactivation by GA 2-oxidase activity due to the presence of a carbon double-bond at C-1,2. The observed reduction in fertility is thus thought to be caused by a persisting GA response or 'GA overdose', although how this results in reduced yield remains undetermined. GA overdose conditions can also be replicated using mutants associated with GA signal transduction. Loss of DELLA repression has been shown to phenocopy wild-type plants chemically treated with GA in numerous dicot and monocot species (Lanahan & Ho, 1988; Peng et al., 1997; Silverstone et al., 1998; Ikeda et al., 2001; Bassel et al., 2008), indicative of increased or constitutive GA signalling in these mutants.

In rice, loss of its single DELLA protein SLENDER RICE 1 (SLR1) is reported to cause sterility (Ikeda et al., 2001), though this phenotype has not been characterised more closely. The equivalent loss-of-function DELLA mutant in barley, *slender* (*sln*), is also reported to be sterile, demonstrating a pollenless phenotype (Lanahan & Ho, 1988). In *Arabidopsis* (which carries five DELLA paralogues, see section 1.3.2), loss of both *RGA* and *GAI* in the Landsberg *erecta* (L*er*) ecotype causes impaired fertility (King et al., 2001), with both a reduction in the amount of pollen produced and shorter stamens relative to the pistil (Dill & Sun, 2001). The severity of this phenotype is apparently not exacerbated by loss of additional DELLA paralogues (Cheng et al., 2004). However, recent work in the Columbia-0 (Col-0) ecotype using a novel *GAI* loss-of-function allele, *gai-td1* (derived from the SAIL collection, line 587_C02, Sessions et al., 2002), in combination with the loss-of-function allele *rga-28* (Tyler et al., 2004), identified an associated male-sterile phenotype (Thomas, S., unpublished data), a result that obviously conflicts with the equivalent L*er* mutant phenotype.

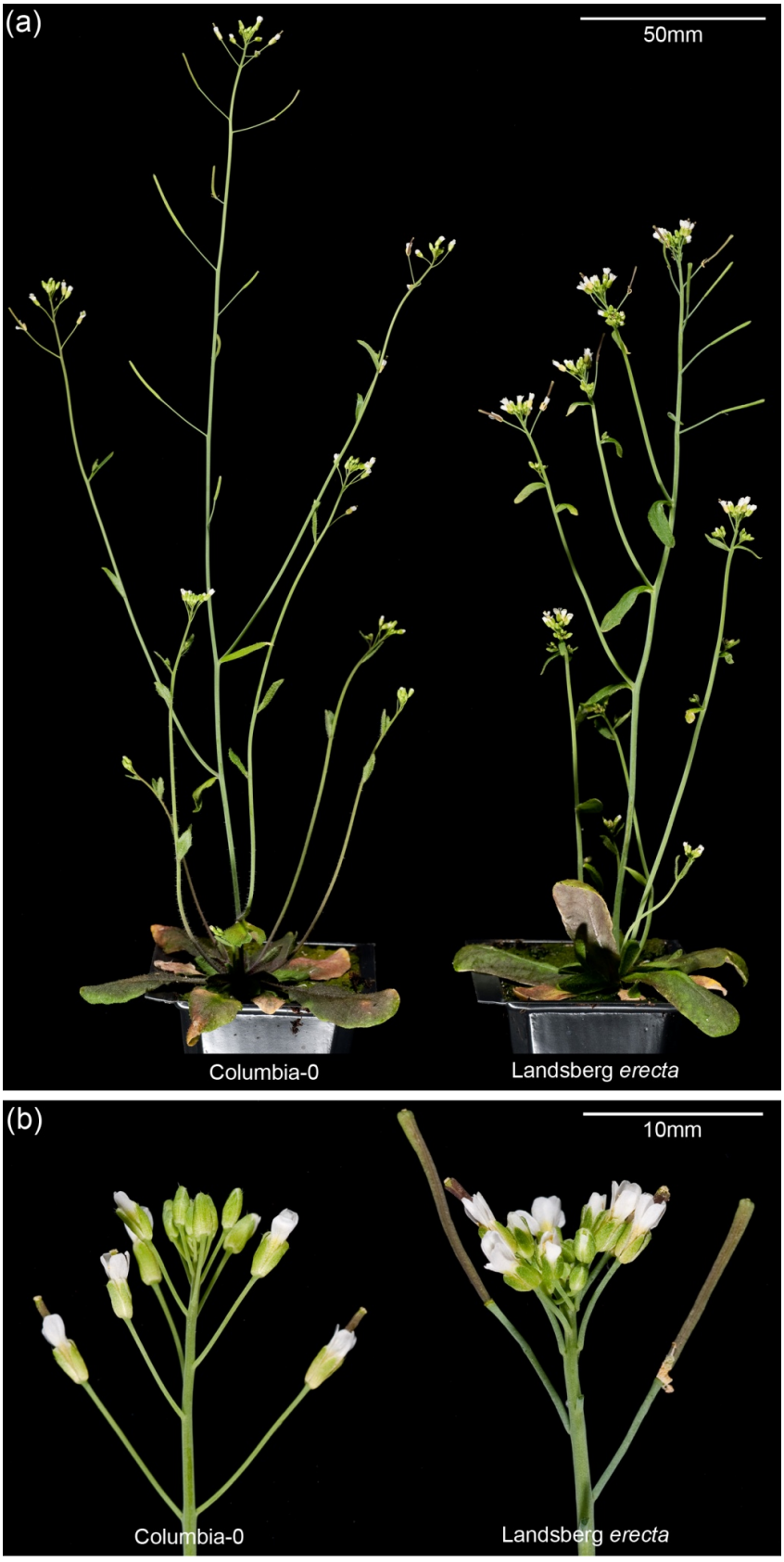

Figure 6.1: Columbia-0 and Landsberg *erecta* inflorescence phenotypes.

Comparison between 27 day-old wild-type Col-0 and Ler plants, showing differences in whole plant phenotype (a) and architecture of the primary inflorescence floral cluster (b).

The phenotypes of these two ecotypes are quite distinct, with Col-0 displaying increased stature due in part to increased elongation of inflorescence internodes (Figure 6.1a). Clear differences are also visible in the architecture of the floral cluster: internode elongation begins before flower opening in Col-0 but only occurs in L*er* inflorescences beneath opened flowers (Figure 6.1b). One obvious genetic difference between these two ecotypes is the loss of *ERECTA* in L*er*, which has been shown to cause large-scale phenotypic changes in the Col-0 background (Torii et al., 1996), but the extent to which the phenotypic differences between these two ecotypes are a result of altered GA biosynthesis or signalling has not previously been investigated.

Evidence presented in this chapter compares the effects of chemical and genetic GA overdose on both the Col-0 and L*er* ecotypes of *Arabidopsis* and finds that significant differences exist between their underlying growth responses to GA, with L*er* fertility proving more resilient under GA-overdosed conditions. The negative impact of GA-overdose on fertility of the Col-0 ecotype cannot be explained by altered floral organ growth. Male sterility of *rga-28 gai-td1* is caused by disrupted pollen development, either during or shortly after meiosis, and might be associated with defects in pollen wall deposition. Pollen development in this mutant was complemented by reintroduction of functional DELLA protein into either the tapetum cell layer or developing pollen. The difference in male fertility between Col-0 and L*er rga gai* mutants could not be explained by the presence/absence of *ERECTA*, and might instead be due to altered expression patterns of other DELLA paralogues within floral tissues.

6.2 RESULTS AND DISCUSSION

6.2.1 The *Arabidopsis* Ecotypes Columbia-0 and Landsberg *erecta* Respond Differently to GA Overdose

To test for differences in the response of the *Arabidopsis* ecotypes Col-0 and L*er* to chemical and genetic GA overdose, the growth and fertility of wild-type and mutant plants was compared under control growth conditions and exogenous treatment with GA_3 (n = 144). Genetic GA overdose was achieved in the Col-0 ecotype by three separate approaches: constitutive expression of the GA biosynthetic gene *AtGA20ox1* under the viral 35S promoter

(previously shown to cause GA-overdose phenotypes, Coles et al., 1999), loss of C_{19}-GA catabolism by GA 2-oxidase activity, as established previously in the *ga2ox1-1 ga2ox2-1 ga2ox3-1 ga2ox4-1 ga2ox6-2* mutant (herein referred to as the *ga2ox* quintuple mutant, Rieu et al., 2008a) and loss of DELLA repression of downstream GA responses in the *rga-28 gai-td1* mutant. These were compared against L*er* wild type and the previously described L*er* *rga-24 gai-t6* mutant, in which reduced fertility was observed (Dill & Sun, 2001).

Both GA treatment and genotype had significant effects on all vegetative phenotypes characterised (Table 6.1), though in the case of mature rosette diameter no significant interaction between these two factors was found ($p = 0.159$), suggesting that GA treatment affected all genotypes equally. Averaged across GA treatments, rosette diameter of both *35S::GA20ox1* and *rga-28 gai-td1* was significantly different from wild-type Col-0 ($p < 0.01$, Table 6.1a), displaying reduced rosette size, as did *rga-24 gai-t6* in comparison with wild-type L*er* ($p < 0.01$). In contrast, the effect of chemical GA treatment averaged across all genotypes was to increase rosette diameter ($p < 0.01$), a finding supported by previous experiments in this project (see sections 3.2.2 and 4.2.2).

Genotype and GA treatment showed a significant interaction in the three other vegetative characters studied ($p < 0.001$ for each, Table 6.1b), indicating differential responses. The total height of all genetically GA-overdosed Col-0 genotypes was significantly different from wild-type Col-0 ($p < 0.01$), all three demonstrating similarly increased growth. In contrast, *rga-24 gai-t6* did not differ significantly from wild-type L*er*. All genotypes responded to chemical GA treatment ($p < 0.01$) except wild-type L*er*, which did not. This demonstrates a difference between Col-0 and L*er* in their responsiveness to GA, and also suggests that loss of *RGA* and *GAI* in L*er* increases its responsiveness to chemical GA treatment, presumably through depletion of DELLA protein repressing growth. The saturation of GA response by *35S::GA20ox1* has not previously been tested, but Rieu et al. (2008a) found that loss of *ga2ox* activity did not fully replicate chemical GA overdose of plant stature, consistent with the results of this experiment.

(a)

Genotype (All GA treatments)	Rosette Diameter (mm)
Wild type (Col-0)	97.58
***35S::GA20ox1* (Col-0)**	79.04[a]
***ga2ox* quint. K.O. (Col-0)**	96.29
***rga-28 gai-td1* (Col-0)**	72.50[a]
Wild type (L*er*)	85.50[a]
***rga-24 gai-t6* (L*er*)**	68.74[b]
1% LSD	***8.506***

GA Treatment (All Genotypes)	Rosette Diameter (mm)
-GA	77.40
+GA	89.15*
LSD1%	***8.895***

(b)

Genotype	Primary Inflorescence Height (mm)		Number of Vegetative Internodes (V.I.)		Mean V.I. Length (mm)	
	-GA	+GA	-GA	+GA	-GA	+GA
Wild type (Col-0)	403.5	526.2*	2.500	4.167*	28.60 [1.4503]	31.60 [1.4956]
***35S::GA20ox1* (Col-0)**	485.6[a]	597.8[c]*	4.250[a]	4.250	32.33 [1.5028]	39.63[c]* [1.5939]
***ga2ox* quint. K.O. (Col-0)**	461.6[a]	521.9*	3.580[b]	4.417*	26.88 [1.4237]	32.63 [1.5093]
***rga-28 gai-td1* (Col-0)**	453.9[a]	571.7c*	3.500[b]	4.500*	22.15[a] [1.3413]	33.24* [1.5158]
Wild type (L*er*)	277.9[b]	289.9[d]	3.000	4.083*	36.92[b] [1.5329]	32.60 [1.5085]
***rga-24 gai-t6* (L*er*)**	295.5[b]	338.1[e]*	2.917	2.997[c]	29.40' [1.4608]	35.89 [1.5507]
1% LSD	***36.15*** *(40.92)*		***0.5954*** *(0.6093)*		***[0.06842]*** *([0.09006])*	

Table 6.1: Effects of GA overdose on *Arabidopsis* vegetative growth.

*A comparison of GA-overdose mutants in the Col-0 and L*er *ecotypes against their respective wild-type controls under control growth conditions and chemical GA treatment, comparing rosette diameter (a) and primary inflorescence characteristics (b). Values given are the mean of 24 independent measurements (a), and 12 independent measurements (b), respectively. V.I. length was analysed on a transformed scale (log), transformed values denoted by square brackets. Pairwise comparisons were made within each phenotypic character using 1% LSDs. LSDs comparing means between genotypes within a GA treatment*

are highlighted in bold, those comparing means between GA treatments in rounded brackets. Superscript letters indicate means significantly different from the Col-0 wild type within that GA treatment, with different letters denoting groups of values significantly different from one another. Where not otherwise indicated, significant difference between rga-24 gai-t6 *and L*er *wild type is marked by an apostrophe. Asterisks denote a significant difference between GA treatments within the same genotype. Comparisons were not made between genotypes in different GA treatments.*

All genetic GA-overdose mutants in Col-0 demonstrated increased numbers of elongating vegetative internodes (V.I., $p < 0.01$), with greater numbers elongating in *35S::GA20ox1* than the *ga2ox* quintuple or *rga-28 gai-td1* ($p < 0.01$). In contrast, loss of *RGA* and *GAI* in the L*er* ecotype did not have a significant effect, even though wild-type Col-0 and L*er* both responded to chemical GA treatment ($p < 0.01$), as did the *ga2ox* quintuple and *rga-28 gai-td1* genotypes ($p < 0.01$). *35S::GA20ox1* was not affected by additional chemical GA overdose, suggesting that its response to GA is already saturated. The length of individual vegetative internodes was less sensitive to genetic GA overdose, with only *rga-28 gai-td1* being significantly different from wild-type Col-0 ($p < 0.01$), and in fact displaying reduced length. *rga-24 gai-t6* internode length is similarly different from its respective wild type ($p < 0.01$). However, whilst internode length in *rga-28 gai-td1* is significantly affected by chemical GA treatment ($p < 0.01$), again, *rga-24 gai-t6* internodes are not ($p > 0.01$).

Collectively, these results indicate that differences exist between the Col-0 and L*er* ecotypes in their responses to GA overdose. Rieu et al. (2008a) found similar phenotypes in the *ga2ox* quintuple mutant for plant stature and the number and length of vegetative internodes to those seen in this experiment, although they report a reduction of vegetative internode length in both wild-type Col-0 and the *ga2ox* quintuple mutant under GA treatment, which was not observed here. Interestingly, *35S::GA20ox1* showed a further increase in internode length under GA treatment ($p < 0.01$), becoming significantly different from GA-treated wild-type ($p < 0.01$). The reasons for these contradictions are not clear, but may relate to differences in the size of experimental populations affecting data analysis (12 vs. 18), or to other technical differences

in methodology. The effects of GA treatment on wild-type Col-0 in this experiment are consistent with those seen previously in this project (Table 3.1).

Differential responses to GA between ecotypes were also observed in reproductive phenotypes. Analysis of flowering time (as measured by days from sowing) found no significant interaction between genotype and chemical GA treatment ($p = 0.223$, Figure 6.2a and b), and GA treatment was not a significant factor in flowering when measured by the number of leaves, ($p = 0.096$, Figure 6.2c). The effect of GA treatment on chronological flowering time (averaged across all genotypes) was to marginally accelerate flowering ($p < 0.01$, Figure 6.2b). *rga-28 gai-td1* is not significantly different from wild-type Col-0 on either scale of measurement, but *rga-24 gai-t6* does differ significantly from wild-type L*er* on both ($p < 0.01$, Figure 6.2a, c), with flowering accelerated. The only Col-0-derived genotype to differ significantly from wild type is *35S::GA20ox1* ($p < 0.01$), with flowering again accelerated. Previously, however, both *35S::GA20ox1* and the *ga2ox* quintuple mutant have been separately found to demonstrate accelerated flowering (Coles et al. 1999; Rieu et al., 2008a), though in the case of the *ga2ox* quintuple this response remained unsaturated in its response to GA (Rieu et al., 2008a). The same explanations for these differences apply here as for vegetative characters, as outlined above. Whilst flowering time between wild-type Col-0 and L*er* is not significantly different when measured chronologically, it does differ significantly when measured developmentally ($p < 0.01$, Figure 6.1c), L*er* flowering after fewer leaves have been produced, a phenotype further enhanced by the absence of *RGA* and *GAI* ($p < 0.01$). Whether this ecotypic difference is entirely GA-dependent remains unclear.

The effect of genetic GA overdose on fertility was measured indirectly through silique phenotypes. The lengths of *35S::GA20ox1* and *ga2ox* quintuple mutant siliques were significantly different from wild-type Col-0 under control growth conditions ($p < 0.01$, Figure 6.2d), being reduced in size. This correlates with a reduction in the number of seeds per silique in both genotypes ($p< 0.01$, Figure 6.2e), seen previously in the *ga2ox* quintuple mutant (Rieu et al., 2008a). Because silique length is dependent on seed number (Cox and Swain, 2006), inferences about the effect of genetic GA overdose on growth of silique tissues

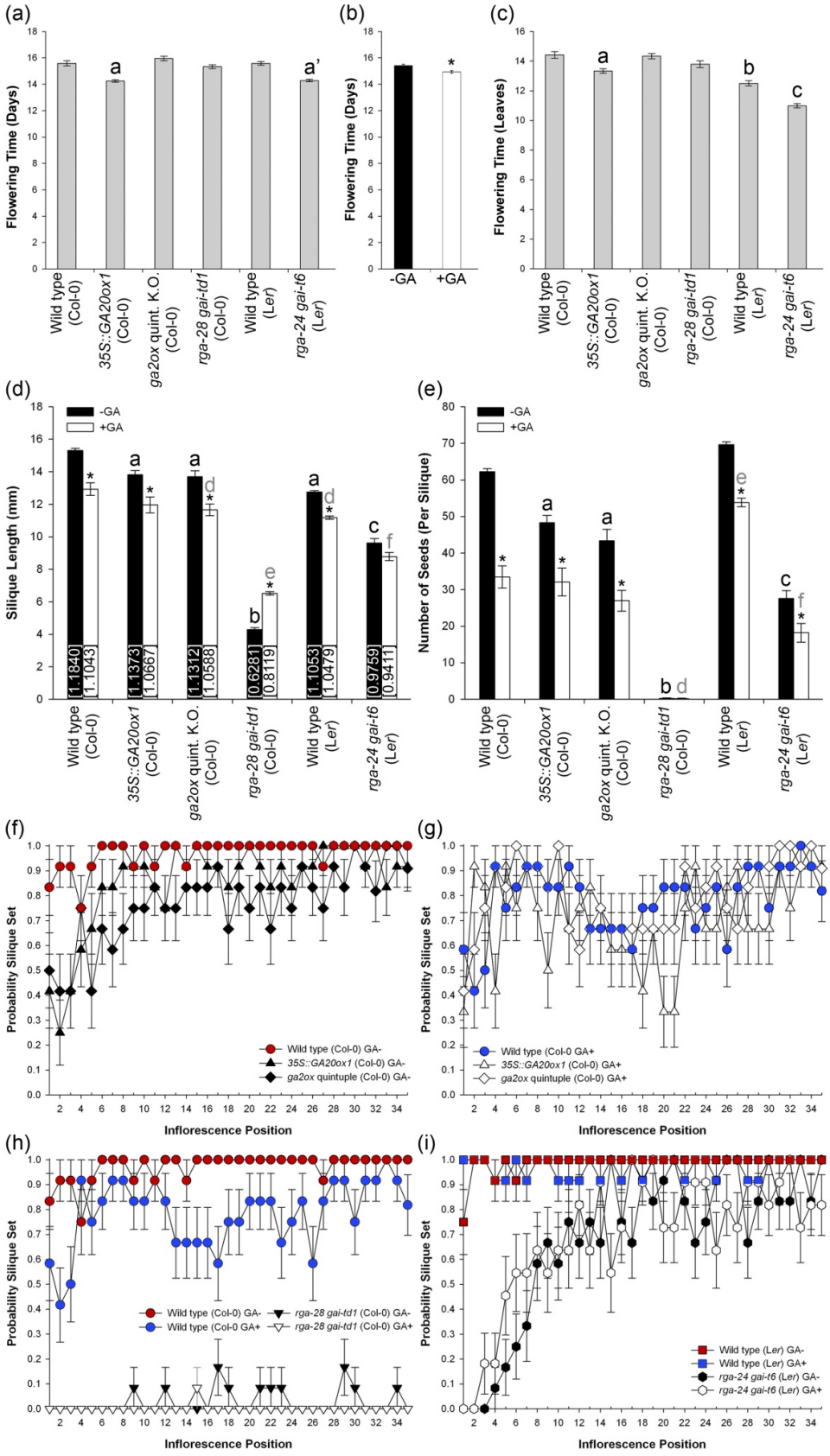

Figure 6.2: Effects of GA overdose on *Arabidopsis* flowering and fertility.

*Comparison of GA-overdose mutants in the Col-0 and L*er *ecotypes against their respective wild-type controls under control growth conditions and chemical GA treatment, comparing*

flowering time (a-c), silique length (d), number of seeds per silique (e) and silique-set as a measure of fertility during flowering of the primary inflorescence (f-i). Flowering time in days is represented as two independent main effects: genotype averaged across GA treatments (a) and GA treatment averaged across all genotypes (b). GA treatment was not a significant factor in flowering time as measured by the number of leaves (p = 0.096): values for each genotype were hence averaged across GA treatments (c). Silique length was analysed on a transformed scale (log), transformed values shown in square brackets. Three siliques were measured per plant, harvested between inflorescence positions 15 and 20.
Graphs represent the mean of 24 measurements (a, c), 72 measurements (b), 36 measurements (d, e), and 12 measurements (f-i) respectively. Error bars represent one S.E. Pairwise comparisons were made using a 1% LSD ((a) 0.4758; (b) ; (c) 0.6327; (d) 0.04383 between genotypes, 0.0502 between GA treatments; (e) 8.752 between genotypes, 9.717 between GA treatments). Superscript letters indicate means significantly different from the Col-0 wild type within that GA treatment, with different letters denoting groups of values significantly different from one another. Where not otherwise indicated, a significant difference between rga-24 gai-t6 *and L*er *wild type is marked by an apostrophe. Asterisks denote significant difference between GA treatments within a genotype. No comparisons were made between genotypes in different GA treatments. Statistical analysis was not performed on silique-set data (f-i).*

cannot be drawn from this data. A significant difference in silique length was found between wild-type Col-0 and L*er* ($p < 0.01$), with L*er* setting shorter siliques. However, there was no reduction in the numbers of seed per silique ($p > 0.01$). GA treatment had a significant negative effect on both silique length and seed number in each of these four genotypes ($p < 0.01$, Figure 6.2d and e). These results contrast with the previous findings of Rieu et al. (2008a) that both silique length and seed number in the *ga2ox* quintuple mutant are saturated for GA response. Col-0 exhibits a far greater reduction in seed number than L*er* under GA treatment (to approximately 50% of yield under control growth conditions), resulting in a significant difference between these two genotypes ($p < 0.01$, Figure 6.2e).

Silique phenotypes of *rga-24 gai-t6* are significantly different from wild-type L*er* under control growth conditions ($p < 0.01$, Figure 6.2d and e), exhibiting a reduction of both silique length and seed number. Whilst silique length was not significantly affected by GA treatment, the number of seeds was found to be further reduced ($p < 0.01$). The *rga-28 gai-td1* mutant phenotype is far more severe, however, exhibiting much shorter siliques than either wild-type Col-0 or *rga-24 gai-t6* ($p < 0.01$, Figure 6.2d). These siliques were mostly empty (Figure 6.2e), with at most one or two seeds occasionally present. Chemical GA treatment significantly affects *rga-28 gai-td1* silique length ($p < 0.01$), causing it to increase (in contrast to all other genotypes), but seed-set was not rescued (Figure 6.2e). Elongation of siliques in this mutant under chemical GA treatment is probably due to parthenocarpic growth of unfertilised pistils, which is induced by exogenous GA treatment (Vivian-Smith & Kolutnow, 1999).

In addition to silique characters, silique-set on the primary inflorescence of each plant was scored as a measure of pollination success, previously found to be reduced by GA treatment (see section 3.2.5). Under control growth conditions both wild-type Col-0 and L*er* demonstrate an early period of reduced fertility before successful silique-set is established, fertility remaining consistently high from this point (Figure 6.2f and i). *35S::GA20ox1* and the *ga2ox* quintuple mutant demonstrate a more severe and prolonged period of reduced silique-set at the start of flowering (Figure 6.2f), fertility subsequently rising but never becoming as robust as in wild-type Col-0. Under chemical GA treatment the probability of silique-set in Col-0 was reduced throughout flowering, becoming similar to *35S::GA20ox1* and the *ga2ox* quintuple mutant, which are relatively unaffected by GA treatment (Figure 6.2g and h). This result correlates with the findings of previous experiments investigating the effect of GA on early fertility (see section 3.2.5). A sporadic reduction in silique-set was previously observed (though not directly measured) in the *ga2ox* quintuple mutant, which was ascribed to pistil overgrowth (Rieu et al., 2008a). However, GA treatment was reported to suppress this phenotype, leading to the conclusion that the defects were due to inequalities between the levels of bioactive GA in floral organs. The results presented here contradict this

and suggest instead that an increase in the absolute amount of bioactive GA negatively affects fertility.

In contrast to Col-0, silique-set of wild-type L*er* was not affected by GA treatment and remained uniformly high (Figure 6.2i). Despite this, loss of *RGA* and *GAI* in the L*er* ecotype negatively affects fertility, with greatly reduced silique-set observed early in flowering (Figure 6.2i). Fertility of the primary inflorescence gradually recovered, but remained less robust than wild-type L*er*. Silique-set of *rga-24 gai-t6* was not obviously affected by chemical GA treatment. In Col-0, loss of *RGA* and *GAI* causes a near-complete loss of silique-set on the primary inflorescence throughout flowering, with only sporadic siliques developing (Figure 6.2h) which contain almost no seed (see above), a phenotype that was not restored by GA treatment.

The results of this characterisation demonstrate that aspects of Col-0 and L*er* plant growth respond differently to GA overdose, though not in all characters observed and not in a consistent manner, suggesting that the underlying differences between these ecotypes is complex. Whilst GA overdose is sub-optimal for both silique-set and seed-set in wild-type Col-0, silique-set in L*er* is far more robust under the same GA-treatment regime, nor is seed-set as strongly affected. The effect of genetic GA overdose through manipulating the GA metabolic pathway partially replicates the phenotypes seen under chemical GA overdose. In general, over-expressing *AtGA20ox1* had a stronger effect on phenotype than that caused by reducing *GA2ox* catabolism of bioactive GA. Genetic manipulation of GA biosynthesis did not saturate GA responsiveness in many phenotypic characters, including some that were previously reported as being so. The effect of removing DELLA inhibition was similar to that of ectopic GA biosynthesis in vegetative characters. In many cases these GA responses were not saturated, thus indicating additional roles for the remaining DELLA paralogues. Differences between *rga-28 gai-td1* and *rga-24 gai-t6* are apparent in both vegetative and reproductive phenotypes, suggesting that the functions of these two paralogues differ between the two ecotypes.

The results obtained here confirm the previous finding that loss of *RGA* and *GAI* impairs fertility in the L*er* background (Dill & Sun, 2001), but loss of these same two paralogues from Col-0 is apparently sufficient to induce complete sterility. Interestingly, this phenotype could not be replicated by chemical GA overdose in either ecotype. The population of DELLA protein is unlikely to be entirely depleted by GA treatment, as evidenced by Western blotting (Dill et al., 2004; Feng et al., 2008) and homeostatic up-regulation of DELLA expression in response to GA signalling (Ueguchi-Tanaka et al., 2008). As such, some DELLA protein is likely to remain in plants carrying functional DELLA paralogues even under chemical GA treatment. On the assumption that the observed male-sterility of Col-0 is DELLA-dependent, the ecotypic differences in fertility suggest that additional factors in the L*er* background are maintaining fertility in the absence of *RGA* and *GAI*. Two additional mutant loci present in *rga-24 gai-t6* are *erecta* and *transparent testa 1* (*tt1*) (Dill & Sun, 2001). *ERECTA* represents a putative Leucine-Rich Repeat Receptor-Like Kinase (LRR-RLK, Torii et al., 1996) that has been shown to promote floral development in conjunction with two closely related genes, *ERECTA-LIKE 1* (*ERL1*) and *-2*. The *ER* triple loss-of-function mutant produces small, under-developed flowers with both anther and ovule developmental defects occurring at an early stage (Shpak et al., 2004; Hord et al., 2008). Loss of ER has been shown to affect the phenotypes of mutants *shi* and *spy*, in which GA signalling is also affected (Fridborg et al., 2001; Swain et al., 2001), but the additive nature of the phenotypes suggests that ERECTA does not directly alter GA signalling. Furthermore, *er* dwarf phenotypes are associated with reduced cell proliferation rather than reduced cell expansion (reviewed in van Zanten et al., 2009), which is more closely associated with GA-deficiency. There is some evidence for an interaction between the ER and auxin signalling pathways to regulate fertility and silique growth (Woodward et al., 2005).

Previous experiments found that GA treatment disrupts patterning and development of *Arabidopsis* flowers (see section 3.2.6). In a separate experiment, the genotypes characterised above were screened for floral abnormalities under control growth conditions and GA treatment (n = 96), to determine whether the same abnormalities were also caused by genetic GA overdose, restricting observations to the 10th inflorescence position. No significant

interaction was found between genotype and GA treatment in this experiment ($p = 0.339$), though both factors were themselves significant ($p < 0.001$ and $p = 0.042$, respectively). Averaging the occurrence of floral abnormalities across GA treatments, it was found that the only genotype significantly different from wild-type Col-0 was wild-type L*er* ($p < 0.05$, Figure 6.3a), which demonstrates a greater frequency of floral abnormalities. Interestingly, the *rga-24 gai-t6* mutant differs significantly from wild-type L*er* ($p < 0.05$), with a reduced occurrence of floral abnormalities, whilst in contrast *rga-28 gai-td1* does not differ significantly from wild-type Col-0. Averaging across all genotypes, chemical GA treatment has a significant positive effect on the frequency of floral abnormalities ($p < 0.05$, Figure 6.3b), supporting the findings in section 3.2.6. Comparing between effects on floral organ number (Figure 6.3c and d) and subsequent floral organ development (Figure 6.3e and f) the greatest effect of GA treatment is again on floral organ number. Surprisingly, wild-type L*er* sepals and petals are apparently the most susceptible organs, rather than stamens. Under either growth condition the number of short stamens is less than expected across a number of genotypes, similar to the effects observed in section 3.2.6.

These results suggest that neither genetic nor chemical GA overdose in the Col-0 ecotype disrupts floral organisation or development, which conflicts with the findings detailed in section 3.2.6. This may be for technical reasons, namely that in this experiment observations are restricted to the 10^{th} inflorescence position, by which time the frequency of abnormalities in the absence of GA treatment was previously found to be very low (Figure 3.14b). This experimental population is also far smaller, potentially reducing the statistical sensitivity. Despite these reservations, these results demonstrate a clear difference between the Col-0 and L*er* ecotypes, suggesting that the L*er* floral plan is more susceptible to perturbation by chemical GA treatment. Loss of repression by RGA and GAI strongly reduces the susceptibility of the L*er* floral plan to GA treatment, suggesting that these two DELLA paralogues are involved in regulating this response. Flowers of the *er105 erl1 erl2* triple mutant are reported as having variable numbers of floral organs (Shpak et al., 2004), and so the greater susceptibility of L*er* might possibly be connected with the absence of *ERECTA*. This is consistent with the role of ERECTA in cell-cell signalling.

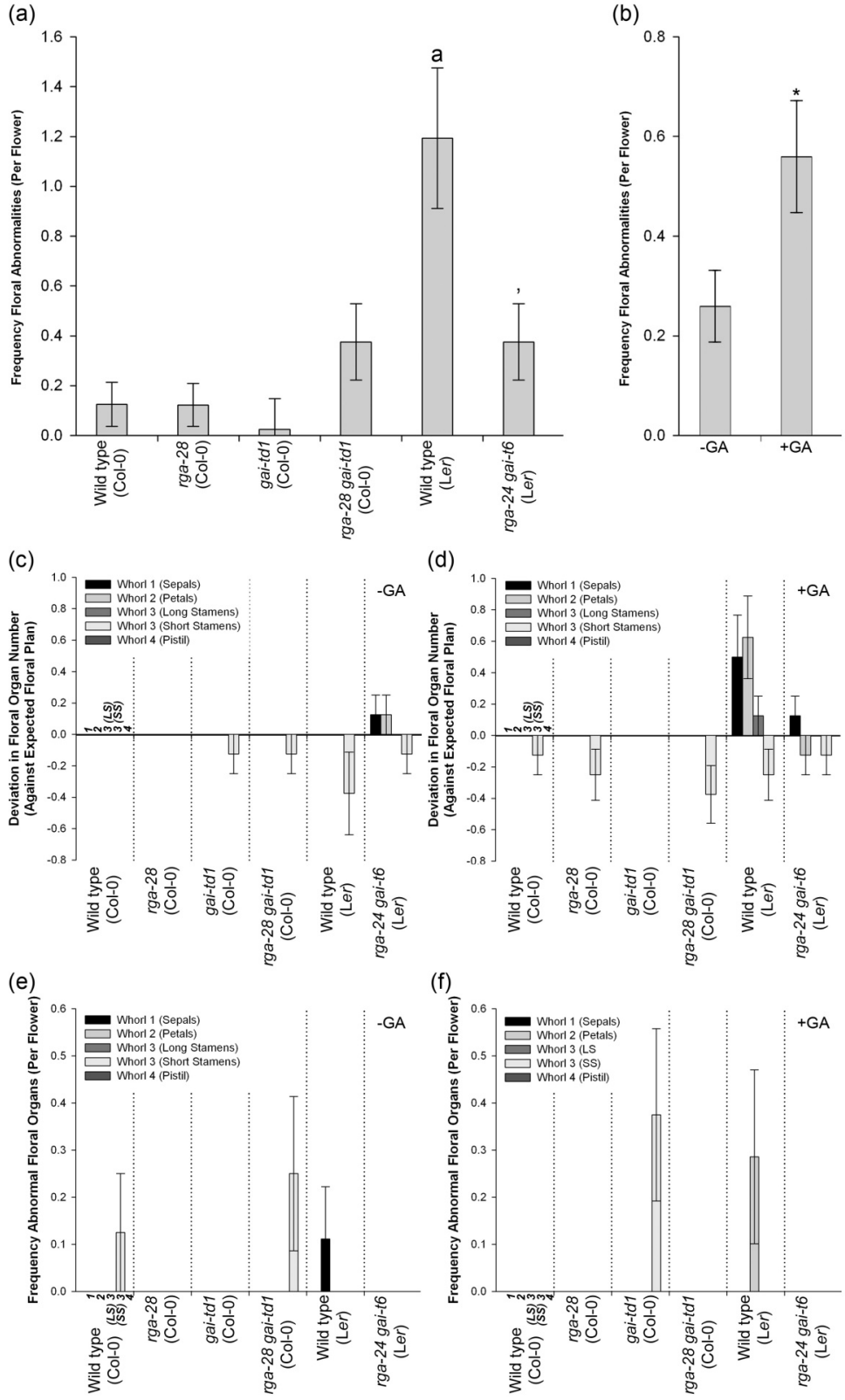

Figure 6.3: Effect of GA overdose on *Arabidopsis* floral organisation.

Comparison of the occurrence of floral abnormalities at the 10th inflorescence position, between genotypes averaged across GA treatments (a) and between GA treatments averaged across all genotypes (b). No significant interaction between genotype and GA treatment was

*found (p = 0.339). Floral abnormalities were subsequently categorised into effects on floral organ number (c, d) and organ development abnormalities (e, f) by floral organ type under control growth conditions (c, e) and under chemical GA treatment (d, f). Graphs represent the mean of 16 measurements (a), 48 measurements (b) and 8 measurements (c-f), respectively. Error bars represent one S.E. Pairwise comparisons were made using a 5% LSD (individual LSDs calculated for each comparison, not shown). No statistical comparisons were made between floral organ numbers or frequency of abnormal development in individual organ types. Letters denote a significant difference from Col-0 wild type. Significant difference between wild-type L*er *and* rga-24 gai-t6 *is denoted by an apostrophe. Significant difference between GA treatments is denoted by an asterisk.*

6.2.2 Reduced Col-0 Fertility Under GA-Overdosed Conditions is Not Associated with Mismatched Floral Organ Growth

Previous experimental results gathered during this project imply that reduced fertility of GA-overdosed Col-0 is not caused by a mismatch in floral organ growth (see section 3.2.5). To test this hypothesis directly, the growth of Col-0 reproductive organs under control growth conditions and GA treatment was compared across floral development by serial dissection of floral clusters, synchronising inflorescence development at the opening of the 10th flower (n = 20). The number of developing floral buds at this stage of flowering was found to be significantly different between untreated and chemically GA-overdosed Col-0 ($p < 0.001$, Figure 6.4a), and consequently, as discussed in section 3.2.5, direct comparisons between particular bud positions with reference to flower opening is not strictly valid. This experiment also included post-anthesis organ growth because this might have a significant impact on reproductive success, and as such it was not feasible to synchronise development between fixed developmental events (the approach taken in section 5.2.1). To overcome the changes in developmental interval between floral buds in different inflorescences, organ lengths were measured across a fixed range of bud positions around flower opening (bud -8 to bud 4, see section 5.2.1) and a correction factor was subsequently applied to place measurements from each inflorescence on a common developmental scale (Figure 6.4b and c). The interval of time between individual floral buds was calculated for each inflorescence (assuming an equal

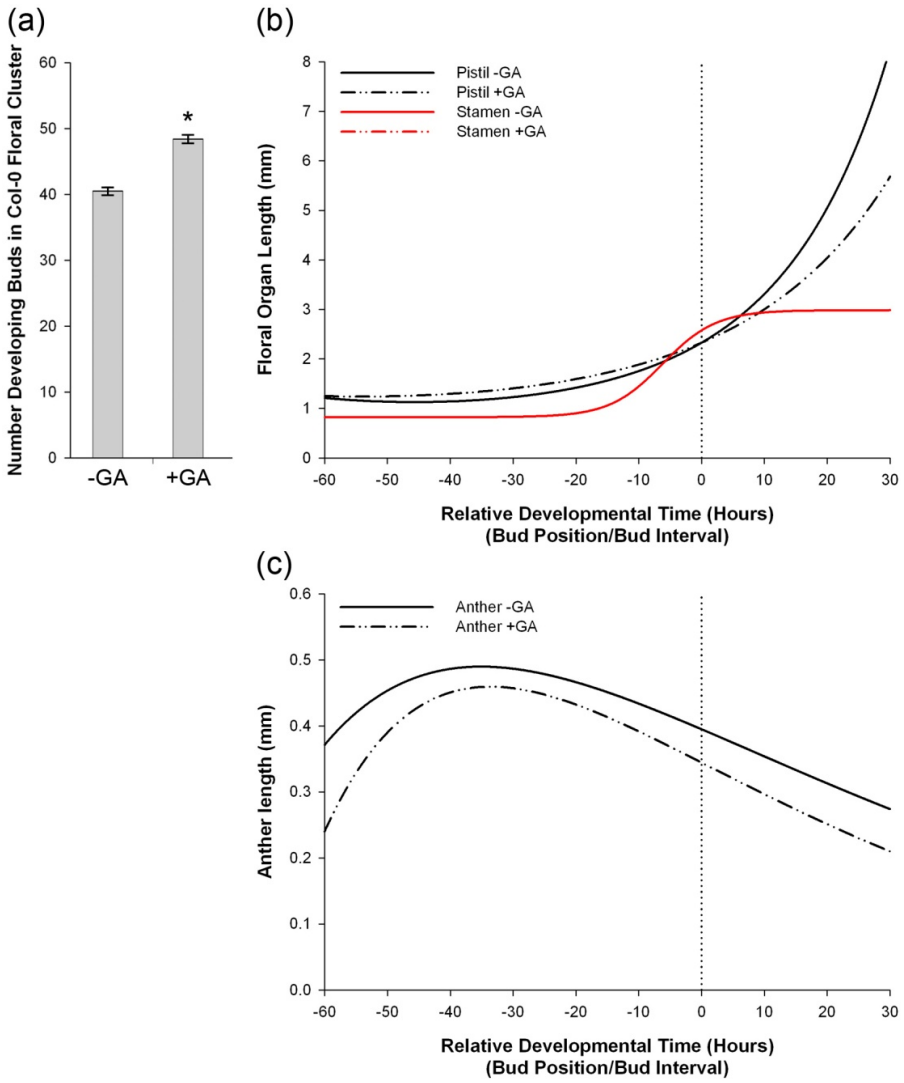

Figure 6.4: Effect of chemical GA overdose on growth of Col-0 reproductive organs.

(a) Comparison between the number of developing floral buds in Col-0 inflorescences between control and GA-treated growth conditions. Inflorescence development was synchronised to the 10th open flower. Bars represent the mean of 10 inflorescences, error bars represent one S.E. Statistical comparison was made using a two-tailed student's T-test. Asterisk denotes significant difference between GA-treated and control inflorescences ($p < 0.001$).

(b) Growth relationships between wild-type pistil and stamens under control and GA-treated growth conditions during floral development around flower opening (vertical dotted line). Stamen growth is not affected by GA treatment: control and GA-treated lines overlap.

(c) Anther size change during floral development under control and GA-treated conditions.

The growth relationships shown are derived from model formulae calculated by regression analysis for each individual inflorescence (10 per GA treatment), using the mean parameters subsequently calculated (given in Table 6.2). Where parameters are not significantly different, the common mean between GA treatments was used (not shown).

interval between each bud), based on the duration between the start of flowering and harvesting of each particular inflorescence. Regression analysis was applied to each inflorescence to calculate the growth relationship for each organ type over developmental time, and comparisons between control and GA-treated conditions were subsequently made at the population level using the growth parameters obtained for each individual plant.

Chemical GA overdose was found to have a significant effect on pistil growth during development, which in this experiment was modelled by the non-linear equation:

$$y = \exp\hat{}(A + Bx + Cx^2)$$

which can be expressed on the logarithmic scale as:

$$\ln(y) = A + Bx + Cx^2$$

where y = pistil length, x = developmental time, parameter A is an estimate of pistil length at developmental time 0 (flower opening) and B and C represent the linear and non-linear (quadratic) coefficients of pistil growth, respectively, in terms of developmental time. The only significant difference found between the two growth conditions was in parameter B ($p < 0.05$, Table 6.2a), with the linear rate of pistil growth reduced under GA treatment. The difference in the value of parameter C between these two treatments borders on significance ($p = 0.052$). Importantly, pistil length at flower opening (represented by the value of parameter A) is not significantly different between control and GA-overdosed floral development ($p = 0.103$). These results indicate that whilst chemical GA overdose does not affect pistil length at flower opening, the subsequent rate of pistil elongation is reduced.

(a)

GA Treatment	Pistil ($y = exp^{(A + Bx + Cx^2)}$)		
	A	**B**	**C**
-GA	0.897000	0.031800	0.000348
+GA	0.794000	0.023300[a]	0.000215
5% LSD	***0.126400***	***0.005440***	***0.0001349***

(b)

GA Treatment	Stamen ($y = D + (E/(1 + exp^{(-F*(x - G))}))$)			
	D	**E**	**F**	**G**
-GA	0.825	2.430	0.249	-5.600
+GA	0.817	1.890	0.225	-6.800
5% LSD	***0.0996***	***1.0460***	***0.1109***	***6.4700***

(c)

GA Treatment	Anther ($y = (H + Jx)*exp^{(-Kx)}$)		
	H	**J**	**K**
-GA	0.394800	0.004950	0.022970
+GA	0.344400[a]	0.005450	0.028590[a]
5% LSD	***0.019020***	***0.000606***	***0.003863***

Table 6.2: Models of reproductive organ growth between control and GA-treated Col-0. *Values given in the tables are the mean parameters governing the growth of pistils (a), whole stamens (b) and anthers (c). Measurements were restricted to long stamens only. Individual growth models were calculated for each inflorescence harvested (10 from each GA treatment) using regression analysis, and parameters were subsequently compared using ANOVA. Comparisons were made between genotypes within each parameter using a 5% LSD, as shown. Superscript letters denote genotypes that are significantly different from -GA ($p < 0.05$). No comparisons were made between parameters.*

Stamen growth was modelled in this experiment by the logistic relationship:

$$y = D + (E/(1 + \exp^{(-F*(x - G))}))$$

where parameter D represents the minimum stamen length, E the total increase in stamen length over time from D (so that maximum stamen length = D + E), F the rate of stamen growth and G the time at which half of the observed growth has occurred (i.e. when y = D + (E/2)). No significant difference was found between control and GA-treated stamens for any parameter ($p = 0.874$, $p = 0.294$, $p = 0.659$ and $p = 0.700$, respectively, Table 6.2b), indicating that stamen growth and final length are unaffected by chemical GA overdose. A comparison with pistil growth (Figure 6.4b) demonstrates that stamens are longer than pistils at flower opening, indicating that there is no mechanical barrier to pollination through mismatched reproductive organ growth under chemical GA treatment. An alternative hypothesis to explain the GA-dependent reduction in fertility relates to defects in pollen or anther development. The timing of anthesis (release of pollen from the anther) relative to flower opening was recorded for each inflorescence during dissection, but chemical GA overdose was found not to have any significant effect ($p = 0.573$). Under either growth condition, anthesis slightly preceded flower opening (-5.448 hours and -4.474 hours under control and GA-treated conditions, respectively). This suggests that there is no obvious physical barrier preventing pollen transfer to the pistil.

A previous experiment found evidence that GA treatment causes a reduction in anther length (Figure 3.13), so anther length during flower opening was also measured in this experimental population, modelled by the critical exponential relationship:

$$y = (H + Jx)*\exp^{(-Kx)}$$

where parameter H represents the estimated anther length at flower opening (i.e. when x = 0), J the linear rate of anther growth observed at flower opening, and K the coefficient for exponential growth. Parameters H and K are significantly different between control and GA-treated anthers ($p < 0.001$ and $p = 0.007$, respectively, Table 6.2c), whilst parameter J is not significantly different ($p = 0.095$). These results indicate that GA-treated anthers are smaller

at flower opening, and that their rate of growth is also affected. When anther growth is modelled across developmental time (Figure 6.4c), chemical GA overdose is shown to cause a reduction in anther size throughout this phase in development, though the biological causes underlying this are currently unknown. Anther length begins to decrease before flower opening (and anthesis, not shown) under both growth conditions, possibly due to water loss from anther tissues during the late stages of anther development (Wilson et al., 2011).

These results make it unlikely that the negative effect on silique-set caused by chemical GA overdose of wild-type Col-0 is due to a mechanical barrier to pollination, and might instead reflect changes associated with pollen or anther development. However, this statistical analysis is based on the assumption of an equal interval of time/development between individual floral buds on an inflorescence, i.e. that new floral meristems arise from the inflorescence meristem at regular intervals and that subsequent floral development progresses at a steady rate. These assumptions are not likely to be met in reality- cumulative flowering experiments suggest that the rate of flower opening on the primary inflorescence is not linear (Footitt et al., 2007). By the opening of the 10th flower, GA-treated floral clusters have significantly more floral buds present, but whether this represents a linear increase in bud production or a shift in the timing of accelerated flowering is currently unknown. The greatest discrepancies caused by different bud numbers will be between buds furthest from flower opening, around which development was synchronised, whilst bud around flower opening remain broadly comparable. An important difference observed between the Col-0 and L*er* ecotypes is the apparent resistance of L*er* silique-set to chemical GA overdose (Figure 6.2i). In future it would be interesting to compare floral organ development in this ecotype to determine whether there are any differences in behaviour under GA treatment compared to Col-0.

6.2.3 Loss of *RGA* and *GAI* Causes Male Sterility in the Col-0 Ecotype, But Not L*er*

Having established that an infertility phenotype is associated with *rga-28 gai-td1*, the cause was investigated in more detail. The single mutants *rga-28* and *gai-td1* are both fully fertile

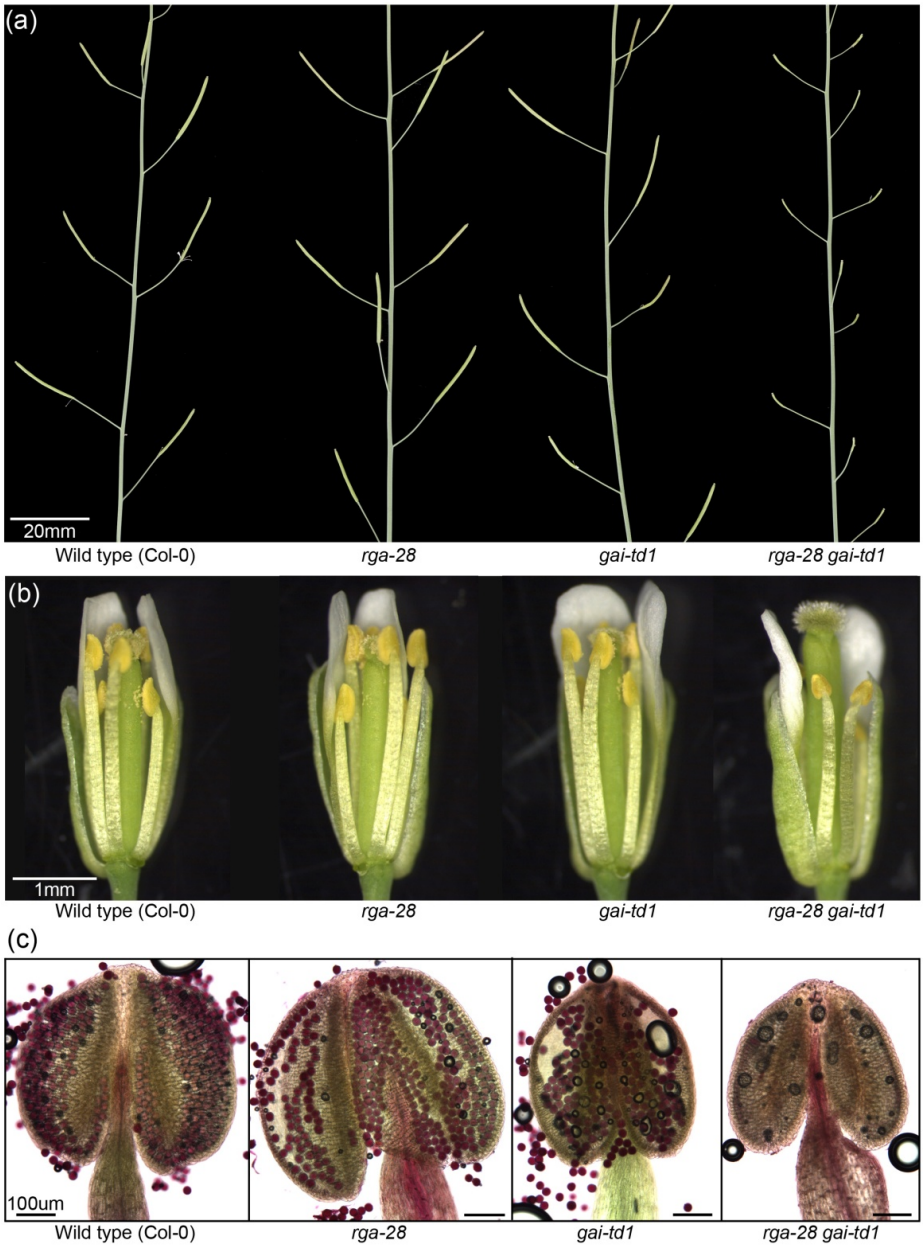

Figure 6.5: Effect of loss of *RGA* and *GAI* on Col-0 floral development.

Comparison of reproductive phenotypes of the rga28, gai-td1 *and* rga-28 gai-td1 *mutants against wild-type Col-0, showing silique-set (a), floral phenotype (b) and pollen viability (c). Pollen viability staining was performed on whole anthers using Alexander pollen viability discrimination stain (Alexander, 1969). Viable pollen stains as dark red, inviable pollen stains as pale green. Scale bars are as indicated.*

as measured by silique-set (Figure 6.5a), indicating that RGA and GAI probably have redundant functions in promoting fertility. Flowers of *rga-28* and *gai-td1* resemble those of wild type (Figure 6.5b), whilst stamens of *rga-28 gai-td1* flowers appear to be relatively short

with shrunken anthers, suggesting that sterility in this mutant is linked to male reproductive development. Dill and Sun (2001) reported that stamen growth is also reduced in *rga-24 gai-t6* flowers. Crosses performed using *rga-28 gai-td1* homozygous mutants plants as female recipients successfully produce seed (Thomas, S., personal communication), indicating that female fertility is not impaired. *rga-28 gai-td1* anthers taken from newly-opened flowers were found to contain no pollen, in contrast to wild-type Col-0, *rga-28* or *gai-td1* (Figure 6.5c). This phenotype suggests that inappropriate GA signalling through loss of repression by RGA and GAI has a pollen-lethal effect. This pollen-less phenotype is reminiscent of that reported in the DELLA loss-of-function sterile barley mutant *slender1* (*sln1*, Lanahan & Ho, 1988), though this phenotype has not been described in more detail. The absence of a pollen-less phenotype in the *rga-28* or *gai-td1* single mutants supports the hypothesis that this phenotype is DELLA-related, and not caused by a separate mutation.

To further investigate DELLA function during stamen development, the *rga-28 gai-td1* genotype was recapitulated in the *gid1a-1 gid1b-1 gid1c-1* GA-insensitive background (Griffiths et al., 2006). *rga-28 gid1a gid1b gid1c* demonstrates partial suppression of the *gid1a gid1b gid1c* vegetative phenotype (Griffiths et al., 2006, Figure 6.6a and b) and floral development, with substantially increased growth of all floral organs, although stamen elongation is not fully rescued (Figure 6.7a). Microscopic analysis of *rga-28 gid1a gid1b gid1c* anthers found viable pollen present (Figure 6.7b), and self-fertilised seed was recovered, suggesting that loss of RGA suppresses developmental arrest in *gid1a gid1b gid1c* anthers (Figure 6.7b). In contrast, the vegetative and floral phenotypes of *gai-td1 gid1a gid1b gid1c* do not differ substantially from *gid1a gid1b gid1c* (Figure 6.6a and Figure 6.7), although a slight difference in rosette size is observed in older plants (Figure 6.6c). The vegetative phenotype of *rga-28 gai-td1 gid1a gid1b gid1c* is indistinguishable from *rga-28 gai-td1* (Figure 6.6a), supporting the findings of Willige et al. (2007) who created similar quintuple and quadruple mutants using the L*er* alleles *rga-24* and *gai-t6*. These results correlate with further experiments in L*er* by Dill and Sun (2001), who found that RGA and GAI act as the predominant DELLAs regulating plant growth, and that loss of *RGA* suppresses dwarfism in *ga1-3* to a far greater extent than loss of *GAI*. The dominance of RGA over vegetative growth

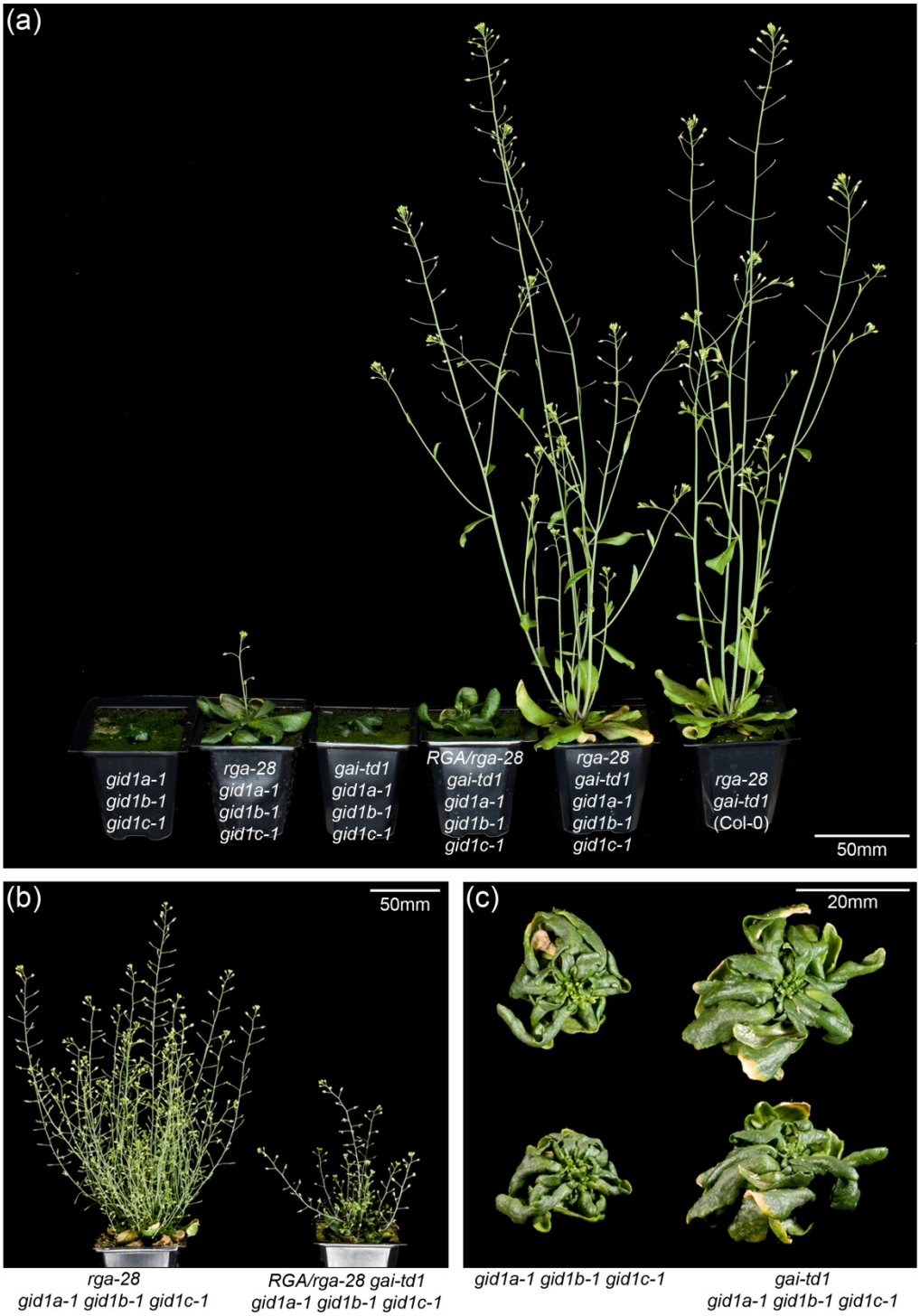

Figure 6.6: *rga-28 gai-td1* mutant suppression of the *gid1* GA-insensitive vegetative phenotype.

Phenotypic comparison of rga-28 *and* gai-td1 *combinatorial mutants in the* gid1a gid1b gid1c *background (as shown) against* gid1a gid1b gid1c *and* rga-28 gai-td1 *control lines at 33 days (a), with selected phenotypic comparisons shown at 48 days (*RGA/rga-28 gid1a gid1b gid1c *vs.* rga-28 gid1a gid1b gid1c *(b) and* gai-td1 gid1a gid1b gid1c *vs.* gid1a gid1b gid1*(c).*

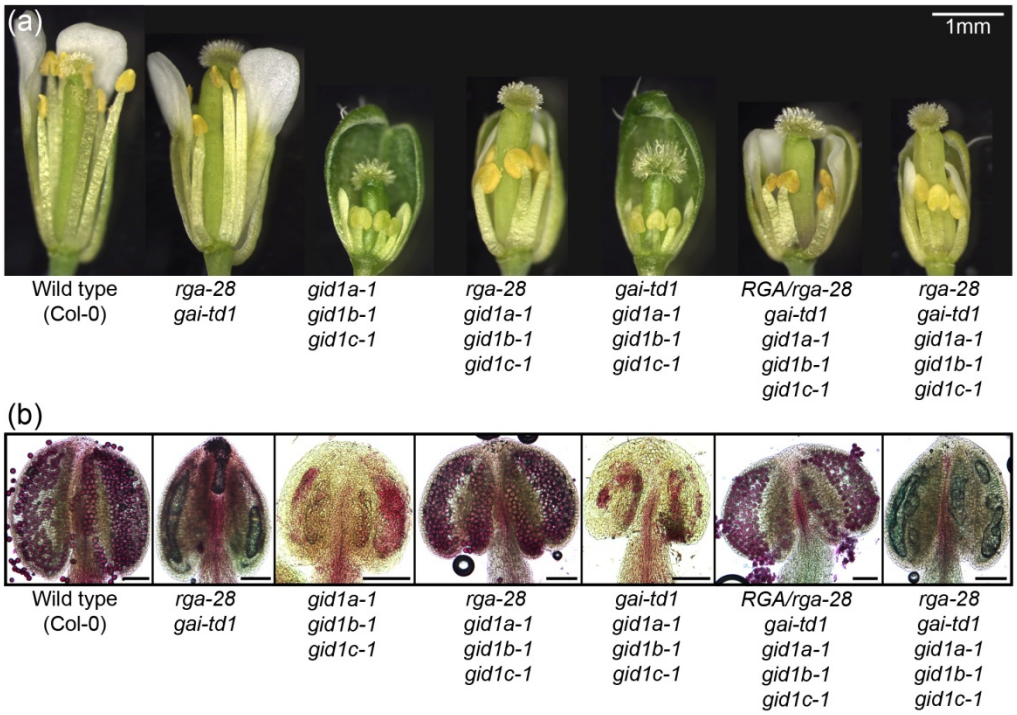

Figure 6.7: *rga-28 gai-td1* mutant suppression of the *gid1* GA-insensitive floral phenotype. *Phenotypic comparison of flowers from* rga-28 *and* gai-td1 *combinatorial mutants in the* gid1a gid1b gid1c *background (as shown) against wild-type Col-0,* gid1a gid1b gid1c *and* rga-28 gai-td1 *control lines, showing floral (a) and anther phenotypes (b). Flowers harvested from the 10th inflorescence position at flower opening (or equivalent to same). Pollen viability staining was performed on whole anthers using Alexander pollen viability discrimination stain (Alexander, 1969). Viable pollen stains as dark red, inviable pollen stains as pale green. Black scale bars represent 100µm.*

is further demonstrated by the ability of a single functional *RGA* allele to repress growth in the *gai-td1 gid1a gid1b gid1c* background, compared to plants in which RGA is entirely absent (Figure 6.6b). This phenotype also demonstrates a clear dosage effect associated with RGA, similar to one previously shown for GAI in the *ga1-3 rga-24* background (King et al., 2001). The dosage effect of RGA in the *gid1a gid1b gid1c* background in the presence of functional GAI was not investigated as part of this project, but future investigation of this relationship could be instructive.

In contrast to *rga-28 gid1a gid1b gid1c*, the *gai-td1 gid1a gid1b gid1c* stamen phenotype resembles that of *gid1a gid1b gid1c* (Figure 6.7), suggesting that RGA also acts as the dominant DELLA regulating at least the early stages of anther development. Nevertheless, *rga-28 gai-td1 gid1a gid1b gid1c* stamens are pollenless (Figure 6.7b), suggesting that GAI is critical to pollen development. The floral expression patterns of *RGA* and *GAI* are currently unknown, but the absence of other phenotypes associated with loss of GAI suggests that its functions (and potentially expression) during floral development could be highly specific, whilst RGA is likely to be more widely expressed. One consequence of this is that tissues which express *GAI* are also likely to express *RGA*, which could explain the lack of phenotypes observed in *gai-td1 gid1a gid1b gid1c*. Expression analysis by Tyler et al. (2004) found that *RGA* was more highly-expressed than *GAI*, in floral tissues and elsewhere, so its loss might have a greater effect on the amount of DELLA protein present in plant tissues. However, the same study found relatively high GAI expression in floral clusters, suggesting that the precise expression pattern could be the more important factor. Interestingly, analysis of transcriptomic data from developing pollen (Honys and Twell, 2004) identifies similar levels of *RGA* and *GAI* transcript in unicellular and bicellular stages, each more highly expressed than other DELLA paralogues. One clear difference between the *rga-28 gai-td1* and *rga-28 gai-td1 gid1a gid1b gid1c* floral phenotypes is that stamen elongation is not completely rescued in the quintuple mutant (Figure 6.7a), indicating the presence of an additional DELLA restricting filament growth in this mutant. Cheng et al. (2004) demonstrated that loss of *RGL2* activity enhances filament elongation in the *ga1-3 rga-t2 gai-t6* (L*er*) background. *RGL2* mRNA has been shown to be highly expressed in inflorescence tissue, with a GUS reporter line further specifying stamen expression to the filament (Lee et al., 2002). *RGL2::GUS* staining was not reported in the anther, suggesting a clear functional differentiation between DELLA paralogues based on tissue expression.

Interestingly, the *rga-24 gai-t6 gid1a gid1b gid1c* quintuple mutant of Willige et al. (2007) fails to set seed (Schwechheimer, C., personal communication), although the cause for this has not been explored. In addition to *rga-28 gai-td1*, other novel *rga gai* loss-of-function double mutant combinations in the Col-0 ecotype display sterility phenotypes (Thomas, S., personal

Figure 6.8: Effect of loss of *RGA* and *GAI* on L*er* floral development.

Comparison of reproductive phenotypes of the rga-24 gai-t6 *(*tt1*) and* rga-t2 gai-t6 *mutants against wild-type* Ler*, showing silique-set across flowering (a) and both floral and pollen development phenotypes exhibited early in flowering (inflorescence positions 1-5 (b)) and after restoration of silique-set (inflorescence positions 20-25 (c)).*

Unless specified otherwise, white scale bars represent 1mm, black scale bars represent 100µm.

communication), supporting the hypotheses that male sterility in *rga-28 gai-td1* is DELLA-dependent, and that the fertility differences between published L*er rga gai* mutants and *rga-28 gai-td1* are dependent on ecotype. To compare the differential effects of the Col-0 and L*er* ecotypes on *rga gai* mutant fertility, the L*er rga gai* floral phenotype was re-examined. As *rga-24 gai-t6* also carries the *tt1* mutation, a second line carrying *gai-t6* in combination with the loss-of-function allele *rga-t2* (Lee et al., 2002) was included to confirm that rescue of fertility was not due to *tt1*. Both mutant lines demonstrate similar fertility defects, setting few

siliques during early flowering but displaying subsequent recovery (Figure 6.8a), as was previously found for *rga-24 gai-t6* (Figure 6.2i). Floral phenotypes were compared between these two phases of fertility, harvesting flowers between inflorescence positions 1-5 (Figure 6.8b) and 20-25 (Figure 6.8c), respectively. Newly-opened flowers from both *rga gai* mutants released visibly less pollen than wild-type L*er* flowers (Figure 6.8b and c), and under microscopic examination individual locules of *rga gai* mutant anthers were frequently empty. However, viable pollen was still in evidence, and no completely empty anthers were observed. This phenotype was seen during both the infertile and fertile phases of flowering, suggesting that pollen production is consistently reduced in these mutants and thus cannot explain the observed rescue of fertility. Dill and Sun (2001) report reduced growth of *rga-24 gai-t6* stamens compared to L*er*. This phenotype was observed in both *rga gai* double mutants later in flowering (Figure 6.8b), although it was not evident in early flowers (Figure 6.8c). The results obtained from both *rga gai* mutants here confirms the floral phenotypes reported by Dill and Sun (2001), and suggests that they can be attributed to loss of *RGA* and *GAI*, rather than *tt1* or other mutations.

Together with evidence from the Col-0 ecotype, these results strongly support the hypothesis that the presence of DELLA protein promotes successful pollen development, and also demonstrate a clear difference in pollen development between the Col-0 and L*er rga gai* backgrounds. To determine whether this is due to the absence of *ERECTA*, the *rga-28 gai-td1* mutant was recapitulated in the Col-0 *er105* background, in which ERECTA is non-functional (Torii et al., 1996) and whose growth phenotype closely resembles that of L*er* (Figure 6.9a). The *er105 rga-28 gai-td1* mutant did not set siliques (Figure 6.9b), and analysis of the *er105 rga-28 gai-td1floral* phenotype demonstrates that loss of *ERECTA* does not complement defects in stamen growth and pollen development (Figure 6.9c), suggesting that successful pollen development in L*er rga gai* mutants is not due to the loss of *ERECTA*.

Another possible explanation for the robust pollen development in L*er rga gai* mutants is the action of another DELLA protein. Differences in DELLA regulation between Col-0 and L*er* stamen tissues can be deduced through comparisons of existing mutant phenotypes: loss of

Figure 6.9: Effect of loss of *ERECTA* function on *rga-28 gai-td1* fertility.

Phenotypic comparison of rga-28*,* gai-td1*and* rga-28 gai-td1 *mutants in the Col-0 er105 background, showing whole plant stature (a) fertility as measured by silique-set on the primary inflorescence (b) and the associated floral and pollen viability phenotypes (c). Plants shown are 36 days old. Newly-opened flowers were harvested from the 10th inflorescence position.*

RGA alone is sufficient to restore stamen development and growth in GA-deficient Col-0 backgrounds (Tyler et al., 2004), whilst stamens remain small and underdeveloped even when both *RGA* and *GAI* are lost from the L*er ga1-3* background (Dill & Sun, 2001), with pollen development blocked (Cheng et al., 2004). This indicates that other DELLA paralogues continue to repress GA signalling in L*er rga gai* anthers. Cheng et al. (2004) show that the combined loss of *RGA*, *RGL1* and *RGL2* restores pollen development in *ga1-3* (L*er*), suggesting that both *RGL1* and *RGL2* are expressed in L*er* anther tissues. This is supported by Honys and Twell (2004), who identify expression of both *RGL1*and *-2* in developing L*er* pollen alongside *RGA* and *GAI*. However, one critical argument against this hypothesis is that the DELLA *global* mutant, in which all five DELLA paralogues are non-functional in the L*er* background (Feng et al., 2008), retains fertility (Thomas, S., personal communication), though to what extent remains undetermined. This mutant combination has not yet been recapitulated in the Col-0 background. One possible technical explanation could be that DELLA expression is not entirely abolished in the *global* background. The T-DNA insertion of the *rgl1-1* allele used in this line occurs 5' of the translational start codon, and so the potential exists for transcription of full length *RGL1* mRNA.

Having obtained supporting evidence that successful pollen development requires DELLA activity, a more detailed analysis of *rga-28 gai-td1* pollen development was undertaken to identify the processes affected in this mutant. Abnormal pollen development was found to manifest during or shortly after meiosis. Whereas wild-type anthers successfully completed meiosis, resulting in the release of free microspores into the locule (Figure 6.10a and b), no morphologically normal microspores were observed in *rga-28 gai-td1* anthers. Instead, microspore degeneration was observed immediately after the completion of meiosis (Figure

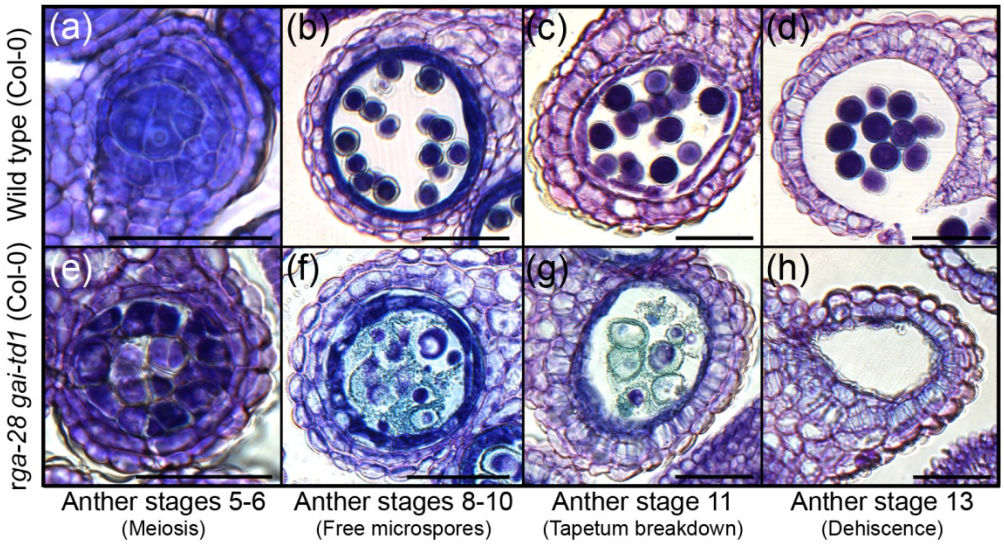

Figure 6.10: Pollen development in the *rga-28 gai-td1* mutant.

Comparison of pollen development between anthers of wild-type Col-0 (a-d) and rga-28 gai-td1 *(e-h) at equivalent developmental stages (as indicated). Scale bars represent 50µm.*

6.10e and f), eventually resulting in empty locules (Figure 6.10h) whilst wild-type anther development resulted in the formation of mature pollen (Figure 6.10c and d). An accumulation of abnormal material was observed in mutant locules during microspore degeneration (Figure 6.10f and g) suggesting that pollen wall formation is disrupted in this mutant. As discussed in detail in section 1.5.3, tapetum function is critical for successful pollen development, including the synthesis and deposition of pollen wall components. Downstream targets of GA signalling include transcription factors involved in tapetum secretory functions (see section 1.5.3) and GA signalling has also been shown to be an important trigger of tapetum programmed cell death (PCD, Aya et al., 2009), resulting in the deposition of pollen coat components. This raises the hypothesis that male sterility in the *rga-28 gai-td1* mutant is related to tapetum function. Morphological analysis did not find clear evidence of early tapetum degeneration, which remains apparently whole in locules where microspore degeneration has already begun (Figure 6.10f), though further tests might identify defects in tapetal structure. Although the tapetum has an important function in pollen wall synthesis and deposition, microspores also contribute (Scott et al., 2004). Expression of GA biosynthesis and signalling genes has been observed in both the tapetum and microspores at

this developmental stage (see section 1.5.3), and so the failure of pollen development might be caused by inappropriate GA signalling within the developing microspores themselves.

6.2.4 Reintroduction of RGA into the Tapetum or Developing Microspores of *rga-28 gai-td1* Rescues Pollen Development

To confirm that *rga-28 gai-td1* male sterility is truly DELLA-dependent, transgenic lines were generated in which functional *RGA* was reintroduced into the *rga-28 gai-td1* background under the control of tissue-specific promoter fragments, derived from either *LIPID TRANSFER PROTEIN 12* (*LTP12*) or *LAT52* (see section 2.1.2). Expression driven by the *LTP12* promoter fragment has been previously shown to be tapetum-specific, expressed post-meiotically between anther stages 8 and 11 (when unicellular and bicellular pollen are present, Ariizumi et al., 2002), whilst the tomato-derived *LAT52* promoter sequence (Twell et al., 1989) has been shown to be specific to developing pollen when introduced into *Arabidopsis*, expression first detectable in uninucleate microspores shortly prior to pollen mitosis and continuing in bicellular and tricellular pollen (Twell et al., 1990; Eady et al., 1994). RGA was expressed as a GFP C-terminal fusion (Nakagawa et al., 2007) to confirm the presence of RGA in the correct tissues. In order to ensure the set of T_1 seed after transformation, the T_0 population transformed was segregating for *gai-td1*, and the subsequent transformant progeny were genotyped to identify those with an *rga-28 gai-td1* double mutant background (see section 2.1.2 for further discussion).

Transgenic *rga-28 gai-td1* plants in the T_1 and T_2 generations expressing either *LTP12::RGA::GFP* or *LAT52::RGA::GFP* demonstrated restored fertility based on silique-set (data not shown), allowing the establishment of homozygous transgenic *rga-28 gai-td1* lines in the T_3 generation for analysis. Three homozygous lines representing independent transformation events were analysed for each transgene. These lines did not demonstrate any pleiotropic effects on stature due to ectopic expression of *RGA* (Figure 6.11a). Successful silique-set by these lines demonstrates that fertility has been restored (Figure 6.12b). However, in two lines carrying *LTP12::RGA::GFP* (tA and tB), a reduction in fertility was observed compared to that seen in earlier generations, with silique-set only recovering late in

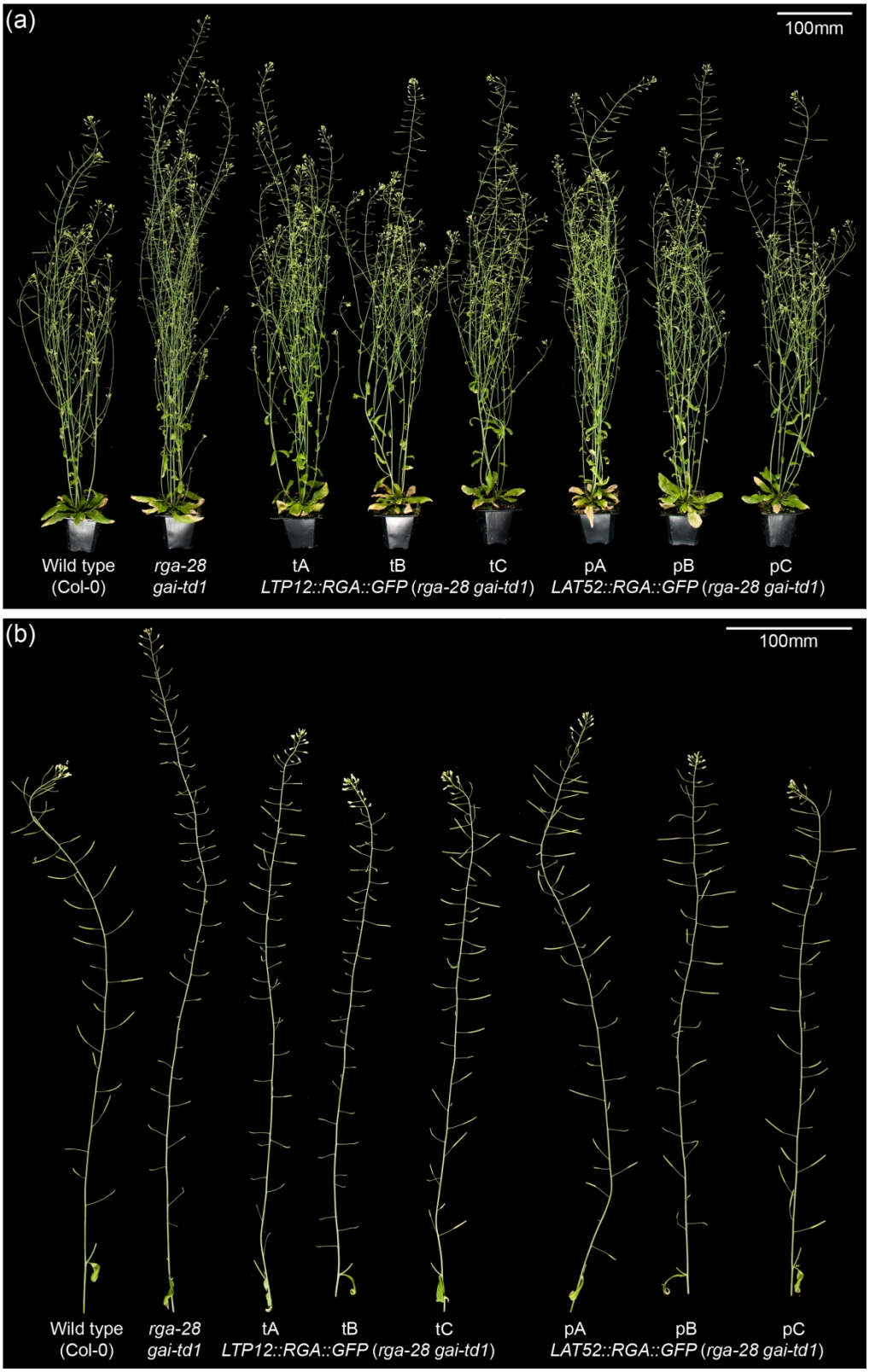

Figure 6.11: Complementation of *rga-28 gai-td1* infertility by reintroduction of RGA. *Comparison of promoter::RGA transgenic lines (as shown) against wild type and* rga-28 gai-td1 *controls at 39 days old, showing both whole plant (a) and primary inflorescence phenotypes (b). Three independent transgenic lines are represented per construct.*

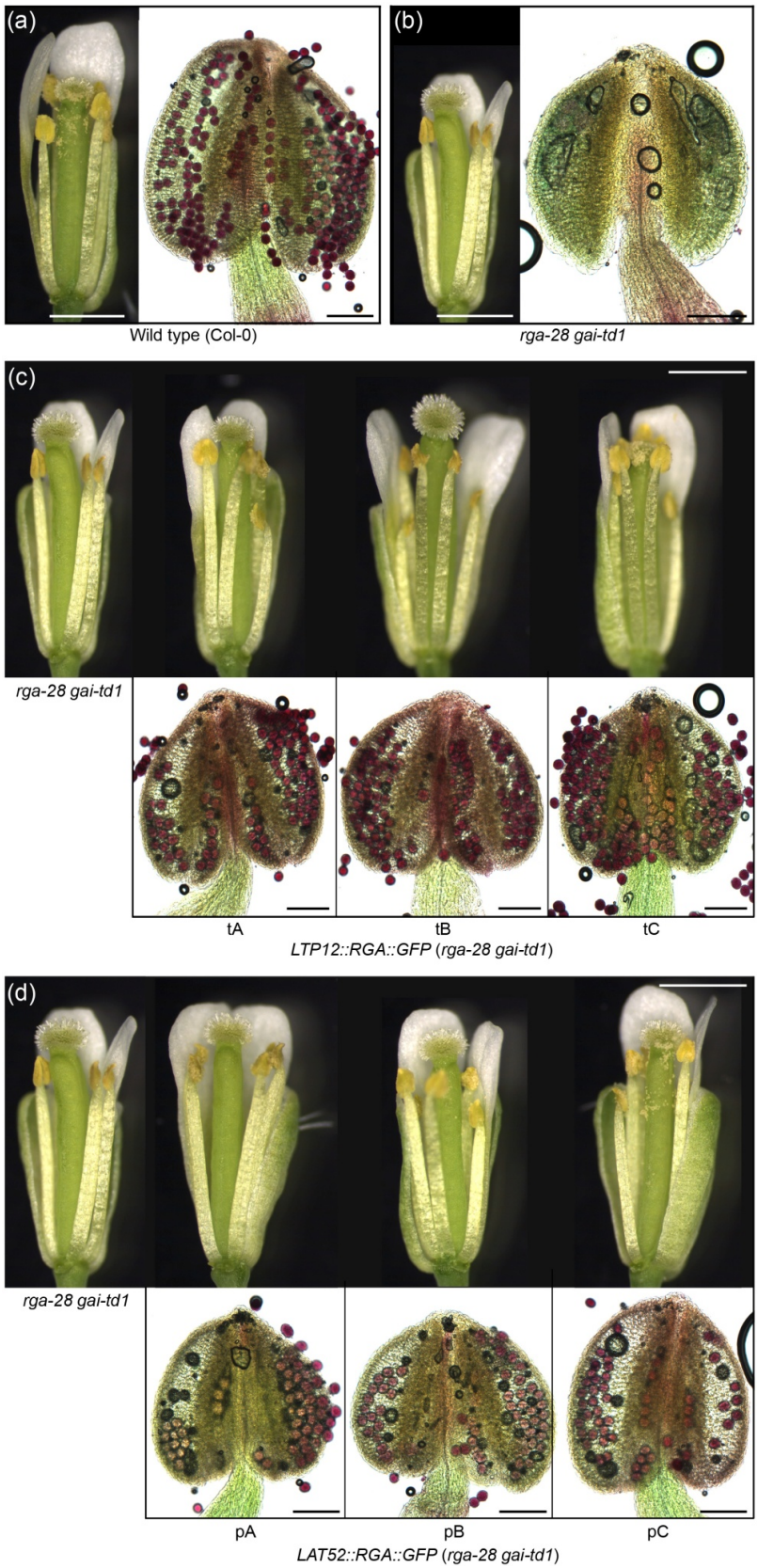

Figure 6.12: Complementation of *rga-28 gai-td1* pollen development by expression of RGA. *Comparison of floral and pollen development phenotypes between wild type (a),* rga-28 gai-td1 *(b) and transgenic lines expressing RGA in the* rga-28 gai-td1 *background (c and d), as*

shown. Three independent lines were analysed for each transgenic construct (denoted tA, tB, tC and pA, pB, pC, respectively). All flowers shown represent newly-opened flowers (bud position 0), with anthers being harvested from the same developmental stage. White scale bars represent 1mm, black scale bars represent 100µm.

flowering (Figure 6.11b). In contrast, *LTP12::RGA::GFP* line tC and all *LAT52::RGA::GFP* lines showed restoration of silique-set across the entire primary inflorescence. To confirm complementation of the *rga-28 gai-td1* male sterility by RGA, pollen development in newly-opened flowers was checked at the 10th inflorescence position for each line. All transgenic anthers were found to contain viable pollen (Figure 6.12c and d) in contrast to untransformed *rga-28 gai-td1* (Figure 6.12b). This result suggests that the re-introduction of DELLA signalling complements the male sterility of *rga-28 gai-td1*, and thus strongly supports the hypothesis that successful pollen development is dependent on DELLA activity.

The restoration of pollen development in early flowers does not explain the late restoration of silique-set during flowering of the lines tA and tB. Viable pollen was found in flowers at inflorescence positions within the infertile phase, suggesting that this phenomenon cannot be explained by silencing of the transgene. The timing of pollen release could create a mechanical block to pollination, but this is unlikely to be the case because dehiscent anthers were observed in newly-opened flowers of these lines (Figure 6.12c and d). Female fertility is not significantly affected in the *rga-28 gai-td1* mutant, so it is unlikely (but not impossible) that female fertility is disrupted in these transgenic flowers. Alternatively, development of male and female floral organs may have become uncoordinated, with unequal lengths of reproductive organs at flower opening causing a mechanical block to pollination. The observed floral phenotypes provide some support for this latter hypothesis (Figure 6.12c and d), with little or no pollen visible on the stigmas. However, whilst the photographic evidence presented in this project and previous publications suggests that loss of *RGA* and *GAI* expression is associated with reduced filament elongation relative to the pistil, the point must be made that the absolute lengths of floral organs in these mutants have not been rigorously compared against their respective wild types. Some observations of the *rga-28 gai-td1* floral

phenotype suggest that increased pistil growth could contribute to mismatched lengths of reproductive organs at flower opening (Figure 6.5b; Figure 6.8), and thus affect fertility independently of pollen development. Our understanding of the mechanism by which GA signalling regulates filament elongation is still incomplete (see section 1.5.4), including whether GA signalling in the anther contributes to it, but at least one additional DELLA paralogue is also expressed in filament tissues (*RGL2*, see section 6.2.2). Without further detailed analysis of the *rga-28 gai-td1* phenotype, we cannot yet conclude whether mismatched floral organ growth is due to reduced filament growth (suggesting that increased GA signalling inhibits filament elongation) or increased pistil growth (consistent with the known growth-repressive function of DELLA proteins).

These results are very interesting, as they indicate that restoring DELLA repression of GA signalling to either the tapetum or developing pollen is sufficient to restore successful pollen development. The precise nature and originating tissue(s) of the *rga-28 gai-td1* anther developmental defects have not yet been established, but both promoters used are reportedly expressed at the unicellular microspore stage (anther stage 8-9, Eady et al., 1994; Ariizumi et al., 2002), suggesting that it is at this stage at which development is rescued. Furthermore, the implication of these results is that there is at least one-directional communication between the two tissue layers to allow rescue of fertility by reintroduction of RGA into either tissue. Different regulatory mechanisms can be hypothesised to explain the role of GA signalling in coordinating development between these two tissues (Figure 6.13). The simplest model is for the tapetum and microspores to be each regulated independently by GA signalling, with GA itself acting to as a coordinating signal (Figure 6.13a). In rice both the tapetum and developing pollen have been shown to express elements of the GA signal transduction pathways (Hirano et al., 2008; Aya et al., 2009). As mentioned in section 6.2.3, transcriptome data from developing *Arabidopsis* (L*er*) pollen (Honys and Twell, 2004) identifies DELLA expression in both unicellular microspores and bicellular pollen. Similar data for the tapetum is not yet available. However, depending on the cause of pollen abortion in *rga-28 gai-td1* (and on the assumption that a single tissue is the proximal cause), the prediction arising from this model is that only reintroduction of RGA into the affected tissue will restore pollen

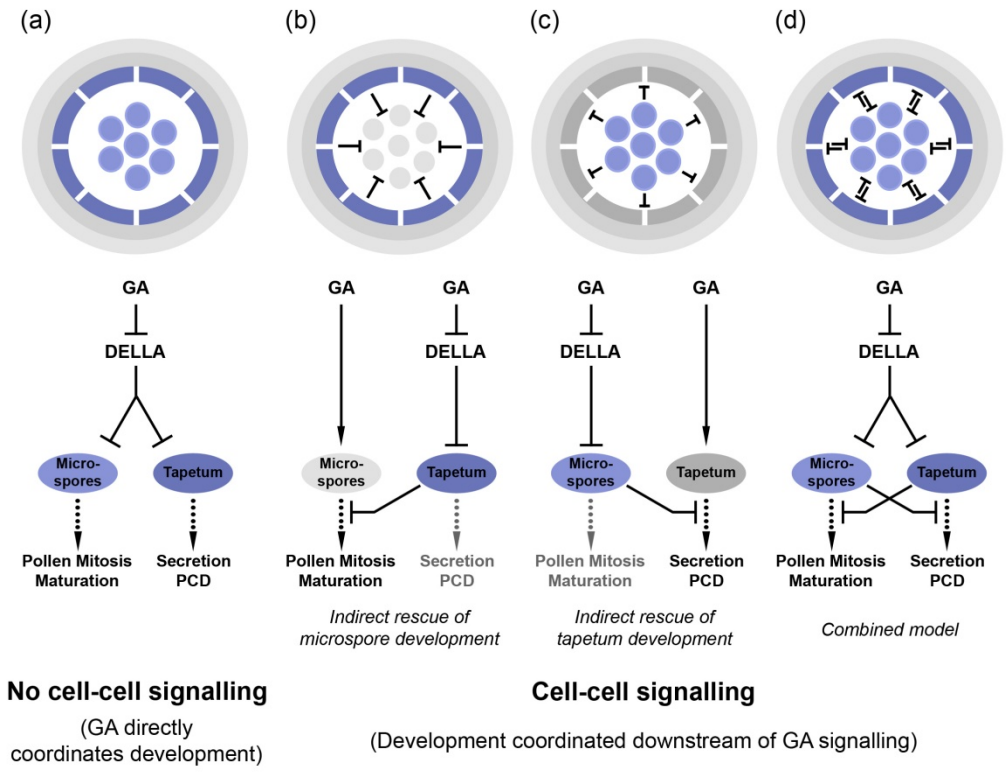

Figure 6.13: Models of GA-dependent coordination of tapetum and microspore development.

(a) *Tapetum and microspore development are independent, each coordinated through GA signalling.*

(b) *Sporophytic rescue of pollen development. Reintroduction of functional DELLA into the tapetum (blue) either restores tapetum function directly or rescues pollen development indirectly through inhibiting inappropriate pollen development.*

(c) *Gametophytic rescue of pollen development. Reintroduction of functional DELLA into the microspores either restores tapetum function directly or rescues pollen development indirectly through inhibiting inappropriate pollen development.*

(d) *Hypothetical model of wild-type anther development combining the models in (b) and (c), with DELLA-dependent GA signalling in both tissues and downstream cross-talk coordinating the progression of tapetum and microspore development.*

The presence of DELLA protein in the tapetum cell layer and/or microspores is indicated by blue highlighting. Solid arrows indicate positive regulation promoting progression through development, bars indicate negative or inhibitory regulation. Dotted arrows indicate downstream developmental processes (as shown).

development, whilst expression in the other tissue will not rescue fertility. This prediction is not met by the experimental results presented above, and so more complex models involving interactions between these two cell types downstream of GA perception and signal transduction are necessary to explain the observed results (Figure 6.13b-d).

The principle of cell-cell signalling between these two tissues has been previously established, one clear example being the EXS/EMS-TPD1 receptor-ligand mechanism specifying tapetum identity in relation to developing PMCs during tissue differentiation (described in section 1.5.3). Post-meiotic development of these two tissue layers is also coordinated, with tapetum secretory functions and PCD synchronised with pollen development. Mis-timing of events such as callase secretion can cause pollen development to fail (Scott et al., 2004), as does a delay in tapetal PCD (Kawanabe et al. 2006). Given their function in GA signal transduction, the nature of the cell-cell signalling related to the reintroduction of DELLA protein is likely to be negative or repressive in nature, either by inhibition of an overactive signal that promotes inappropriate progression through development, or by promoting an inhibitory signal blocking progression through development that is absent in the *rga-28 gai-td1* mutant. Both DELLA down-regulated and DELLA up-regulated genes have been previously identified in floral tissues (Hou et al., 2008).

The appropriate model to explain the experimental results presented above depends on the nature and originating tissue of the *rga-28 gai-td1* developmental defect, and can be distinguished by sporophytic rescue of gametophyte development or gametophytic rescue of sporophyte development. Under the sporophytic rescue model (Figure 6.13b), reintroduction of DELLA protein into the tapetum either directly complements the mutant phenotype if sterility relates to tapetum function, whilst if the defect is in microspore development then the presence of DELLA in the tapetum rescues pollen development indirectly, with a tapetum-derived signal inhibiting aberrant pollen development. In the gametophtic rescue model, in which DELLA protein in reintroduced to the developing microspores (Figure 6.13c), the converse applies. Whilst either of these models can explain the experimental results obtained in this project, given the information available in rice regarding the distribution of DELLA

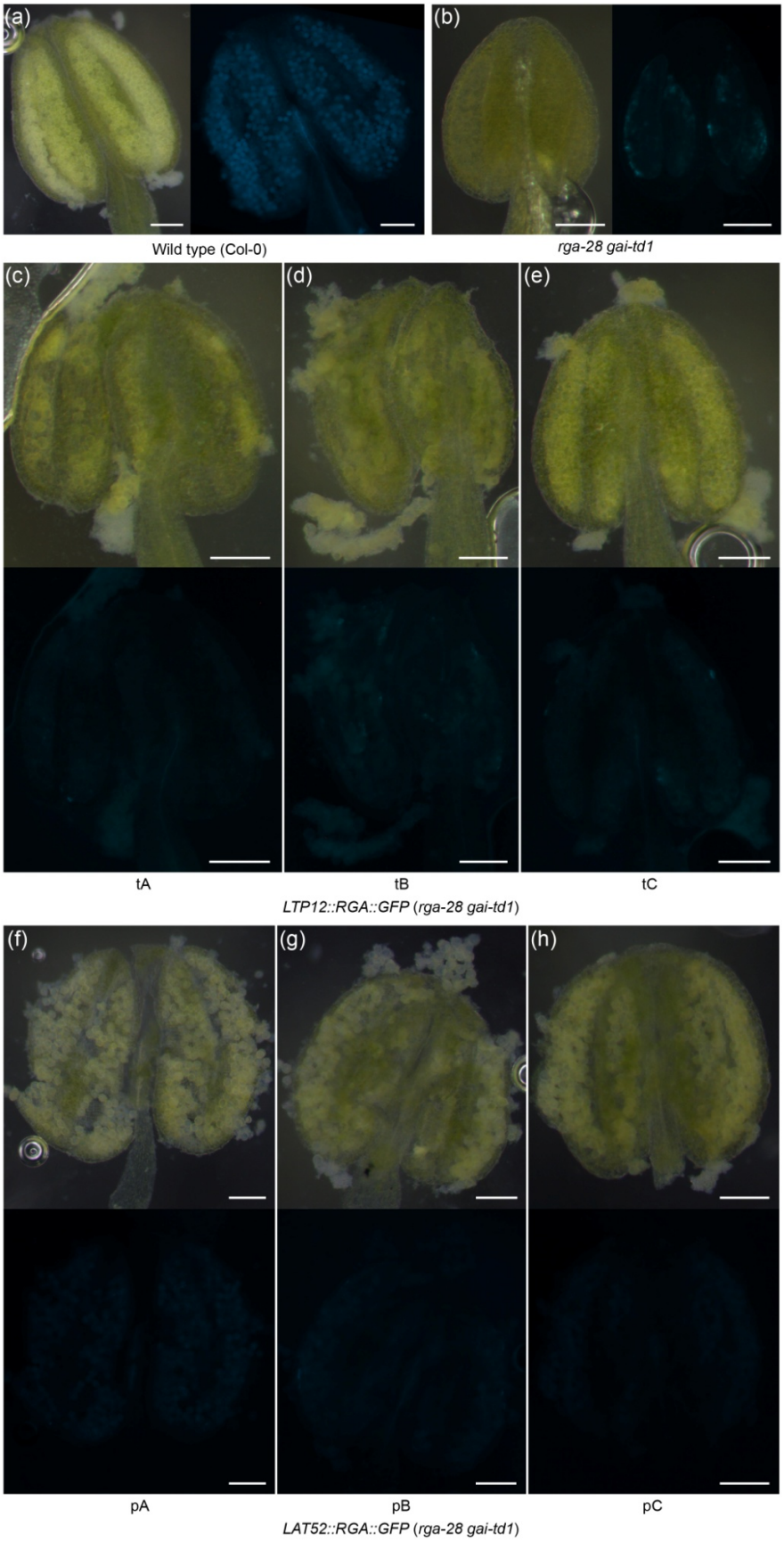

Figure 6.14: GFP fluorescence screening of promoter*::RGA::GFP* (*rga-28 gai-td1*) transgenic lines.

Under a fluorescence microscope with GFP-specific filters (see 2.3.2), wild-type anthers (a) demonstrate some autofluorescence, mostly attributable to developing pollen, though some autofluorescence is also visible in anther walls from empty rga-28 gai-td1 *anthers (b). Under the same settings, fluorescence in anthers of transgenic lines of either construct (c-e and f-h, respectively) was not any greater than that seen in control samples. Anthers shown were harvested from bud developmental positions -7 to -10, at which point the* rga-28 gai-td1 *pollen development phenotype is manifest and wild-type anthers contain post-meiotic developing pollen. Scale bars represent 100µm.*

protein (see above) and the evidence from this project that signalling exists between the tapetum and microspores at this stage of development, a more complex model can be hypothesised for wild-type anther development in which DELLA protein is expressed in both tissues, with the potential subsequent downstream cross-talk in both directions ensuring coordinated development between these two tissues (Figure 6.13d). However, until the precise nature of the *rga-28 gai-td1* phenotype is known, it is not possible to decide which of these models (if any) is most appropriate.

The models described above are based on the assumption that expression of RGA under either the *LTP12* or *LAT52* promoter fragments is restricted to the published expression patterns. Another possibility that must be considered is that the mobile signal is in fact DELLA transcript or protein: there are two previous reports suggesting that intercellular trafficking of GAI mRNA occurs through phloem sieve tubes in pumpkin, tomato and *Arabidopsis* (Ruiz-Medrano et al., 1999; Haywood et al., 2005). To confirm that *RGA* expression is restricted to the appropriate tissue in each line, anthers from T_3 plants representing each transgene were screened for GFP expression. However, no clear GFP fluorescence was observed in transgenic anthers that could not alternatively be attributed to background fluorescence seen in wild-type anthers (Figure 6.14). The presence of RGA-GFP transcript was identified by RT-PCR in cDNA created from whole floral clusters for each transgenic line (Figure 6.15), suggesting that the RGA-GFP fusion is being expressed and, furthermore, that full-length GFP mRNA is transcribed (Figure 6.15c). Sequence analysis of the RGA-GFP transgene prior to

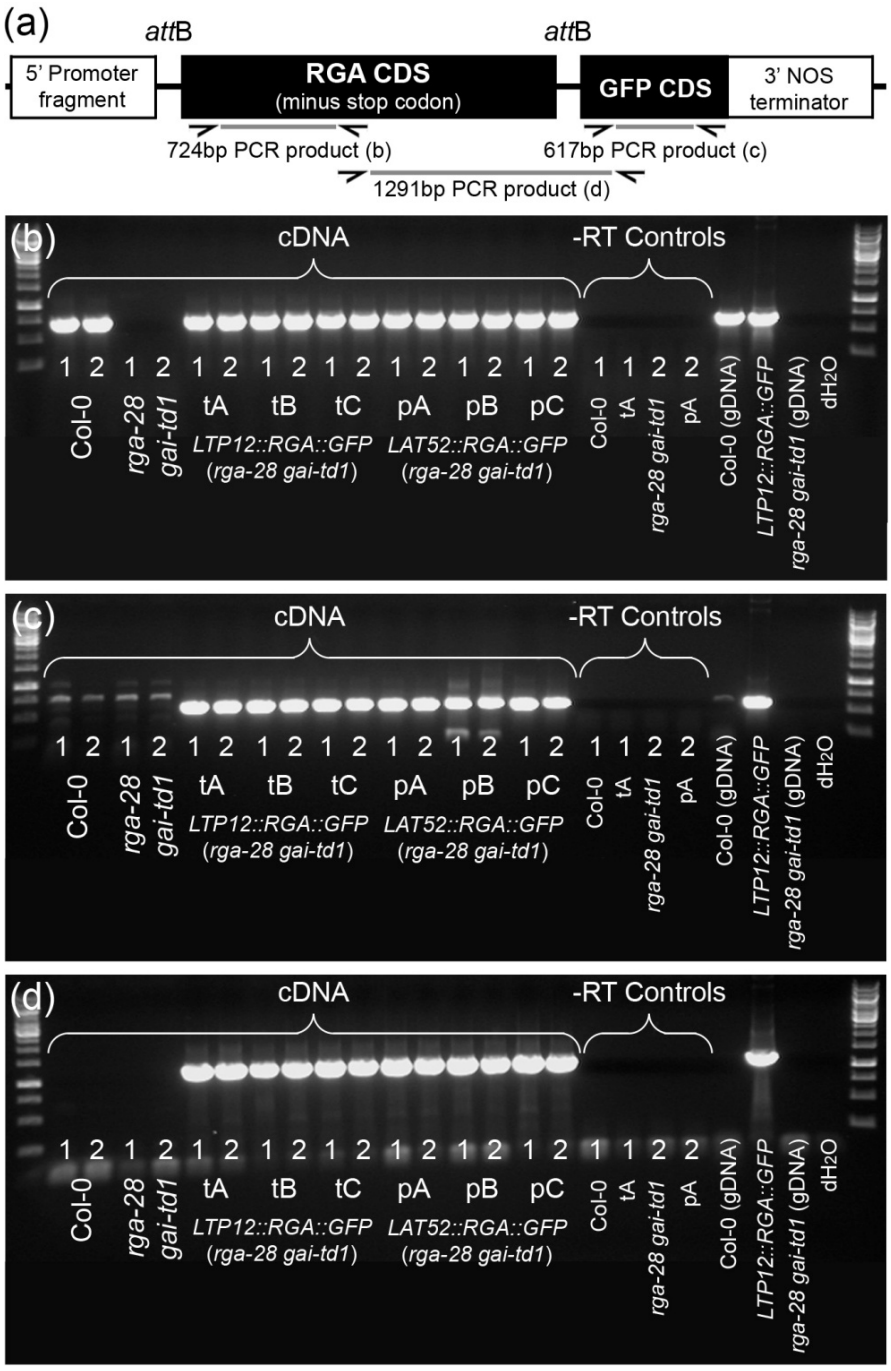

Figure 6.15: RT-PCR analysis of RGA-GFP expression in *LTP12::RGA::GFP* and *LAT52::RGA::GFP* transgenic lines.

Schematic of promoter::RGA::GFP *transgene structure (a), marking RT-PCR targets to test for the presence of RGA (b), GFP (c) and RGA-GFP fusion transcript (d) in RNA extracted from whole inflorescence tissues, against -RT and DNA controls. Two biological replicates of each genotype/transgenic line were tested (as numbered), each comprising three floral clusters from one individual plant. PCR products are shown against 1kb DNA ladder.*

transformation did not identify any mutations in the linking *att*B site (Figure 6.15a) or the GFP CDS (not shown), and as such there is no technical reason preventing GFP fluorescence. The complementation of the fertility phenotype also suggests that the RGA component of the transgene is functioning effectively. Although the absolute level of transgene expression has not been quantified in these lines, this data suggests that the lack of observed fluorescence was caused by technical problems with GFP fluorescence microscopy screening rather than with a failure of GFP expression. Unfortunately it was not possible to optimise screening for GFP fluorescence within the time-frame of this project, and thus the sites of RGA expression in anthers could not be confirmed. Despite the lack of positional information, this transgenic approach has still supplied strong and direct evidence for the necessity of DELLA repression of GA signalling to maintain successful pollen development in *Arabidopsis*.

6.3 CONCLUSIONS

From the experimental results presented in this chapter, it can be concluded that the responses of the Columbia and Landsberg *erecta* ecotypes to GA overdose are significantly different, though the underlying cause of these differences has not been investigated directly. Chemical GA overdose has a negative effect on the fertility of Col-0 (as measured by silique-set) which cannot be explained by mismatched floral organ growth and instead is associated with reduced anther size. In contrast, the fertility of L*er* is not significantly affected by chemical GA overdose following the same criteria. These results suggest that underlying differences in GA response exist between the reproductive systems of these two ecotypes, presumably relating to GA signal transduction and downstream responses.

Loss of the two DELLA paralogues *RGA* and *GAI* negatively affects fertility in both ecotypes, though the impact on phenotype is far more severe in Col-0, where it causes complete male sterility. In this respect, the Col-0 phenotype more closely matches DELLA loss-of-function mutants from other species, such as *sln1* in barley. These fertility phenotypes were more severe than those achieved by either chemical GA treatment or genetic GA overdose through manipulation of GA biosynthesis and metabolism. Loss of DELLA action in Col-0 was found to disrupt pollen development after the completion of meiosis, with a potential defect in pollen

wall synthesis/deposition leading to collapse of the developing microspores. This phenotype was complemented by reintroduction of RGA into either the tapetum or developing microspores, raising the possibility that GA-dependent communication occurs between these two tissues downstream of GA signalling. The observations made of the L*er* phenotype as part of this project support previous reports that loss of *RGA* and *GAI* negatively impacts pollen development in this ecotype (Dill & Sun, 2001), but that plants remain partially male-fertile. Recapitulation of the *rga-28 gai-td1* male-sterile phenotype in the Col-0 *er105* background makes it highly unlikely that successful pollen development in *rga gai* (L*er*) mutants is due to the loss of ER function. Differences in DELLA loss-of-function mutant phenotypes in the Col-0 and L*er* backgrounds highlights the possibility of differential stamen expression patterns of DELLA paralogues between these ecotypes, which might explain the continuing success of pollen development in L*er* anthers in the absence of *RGA* and *GAI*. However, this question remains to be addressed directly, and needs to be squared with the apparent retention of male fertility in the L*er* DELLA *global* quintuple loss-of-function mutant.

CHAPTER 7: GENERAL DISCUSSION

7.1 THE *ATGA20OX* GENE FAMILY EXHIBITS A FUNCTIONAL HIERARCHY

The existence of a *GA20ox* multigene family is conserved across higher plants, with multiple *GA20ox* genes found in each species studied to date, including rice (4 paralogues, Sakamoto et al., 2004), pumpkin (3 paralogues, Lange et al., 2005), tomato (3 paralogues, Rebers et al., 1999) and pea (2 paralogues, Ait-Ali et al., 1999), although with the exception of *Arabidopsis* and rice (in which the complete genomes have been sequenced) cataloguing of GA biosynthetic genes has not been exhaustive. The principle of *GA20ox* paralogues having individual, complex developmental and spatial expression patterns has been established previously by expression analysis in numerous species (Phillips et al., 1995; Rebers et al., 1999; Yamaguchi et al., 2001; Lange et al., 2005; Rieu et al., 2008).

Prior to this project, specific developmental functions had been established for two of the five known *GA20ox* paralogues in *Arabidopsis* (*AtGA20ox1* and *AtGA20ox2*) through mutant analysis (Rieu et al., 2008), but significant differences remained between the growth phenotypes of the *ga20ox1 ga20ox2* double mutant and the GA-deficient mutant *ga1-3*. This study represents the first instance in which the entire *GA20ox* gene family of any plant species has been so characterised. Mutant phenotypic analyses demonstrate that GA20ox activity during *Arabidopsis* development is accounted for almost entirely by a combination of *AtGA20ox1*, *-2* and *-3*. Although initial comparisons between the *ga20ox1 ga20ox2 ga20ox3-1* and *ga1-3* mutants suggested some small remaining differences between these two genotypes, these were not verified in subsequent comparisons against the alternative triple mutant *ga20ox1 ga20ox2 ga20ox3-3* and the two quadruple mutants *ga20ox1 ga20ox2 ga20ox3-1 ga20ox4-2* and *ga20ox1 ga20ox2 ga20ox3-1 ga20ox5-2*. That said, a number of these new alleles (*ga20ox3-3*, *ga20ox4-2* and *ga20ox5-2*) were derived from *Arabidopsis* ecotypes other than Col-0, and their introduction into the Col-0 background through crossing raises the possibility that the phenotypes of these combinatorial mutants are also influenced by other, ecotype-specific variations in unrelated genes. Subtle differences in flowering time and stamen growth between *ga20ox1 ga20ox2 ga20ox3-1* and *ga1-3* could not be completely

discounted in subsequent analyses. *In vitro* functional assays and mutant analysis suggest that any remaining GA20ox function is likely to be due to *AtGA20ox4*, with *AtGA20ox5* unable to catalyse the final oxidative step of canonical GA20ox activity and convert GA_{24} to GA_9.

The conservation of multiple *GA20ox* paralogues across numerous plant species, in conjunction with individual expression patterns, has led to speculation that each paralogue might possess specific functions in plant development. Whilst functional specification has been previously shown between *AtGA20ox1* and *AtGA20ox2* (Rieu et al., 2008), the results presented here suggest that a more complex relationship exists between other members of the *AtGA20ox* gene family. Mutant analysis indicates that the function of *AtGA20ox3* appears to be in support of either *AtGA20ox1*, *-2* or both (acting as primary contributors of GA20ox function), with very few aspects of plant development in which its presence or absence affects growth phenotypes when at least one of these other paralogues remains. Notable exceptions include flowering time and 7-day root length, in which loss of *AtGA20ox3* exacerbated the *ga20ox2* mutant phenotype, and could not be compensated for by *AtGA20ox1* (see sections 3.2.2 and 3.2.3). The difference in flowering time is particularly interesting, as no significant difference in the level of bioactive GA present in whole rosettes was found between the *ga20ox2* and *ga20ox2 ga20ox3-1* mutants (whilst, in contrast, *ga20ox1 ga20ox3-1* contained less bioactive GA than *ga20ox1*, with no appreciable effect on phenotype). This probably reflects the importance of the site of expression of each paralogue on its contribution towards any particular aspect of plant growth and development. As yet, tissue expression patterns for all three paralogues during floral transition have not been established. The functional redundancy between these three paralogues is perhaps best typified during germination, where two independent analyses found that *AtGA20ox3* is far more highly expressed than either *AtGA20ox1* or *-2* (Ogawa et al., 2003; Rieu et al., 2008). Despite this, the frequency of germination is only affected by simultaneous loss of all three paralogues. The presence of functional *AtGA20ox4* and *-5* is not enough to stimulate germination in *ga20ox1 ga20ox2 ga20ox3* seed, despite both being expressed to some degree (Rieu et al., 2008). This may reflect a high minimum requirement for bioactive GA during the germination process, which is satisfied by the activity of either *AtGA20ox1*, *-2* or *-3*, the expression of each being

approximately two orders of magnitude greater than that of *AtGA20ox5* (Rieu et al., 2008). Whilst germination success was unaffected in single or double mutants, future phenotypic analysis may find subtle differences in other germination phenotypes, for example germination speed or length of dormancy. The embryo tissue expression patterns of these three paralogues during germination have not yet been resolved, but the GUS reporter lines developed during this project now provide the tools to be able to do so.

The evidence presented relating to expression of *AtGA20ox1*, *-2*, *-3* and *-4* during floral development (as reported by GUS expression), supports the hypothesis that each paralogue is expressed in a unique tissue pattern, further supported by the expression mapping by qPCR performed on late floral development. Intriguingly, whereas GUS staining patterns had led to the expectation of overlapping expression within floral tissues during late floral development it was found that *GA20ox* expression in particular floral organs was instead restricted almost exclusively to individual paralogues. Even more surprisingly, expression in wild-type floral tissues was limited to *AtGA20ox1* and *-2*, with very low expression of *AtGA20ox3*, *-4* or *-5* in comparison to these two. This is inconsistent with the floral phenotypes of the *ga20ox1 ga20ox2* and *ga20ox1 ga20ox2 ga20ox3-1* mutants, which indicate a function for *AtGA20ox3* in floral development. Previous expression analysis has concluded that multiple *AtGA20ox* paralogues are co-expressed in most reproductive and vegetative tissues across plant development (Rieu et al., 2008), which would appear to contradict this result. The functional redundancy found between *AtGA20ox1*, *-2* and *-3* by mutant analysis further argues for co-expression. However, the previous expression analysis was conducted at a very low resolution, for instance using entire floral clusters as source tissue for studying floral development (Griffiths et al., 2006; Rieu et al., 2008), whereas the work presented here was conducted using individual floral organ types. As such, whilst numerous *AtGA20ox* paralogues may by expressed within the whole floral cluster during floral development, finer-resolution mapping suggests that (in the case of late floral development at least) expression of *AtGA20ox* paralogues is in fact more compartmentalised. Similar discrepancies between qPCR and GUS staining were observed during an earlier stage of floral development. Mutant analysis indicates that *AtGA20ox1*, *-2* and *-3* all function to promote entry of the tapetum cell

layer into PCD as part of normal anther development, a conclusion supported by GUS staining analysis, with *AtGA20ox1*, *-2*, *-3* and *-4* all reported exclusively within the tapetum (in the context of anther tissues) between meiosis and tapetum PCD. However, qPCR analysis found floral development at this stage to be dominated by *AtGA20ox1* expression, with *AtGA20ox2* present at far lower levels and *AtGA20ox3*, *-4* and *-5* barely detectable in comparison. This expression analysis was performed on whole floral buds, thereby encompassing other sites of *AtGA20ox* expression including the stamen filament, the pistil and receptacle. As such, expression analyses are required at a higher resolution, both in this and other developmental contexts, to confirm or refute whether compartmentalised expression of *AtGA20ox* paralogues occurs more generally during plant development. An additional source of information will be high-resolution transcriptomes for particular tissues during development, such as that now available for post-meiotic development of *Arabidopsis* pollen (Honys and Twell, 2004). Whilst broadly in agreement with the observed GUS staining patterns of the *AtGA20ox* reporters, mining of this dataset identifies distinctions in the timing of expression during pollen development not identifiable from the GUS expression patterns. However, the transcriptomic analysis finds fewer *AtGA20ox* and *AtGA3ox* paralogues in developing pollen than predicted by GUS reporters, and similarly *AtCPS* expression is not identified in the stages predicted by GUS expression. Whether this is due to false expression by over-sensitive GUS reporter lines, or to low expression of these biosynthetic genes falling beneath the detection threshold of the microarray, remains to be determined.

Compartmentalisation of *AtGA20ox* expression can theoretically by explained by transcriptional feedback regulation of *AtGA20ox1*, *-2* and *-3*. Evidence for a hierarchical relationship between *AtGA20ox* paralogues has been previously published (Rieu et al., 2008). In wild-type stem tissues, expression analysis indicates that GA20ox function is dominated almost exclusively by *AtGA20ox1*, but internode expression of *AtGA20ox2* is dramatically increased in the *ga20ox1* mutant background. In contrast, *AtGA20ox1* expression is either unaffected or slightly reduced in *ga20ox2* stem tissues. Whilst *AtGA20ox3* expression was found to be slightly increased in *ga20ox1* tissues, the most significant increase was found in the absence of both *AtGA20ox1* and *-2*. These responses do not support a model in which the

expression of each paralogue responds independently to GA signalling, but instead a more complex relationship in which expression of one paralogue can influence the expression of others, (i.e. *AtGA20ox1* represses *AtGA20ox2* and both *AtGA20ox1* and *-2* represses expression of *AtGA20ox3*). Application of these rules more generally could explain both the apparent compartmentalisation of *AtGA20ox* expression between different floral tissues and the unexpected absence of *AtGA20ox3* expression from floral tissues. In support of this hypothesis, *AtGA20ox3* expression was found to be significantly up-regulated in specific *ga20ox1 ga20ox2* floral tissues.

Homeostatic regulation of these paralogues acts through GA signalling as demonstrated by the effect of GA treatment on *AtGA20ox* expression (Rieu et al., 2008), and transcriptomics analyses have identified both *AtGA20ox1* (Cao et al., 2006) and *AtGA20ox2* (Zentella et al., 2007) as DELLA transcriptional targets. As an alternative hypothesis to direct sideways interactions between *AtGA20ox* paralogues to affect each other's expression, their behaviour might be explicable by differing sensitivities to GA, although GA treatment studies did not observe any gross differences in behaviour between paralogues to changing GA concentrations (Rieu et al., 2008). It is important to bear in mind that GA20ox activity does not directly create bioactive GA, requiring additional GA3ox activity, which, given the physical separation of the GA biosynthetic pathway between plant tissues (see section 1.2), could potentially be acting at a distant site. Furthermore, *AtGA3ox1* is also under homeostatic regulation via the GA signal transduction pathway (Zentella et al., 2007), and so the expression behaviour of the *AtGA20ox* paralogues is likely to be complicated by the behaviour of GA 3-oxidases. The transcriptional regulation of particular *AtGA20ox* paralogues is further complicated by other environmental or endogenous signals. Both *AtGA20ox1* and *-2* are subject to different types of transcriptional regulation by environmental factors, including light (Hisamatsu et al., 2005) and temperature (Yamauchi et al., 2004), as well as circadian regulation (Hisamatsu et al., 2005, see section 1.2.1 for further discussion). In contrast, expression of *AtGA20ox3* has been shown to not be affected by temperature during germination (Yamauchi et al., 2004). The interaction between environmental and homeostatic regulation of *AtGA20ox* gene expression (and of other GA biosynthetic genes) has not yet

been investigated. Past expression studies have focussed on particular tissues or developmental events, and it is not known how (or if) regulation of *AtGA20ox* expression alters between developmental contexts. The mobility of bioactive GA (see section 1.2) means that homeostasis must also be considered in the context of multicellular tissues, rather than just within individual cells. Given the dependence of GA homeostasis on GA signal transduction and the potential separation of the sites of GA biosynthesis and GA signalling, one possible way to reconcile these two regulatory mechanisms is by homeostatic regulation only affecting *AtGA20ox* expression in cells where GA signalling actively occurs, whilst developmental regulation of GA biosynthesis might occur in tissues where GA signalling components (specifically DELLA proteins) are not expressed. That said, *AtGA3ox1* expression is also regulated by environmental signals in some tissues (Yamaguchi et al., 1998; Yamauchi et al., 2004), and the direct production of bioactive GA by GA3ox makes it unlikely that environmental and homeostatic signals can be separated in this manner.

One way in which the observed disparity between expression patterns found between qPCR analysis and GUS reporter lines might be explained is that the *GA20ox::GUS* transcriptional fusion transgenes created for this project are not subject to homeostatic regulation because they lack native *GA20ox* intronic sequence. A comparison of transcriptional and translational fusion GUS lines reporting *AtCPS* (Silverstone et al., 1997) and *AtGA3ox* expression (Mitchum et al., 2006, Hu et al., 2008), suggests that intronic regulatory elements affect reporter gene expression, and clear differences in expression were observed between the transcriptional and translational forms of GUS reporters (which included intronic sequences) for *AtGA20ox1* and *-2*. However, alternative explanations can also be proposed, including regulation at the post-transcriptional or post-translational level. An important test of this hypothesis will be the responsiveness of the *AtGA20ox::GUS* reporter lines created for this project to chemical GA treatment, which has not yet been established.

Another unexpected result from this project is the phenotypic rescue of *ga20ox* loss-of-function mutant phenotypes by constitutive expression of *AtGA20ox5*. As mentioned above, this paralogue was found to have incomplete GA20ox activity *in vitro*. The initial hypothesis

that AtGA20ox5 activity enhanced the biosynthesis of GA in the *ga20ox1 ga20ox2 ga20ox3-1* background by increasing flux through the pathway in collaboration with AtGA20ox4 was not supported by subsequent evidence that phenotypic rescue by *35S::AtGA20ox5* occurs even in the absence of any other (currently known) fully-functional *AtGA20ox* paralogue. Whilst this result could be explained by residual conversion of GA_{24} to GA_9 by AtGA20ox5 (or potentially an unrelated enzyme), it might also indicate an alternative biosynthesis pathway that is not dependent on full GA20ox activity. Examples of unorthodox catalytic behaviour by GA biosynthetic enzymes have been reported previously in pumpkin (*Cucurbita maxima*), including a GA 20-oxidase (CmGA20ox1) which predominantly produces C_{20}-GA products (GA_{25} and GA_{17}) in preference to the more typical C_{19}-GAs (Lange, 1994; Lange et al. 1994) and a GA 3-oxidase (CmGA3ox1) that preferentially 3β-hydroxylates C_{20}-GAs (Frisse et al., 2003) as well as displaying dual 3β and 2β-hydroxylation activity (Lange et al., 1997). These unorthodox functions have been confirmed *in planta* through heterologous expression in *Arabidopsis* (Radi et al., 2006), the transgenic lines consequently demonstrating altered GA biosynthesis.

Although the most recent reviews of GA biosynthesis have focussed almost exclusively on the canonical pathway (outlined in Figure 1.3) that has been established as the primary route of GA biosynthesis in numerous higher plants (Yamaguchi, 2008), earlier summaries emphasise a more complex metabolic pathway and highlight the potential for alternative routes (e.g. MacMillan, 1997). One alternative, termed the 'early 3β-hydroxylation pathway', may explain the phenotypic rescue by AtGA20ox5 through 3β-hydroxylation of the GA20ox intermediates GA_{15} and GA_{24} to GA_{37} and GA_{36}, respectively, a possibility supported by biochemical analysis of AtGA3ox1 substrate specificity (Williams et al., 1998). Bioassay data summarised in Graebe and Ropers (1978) show that application of GA_{37} and GA_{36} cause significant plant growth responses in several plant species, as do numerous other GA species in addition to the accepted bioactive forms of GA. Both of these forms of GA have been identified in wild-type *Arabidopsis* tissues by GC-MS (Talon et al., 1990). The expanded GA metabolic pathway summarised by MacMillan (1997), based on the activity of GA biosynthetic enzymes *in vitro*, suggests that in many cases the apparent bioactivity of these

other GA forms could be explained by inter-conversion to GA_1 or GA_4 by native GA biosynthetic enzymes- for example, conversion of GA_{36} to GA_4 by GA20ox activity (demonstrated in pumpkin, Macmillan, 1997). In this situation GA biosynthesis is better represented as a metabolic grid than a linear pathway. However, whilst the conversion of GA_{37} to GA_{36} (and on through to GA_4) is postulated, this step has not been directly demonstrated, and, importantly, these conversions are still dependent on the presence of fully-active AtGA20ox activity. As such, it is unlikely that the phenotypic rescue by *35S::GA20ox5* is through production of GA_4, suggesting that GA_{36} or GA_{37} themselves could possess innate bioactivity. In particular, the structure of GA_{37} closely mimics GA_4 (Figure 4.9b), and conversion of GA_{15} to GA_{37} *in vitro* was far more efficient than that of GA_{24} to GA_{36} (Williams et al., 1998). This hypothesis is supported by the phenotype of *AtGA20ox5* overexpression lines, in which growth is only partially restored in comparison with *AtGA20ox1* overexpression, despite a demonstrably high level of *AtGA20ox5* expression in these lines, a difference that could be explained through the production of an alternative bioactive GA with reduced effectiveness compared to GA_4.

Whilst attractive, this hypothesis has yet to be tested directly, for example through GA analysis of the transgenic lines produced during this project. A potential genetic test for the reliance of this hypothesised pathway on GA3ox activity would be to introduce existing *ga3ox* loss-of-function alleles (Mitchum et al., 2006; Hu et al., 2008) into *35S::GA20ox5* (*ga20ox1 ga20ox2 ga20ox3-1 ga20ox4-2*). The bioactivity of GA_{37} itself can be directly tested *in vitro* using a GA-dependent yeast-2-hybrid interaction between GID1 and DELLA protein, as used in numerous previous studies (Griffiths et al., 2006; Ueguchi-Tanaka et al., 2007). Any contribution by this putative pathway to GA biosynthesis is extremely minor, as demonstrated by the severity of the *ga20ox1 ga20ox2 ga20ox3-1 ga20ox4-2* dwarf phenotype, but this finding does highlight the potential flexibility of GA biosynthesis in higher plants.

7.2 *ARABIDOPSIS* FERTILITY IS DEPENDENT ON AN OPTIMUM LEVEL OF GA SIGNALLING

Successful reproduction of angiosperms is well-known to be dependent on GA, with reduced GA biosynthesis negatively impacting fertility in numerous plant species through defects in both male and female reproductive development (Pharis & King, 1985). In the absence of bioactive GA, pollen development in both rice and *Arabidopsis* has been shown to be arrested shortly after meiosis (Cheng et al., 2004; Aya et al., 2009). A post-meiotic developmental arrest has also been observed in GA-deficient petunia flowers (Izhaki et al., 2002), whilst in GA-deficient tomato a pre-meiotic developmental block occurs (Jacobsen & Olszewski, 1991). In rice it has been clearly demonstrated that entry of the tapetum into PCD is GA-dependent (Aya et al., 2009); a similar defect in PCD was observed during this project in the *ga20ox1 ga20ox2 ga20ox3-1* triple mutant. Analysis of the expression of GA-biosynthetic genes in both rice and *Arabidopsis* (Kaneko et al., 2003; Hirano et al., 2008; Hu et al., 2008) suggests that the tapetum is a strong source of GA within anther tissues at this stage of development, in conjunction with the stamen filament. GUS staining performed during this project indicates that the tapetum is the near-exclusive site of GA20ox activity in anther tissues prior to tapetum PCD, with weak expression seen in meiotic PMCs (*AtGA20ox1* and -*2*) and post-meiotic microspores (*AtGA20ox1*). GA signalling occurs in both the tapetum and developing microspores at this stage (Kaneko et al., 2004; Millar & Gubler 2005; Aya et al., 2009), and it remains unclear in which tissue this developmental block originates, and what its cause is.

Less severe *Arabidopsis* GA biosynthesis and signalling mutants progress beyond this checkpoint through to stamen maturation. Phenotypic analysis of the *ga3ox1 ga3ox3* double mutant (Hu et al., 2008), and evidence from stamen growth of the *ga20ox1 ga20ox2* mutant acquired during this project, support the existence of a separate, late-stage checkpoint in stamen development dependent on GA at approximately floral stage 10, just prior to stamen maturation and anthesis. This is strongly reminiscent of floral phenotypes of JA-biosynthetic and signalling mutants (Feys et al., 1994; Stintzi & Browse, 2000). Given that JA signalling has been found to act downstream of GA signalling during late stamen development (Cheng et

al., 2009), it may well be that the developmental block in very early flowers of these mutants is related to JA-dependent anther developmental processes. Both the *ga20ox1 ga20ox2* and *ga3ox1 ga3ox3* mutants display reduced silique-set in early flowers, after which fertility recovers. This can be ascribed to mismatched floral organ growth in these flowers creating a mechanical barrier to pollination (Hu et al., 2008; Rieu et al., 2008), whilst pollen development and viability, both of which are GA-dependent (Singh et al., 2002; Chhun et al., 2007), remain largely unaffected. Segregation analysis of *ga20ox* mutant alleles found little evidence of a pollen fitness penalty *in vivo*, even for triple and quadruple mutant pollen, in contrast to the effects seen in pollen of GA-deficient rice mutants (Chhun et al., 2007). However, segregation analyses by Chhun et al. only included GA mutants from biosynthetic steps governed by single copy genes (Sakamoto et al., 2004), whereas maternal tissues in the segregation analyses performed in this study still contained functional *AtGA20ox* paralogues, which thus could have masked pollen growth phenotypes by supplying bioactive GA.

Mutant analysis in this project suggests that both *AtGA20ox1* and *-2* promote pistil growth. Expression mapping indicates that *AtGA20ox2* is expressed directly in pistil tissues, whilst *AtGA20ox1* may act indirectly to promote pistil growth from other floral tissues. The greatest change in floral organ growth across these early flowers was found in stamens, the growth of which is promoted late in development by *AtGA20ox1* expression in the stamen filament and in the underlying receptacle. Expression analysis suggests that by this stage in development the anther only makes a small contribution to stamen GA biosynthesis, with a low level of *AtGA20ox2* expression found in anther tissues. Modelling changes in stamen growth across early flowers in the *ga20ox1 ga20ox2* mutant indicates that the rescue of stamen growth is a not gradual, indicative of a developmental block in very early flowers. An underlying trend of increasing stamen growth by the time of flower opening with increasing inflorescence position was also found, in this and all other genotypes studied, to which recovery of fertility in less-severely infertile genotypes (e.g. *ga20ox1*) could be ascribed. Petal growth demonstrated a similar trend, suggesting that their growth is affected by the same mechanism. Petal growth has previously been linked to that of stamens through GA, with a lack of *GA3ox* expression in rice and *Arabidopsis* petals (Mitchum et al., 2006, Hu et al., 2008, Kaneko et al., 2003) and

GA analysis of rice flowers (Kobayashi et al., 1988) suggesting that petals are dependent on stamens as a source of bioactive GA. Results from this project partly support this hypothesis, with no *AtGA20ox* expression detected in petals during floral development, and with petal and stamen growth in early *ga20ox1 ga20ox2* flowers displaying correlated phenotypes. However, whereas stamen growth in *ga20ox1 ga20ox2 ga20ox3-1* and *ga1-3* flowers was found to arrest during floral development, petal growth continued, suggesting that their dependence on GA for growth is not absolute. Though less so than developing stamens, other floral tissues such as the receptacle are likely to be alternative sources of bioactive GA (Mitchum et al., 2006, Hu et al., 2008), as indicated from *AtGA3ox* expression distribution. Furthermore, the difference in growth between *ga20ox1 ga20ox2 ga20ox3-1* and *ga1-3* floral organs was greater for petals than for stamens. This might be due to the dependence of petals on external GA sources, amplifying the phenotypic impact of small changes to the availability of GA in floral tissues.

Work previously published and also that presented in this project demonstrates that, in addition to GA-deficiency, GA treatment to excess negatively affects fertility of wild-type *Arabidopsis* (Jacobsen & Olszewski, 1993), reducing both the probability of silique-set and the number of seeds per silique. Floral organ growth under control conditions and chemical GA treatment did not differ at flower opening, neither did the timing of anther dehiscence, suggesting that this is not due to mismatched floral organ growth or development, as is the case under GA-deficient conditions (see above). However, chemical GA treatment was found to have a consistent negative effect on anther size, both at flower opening and at other surrounding developmental stages, raising the possibility that fertility is negatively affected by other problems associated with anther or pollen development. Pollen tube growth *in vitro* is negatively affected by high concentrations of bioactive GA (Singh et al., 2002), which might explain the observed negative impact on seed set (although this has not been directly tested), but cannot easily explain the negative effect of GA-overdose on silique-set, as high concentrations of GA does not completely inhibit pollen tube growth, as evidenced by *in vitro* assays (Singh et al., 2002) and the continuation of seed set under GA overdosed conditions.

Silique-set phenotypes seem to be more closely linked to pollination success rather than subsequent fertilisation success.

Mutants in the L*er* ecotype in which repression of downstream GA signalling by RGA and GAI is lost demonstrate similar fertility defects to those caused by chemical GA treatment, which in these mutants have been ascribed to reduced pollen production and, anecdotally, mismatched growth between stamens and pistils (Dill & Sun, 2001). The equivalent Col-0 mutant was found to be entirely male-sterile, with a post-meiotic defect in pollen development resulting in pollen abortion, a phenotype that was complemented by reintroduction of functional RGA. This suggests that, whilst successful pollen development requires GA signalling in order to progress through key checkpoints, it is also necessary that GA signalling be restricted, a hypothesis that fits well with the complex temporal and spatial expression patterns of GA-biosynthetic genes seen during anther development. Inappropriate GA signalling leading to pollen developmental defects can explain the reduced fertility phenotypes of both L*er rga gai* mutants and chemically GA-overdosed plants, though the reasons for the difference in phenotype between the Col-0 and L*er* ecotypes are still not clear. The responses of Col-0 and L*er* fertility to chemical GA treatment were found to be quite distinct, with L*er* fertility remaining highly robust whilst Col-0 fertility is reduced. Interestingly, although L*er* fertility is unaffected by chemical GA-overdose, increased GA signalling caused by loss of RGA and GAI does negatively affect fertility as described above. This suggests that the same principles underlie pollen development in both ecotypes, but L*er* pollen development appears to be far more resistant to inappropriate GA signalling. The male-sterile phenotype of the Col-0 *er105 rga-28 gai-td1* mutant characterised during this project suggests that this is not due to the loss of *ERECTA* function in the L*er* background.

Multiple DELLA paralogues act to repress GA signalling during stamen development, as demonstrated through phenotypic analysis of DELLA loss-of-function mutants in the *ga1-3* background (Cheng et al., 2004; Tyler et al., 2004). These indicate that, in addition to RGA and GAI, RGL1 and RGL2 are important contributors to the repression of GA signalling during floral development, though their importance in different aspects of development varies.

RGL2 expression has been reported in the pistil, sepals and stamen filaments of developing flowers, but apparently not the anther (Lee et al., 2002). That said, *RGL2* expression has detected at a relatively low level in the transcriptome of developing pollen (Honys and Twell, 2004). Results presented in this project demonstrate that loss of RGA and GAI in the *gid1c gid1b gid1c* GA-insensitive background (Griffiths et al., 2006) was not sufficient to restore full stamen filament elongation, suggesting that other DELLA proteins continue to restrict growth. In contrast, loss of RGA and GAI was shown to cause male sterility through disruption of pollen development in this GA-insensitive background, suggesting that (in the Col-0 ecotype) the remaining DELLA paralogues do not repress GA signalling sufficiently in relevant anther/pollen tissues to maintain successful pollen development. Loss of *RGA* alone is sufficient to overcome pollen developmental arrest in the *gid1a gid1b gid1c* background (Griffiths et al., 2006). In contrast, loss of *GAI* alone from this background had no effect on *gid1a gid1b gid1c* stamen development. As such, although GAI is necessary for successful pollen development its role is apparently minor compared to RGA. A similar hierarchy is observed throughout vegetative tissues as well (Dill & Sun, 2001), with loss of RGA sufficient to substantially rescue GA-dependent dwarfism in GA-deficient and insensitive backgrounds (Dill & Sun, 2001, Tyler et al., 2004, Griffiths et al., 2006). In both vegetative and reproductive contexts this could be explained by *RGA* having a far broader tissue expression pattern than *GAI*.

If DELLA mutant analyses are compared between the L*er* and Col-0 ecotypes, it can be seen that rescue of stamen growth by loss of *RGA* is far greater in GA-deficient Col-0 (Tyler et al., 2004) than when both *RGA* and *GAI* are absent from GA-deficient L*er* (Dill & Sun, 2001; King et al., 2001; Cheng et al., 2004). A comparison of the amino acid sequence between Col-0 and L*er* RGA proteins finds a difference of two amino acids (Thomas, S., personal communication), but whether this affects RGA activity has not been tested. Loss of additional DELLA proteins in the L*er* background rescues stamen development (Cheng et al., 2004), suggesting that the ecotype-specific differences observed in stamen development could be due to differences in the expression of the DELLA paralogues. Importantly, whilst results presented here found that loss of RGA alone was sufficient to overcome arrested pollen

development in the Col-0 GA-insensitive *gid1a gid1b gid1c* mutant, pollen development in the L*er ga1-3* mutant is only restored by the simultaneous loss of *RGA*, *RGL1* and *RGL2* (Cheng et al., 2004). Analysis of gene expression in L*er* pollen (Honys and Twell, 2004) supports this, with four DELLA paralogues (*RGA*, *GAI*, *RGL1* and *RGL2*) expressed prior to and during pollen mitosis (the timing of developmental arrest in *ga1-3*). The observed differences between mutants in different ecotypes suggest that in the L*er* ecotype additional DELLA paralogues are acting in anther tissues, though whether this is due to altered levels of expression or qualitatively different tissue expression patterns is unknown.

It is possible that differences in DELLA expression are sufficient to explain the different responses of Col-0 and L*er* fertility to chemical GA treatment. However, the L*er* global DELLA mutant (carrying loss-of-function mutations in all five DELLA paralogues) is not completely male-sterile (unpublished data), displaying similar fertility phenotypes to Ler *rga gai* mutants (Thomas, S., personal communication). If accurate, this indicates that differences between the Col-0 and L*er* ecotypes other than at the level of DELLA expression maintain L*er* pollen development in the absence of GA signalling, and if so, likely candidates are downstream targets of GA signalling or DELLA-interacting proteins. An alternative possibility, however, is that not all of the alleles used in the L*er* DELLA global mutant are complete loss-of-function alleles: the *rgl1-1* allele contains a T-DNA insertion 68 bp upstream of the start codon (Lee et al., 2002), and current work recreating the global DELLA mutant in the Col-0 background using the *rgl1-2* allele (Tyler et al., 2004) has raised the possibility that the *rgl1-1* allele may still have some residual expression (Thomas, S., personal communication). The creation of a corresponding quintuple DELLA mutants in the Col-0 ecotype will be an important step toward answering this question, as will the mapping of DELLA expression patterns between these two ecotypes.

Beyond determining that the failure in pollen development in the *rga-28 gai-td1* (Col-0) mutant relates to a loss of DELLA repression in stamen tissues, the precise nature of the developmental defect remains unclear. Morphological analysis indicates that the mutant phenotype manifests after the completion of meiosis, with pollen wall deposition visibly

disrupted prior to pollen abortion. Both the tapetum cell layer and developing microspores contribute to pollen wall formation (reviewed in Scott et al., 2004), and there is evidence of GA signalling occurring in both cell types during this stage of development (see above). Whether (and how) inappropriate GA signalling disrupts the development of either or both of these tissues can be tested through ultrastructural analysis via transmission electron microscopy (TEM). Other tools to address this question have been developed during this project. Tissue-specific reintroduction of RGA under either the tapetum-specific *LTP12* (Ariizumi et al., 2002) or pollen-specific *LAT52* (Twell et al., 1989, 1990; Eady et al., 1994) promoters restored male fertility of *rga-28 gai-td1*. The published expression patterns of these two promoter fragments, the timing of which overlaps, suggests that the developmental defect is post-meiotic, occurring at the unicellelular microspore stage (anther stage 8-9). It is during this phase of development that deposition of the pollen wall begins.

The fact that reintroduction of RGA into either tissue is sufficient to rescue pollen development suggests that, rather than both tissues being separately regulated (and their progression through development coordinated) by GA signalling, communication might occur between these two tissues downstream of GA signalling at this stage of anther development. The principle of cell-to-cell communication between the tapetum and developing pollen has been demonstrated during the determination of cell fate, where signalling via EXS/EMS-TPD causes secondary parietal cells to adopt tapetal cell fate instead of becoming pollen mother cells (Canales et al.,2002; Zhao et al., 2002; Yang et al. 2003, Jia et al. 2008). Development continues to be tightly co-ordinated between these two cell types, with the tapetum secreting callase to release post-meiotic microspores from tetrads and tapetal PCD releasing crucial pollen wall components from specific organelles. Premature release of microspores from tetrads results in pollen abortion in both tobacco and petunia (Worral et al., 1992), and whilst pollen degradation through premature activation of tapetal PCD can be ascribed to failed release of pollen from tetrads (Mariani et al., 1990; Hird et al., 1993), inhibition of tapetal PCD also disrupts microspore development after release from tetrads (Kawanabe et al, 2006). The signalling mechanisms through which these events are coordinated are not currently well understood, and the results from this project indicate that GA signalling has a function in

regulating this communication. Alternatively, DELLA could conceivably move between the two tissues, either as protein or mRNA. Previous experimental studies have found evidence supporting trafficking of GAI mRNA through phloem sieve tubes in pumpkin, tomato and *Arabidopsis* (Ruiz-Medrano et al., 1999; Haywood et al., 2005). However, as yet it has not been possible to validate the tissue-specificity of the RGA-expressing transgenic lines produced in this project via GFP fluorescence as was intended, so the possibility remains that expression under one or both of these promoters is leaky, with functional RGA being expressed simultaneously in both tapetum and developing pollen.

7.3 GA SIGNALLING STABILISES PATTERNING OF THE FLORAL MERISTEM AND STAMEN DEVELOPMENTAL IDENTITY

In addition to its functions promoting pollen development and floral organ growth, GA signalling also regulates aspects of early floral development. GA signalling has been shown to promote organogenesis at the shoot apical meristem (SAM) during the vegetative phase of development (Hay et al., 2002), and observations made during this project suggests that the same function exists in the succeeding inflorescence meristem (IM) during reproductive development. GA signalling up-regulates expression of the inflorescence and floral-meristem identity transcription factor *LFY* (Blazquez et al., 1998; Yu et al., 2004), and the floral homeotic genes *AP3* and *AG* (Yu et al., 2004), which themselves are also up-regulated by LFY during very early floral development to establish floral organ identity. However, whilst *LFY* expression declines after the establishment of floral organs (Weigel et al., 1992), GA signalling maintains expression of *AP3* and in particular *AG* (Yu et al., 2004), prolonged expression of which is necessary for successful stamen development (Ito et al., 2007), which is potentially achieved through a self-supporting positive feedback loop with GA (Gomez-Mena et al., 2005).

Despite this interaction with AG, no role for GA signalling in the floral meristem prior to floral organ outgrowth has been previously identified, supported by the phenotype of GA-deficient and GA-insensitive flowers, which show superficially normal early floral development until they experience developmental arrest (Goto & Pharis, 1999; Cheng et al.,

2004; Griffiths et al. 2006). Phenotypic analysis in this project has for the first time identified GA-dependent effects on floral organisation and stamen identity. Chemical GA treatment had a significant destabilising effect on floral development, an effect replicated by loss of *AtGA20ox1* and *-3* but not in the *ga20ox1 ga20ox2 ga20ox3-1* or *ga1-3* mutants. This could be explained not by an absolute requirement for GA in early floral development but through an imbalance in GA signalling across the floral meristem, which in turn suggests that GA signalling stabilises floral patterning by expression in very precise locations in the floral meristem. The most significant phenotypes were seen in stamens, in particular the repression of outgrowth of short stamens leaving gaps in the floral plan, partial homeosis of stamens to petals and the occurrence of split or branched stamens, in which two whole or partial stamens arose from the same floral organ primordium.

Homeotic phenotypes suggest involvement of the floral homeotic genes, which have previously been linked with GA signalling (see above). The floral homeotic genes encode MADS-box transcription factors that are expressed in overlapping domains across the floral meristem, with floral organ identity established through the formation of protein complexes, the precise composition of which determining the identity of each whorl according to the ABCE model (reviewed in Airoldi, 2010; Irish, 2010). The precise mechanisms through which these complexes establish specific floral identities is not yet known, but they are likely to direct the activation of specific developmental programmes to direct cell fate. AG acts in stamen primordia to directly promote expression of *SPL/NZZ* (Ito et al., 2004), which encodes a key transcription factor that initiates the specification of many anther tissues (see section 1.5.3). AG also regulates stamen development through indirect mechanisms, for example via JA signalling in late stamen development (Ito et al., 2007). Experiments using DEX-inducible *AG* expression in an *ag* mutant background demonstrated that stamen identity specification is neither switch-like nor absolutely determined at the very start of floral development, and that instead prolonged *AG* expression was necessary to restore full stamen identity, the default identity of organs in whorl 3 in the absence of AG being petals (Ito et al., 2007). One of the mechanisms through which AG acts might be GA signalling.

Floral organ primordia outgrowth begins after the establishment of homeotic gene expression domains across the floral meristem. Floral development can be viewed as the successive creation of boundaries- firstly between the nascent floral primordium and the inflorescence meristem, then between whorls within the floral meristem and then within whorls to demarcate individual floral organs (Irish, 2010). The other GA-related floral phenotypes identified here suggest that GA signalling may be involved in regulating the formation of these final subdivisions, the cells of which demonstrate altered cell division rates and asymmetric growth compared to cells within developing primordia (Aida & Tasaka, 2006). Auxin signalling has been implicated in regulating the formation of boundary layers between lateral organs through limiting the spatial expression of the NAC genes *CUP-SHAPED COTYLEDON1* (*CUC1*) and *CUC2* (Vernoux et al., 2000; Furutani et al., 2004), as well as the KNOX gene *SHOOTMERISTEMLESS* (*STM*; Furutani et al., 2004). During embryo development *CUC1* and *CUC2* are antagonised by *STM* (Aida et al., 1999), which has also been shown to repress the expression of *AtGA20ox1* in the SAM (Hay et al., 2002). Other genes associated with establishing boundaries between floral organs include *UNUSUAL FLORAL ORGANS* (*UFO*, Levin & Meyerowitz, 1995; Wilkinson & Haughn, 1995) and *FUSED FLORAL ORGANS1* (*FFO1*), *-2* and *-3* (Levin et al., 1998). The mechanisms through which GA may affect boundary formation, directly or indirectly, are currently unknown. *AtGA3ox1* expression is reported beneath the floral meristem of very early flowers from floral stage 3 (Hu et al., 2008), by which time floral organ primordia are beginning to arise. More detailed information regarding the sites of GA signalling in developing flowers will be gained from future analysis of DELLA expression in these tissues.

7.4 STAMEN GROWTH AND DEVELOPMENT IS MODULATED BY A PATHWAY INDEPENDENT OF GA BIOSYNTHESIS

As discussed in section 7.2, a significant trend of increasing stamen length at flower opening with increasing inflorescence position was identified across positions 1-10 on the primary inflorescence, irrespective of genotype. This trend correlates with measurements of the probability of silique-set across this same range of flowering Importantly, this trend was not affected by GA treatment, although there was a uniform reduction in the probability of

successful silique-set across all inflorescence positions. Although not measured as rigorously, it was similarly observed that floral organ growth increased in later flowers of more severely GA-deficient mutants, including *ga20ox1 ga20ox2 ga20ox3-1*, *ga20ox1 ga20ox2 ga20ox3-3*, *ga20ox1 ga20ox2 ga20ox3-1 ga20ox4-2*, *ga20ox1 ga20ox2 ga20ox3-1 ga20ox5-2* and *ga1-3*, in the absence of chemical GA treatment, as well as in plants over-expressing *AtGA20ox1* and *-5* (see section 4.2.3). This phenotypic recovery has not been previously reported for *ga1-3*. These results collectively suggest that the changes in floral length observed are unlikely to be dependent on changes in GA biosynthesis. Alternatively, these phenotypic changes could be effected by modulating GA signal transduction in the absence of GA. There is evidence that both the GID1 and DELLA components are under homeostatic regulation, with GID1 expression down-regulated (Griffiths et al., 2006) and DELLA expression up-regulated (Ueguchi-Tanaka et al., 2008) by GA signalling. In consequence, a reduction in GA signalling might be expected to both increase sensitivity to GA and reduce the abundance of DELLA repressing downstream GA responses. However, similar changes in stamen length were also observed in *rga-28 gai-td1 gid1a gid1b gid1c* mutant inflorescences (data not shown), where modulation of GA signal perception should be impossible. Further indirect evidence of changing stamen length in GA-insensitive backgrounds comes from the *rga-28 gid1a gid1b gid1c* quadruple mutant, in which seed set is eventually restored despite evidence that filament elongation is repressed by RGL2 in earlier flowers of this mutant (see section 7.2).

Importantly, tricellular pollen was found in phenotypically-rescued flowers from severely GA-deficient genotypes, suggesting that the GA-dependent arrest of pollen development is also overcome through this mechanism. This conclusion is reinforced by the observation that seed set eventually recovers in the *ga20ox1 ga20ox2 ga20ox3-1* background without GA treatment. These seed proved to be self-fertilised, indicating that pollen viability and development in *ga20ox1 ga20ox2 ga20ox3-1* flowers had recovered. Pollen development is reported to arrest at the uninucleate state in both *ga1-1* (Goto & Pharis, 1999) and *ga1-3* (Cheng et al., 2004). Where this phenotype has been assessed quantitatively in *ga1-3*, a minority of pollen within *ga1-3* anthers (6%) was found to develop further even in the absence

of GA treatment. Depending on the stage of flowering where pollen development was analysed in these studies (which is not specified), these results do not necessarily conflict with the developmental rescue observed during this project. The extent to which the subsequent filament elongation phenotypes of GA-deficient and insensitive mutants is due to direct repression of elongation or to indirect inhibition from the anther developmental block is currently unknown. Further investigation into this mechanism would be very instructive, as it could identify components downstream of GA signalling that are involved in anther developmental arrest, and thus increase our understanding of the functions of GA signalling at this stage of anther development.

Assuming that these changes all relate to the same underlying process, these results suggest that another pathway, independent of GA biosynthesis or perception, causes GA-dependent aspects of stamen development to recover in later flowers even in the absence of a GA signal. The evidence across inflorescence positions 1-10 suggests that these phenotypic changes are gradual rather than a sudden increase in elongation occurring in later flowers, which supports the hypothesis that the changes are a result of gradual modulation of existing processes rather than the switching on of an entirely separate pathway. With evidence mounting against the likely explanations that the changes in stamen development seen in these mutants are related to GA biosynthesis or signalling, another possibility is that the phenotypic changes occur due to modulation of downstream GA signalling targets in a GA-independent manner. As mentioned in section 7.2, as a result of GA-dependent up-regulation of the JA biosynthesis gene *DAD1*, JA signalling transmits a subset of the GA signalling responses (Cheng et al., 2009), and a physical interaction has also been demonstrated between DELLA proteins and the equivalent component in JA signal transduction, the JAZ proteins (Hou et al., 2010). Although chemical treatment with JA was shown to be insufficient to rescue growth of GA-deficient stamens (Cheng et al., 2009), the phase of flowering tested was not specified. Small changes to JA signalling in later flowers might well contribute to the phenotypic rescue observed. A relatively simple genetic method of testing this hypothesis would be to create combinatorial *Arabidopsis* mutants insensitive to, or deficient in the biosynthesis of, both GA and JA. Another hormone possibly involved in this process is auxin, which also has functions

across stamen development (see section 1.5.4). At present the relationship between these three signalling mechanisms is not well understood, and whilst links between auxin and JA signalling have been suggested through ARF proteins (Nagpal et al., 2005), the relationship between GA and auxin in stamen development remains unclear. The similarities between the floral phenotypes of *ar6 arf8* (Nagpal et al., 2005) and early *ga20ox1 ga20ox2* flowers (Rieu et al., 2008) is suggestive, but a direct comparison has yet to be made. Future investigation into the interactions between these three hormones to collectively regulate stamen development should be a research priority.

CHAPTER 8: REFERENCES

Aach, H., Bose, G. and Graebe, J.E. (1995). *Ent*-kaurene biosynthesis in a cell-free system from wheat (*Triticum aestivum* L.) seedlings and the localisation of ent-kaurene synthetase in plastids of three species. Planta **197**, 333-342

Aarts, M.G.M., Hodge, R., Kalantidis, K., Florack, D., Wilson, Z.A., Mulligan, B.J., Stiekema, W.J., Scott, R. and Pereira, A. (1997). The *Arabidopsis MALE STERILITY 2* protein shares similarity with reductases in elongation/condensation complexes. Plant J. **12**, 615-623

Achard, P., Baghour, M., Chapple, A., Hedden, P., Van Der Straeten, D., Genschik, P., Moritz, T. and Harberd, N. (2007). The plant stress hormone ethylene controls floral transition via DELLA-dependent regulation of floral meristem-identity genes. PNAS **104**, 6484-6489

Achard, P., Cheng, H., De Grauwe, L., Decat, J., Schoutteten, H., Moritz, T., Van Der Straeten, D., Peng, J. and Harberd, N.P. (2006). Integration of plant responses to environmentally activated phytohormonal signals. Science **311**, 91-94

Achard, P., Herr, A., Baulcombe, D. and Harberd, N.P. (2004). Modulation of floral development by a gibberellin-regulated microRNA. Dev. **131**, 3357-3365

Achard, P., Vriezen, W.H., Van Der Straeten, D. and Harberd, N.P. (2003). Ethylene regulates *Arabidopsis* development via the modulation of DELLA protein growth repressor function. Plant Cell **15**, 2816-2825

Aida, M., Ishida, T. and Tasaka, M. (1999). Shoot apical meristem and cotyledon formation during *Arabidopsis* embryogenesis: interaction among the *CUP-SHAPED COTYLEDON* and *SHOOT MERISTEMLESS* genes. Dev. **126**, 1563-1570

Aida, M. and Tasaka, M. (2006). Morphogenesis and patterning at the organ boundaries in the higher plant shoot apex. Plant Mol. Biol. **60**, 915-928

Airoldi, C. (2010). Determination of sexual organ development. Sex. Plant Repro. **23**, 53-62

Ait-Ali, T., Frances, S., Weller, J.L., Reid, J.B., Kendrick, R.E. and Kamiya, Y. (1999). Regulation of gibberellin 20-oxidase and gibberellin 3β-hydroxylase transcript accumulation during de-etiolation of pea seedlings. Plant Physiol. **121**, 783-791

Alexander, M.P. (1969). Differential staining of aborted and non-aborted pollen. Stain Technology **44**, 117-122

Allen, R.S., Li, J.Y., Stahle, M.I., Dubroue, A., Gubler, F. and Millar, A.A. (2007). Genetic analysis reveals functional redundancy and the major target genes of the *Arabidopsis* miR159 family. PNAS **104**, 16371-16376

Alonso, J.M., Stepanova, A.N., Leisse, T.J., Kim, C.J., Chen, H., Shinn, P. and Stevenson, D.K. (2003). Genome-wide insertional mutagenesis of *Arabidopsis thaliana*. Science **301**, 653-657

Ariizumi, T., Amagai, M., Shibata, D., Hatakeyama, K., Watanabe, M. and Toriyama, K. (2002). Comparative study of promoter activity of three anther-specific genes encoding lipid transfer protein, xyloglucan endotransglucosylase/hydrolase and polygalacturonase in transgenic *Arabidopsis thaliana*. Plant Cell Rep. **21**, 90-96

Ariizumi, T., Lawrence, P.K. and Steber, C.M. (2011). The role of two F-box proteins, SLEEPY1 and SNEEZY, in *Arabidopsis* gibberellin signaling. Plant Physiol. **155**, 765-775

Ariizumi, T., Murase, K., Sun, T.P. and Steber, C.M. (2008). Proteolysis-independent downregulation of DELLA repression in *Arabidopsis* by the gibberellin receptor GIBBERELLIN INSENSITIVE DWARF1. Plant Cell **20**, 2447-2459

Aya, K., Ueguchi-Tanaka, M., Kondo, M., Hamada, K., Yano, K., Nishimura, M. and Matsuoka, M. (2009). Gibberellin modulates anther development in rice via the transcriptional regulation of GAMYB. Plant Cell **21**, 1453-1472

Bartrina, I., Otto, E., Strnad, M., Werner, T. and Schmülling, T. (2011). Cytokinin regulates the activity of reproductive meristems, floral organ size, ovule formation, and thus seed yield in *Arabidopsis thaliana*. Plant Cell **23**, 69-80

Bassel, G.W., Mullen, R.T. and Bewley, J.D. (2008). *procera* is a putative DELLA mutant in tomato (*Solanum lycopersicum*): effects on the seed and vegetative plant. J. Exp. Bot. **59**, 585-593

Bensen, R.J., Johal, G.S., Crane, V.C., Tossberg, J.T., Schnable, P.S., Meeley, R.B. and Briggs, S.P. (1995). Cloning and characterization of the maize *An1* gene. Plant Cell **7**, 75-84

Blázquez, M.A., Green, R., Nilsson, O., Sussman, M.R. and Weigel, D. (1998). Gibberellins promote flowering of *Arabidopsis* by activating the *LEAFY* promoter. Plant Cell **10**, 791-800

Bohlmann, J., Meyer-Gauen, G. and Croteau, R. (1998). Plant terpenoid synthases: Molecular biology and phylogenetic analysis. PNAS **95**, 4126-4133

Boss, P.K., Bastow, R.M, Mylne, J.S. and Dean, C. (2004). Multiple pathways in the decision to flower: Enabling, promoting and resetting. Plant Cell **16**, S18-S31

Bowman, J.L. (1994). *Arabidopsis*: An atlas of morphology and development. (Springer-Verlag).

Bowman, J.L., Drews, G.N. and Meyerowitz, E.M. (1991). Expression of the *Arabidopsis* floral homeotic gene *AGAMOUS* is restricted to specific cell types late in flower development. Plant Cell **3**, 749-758

Cao, D.N., Cheng, H., Wu, W., Soo, H.M. and Peng, J.R. (2006). Gibberellin mobilizes distinct DELLA-dependent transcriptomes to regulate seed germination and floral development in *Arabidopsis*. Plant Physiol. **142**, 509-525

Canales, C., Bhatt, A.M., Scott, R. and Dickinson, H. (2002). *EXS*, a putative LRR receptor kinase, regulates male germline cell number and tapetal identity and promotes seed development in *Arabidopsis*. Curr. Biol. **12**, 1718-1727

Carrera, E., Jackson, S.D. and Prat, S. (1999). Feedback control and diurnal regulation of gibberellin 20-oxidase transcript levels in potato. Plant Physiol. **119**, 765-776

Causton, D.R. and Venus, J.C. (1981). The biometry of plant growth. Edward Arnold (Publishers) Ltd.

Cecchetti, V., Altamura, M.M., Falasca, G., Costantino, O. and Cardarelli, M. (2008). Auxin regulates *Arabidopsis* anther dehiscence, pollen maturation and filament elongation. Plant Cell **20**, 1760-1774

Chandler, P.M., Harding, C.A., Ashton, A.R., Mulcair, M.D., Dixon, N.E. and Mander, L.N. (2008). Characterization of gibberellin receptor mutants of barley (*Hordeum vulgare* L). Mol. Plant **1**, 285-294

Chen, H., Banerjee, A.K. and Hannapel, D.J. (2004). The tandem complex of BEL and KNOX partners is required for transcriptional repression of *ga20ox1*. Plant J. **28**, 276-284

Cheng, H., Qin, L.J., Lee, S.C., Fu, X.D., Richards, D.E., Cao, D.N., Luo, D., Harberd, N.P. and Peng, J.R. (2004). Gibberellin regulates *Arabidopsis* floral development via suppression of DELLA protein function. Dev. **131**, 1055-1064

Cheng, H., Song, S.S., Xioa, L.T., Soo, H.M., Cheng, Z.W., Xie, D.X. and Peng, J.R. (2009). Gibberellin acts through jasmonate to control the expression of *MYB21*, *MYB24* and *MYB57* to promote stamen filament growth in *Arabidopsis*. PLoS Genet. **5**, 1-13

Cheng, Y.F., Dai, X.H. and Zhao, Y.D. (2006). Auxin biosynthesis by the YUCCA flavin monooxygenases controls the formation of floral organs and vascular tissues in *Arabidopsis*. Genes Dev. **20**, 1790-1799

Chhun, T., Aya, K., Asano, K., Yamamoto, E., Morinaka, Y., Watanabe, M., Kitano, H., Ashikira, M., Matsuoka, M. and Ueguchi-Tanaka, M. (2007). Gibberellin regulates pollen viability and pollen tube growth in rice. Plant Cell **19**, 3876-3888

Colbert, T., Till, B.J., Tompa, R., Reynolds, S., Steine, M.N., Yeung, A.T., McCallum, C.M., Comai, L. and Henikoff, S. (2001). High-throughput screening for induced point mutations. Plant Physiol. **126**, 480-484

Coles, J.P., Phillips, A.L., Croker, S.J., Garcia-Lepe, R., Lewis, M.J. and Hedden, P. (1999). Modification of gibberellin production and plant development in *Arabidopsis* by sense and antisense expression of gibberellin 20-oxidase genes. Plant J. **17**, 547-556

Cox, C.M. and Swain, S.M. (2006). Localised and non-localised promotion of fruit development by seeds in *Arabidopsis*. Funct. Plant Biol. **33**, 1-8

Czechowski, T., Stitt, M., Altmann, T., Udvardi, M.K. and Scheible, W.-R. (2005). Genome-wide identification and testing of superior reference genes for transcript normalization in *Arabidopsis*. Plant Physiol. **139**, 5-17

Davidson, S.E., Elliott, R.C., Helliwell, C.A., Poole, A.T. and Reid, J.B. (2003). The pea gene *NA* encodes *ent*-kaurenoic acid oxidase. Plant Physiol. **131**, 335-344

de Lucas, M., Daviere, J.M., Rodriguez-Falcon, M., Pontin, M., Iglesias-Pedraz, J.M., Lorrain, S., Fankhauser, C., Blázquez, M.A., Titarenko, E. and Prat, S. (2008). A molecular framework for light and gibberellin control of cell elongation. Nature **451**, 480-484

Dill, A., Jung, H.S. and Sun, T.P. (2001). The DELLA motif is essential for gibberellin-induced degradation of RGA. PNAS **98**, 14162-14167

Dill, A. and Sun, T.P. (2001). Synergistic derepression of gibberellin signaling by removing RGA and GAI function in *Arabidopsis thaliana*. Genetics **159**, 777-785

Dill, A., Thomas, S.G., Hu, J.H., Steber, C.M. and Sun, T.P. (2004). The *Arabidopsis* F-box protein SLEEPY1 targets gibberellin signaling repressors for gibberellin-induced degradation. Plant Cell **16**, 1392-1405

Eady, C., Lindsey, K. and Twell, D. (1994). Differential activation and conserved vegetative cell-specific activity of a late pollen promoter in species with bicellular and tricellular pollen. Plant J. **5**, 543-550

Endrizzi, K., Moussian, B., Haecker, A., Levin, J.Z. and Laux, T. (1996). The *SHOOT MERISTEMLESS* gene is required for maintenance of undifferentiated cells in *Arabidopsis* shoot and floral meristems and acts at a different regulatory level than the meristem genes *WUSCHEL* and *ZWILLE*. Plant J. **10**, 967-979

Ergün, N., Topcuoğlu, Ş.F. and Yildiz, A. (2002). Auxin (indole-3-acetic acid), gibberellic acid (GA_3), abscisic acid (ABA) and cytokinin (zeatin) production by some species of mosses and lichens. Turk. J. Bot. **26**, 13-18

Eriksson, M.E., Israelsson, M., Olsson, O. and Moritz, T. (2000). Increased gibberellin biosynthesis in transgenic trees promotes growth, biomass productions and xylem fiber length. Nat. Biotechnol. **18**, 785-788

Eriksson, S., Bohlenius, H., Moritz, T and Nilsson, O. (2006). GA_4 is the active gibberellin in the regulation of *LEAFY* transcription and *Arabidopsis* floral transition. Plant Cell **18**, 2172-2181

Feng, S.H., Martinez, C., Gusmaroli, G., Wang, Y., Zhou, J.L., Wang, F., Chen, L.Y., Yu, L., Iglesias-Pedraz, J.M., Kircher, S., Schafer, E., Fu, X.D., Fan, L.M. and Deng, X.W. (2008). Coordinated regulation of *Arabidopsis thaliana* development by light and gibberellins. Nature **451**, 475-479

Feys, B.J.F., Benedetti, C.E., Penfold, C.N. and Turner, J.G. (1994). *Arabidopsis* mutants selected for resistant to the phytotoxin coronatine are male sterile, insensitive to methyl jasmonate, and resistant to a bacterial pathogen. Plant Cell **6**, 751-759

Fleck, B. and Harberd, N.P. (2002). Evidence that the *Arabidopsis* nuclear gibberellin signalling protein GAI is not destabilised by gibberellin. Plant J., **32**, 935-947

Fleet, C.M. and Sun, T.P. (2005). A DELLAcate balance: the role of gibberellin in plant morphogenesis. Curr. Op. Plant Biol. **8**, 77-85

Footitt, S., Dietrich, D., Fait, A., Fernie, A.R., Holdsworth, M.J., Baker, A. and Theodoulou, F.L. (2007). The COMATOSE ATP-binding cassette transporter is required for full fertility in *Arabidopsis*. Plant Physiol. **144**, 1467-1480

Fridborg, I., Kuusk, S., Robertson, M. and Sundberg, E. (2001). The *Arabidopsis* protein SHI represses gibberellin responses in *Arabidopsis* and barley. Plant Physiol. **127**, 937-948

Frisse, A., Pimenta, M.J. and Lange, T. (2003). Expression studies of gibberellin oxidases in developing pumpkin seeds. Plant Physiol. **131**, 1220-1227

Fu, X.D. and Harberd, N.P. (2003). Auxin promotes *Arabidopsis* root growth by modulating gibberellin response. Nature **421**, 740-743

Fu, X.D., Richards, D.E., Fleck, B., Xie, D., Burton, N and Harberd, N.P. (2004). The *Arabidopsis* mutant *sleepy1*$^{gar\text{-}2}$ protein promotes plant growth by increasing the affinity of the SCF^{SLY1} E3 ubiquitin ligase for DELLA protein substrates. Plant Cell **16**, 1406-1418

Furutani, M., Vernoux, T., Traas, J., Kato, T., Tasaka, M. and Aida, M. (2004). *PIN-FORMED1* and *PINOID* regulate boundary formation and cotyledon development in *Arabidopsis* embryogenesis. Dev. **131**, 5021-5030

Gallego-Bartolomé, J., Minguet, E.G., Marin, J.A., Prat, S., Blázquez, M.A. and Alabadi, D. (2010). Transcriptional diversification and functional conservation between DELLA proteins in *Arabidopsis*. Mol. Biol. Evol. **27**, 1247-1256

Gilroy, S. and Jones, R.L. (1994). Perception of gibberellin and abscisic acid at the external face of the plasma membrane of barley (*Hordeum vulgare* L) aleurone protoplasts. Plant Physiol. **104**, 1185-1192.

Gleave, A.P. (1992). A versatile binary vector system with T-DNA organisational structure conducive to efficient integration of cloned DNA into the plant genome. Plant Mol. Biol. **20**, 1203-1207

Gocal, G.F.W., Sheldon, C.C., Gubler, F., Moritz, T., Bagnall, D.J., MacMillan, C.P., Li, S.F., Parish, R.W., Dennis, E.S., Weigel, D. and King, R.W. (2001). *GAMYB-like* genes, flowering, and gibberellin signaling in *Arabidopsis*. Plant Physiol. **127**, 1682-1693

Gomez, K.A. and Gomez, A.A. (1984). Statistical procedures for agricultural research. New York: John Wiley & Sons.

Gómez-Mena, C., de Folter, S., Costa, M.M.R., Angenent, G.C. and Sablowski, R. (2005). Transcriptional program controlled by the floral homeotic gene *AGAMOUS* during early organogenesis. Dev. **132**, 429-438

Gomi, K., Sasaki, A., Itoh, H., Ueguchi-Tanaka, M., Ashikira, M., Kitano, H. and Matsuoka, M. (2004). GID2, an F-box subunit of the SCF E3 complex, specifically interacts with phosphorylated SLR1 protein and regulates the gibberellin-dependent degradation of SLR1 in rice. Plant J. **37**,626-634

Goto, N. and Pharis, R.P. (1999). Role of gibberellins in the development of floral organs of the gibberellin-deficient mutant, *ga1-1*, of *Arabidopsis thaliana*. Can. J. Bot. **77**, 944-954

Graebe, J.E. and Ropers, H.J. (1978). Gibberellins. *In* 'Phytohormones and related compounds- a comprehensive Treatise, Vol. I. The biochemistry of phytohormones and related compounds'. Eds. Letham, D.S., Goodwin, P.B. and Higgins T.J.V. Elsevier/North-Holland Biomedical Press, pp 107-204

Griffiths, J., Murase, K., Rieu, I., Zentella, R., Zhang, Z.L., Powers, S.J., Gong, F., Phillips, A.L., Hedden, P., Sun, T.P. and Thomas, S.G. (2006). Genetic characterisation and functional analysis of the GID1 gibberellin receptors in *Arabidopsis*. Plant Cell **18**, 3399-3414

Gubler, F., Chandler, P.M., White, R.G., Llewellyn, D.J. and Jacobsen, J.V. (2002). Gibberellin signaling in barley aleurone cells. Control of *SLN1* and *GAMYB* expression. Plant Physiol. **129**, 191-200

Gubler, F., Kalla, R., Roberts, J.K. and Jacobsen, J.V. (1995). Gibberellin-regulated expression of a *myb* gene in barley aleurone cells: evidence for MYB transactivation of a high-pL α-amylase gene promoter. Plant Cell **7**, 1879-1891

Harberd, N.P., Belfield, E. and Yasumura, Y. (2009). The angiosperm gibberellin-GID1-DELLA growth regulatory mechanism: How an "inhibitor of an inhibitor" enables flexible response to fluctuating environments. Plant Cell **21**, 1328-1339

Hartlet, J.L., Temple, G.F. and Brasch, M.A. (2000). DNA cloning using *in vitro* site-specific recombination. Genome Research **10**, 1788-1795

Hay, A., Kaur, H., Phillips, A.L., Hedden, P., Hake, S. and Tsiantis, M. (2002). The gibberellin pathway mediates KNOTTED1-type homeobox function in plants with different body plans. Curr. Biol. **12**, 1557-1565

Haywood, V., Yu, T.S., Huang, N.C. and Lucas, W.J. (2005). Phloem long-distance trafficking of *GIBBERELLIC ACID-INSENSTIVE* RNA regulates leaf development. Plant J. **42**, 49-68

Hedden, P. (1997). The oxidases of gibberellin biosynthesis: Their function and mechanism. Physiol. Plant. **101**, 709-719

Hedden, P. and Phillips, A.L. (2000). Gibberellin metabolism: new insights revealed by the genes. Trends Plant Sci. **5**, 523-530

Hedden, P., Phillips, A.L., Rojas, M.C., Carrera, E. and Tudzynski, B. (2002). Gibberellin biosynthesis in plants and fungi: a case of convergent evolution? J. Plant Growth Regul. **20**, 319-331

Helliwell, C.A., Sheldon, C.C., Olive, M.R., Walker, A.R., Zeevaart, J.A.D., Peacock, W.J. and Dennis, E.S. (1998). Cloning of the *Arabidopsis ent*-kaurene oxidase gene *GA3*. PNAS. **95**, 9019-9024

Helliwell, C.A., Sullivan, J.A., Mould, R.M., Gray, J.C., Peacock, W.J. and Dennis, E.S. (2001). A plastid envelope location of *Arabidopsis ent*-kaurene oxidase links the plastid and endoplasmic reticulum steps of the gibberellin biosynthesis pathway. Plant J. **28**, 201-208

Hepler, P.K., Vidali, L. and Cheung, A.Y. (2001). Polarized cell growth in higher plants. Ann. Rev. Cell Dev. Biol. **17**, 159-187

Hernández-Pinzón, I., Ross, J.H.E., Barnes, K.A., Damant, A.P. and Murphy, D.J. (1999). Composition and role of tapetal lipid bodies in the biogenesis of the pollen coat of *Brassica napus*. Planta **208**, 588-598.

Hirano, K., Asano, K., Hiroyuki, T., Kawamura, M., Mori, H., Kitano, H., Ueguchi-Tanaka, M. and Matsuoka, M. (2010). Characterization of the molecular mechanism underlying gibberellin perception complex formation in rice. Plant Cell **22**, 2680-2696

Hirano, K., Aya, K., Hobo, T., Sakakibara, H., Kojima, M., Shim, R.A., Hasegawa, Y., Ueguchi-Tanaka, M. and Matsuoka, M. (2008). Comprehensive transcriptome analysis of phytohormone biosynthesis and signaling genes in microspore/pollen and tapetum of rice. Plant Cell Physiol. **49**, 1429-1450

Hird, D.L., Worrall, D., Hodge, R., Smarrtt, S., Paul, W. and Scott, R. (1993). The anther-specific protein encoded by the *Brassica napus* and *Arabidopsis thaliana* A6 gene displays similarity to β-1,3- glucanases. Plant J. **4**, 1023-1033

Hisamatsu, T., King, R.W., Helliwell, C.A. and Koshioka, M. (2005). The involvement of gibberellin 20-oxidase genes in phytochrome-regulated petiole elongation of *Arabidopsis*. Plant Physiol. **138**, 1106-1116

Hisamatsu, T. and King, R.W. (2008). The nature of floral signals in *Arabidopsis*. II. Roles for *FLOWERING LOCUS T* (*FT*) and gibberellin. J. Exp. Bot. **59**, 3821-3829

Hoad, G. (1983). Gibberellin bioassays and structure-activity relationships. *In* 'The Biochemistry and Physiology of Gibberellins Volume 2', Ed. A. Crozier (Praeger), pp. 57-94

Honys, D. and Twell, D. (2004). Transcriptome analysis of haploid male gametophyte development in *Arabidopsis*. Gen. Biol. **5**, R85

Hooley, R., Beale, M.H. and Smith, S.J. (1991). Gibberellin perception at the plasma membrane of *Avena fatua* aleurone protoplasts. Planta **183**, 274-280

Hord, C.L.H., Sun, Y.J., Pillitteri, L.J., Torii, K.U., Wang, H., Zhang, S. and Ma, H. (2008). Regulation of *Arabidopsis* early anther development by the mitogen-activated protein kinases MPK3 and MPK6, and the ERECTA and related receptor-like kinases. Mol. Plant **1**, 645-658

Hou, X.L., Hu, W.W., Shen, L., Lee, L.Y.C., Tao, Z., Han, J.H. and Yu, H. (2008). Global identification of DELLA target genes during *Arabidopsis* flower development. Plant Physiol. **147**, 1126-1142

Hou, X.L., Lee, L.Y.C., Xia, K.F., Yan, Y.Y. and Yu, H. (2010). DELLAs modulate jasmonate signalling via competitive binding to JAZs. Dev. Cell **19**, 884-894

Hruz, T., Laule, O., Szabo, G., Wessendorp, F., Bleuler, S., Oertle, L., Widmayer, P., Gruissem, W. and Zimmermann, P. (2008). Genevestigator V3: A reference expression database for the meta-analysis of transcriptomes. Advances in Bioinformatics **2008**, Article ID 420747 (5 pages)

Hu, J.H., Mitchum, M.G., Barnaby, N., Ayele, B.T., Ogawa, M., Nam, E., Lai, W.C., Hanada, A., Alonso, J.M., Ecker, J.R., Swain, S.M., Yamaguchi, S., Kamiya, A. and Sun, T.P. (2008). Potential sites of bioactive gibberellin production during reproductive growth in *Arabidopsis*. Plant Cell **20**, 320-336

Huang, S.S., Raman, A.S., Ream, J.E., Fujiwara, H., Cerny, R.E. and Brown, S.M. (1998). Overexpression of 20-oxidase confers a gibberellin-overproduction phenotype in *Arabidopsis*. Plant Physiol. **118**, 773-781

Huysmans, S., El-Ghazaly, G. and Smets, E. (1998). Orbicules in angiosperms: morphology, function, distribution and relation with tapetum types. Bot. Rev. **64**, 240-272

Ikeda, A., Ueguchi-Tanaka, M., Sonoda, Y., Kitano, H., Koshioka, M., Futsuhara, Y., Matsuoka, M. and Yamaguchi, J. (2001). *slender rice 1*, a constitutive gibberellin response mutant, is caused by a null mutation of the *SLR1* gene, an ortholog of the height-regulating gene *GAI*/*RGA*/*RHT*/*D8*. Plant Cell **13**, 999-1010

Ingram, T.J. and Reid, J.B. (1987). Internode length in *Pisum*- Gene *na* may block gibberellin synthesis between *ent*-7-alpha-hydroxykaurenoic acid and gibberellin A_{12}-aldehyde. Plant Physiol. **83**, 1048-1053

Inoue, H., Nojima, H. and Okayama, H. (1990). High efficiency transformation of *Escherichia coli* with plasmids. Gene **96**, 23-28

Irish, V.F. (2010). The flowering of *Arabidopsis* flower development. Plant J. **61**, 1014-1028

Ishiguro, S., Kawai-Oda, A., Ueda, J., Nishida, I. and Okada, K. (2001). The *DEFECTIVE IN ANTHER DEHISCENCE1* gene encodes a novel phospholipase A1 catalysing the initial step of jasmonic acid biosynthesis, which synchronises pollen maturation, anther dehiscence, and flower opening in *Arabidopsis*. Plant Cell **13**, 2191-2209

Ishisa, S., Fukazawa, J., Yuasa, T. and Takahashi, Y. (2004). Involvement of 14-3-3 signaling protein binding in the functional regulation of the transcriptional activator REPRESSION OF SHOOT GROWTH by gibberellins. Plant Cell **16**, 2641-2651

Israelsson. M., Mellerowicz, E., Chono, M., Gullberg, J. and Moritz, T. (2004). Cloning and overproduction of gibberellin 3-oxidase in hybrid aspen trees. Effects on gibberellin homeostasis and development. Plant Physiol. **135**, 221-230

Ito, T. (2011). Coordination of flower development by homeotic master regulators. Curr. Op. Plant Biol. **14**, 53-59

Ito, T., Ng, K.H., Lim, T.S., Yu, H. and Meyerowitz, E.M. (2007). The homeotic protein AGAMOUS controls late stamen development by regulating a jasmonate biosynthetic gene in *Arabidopsis*. Plant Cell **19**, 3516-3529

Ito, T., Wellmer, F., Yu, H., Das, P., Ito, N., Alves-Ferreira, M., Reichmann, J.L. and Meyerowitz, E.M. (2004). The homeotic protein AGAMOUS controls microsporogenesis by regulation of SPOROCYTELESS. Nature **430**, 356-360

Itoh, H., Ueguchi-Tanaka, M., Kawaide, H., Chen, X.B., Kamiya, Y. and Matsuoka, M. (1999). The gene encoding tobacco gibberellin 3β-hydroxylase is expressed at the site of GA action during stem elongation and flower organ development. Plant J. **20**, 15-24

Iuchi, S., Suzuki, H., Yim, Y.C., Iuchi, A., Kuromori, T., Ueguchi-Tanaka, M., Asami, T., Yamaguchi, I., Matsuoka, M., Kobayashi, M. and Nakajima, M. (2007). Multiple loss-of-function of *Arabidopsis* gibberellin receptor AtGID1s completely shuts down a gibberellin signal. Plant J. **50**, 958-966

Izhaki, A., Borochov, A., Zamski, E. and Weiss, D. (2002). Gibberellin regulates post-microsporogenesis processes in petunia anthers. Physiol. Plant. **155**, 442-447

Jacobsen, S.E. and Olszewski, N.E. (1991). Characterization of the arrest in anther development associated with gibberellin deficiency of the *gib-1* mutant of tomato. Plant Physiol. **97**, 409-414

Jacobsen, S.E. and Olszewski, N.E. (1993). Mutations in the *SPINDLY* locus of *Arabidopsis* alter gibberellin signal transduction. Plant Cell **5**, 887-896

Jasinski, S., Piazza, P., Craft, J., Hay, A., Woolley, L., Rieu, I., Phillips, A.L., Hedden, P. and Tsiantis, M. (2005). KNOX action in *Arabidopsis* is mediated by coordinate regulation of cytokinin and gibberellin activities. Curr. Biol. **15**, 1560-1565

Jia, G.X., Liu, X.D., Owen, H.A. and Zhao, D.Z. (2008). Signaling of cell fate determination by the TPD1 small protein and EMS1 receptor kinase. PNAS **105**, 2220-2225

Josse, E.M., Gan, Y., Bou-Torrent, J., Stewart, K.L., Gilday, A.D., Jeffree, C.E., Vaistij, F.E., Martínez-García, J.F., Nagy, F., Graham, I.A. and Halliday, K.J. (2011). A DELLA in disguise: SPATULA restrains the growth of the developing *Arabidopsis* seedling. Plant Cell **23**, 1337-1351

Kamiya, Y. and Graebe, J.E. (1983). The biosynthesis of all major pea gibberellins in a cell-free system from *Pisum sativum*. Phytochemistry **22**, 681-689

Kaneko, M., Inukai, Y., Ueguchi-Tanaka, M., Itoh, H., Izawa, T., Kobayashi, Y., Hattori, T., Miyao, A., Hirochika, H., Ashikari, M. and Matsuoka, M. (2004). Loss-of-function mutations of the rice *GAMYB* gene impair α-amylase expression in aleurone and flower development. Plant Cell **16**, 33-44

Kaneko, M., Itoh, H., Inukai, Y., Sakamoto, T., Ueguchi-Tanaka, M., Ashikira, M. and Matsuoka, M. (2003). Where do gibberellin biosynthesis and gibberellin signaling occur in rice plants? Plant J. **35**, 104-115

Kato, J., Purves, W.K. and Phinney, B.O. (1962). Gibberellin-like substances in plants. Nature **196**, 687-688

Kawai, T., Tanaka, K., Niwa, Y., Watanabe, Y., Makamura, K., Kimura, T. and Ishiguro, S. (2007). Improved gateway binary vectors: High-performance vectors for creation of fusion constructs in transgenic analysis of plants. Biosci. Biotech. Biochem. **71**, 2095-2100

Kawanabe, T., Ariizumi, T., Kawai-Yamade, M., Uchimiya, H. and Toriyama, K. (2006). Abolition of the tapetum suicide program ruins microsporogenesis. Plant Cell Physiol. **47**, 784-787

Kilian, J., Whitehead, D., Horak, J., Wanke, D., Weinl, D., Weinl., S., Batistic, O., D'Angelo, C., Bornberg-Bauer, E., Kudla, J. and Harter, K. (2007). The AtGenExpress global stress expression data set: protocols, evaluation and model data analysis of UV-B light, drought and cold stress responses. Plant J. **50**, 347-363

King, K.E., Moritz, T. and Harberd, N.P. (2001). Gibberellins are not required for normal stem growth in *Arabidopsis thaliana* in the absence of GAI and RGA. Genetics **159**, 767-776

King, R.W., Mander, L.N., Asp, T., MacMillan, C.P., Blundell, C.A. and Evans, L.T. (2008). Selective deactivation of gibberellins below the shoot apex is critical to flowering but not to stem elongation of *Lolium*. Mol. Plant **1**, 295-307

Kobayashi, M., Yamaguchi, I., Murofushi, N., Ota, Y. and Takahashi, N. (1984). Endogenous gibberellins in immature seeds and flowering ears of rice. Agric. Biol. Chem. **48**, 2725-2729

Kobayashi, M., Yamaguchi, I., Murofushi, N., Ota, Y. and Takahashi, N. (1988). Fluctuation and localisation of endogenous gibberellins in rice. Agric. Biol. Chem. **52**, 1189-1194

Koornneef, M. and Van der Veen, J.H. (1980). Induction and analysis of gibberellin sensitive mutants in *Arabidopsis thaliana* (L) heyhn. Theor. Appl. Genet. **58**, 257-263

Kurogochi, S., Murofushi, N., Ota, Y. and Takahashi, N. (1979). Identification of gibberellins in the rice plant and quantitative changes of gibberellin-A19 throughout its life-cycle. Planta **146**, 185-191

Lamb, R.S., Hill, T.A., Tan, Q.K.G. and Irish, V.F. (2002). Regulation of *APETALA3* floral homeotic gene expression by meristem identity genes. Dev. **129**, 2079-2086

Lanahan, M.B. and Ho, T.H.D. (1988). *Slender* barley- a constitutive gibberellin response mutant. Planta **175**, 107-114

Landy, A. (1989). Dynamic, structural and regulatory aspects of lambda site-specific recombination. Ann. Rev. Biochem. **58**, 913-949

Lange, T. (1994). Purification and partial amino-acid-sequence of gibberellin 20-oxidase from *Cucurbita maxima* L. endosperm. Planta **195**, 108-115

Lange, T., Hedden, P., and Graebe, J.E. (1994). Expression cloning of a gibberellin 20-oxidase, a multifunctional enzyme involved in gibberellin biosynthesis. PNAS **91**, 8552-8556

Lange, T., Kappler, J., Fischer, A. Frisse, A., Padeffke, T., Schmidtke, S. and Pimenta Lange, M.J. (2005). Gibberellin biosynthesis in developing pumpkin seedlings. Plant Physiol. **139**, 213-223

Lange T., Robatzek, S. and Frisse, A. (1997). Cloning and expression of gibberellin 2β,3β-hydroxylase cDNA from pumpkin endosperm. Plant Cell **9**, 1459-1467

Lee, D.J. and Zeevaart, J.A.D. (2002). Differential regulation of RNA levels of gibberellin dioxygenases by photoperiod in spinach. Plant Physiol. **130**, 2085-2094

Lee, D.J. and Zeevaart, J.A.D. (2005). Molecular cloning on *GA 2-oxidase 3* from spinach and its ectopic expression in *Nicotiana sylvestris*. Plant Physiol. **138**, 243-254

Lee, J., Oh, M., Park, H. and Lee, I. (2008). SOC1 translocated to the nucleus by interaction with ALG24 directly regulates *LEAFY*. Plant J. **55**, 832-843

Lee, S.C., Cheng, H., King, K.E., Wang, W.F., He, Y., Hussain, A., Lo, J., Harberd, N.P. and Peng, J.R. (2002). Gibberellin regulates *Arabidopsis* seed germination via *RGL2*, a *GAI*/*RGA*-like gene whose expression is up-regulated following imbibition. Genes Dev. **16**, 646-658

Levin, J.Z., Fletcher, J.C., Chen, X.M. and Meyerowitz, E.M. (1998). A genetic screen for modifiers of *UFO* meristem activity identifies three novel *FUSED FLORAL ORGANS* genes required for early flower development in *Arabidopsis*. Genetics **149**, 579-595

Levin, J.Z. and Meyerowitz, E.M. (1995). *UFO*: an *Arabidopsis* gene involved in both floral meristem and floral organ development. Plant Cell **7**, 529-548

Li, N., Zhang, D.S., Liu, H.S., Yin, C.S., Li, X.X., Liang, W.Q., Yuan, Z, Xu, B., Chu, H.W., Wang, J., Wen, T.Q., Huang, H., Luo, D., Ma, H. and Zhang, D.B. (2006). The rice *TAPETUM DEGENERATION RETARDATION* gene is required for tapetum degradation and anther development. Plant Cell **18**, 2999-3014

Lo, S.F., Yang, S.Y., Chen, K.T., Hsing, Y.L., Zeevaart, J.A.D., Chen, L.J. and Yu, S.M. (2008). A novel class of gibberellin 2-oxidases control semidwarfism, tillering, and root development in rice. Plant Cell **20**, 2603-2618

Lohmann, J.U., Hong, R.L., Hobe, M., Busch, M.A., Parcy, F., Rüdiger, S. and Weigel, D. (2001). A molecular link between stem cell regulation and floral patterning in *Arabidopsis*. Cell **105**, 793-803

MacMillan, J. (1997). Biosynthesis of the gibberellin plant hormones. Nat. Prod. Rep. **14**, 221-244

MacMillan, J. (2001). Occurrence of gibberellins in vascular plants, fungi and bacteria. J. Plant Growth Regul. **20**, 387-442

MacMillan, J. and Takahashi, N. (1968). Proposed procedure for the allocation of trivial names to the gibberellins. Nature **217**, 170-171

Mandoakar, A. and Browse, J. (2009). MYB108 acts together with MYB24 to regulate jasmonate-mediated stamen maturation in *Arabidopsis*. Plant Physiol. **149**, 851-862

Mandoakar, A., Thines, B., Shin, B., Lange, B.M., Choi, G., Koo, Y.J., Yoo, Y.J., Choi, Y.D., Choi, G. and Browse, J. (2006). Transcriptional regulators of stamen development in *Arabidopsis* identified by transcriptional profiling. Plant J. **46**, 984-1008

Mariani, C., Beuckeleer, M.D., Truettner, J., Leemans, J. and Goldberg, R.B. (1990). Introduction of male sterility in plants by a chimaeric ribonuclease gene. Nature **347**, 737-741

Martienssen, R.A. (1998). Functional genomics: Probing plant gene function and expression with transposons. PNAS **95**, 2021-2026

Martin, D.N., Proebsting, W.M., Parks, T.D., Dougherty, W.G., Lange, T., Lewis, M.J., Gaskin, P. and Hedden, P. (1996). Feed-back regulation of gibberellin biosynthesis and gene expression in *Pisum sativum* L. Planta **200**, 159-166

Matsushita, A., Furumoto, T., Ishida, S. and Takahashi, Y. (2007). AGF1, an AT-hook protein, is necessary for the negative feedback of *AtGA3ox1* encoding GA 3-oxidase. Plant Physiol. **143**, 1152-1162

McGinnis, K.M., Thomas, S.G., Soule, J.D., Strader, L.C., Zale, J.M., Sun, T.P. and Steber, C.M. (2003). The *Arabidopsis SLEEPY1* gene encodes a putative F-box subunit of an SCF E3 ubiquitin ligase. Plant Cell **15**, 1120-1130

Michaels, S.D. and Amasino, R.M. (1999). The gibberellic acid biosynthesis mutant *ga1-3* of *Arabidopsis thaliana* is responsive to vernalization. Dev. Genet. **25**, 194-198

Millar, A.A. and Gubler, F. (2005). The *Arabidopsis* GAMYB-like genes, *MYB33* and *MYB65*, are microRNA-regulated genes that redundantly facilitate anther development. Plant Cell **17**, 705-721

Mitchum, M.G., Yamaguchi, S., Hanada, A., Kuwahara, A., Yoshioka, Y., Kato, T., Tabata, S., Kamiya, Y. and Sun, T.P. (2006). Distinct and overlapping roles of two gibberellin-3-oxidases in *Arabidopsis* development. Plant Cell **45**, 804-818

Moon, J., Suh, S.S., Lee, H., Choi, K.R., Hong, C.B., Paek, N.C., Kim, S.G. and Lee, I. (2003). The *SOC1* MADS-box gene integrates vernalization and gibberellin signals for flowering in *Arabidopsis*. Plant J. **35**, 613-623

Murase, K., Hirano, Y., Sun, T.P. and Hakoshima, T. (2008). Gibberellin-induced DELLA recognition by the gibberellin receptor GID1. Nature **456**, 459-463

Murray, F., Kalla, R., Jacobsen, J. and Gubler, F. (2003). A role for HvGAMYB in anther development. Plant J. **33**, 481-491

Mutasa-Göttgens, E. and Hedden, P. (2009). Gibberellin as a factor in floral regulatory networks. J. Exp. Bot. **60**, 1979-1989

Mutasa- Göttgens, E., Qi, A., Matthews, A., Thomas, S.G., Phillips, A.L. and Hedden, P. (2008). Modification of gibberellin signalling (metabolism and signal transduction) in sugar beet: analysis of potential targets for crop improvement. Transgenic Res. **18**, 301-308

Nagpal, P., Ellis, C.M., Weber, H., Ploense, S.E., Barkawi, L.S., Guilfoyle, T.J., Hagen, G., Alonso, J.M., Cohen, J.D., Farmer, E.E., Ecker, J.R. and Reed, J.W. (2005). Auxin response factors ARF6 and ARF8 promote jasmonic acid production and flower maturation. Dev. **132**, 4107-4118

Nakagawa, T., Suzuki, T., Murata, S., Nakamura, S., Hino, T., Maeo, K., Tabata, R., Nagpal, P., Ellis, C.M., Weber, H., Ploense, S.E., Barkawi, L.S., Guilfoyle, T.J., Hagen, G., Alonso, J.M., Cohen, J.D., Farmer, E.E., Ecker, J.R. and Reed, J.W. (2005). Auxin response factors ARF6 and ARF8 promote jasmonic acid production and flower maturation. Dev. **132**, 4107-4118

Nakajima, M., Shimada, A., Takashi, Y., Kim, Y.C., Park, S.H., Ueguchi-Tanaka, M., Suzuki, H., Katoh, E., Iuchi, S., Kobayashi, M., Maeda, T., Matsuoka, M. and Yamaguchi, I. (2006). Identification and characterisation of *Arabidopsis* gibberellin receptors. Plant J. **46**, 880-889

Neff, M.M., Neff, J.D., Chory, J. and Pepper, A.E. (1998). dCAPS, a simple technique for the genetic analysis of single nucleotide polymorphisms: experimental applications in *Arabidopsis thaliana* genetics. Plant J. **14**, 387-392

Nester, J.E. and Zeevaart, J.A.D. (1988). Flower development in normal tomato and a gibberellin-deficient (*ga-2*) mutant. Am. J. Bot. **75**, 45-55

Ng, M. and Yanofsky, M.F. (2001). Activation of the *Arabidopsis* B class homeotic genes by *APETALA1*. Plant Cell **13**, 739-753

O'Brien, T.P., Feder, N. and McCully, M.E. (1964). Polychromatic staining of plant cell walls by toluidine blue O. Protoplasma **59**, 368-374

Ogawa, M., Hanada, A., Yamauchi, Y., Kuwahara, A., Kamiya, Y. and Yamaguchi, S. (2003). Gibberellin biosynthesis and response during *Arabidopsis* seed germination. Plant Cell **15**, 1591-1604

Ossowski, S., Schneeberger, K., Clark, R.M., Lanz, C., Warthmann, N. and Weigel, D. (2008). Sequencing of natural strains of *Arabidopsis thaliana* with short reads. Genome Res. **18**, 2024-2033

Otsuka, M., Kenmoku, H., Ogawa, M., Okada, K., Mitsuhaski, W., Sassa, T., Kamiya, Y., Toyomasu, T. and Yamaguchi, S. (2004). Emission of *ent*-kaurene, a diterpenoid hydrocarbon precursor for gibberellins, into the headspace from plants. Plant Cell Physiol. **45**, 1129-1138

Parcy, F., Nilsson, O., Busch, M.A., Lee, I. and Weigel, D. (1998). A genetic framework for floral patterning. Nature **395**, 561-566

Penfield, S. and Hall, A. (2009). A role for multiple circadian clock genes in the response to signals that break seed dormancy in *Arabidopsis*. Plant Cell **21**, 1722-1732

Penfield, S., Josse, E.M., Kannangara, R., Gilday, A.D., Halliday, K.J. and Graham, I.A. (2005). Cold and light control seed germination through the bHLH transcription factor SPATULA. Curr. Biol. **15**, 1998-2006

Peng, J.R., Carol, P., Richards, D.E., King, K.E., Cowling, R.J., Murphy, G.P. and Harberd, N.P. (1997). The *Arabidopsis GAI* gene defines a signalling pathway that negatively regulates gibberellin responses. Genes Dev. **11**, 3194-3205

Peng, J.R., Richards, D.E., Hartley, N.M., Murphy, G.P., Devos, K.M., Flintham, J.E., Beales, J., Fish. L.J., Worland, A.J., Pelica, F., Sudhakar, D., Christou, P., Snape, J.W., Gale, M.D. and Harberd, N.P. (1999). 'Green revolution' genes encode mutant gibberellin response modulators. Nature **400**, 256-261

Petroski, M.D. and Deshaies, R.J. (2005). Function and regulation of Cillin-RING ubiquitin ligases. Nat. Rev. Mol. Cell Biol. **6**, 9-20

Pharis, R.P. and King, R.W. (1985). Gibberellins and reproductive development in seed plants. Annu. Rev. Plant Physiol. **36**, 517-568

Phillips, A.L. (2004). Genetic and transgenic approaches to improving crop performance. *In* 'Plant Hormones: Biosynthesis, Signal Transduction, Action!' Ed. Davies, P.J., Kluwer Academic Publishes, Dordrecht, The Netherlands, pp 582-609

Phillips, A.L., Ward, D.A., Uknes, S., Appleford, N.E.J., Lange, T., Huttly, A.K., Gaskin, P., Graebe, J.E. and Hedden, P. (1995). Isolation and expression of three gibberellin 20-oxidase cDNA clones from *Arabidopsis*. Plant Physiol. **108**, 1049-1057

Piffanelli, P., Ross, J.H.E. and Murphy, D.J. (1997). Intra- and extracellular lipid composition and associated gene expression patterns during pollen development in *Brassica napus*. Plant J. **11**, 549-562

Piffanelli, P., Ross, J.H.E. and Murphy, D.J. (1998). Biogenesis and function of the lipidic structures of pollen grains. Sex. Plant Repro. **11**, 65-80

Plackett, A.R.G., Thomas, S.G., Wilson, Z.A. and Hedden, P. (2011). Gibberellin control of stamen development: a fertile field. Trends Plant Sci. **16**, 568-578

Prescott, A.G. and John, P. (1996). Dioxygenases: Molecular structure and role in plant metabolism. Annu. Rev. Plant Physiol. Plant Mol. Biol. **47**, 245-271

Proebsting, W.M., Hedden, P., Lewis, M.J., Croker, S.J. and Proebsting, L.N. (1992). Gibberellin concentration and transport in genetic lines of pea- effects of grafting. Plant Physiol. **100**, 1354-1360

Pysh, L.D., Wysocka-Diller, J.W., Camilleri, C., Bouchez, D. and Benfey, P.N. (1999). The GRAS gene family in *Arabidopsis*: sequence characterisation and basic expression analysis of the *SCARECROW-LIKE* genes. Plant J. **18**, 111-119

Radi, A., Lange, T., Niki, T., Koshioka, M. and Pimenta Lange, M.J. (2006). Ectopic expression of pumpkin gibberellin oxidases alters gibberellin biosynthesis and development of transgenic *Arabidopsis* plants. Plant Physiol. **140**, 528-536

Radley, M. (1961). Gibberellin-like substances in plants. Nature **191**, 684-425

Ratcliffe, O.J., Bradley, D.J. and Coen, E.S. (1999). Separation of shoot and floral identity in *Arabidopsis*. Dev. **126**, 1109-1120

Rebers, M., Kaneta, T., Kawaide, H., Yamaguchi, S., Yang, Y.Y., Imai, R., Sekimoto, H. and Kamiya, Y. (1999). Regulation of gibberellin biosynthesis genes during flower and early fruit development of tomato. Plant J. **17**, 241-250

Regan, S.M. and Moffat, B.A. (1990). Cytochemical analysis of pollen development in wild-type *Arabidopsis* and a male-sterile mutant. Plant Cell **2**, 877-889

Rieu, I., Eriksson, S., Powers, S.J., Gong, F., Griffiths, J., Woolley, L., Benlloch, R., Nilsson, O., Thomas, S.G., Hedden, P. and Phillips, A.L. (2008a). Genetic analysis reveals that C_{19}-GA 2-oxidation is a major gibberellin inactivation pathway in *Arabidopsis*. Plant Cell **20**, 2420-2436

Rieu, I., Ruiz-Rivero, O., Fernandez-Garcia, N., Griffiths, J., Powers, S.J., Gong, F., Linhartova, T., Eriksson, S., Nilsson, O., Thomas, S.G., Phillips, A.L. and Hedden, P. (2008). The gibberellin biosynthetic genes *AtGA20ox1* and *AtGA20ox2* act, partially redundantly, to promote growth and development throughout the *Arabidopsis* lifecycle. Plant J. **53**, 488-504

Rosso, M.G., Li, Y., Strizhov, N., Reiss, B., Dekker, K. and Weisshaar, B. (2003). An *Arabidopsis thaliana* T-DNA mutagenized population (GABI-kat) for flanking sequence tag-based reverse genetics. Plant Mol. Biol. **53**, 247-259

Ruiz-Medrano, R., Xoconostle-Cázares, B. and Lucas, W.J. (1999). Phloem long-distance transport of *CmNACP* mRNA: implications for supracellular regulation in plants. Dev **126**, 4405-4419

Ruzin, S.E. (1999). Plant microtechnique and microscopy. Oxford University Press, New York

Sakamoto, T., Kamiya, N., Ueguchi-Tanaka, M., Iwahori, S. and Matsuoka, M. (2001). KNOX homeodomain protein directly suppresses the expression of a gibberellin biosynthetic gene in the tobacco shoot apical meristem. Genes Dev. **15**, 581-590

Sakamoto, T., Kobayashi, M., Itoh, H., Tagiri, A., Kayano, T., Tanaka, H., Iwahori, S. and Matsuoka, M. (2001a). Expression of a gibberellin 2-oxidase gene around the shoot apex is related to phase transition in rice. Plant Physiol. **125**, 1508-1516

Sakamoto, T., Miura, K., Itoh, H., Tatsumi, T., Ueguchi-Tanaka, M., Ishiyama, K., Kobayashi, M., Agrawal, G.K., Takeda, S., Abe, K., Miyau, A., Hirochika, H., Kitano, H., Ashikira, M. and Matsuoka, M. (2004). An overview of gibberellin metabolism enzyme genes and their related mutants in rice. Plant Physiol. **134**, 1642-1653

Sambrook, J., Fritsch, E.F. and Maniatis, T. (1989). Molecular cloning: a laboratory manual. 2nd ed., Cold Spring Harbor Laboratory Press

Sanders, P.M., Bui, A.Q., Weterings, K., McIntire, K.N., Hsu, Y.C., Lee, P.Y., Truong, M.T., Beals, T.P. and Goldberg, R.B. (1999). Anther development defects in *Arabidopsis thaliana* male sterile mutants. Sex. Plant Repro. **11**, 297-322

Sawhney, V.K. (1992). Floral mutants in tomato: development, physiology, and evolutionary implications. Can. J. Bot. **70**, 701-707

Schomburg, F.M., Bizzell, C.M., Lee, D.J., Zeevaart, J.A.D. and Amasino, R.M. (2003). Overexpression of a novel class of gibberellin 2-oxidases decreases gibberellin levels and creates dwarf plants. Plant Cell **15**, 151-163

Scott, R.J., Spielman, M. and Dickinson, H.G. (2004). Stamen structure and function. Plant Cell **16**, S46-S60

Searle, I. and Coupland, G. (2004). Induction of flowering by seasonal changes in photoperiod. EMBO J. **23**, 1217-1222

Sessions, A., Burke, E., Presting, G., Aux, G., McElver, J., Patton, D., Dietrich, B., Ho, P., Bacwaden, J., Ko, C., Clarke, J.D., Cotton, D., Bullis, D., Snell, J., Miguel, T., Hutchinson, D., Kimmerly, B., Mitzel, T., Katagiri, F., Glazebrook, J., Law, M. and Goff, S.A. (2002). A high-throughput *Arabidopsis* reverse genetics system. Plant Cell **14**, 2985-2994

Shimada, A., Ueguchi-Tanaka, M., Nakatsu, T., Nakajima, M., Naoe, Y., Ohmiya, H., Kato, H. and Matsuoka, M. (2008). Structual basis for gibberellin recognition by its receptor GID1. Nature **191**, 520-523

Shpak, E.D., Berthiaume, C.T., Hill, E.J. and Torii, K.U. (2004). Synergistic interaction of three ERECTA-family receptor-like kinases controls *Arabidopsis* organ growth and flower development be promoting cell proliferation. Dev. **131**, 1491-1501

Silverstone, A.L., Ciampaglio, C.N. and Sun, T.P. (1998). The *Arabidopsis RGA* gene encodes a transcriptional regulator repressing the gibberellin signal transduction pathway. Plant Cell **10**, 155-169

Silverstone, A.L., Chang, C.W., Krol, E. and Sun, T.P. (1997). Developmental regulation of the gibberellin biosynthetic gene *GA1* in *Arabidopsis thaliana*. Plant J. **12**, 9-19

Silverstone, A.L., Jung, H.S., Dill, A., Kawaide, H., Kamiya, Y. and Sun, T.P. (2001). Repressing a repressor: Gibberellin-induced rapid reduction of the RGA protein in *Arabidopsis*. Plant Cell **13**, 1555-1565

Silverstone, A.L., Mak, P.Y.A., Casamitjana-Martinez, E. and Sun, T.P. (1997a). The new *RGA* locus encodes a negative regulator of gibberellin response in *Arabidopsis thaliana*. Genetics **146**, 1087-1099

Singh, D.P., Jermakow, A.M. and Swain, S.M. (2002). Gibberellins are required for seed development and pollen tube growth in *Arabidopsis*. Plant Cell **14**, 3133-3147

Smyth, D.R., Bowman, J.L. and Meyerowitz, E.M. (1990). Early flower development in *Arabidopsis*. Plant Cell **2**, 755-767

Song, S.S., Qi, T.C., Huang, H., Ren, Q.C., Wu, D.W., Chang, C.Q., Peng, W., Liu, Y.L, Peng, J.R. and Xie, D.X. (2011). The Jasmonate-ZIM domain proteins interact with the R2R3-MYB transcription factors MYB21 and MYB24 to affect jasmonate-regulated stamen development in *Arabidopsis*. Plant Cell **23**, 1000-1013

Sorensen, A., Krober, S., Unte, U.S., Huijser P., Dekker, K. and Saedler, H. (2003). The *Arabidopsis ABORTED MICROSPORES* (*AMS*) gene encodes a MYC class transcription factor. Plant J. **33**, 413-423

Spartz, A.K. and Gray, W.M. (2008). Plant hormone receptors: new perceptions. Genes Dev. **22**, 2139-2148

Stintzi, A. and Browse, J. (2000). The *Arabidopsis* male-sterile mutant, *opr3*, lacks the 12-oxophytodienoic acid reductase required for jasmonate synthesis. PNAS **97**, 10625-10630

Strader, L.C., Ritchie, S., Soule, J.D., McGinnis, K.M. and Steber, C.M. (2004). Recessive-interfering mutations in the gibberellin signaling gene *SLEEPY1* are rescued by overexpression of its homologue, SNEEZY. PNAS **101**, 12771-12776

Sun, T.P. (2010). Gibberellin-GID1-DELLA: A pivotal regulatory module for plant growth and development. Plant Physiol. **154**, 567-570

Sun, T.P., Goodman, H.M. and Ausubel, F.M. (1992). Cloning the *Arabidopsis GA1* locus by genomic subtraction. Plant Cell **4**, 119-128

Sun, T.P. and Kamiya, Y. (1994). The *Arabidopsis GA1* locus encodes the cyclise *ent*-kaurene synthetase A of gibberellin biosynthesis. Plant Cell **6**, 1509-1518

Sun, T.P. and Kamiya, Y. (1997). Regulation and cellular localization of *ent*-kaurene synthesis. Physiol. Plant. **101**, 701-708

Sundaresan, V., Springer, P., Volpe, T., Haward, S., Jones, J.D.G., Dean, C., Ma, H. and Martienssen, R. (1998). Patterns of gene action in plant development revealed by enhancer trap and gene trap transposable elements. Genes Dev. **9**, 1797-1810

Swain, S.M., Muller, A.J. and Singh, D.P. (2004). The *gar2* and *rga* alleles increase the growth of gibberellin-deficient pollen tubes in *Arabidopsis*. Plant Physiol. **134**, 694-705

Swain, S.M., Tseng, T.S. and Olszewski, N.E. (2001). Altered expression of *SPINDLY* affects gibberellin response and plant development. Plant Physiol. **126**, 1174-1185

Talon, M., Koornneef, M. and Zeevaart, J.A.D. (1990). Endogenous gibberellins in *Arabidopsis thaliana* and possible steps blocked in the biosynthetic pathways of the semidwarf *ga4* and *ga5* mutants. PNAS **87**, 7983-7987

Tang, X., Zhang, Z.Y., Zhang, W.J., Zhao, X.M., Li, X., Zhang, D., Liu, Q.Q. and Tang, W.H. (2010). Global gene profiling of laser-capture pollen mother cells indicates molecular pathways and gene subfamilies involved in rice meiosis. Plant Physiol. **154**, 1855-1870

Thomas, G., Phillips, A.L. and Hedden, P. (1999). Molecular cloning and functional expression of gibberellin 2-oxidases, multifunctional enzymes involved in gibberellin deactivation. PNAS **96**, 4698-4703

Till, B.J., Reynolds, S.H., Greene, E.A., Codomo, C.A., Enns, L.C., Johnson, J.E., Burtner, C., Odden, A.R., Young., K., Taylor, N.E., Henikoff, J.G., Comai, L. and Henikoff, S. (2003). Large-scale discovery of induced point mutations with high-throughput TILLING. Genome Res. **13**, 524-530

Torii, K.U., Mitsukawa, N., Oosumi, T., Matsuura, Y., Yokoyama, R., Whittier, R.F. and Komeda, Y. (1996). The *Arabidopsis ERECTA* gene encodes a putative receptor protein kinase with extracellular leucine-rich repeats. Plant Cell **8**, 735-746

Tsuji, H., Aya, K., Ueguchi-Tanaka, M., Shimada, Y., Nakazono, M., Watanabe, R., Nishizawa, N.K., Gomi, K., Shimada, A., Kitano, H., Askikira, M. and Matsuoka, M. (2006). GAMYB controls different sets of genes and is differentially regulated by microRNA in aleurone cells and anthers. Plant J. **47**, 427-444

Tuomi, J.M., Voorbraak, F., Jones, D.L. and Ruijter, J.M. (2010). Bias in the C_q value observed with hydrolysis probe based quantitative PCR can be corrected with the estimated PCR efficiency value. Methods **50**, 313-322

Twell. D., Wing, R., Yamaguchi, J. and McCormick, S. (1989). Isolation and expression of an anther-specific gene from tomato. Mol. Gen. Genet. **217**, 240-245

Twell, D., Yamaguchi, J. and McCormick, S. (1990). Pollen-specific gene expression in transgenic plants: coordinate regulation of two different tomato gene promoters during microsporogenesis. Dev. **109**, 705-713

Tyler, L., Thomas, S.G., Hu, J.H., Dill, A., Alonso, J.M., Ecker, J.R. and Sun, T.P. (2004). DELLA proteins and gibberellin-regulated seed germination and floral development in *Arabidopsis*. Plant Physiol. **135**, 1008-1019

Ubeda-Tomas, S., Federici, F., Casimiro, I., Beemster, G.T.S., Bhalerao R., Swarup, R., Doerner, P., Haseloff, J. and Bennett, M.J. (2009) Gibberellin signalling in the endodermis controls *Arabidopsis* root meristem size. Curr. Biol. **19**, 1194-1199

Ueguchi-Tanaka, M., Ashikari, M., Nakajima, M., Itoh, H., Katoh, E., Kobayashi, M., Chow, T.Y., Hsing, Y.I.C., Kitano, H., Yamaguchi, I. and Matsuoka, M. (2005). *GIBBERELLIN INSENSITIVE DWARF1* encodes a soluble receptor for gibberellin. Nature **437**, 693-698

Ueguchi-Tanaka, M., Hirano, K., Hasegawa, Y., Kitano, H. and Matsuoka, M. (2008). Release of the repressive activity of rice DELLA protein SLR1 by gibberellin does not require SLR1 degradation in the *gid2* mutant. Plant Cell **20**, 2437-2446

Ueguchi-Tanaka, M. and Matsuoka, M. (2010). The perception of gibberellins: clues from receptor structure. Curr. Op. Plant Biol. **13**, 1-16

Ueguchi-Tanaka, M., Nakajima, M., Katoh, E., Ohmiya, H., Asano, K., Saji, S., Hongyu, X., Ashikari, M., Kitano, H., Yamaguchi, I. and Matsuoka, M. (2007). Molecular interactions of a soluble gibberellin receptor, GID1, with a rice DELLA protein, SLR1, and gibberellin. Plant Cell **19**, 2140-2155

van Zanten, M., Snoek, L.B., Proveniers, M.C.G. and Peeters, A.J.M. (2009). The many functions of ERECTA. Trends Plant Sci. **14**, 214-218

Varbanova, M., Yamaguchi, S., Yang, Y., McKelvey, K., Hanada, A., Borochov, R., Yu, F., Jikumaru, Y., Ross, J., Cortes, D., Ma, C.J., Noel, J.P., Mander, L., Shulaev, V., Kamiya, Y., Rodermel, S., Weiss, D. and Pichersky, E. (2007). Methylation of gibberellins by *Arabidopsis* GAMT1 and GAMT2. Plant Cell **19**, 32-45

Vernoux, T., Kroneberger, J., Grandjean, O., Laufs, P. and Tras, J. (2000). *PIN-FORMED 1* regulates cell fate at the periphery of the shoot apical meristem. Dev. **127**, 5157

Vivian-Smith, A. and Kolutnow, A.M. (1999). Genetic analysis of growth-regulator-induced parthenocarpy in *Arabidopsis*. Plant Physiol. **121**, 437-451

Ward, J., Jackson, G.J., Beale, M.H., Gaskin, P., Hedden, P., Mander, L.N., Phillips, A.L., Seto, H., Talon, M., Willis, C.J., Wilson, T.M. and Zeevaart, J.A.D. (1997). Stereochemistry of the oxidation of gibberellin 20-alcohols, GA15 and GA44, to 20-aldehydes by gibberellin 20-oxidases. J. Chem. Soc. Chem. Commun. **1**, 13-14

Weigel, D., Alvarez, J., Smyth, D.R., Yanofsky, M.F. and Meyerowitz, E.M. (1992). *LEAFY* controls floral meristem identity in *Arabidopsis*. Cell **69**, 843-859

Weigel, D. and Nilsson, O. (1995). A developmental switch sufficient for flower initiation in diverse plants. Nature **377**, 495-500

Wen, C.K. and Chang, C. (2002). *Arabidopsis RGL1* encodes a negative regulator of gibberellin responses. Plant Cell **14**, 87-100

Wilkinson, M.D. and Haughn, G.W. (1995). *UNUSUAL FLORAL ORGANS* controls meristem identity and organ primordia fate in *Arabidopsis*. Plant Cell **7**, 1485-1499

Williams, J., Phillips, A.L., Gaskin, P. and Hedden, P. (1998). Function and substrate specificity of the gibberellin 3β-hydroxylase encoded by the *Arabidopsis GA4* gene. Plant Physiol. **117**, 559-563

Willige, B.C., Ghosh, S., Nill, C., Zourelidou, M., Dohmann, E.M.N., Maier, A. and Schwechheimer, C. (2007). The DELLA domain of GA INSENSTIVE mediates the interaction with the GA INSENSITIVE DWARF1A gibberellin receptor of *Arabidopsis*. Plant Cell **19**, 1209-1220

Wilson, R.N., Heckman, J.W. and Somerville, C.R. (1992). Gibberellin is required for flowering in *Arabidopsis thaliana* under short days. Plant Physiol. **100**, 403-408

Wilson, Z.A., Song, J., Taylor, B. and Yang, C.Y (2011). The final split: the regulation of anther dehiscence. J. Exp. Bot. **62**, 1633-1649

Wilson, Z.A. and Zhang, D. (2009). From *Arabidopsis* to rice: pathways in pollen development. J. Exp. Bot. **60**, 1479-1492

Woodward, C., Bemis, S.M., Hill, E.J., Sawa, S., Koshiba, T. and Torii, K.U. (2005). Interaction of auxin and ERECTA in elaborating *Arabidopsis* inflorescence architecture revealed by the activation tagging of a new member of the YUCCA family putative flavin monooxygenases. Plant Physiol. **139**, 192-203

Worrall, D., Hird, D.L., Hodge, R., Paul, W., Draper, J. and Scott, R. (1992). Premature dissolution of the microsporocyte callose wall causes male sterility in transgenic tobacco. Plant Cell **4**, 759-771

Wu, K.Q., Li, L., Gage, D.A. and Zeevaart, J.A.D. (1996). Molecular cloning and photperiod-regulated expression of gibberellin 20-oxidase from the long day plant spinach. Plant Physiol. **110**, 547-554

Xu, Y.L., Gage, D.A. and Zeevaart, J.A.D. (1997). Giberellins and stem growth in *Arabidopsis thaliana*- effects of photoperiod on expression of the *GA4* and *GA5* loci. Plant Physiol. **114**, 1471-1476

Xu, Y.L., Li, L., Wu, K., Peeters, A.J.M., Gage, D.A., and Zeevaart, J.A.D. (1995). The *GA5* locus of *Arabidopsis thaliana* encodes a multifunctional gibberellin 20-oxidase: Molecular cloning and functional expression. PNAS **92**, 6640-6644

Yamaguchi, S. (2008). Gibberellin metabolism and its regulation. Annu. Rev. Plant Biol. **58**, 225-251

Yamaguchi, S., Kamiya, Y. and Sun, T.P. (2001). Distinct cell-specific expression patterns of early and late biosynthetic genes during *Arabidopsis* seed germination. Plant J. **28**, 443-453

Yamaguchi, S., Smith, M.W., Brown, R.G.S., Kamiya, Y. and Sun, T.P. (1998). Phytochrome regulation and differential expression of gibberellin 3 beta-hydroxylase genes in germinating *Arabidopsis* seeds. Plant Cell **10**, 2115-2126

Yamamoto, Y., Hirai, T., Yamamoto, E., Kawamura, M., Sato, T., Kitano, H., Matsuoka, M. and Ueguchi-Tanaka, M. (2010). A rice *gid1* suppressor mutant reveals that gibberellin is not always required for interaction between its receptor, GID1, and DELLA proteins. Plant Cell **22**, 3589-3602

Yamauchi, Y., Ogawa, M., Kuwahara, A., Hanada, A., Kamiya, Y and Yamaguchi, S. (2004). Activation of gibberellin biosynthesis and response pathways by low temperature during imbibitions of *Arabidopsis thaliana* seeds. Plant Cell **16**, 367-378

Yamauchi, Y., Takeda-Kamiya, N., Hanada, A., Ogawa, M., Kuwahara, A., Seo, M., Kamiya, Y. and Yamaguchi, S. (2007). Contribution of gibberellin deactivation by *AtGA2ox2* to the suppression of germination of dark-imbibed *Arabidopsis thaliana* seeds. Plant and Cell Physiol. **48**, 555-561

Yang, S.L., Jiang, L.X., Puah, C.S., Xie, L.F., Zhang, X.Q., Chen, L.Q., Yang. W.C. and Ye, D. (2005). Overexpression of *TAPETUM DETERMINANT1* alters the cell fates in the *Arabidopsis* carpel and tapetum via genetic interaction with *EXCESS MICROSPOROCYTES1/EXTRA SPOROGENOUS CELLS*. Plant Physiol. **139**, 186-191

Yang, S.L., Xiea, L.F., Mao, H.Z., Puah, C.S., Yang, W.C., Jiang, L.X., Sundaresan, V. and Ye, D. (2003). *TAPETUM DETERMINANT1* is required for cell specialization in the *Arabidopsis* anther. Plant Cell **15**, 2792-2804

Yasamura, Y., Crumpton-Taylor, M., Fuentes, S. and Harberd, N. (2007). Step-by-step acquisition of the gibberellin-DELLA growth-regulatory mechanism during land-plant evolution. Curr. Biol. **17**, 1225-1230

Yu., H., Ito, T., Zhao, Y.X., Peng, J.R., Kumar, P. and Meyerowitz, E.M. (2004). Floral homeotic genes are targets of gibberellin signaling in flower development. PNAS **101**, 7827-7832

Zeevaart, J.A.D. (1976). Physiology of flower formation. Annu. Rev. Plant Physiol. Plant Mol. Biol. **27**, 321-348

Zeevaart, J.A.D. and Gage, D.A. (1993). *ent*-Kaurene biosynthesis is enhanced by long photoperiods in the long-day plants *Spinichia oleracea* L and *Agrostemma githago* L. Plant Physiol. **101**, 25-29

Zentella, R., Zhang, Z.L., Park, M., Thomas, S.G., Endo, A., Murase, K., Fleet, C.M., Jikumaru, Y., Nambara, E., Kamiya, Y. and Sun, T.P. (2007). Global analysis of DELLA direct targets in early gibberellin signalling in *Arabidopsis*. Plant Cell **19**, 3037-3057

Zhang, W., Sun, Y.J., Timofejeva L., Chen, C.B., Grossniklaus, U. and Ma, H. (2006). Regulation of *Arabidopsis* tapetum development and function by *DYSFUNCTIONAL TAPETUM1* (*DYT1*) encoding a putative bHLH transcription factor. Dev. **133**, 3085-3095

Zhao, D.Z., Wang, G.F., Speal, B. and Ma, H. (2002). The *EXCESS MICROSPOROCYTES1* gene encodes a putative leucine-rich repeat receptor kinase that controls somatic and reproductive cell fates in the *Arabidopsis* anther. Genes Dev. **16**, 2021-2031

Zhu, Y.Y., Nomura, T., Xu, Y.H., Zhang, Y.Y., Peng, Y., Mao, B.Z., Hanada, A., Zhou, H.C., Wang, R.X., Li, P.J., Zhu, X.D., Mander, L.N., Kamiya, Y., Yamaguchi, S. and He, Z.H. (2006). *ELONGATED UPPERMOST INTERNODE* encodes a cytochrome P450 monooxygenase that epoxidizes gibberellins in a novel deactivation reaction in rice. Plant Cell **18**, 442-456

APPENDICES

APPENDIX 1: CLASSIFICATION OF *ARABIDOPSIS* FLORAL AND STAMEN DEVELOPMENT

(a)

Floral Stage	Morphological markers for stage entry	Duration (hours)
1	Flower buttress arises from inflorescence meristem	24
2	Flower primordium forms	30
3	Sepal primordia arise	18
4	Sepals overlie floral meristem	18
5	Petal and stamen primordia arise	6
6	Sepals enclose bud	30
7	Long stamen primordia stalked at base	24
8	Locules appear in long stamens	24
9	Petal primordia stalked at base	60
10	Petals level with short stamens	12
11	Stigmatic papillae appear	30
12	Petals level with long stamens	42
13	Bud opens, petals visible, anthesis	6
14	Long anthers extend above stigma	18
15	Stigma extends above long anthers	24
16	Petals and sepals withering	12
17	All organs fall from green siliques	192
18	Siliques turn yellow	36
19	Valves separate from dry siliques	up to 24
20	Seeds fall	-

Developmental stages in Table (a) are as described by Smyth et al. (1990).

(b)

Anther Stage	Morphological markers for stage entry	Floral Stage
1	Rounded stamen primordia emerge	**5**
2	Archesporial cells arise	
3	Archesporial division: parietal and sporogenous layers arise (primary and seconday) Endothecium layer specified	**7**
4	Four-lobed anther, two developing stomium regions Vascular region initiated	**8**
5	Establishment of four clearly defined locules All anther cell types present and anther organisation defined Appearance of microsporocytes	**9**
6	Entry into meiosis. Middle layer crushed, degenerates Tapetum becomes vacuolated, anther increases in size	
7	Meiosis completed. Tetrads of microspores visible. Remnants of middle layer present	
8	Callose wall surrounding tetrads degenerates. Individual microspores released	**10**
9	Microspores become vacuolated, exine wall generated Growth and expansion of anther continue Septum cells distinguishable with TEM	
10	Tapetum degeneration initiated (entry into PCD)	**11-12**
11	Pollen mitotic divisions occur, tapetum degenerates Expansion of endothecium, secondary thickening appears Septum begins degenerating, stomium differentiation begins	
12	Anther contains tricellular pollen grains Anther becomes bilocular through breakage of septum Stomium distinguishable with TEM	
13	Dehiscence: breakage along stomium and pollen release	**13-14**
14	Stamen senescence, shrinkage of cells	**15-16**
15	Stamen abscission	**17**

Developmental stages in Table (b) are as described by Sanders et al. (1999).

(c)

Pollen Stage	**Morphological markers for** stage **entry**	**Anther Stage**
3	Microsporocytes (Pollen Mother Cells)	**5**
4	Tetrads of microspores surrounded by callose wall	**7**
5	Just released microspores, dense cytoplasm	**8**
6	Early vacuolate microspores	**9**
7	Vacuolated microspores	**9**
8	Pollen Mitosis I: bicellular, vegetative cell and generative cell	**11**
9	Pollen Mitosis II: tricellular, vegetative cell and two gametes	**11**
10	Mature tricellular pollen	**12**

Developmental stages in Table (c) are as described by Regan and Moffat (1990).

APPENDIX 2: PCR CONDITIONS AND PRIMERS

(a)

Locus	Allele	Forward Primer	Reverse Primer	Annealing Temp. (°C)	PCR Product (+Restriction Digest)
GA20ox1	WT	20ox1F	20ox1R	55	370bp
	ga20ox1-1	20ox1F2	LBa1	55	≈600bp
GA20ox2	WT	20ox2F3	20ox2R3	55	947bp
	ga20ox2-3	20ox2F3	GABI-kat LB	55	≈1100bp
GA20ox3	WT	20ox3 dCAPF1	20ox3 dCAPR1	55	93bp + 147bp (DdeI)
	ga20ox3-1	20ox3 dCAPF1	20ox3 dCAPR1	55	93bp + 121bp + 26bp (DdeI)
GA20ox3	WT	ET10670 genoF	ET10670 genoR2	55	308bp
	ga20ox3-3	Ds3-4	ET10670 genoR2	55	325bp
GA20ox4	WT	20ox4dCAP 368F	20ox4dCAP 368R	44	157bp (SpeI)
	ga20ox4-1	20ox4dCAP 368F	20ox4dCAP 368R	44	23bp + 134bp (SpeI)
GA20ox4	WT	GA20ox4 Bur-genoF	GA20ox4 Bur-genoR	55	11bp + 32bp+ 172bp (Hin4I)
	ga20ox4-2	GA20ox4 Bur-genoF	GA20ox4 Bur-genoR	55	214bp (Hin4I)
GA20ox5	WT	20ox5F	20ox5R	55	1295bp
	ga20ox5-2	Ds3-4	20ox5R	55	534bp

(b)

Locus	Allele	Forward Primer	Reverse Primer	Annealing Temp. (°C)	PCR Product (+Restriction Digest)
GA20ox1 ::GUS	WT	20ox1HseqF2	GUSintF5	55	-
	T-DNA	20ox1HseqF2	GUSintF5	55	1616bp
GA20ox2 ::GUS	WT	20ox2seqF	GUSintF5	55	-
	T-DNA	20ox2seqF	GUSintF5	55	1076bp
GA20ox3 ::GUS	WT	20ox3seqF2	GUSintF5	55	-
	T-DNA	20ox3seqF2	GUSintF5	55	1329bp
GA20ox4 ::GUS	WT	20ox4seqF	GUSintF5	55	-
	T-DNA	20ox4seqF	GUSintF5	55	1587bp

(c)

Locus	Allele	Forward Primer	Reverse Primer	Annealing Temp. (°C)	PCR Product (+Restriction Digest)
RGA	WT (Col-0)	RGAgenoF	RGAR-201	55	724bp
	rga-28	rga28-244	LB (rga-28)	65	646bp
GAI	WT (Col-0)	GAI_TDNA_LP3	GAI_TDNA_RP	55	580bp
	gai-td1	LB3	GAI_TDNA_RP	55	494bp
ERECTA	WT	ERWTF	er105R2	55	1085bp
	er105	er105F	er105R2	55	≈600bp
GID1A	WT	GID1A-1F	GID1A-1R	55	552bp
	gid1a-1	LBa1 (T-DNA iso)	GID1A-1R	55	684bp
GID1B	WT	GID1B-1F	GID1B-1R	55	897bp
	gid1b-1	SLAT3'	GID1B-1R	55	354bp
GID1C	WT	GID1C-1F	GID1C-1R	55	570bp
	gid1c-1	LBa1 (T-DNA iso)	GID1C-1R	55	559bp

(d)

Locus	Allele	Forward Primer	Reverse Primer	Annealing Temp. (°C)	PCR Product (+Restriction Digest)
LTP12 ::RGA	WT	pGWBF	LTP12seqR	55	-
	T-DNA	pGWBF	LTP12seqR	55	613bp
LAT52 ::RGA	WT	pGWBF	LAT52seqR	55	-
	T-DNA	pGWBF	LAT52seqR	55	513bp
RGA-GFP	WT	RGAseqF	GFP-R2	55	-
	T-DNA	RGAseqF	GFP-R2	55	1291bp
GFP	WT	GFP-F	GFP-R	55	-
	T-DNA	GFP-F	GFP-R	55	617bp

Tables (a)-(d). Genotyping PCR reactions to distinguish wild-type and mutant alleles in the *GA20ox* (a) and various GA signalling genes (c), and to distinguish the presence of the appropriate transgene insertions in *GA20ox::GUS* reporter (b) and promoter-specific *RGA-GFP* fusion lines (d).

For each reaction the appropriate primer combination is shown, as is the annealing temperature for that reaction and expected PCR product size.

(e)

Amplified Product	Forward Primer	Reverse Primer	PCR Product (bp)
*Hind*III-GA20ox1promoter(I)	20ox1promHindF	20ox1promSpeR	2661bp
GA20ox1promoter(II)-*Nde*I	20ox1promSpeF	20ox1promNdeR	626bp
*Xma*I-GA20ox2promoter-*Nde*I	20ox2promXma2F	20ox2promNdeR	1526bp
*Sal*I-GA20ox3promoter-*Xma*I	20ox3promSalF	20ox3prom XmaATGR	2768bp
*Sal*I-GA20ox4promoter(I)	20ox4promSal2F	20ox4promjoin BamR	1834bp
GA20ox4promoter(II)-*Nde*I	20ox4promjoinBamF	20ox4promNdeR2	373bp
*Xma*I-GA20ox5 promoter(short)-*Nde*I	20ox5promshortXmaF	20ox5promNdeR	620bp
*Xma*I-GA20ox5 promoter(long)-*Nde*I	20ox5promXma2F	20ox5promNdeR	1885bp

(f)

Amplified Product	Forward Primer	Reverse Primer	PCR Product (bp)
*Sal*I-GA20ox1CDS-*Not*I	GA20ox1CDSSalF	GA20ox1CDSNotR	1153bp
*BamH*I-GA20ox3CDS-*Not*I	20ox3F-BamHI	20ox3R-NotI	1193bp
*Sal*I-GA20ox5CDS-*Not*I	GA20ox5CDSSalF	GA20ox5CDSNotR	1177bp
*EcoR*I-GA20ox1CDS-*BamH*I	GA20ox1amp-EcoF	GA20ox1amp-BamR	1154bp
*Xho*I-GA20ox5CDS-*Kpn*I	GA20ox5cDNA amp2-XhoF	GA20ox5cDNA amp-KpnR	1176bp

(g)

Amplified Product	Forward Primer	Reverse Primer	PCR Product (bp)
*Xba*I-LTP12-*Xba*I	LTPXbaF	LTPXbaR	1095bp
*Xba*I-LAT52-*Xba*I	LAT52promXbaF	LAT52promXbaR	613bp
*Sal*I-RGACDS (-stop codon)-*Not*I	rga17SalF	rga17NotR	1779bp

Tables (e)-(g). Amplification PCR reactions involved in the construction of *GA20ox::GUS* reporter (e), *in vitro* expression and *35S::GA20ox* overexpression analysis (f) and promoter-specific *RGA-GFP* fusion transgenic lines (g). *PCR products were amplified from either gDNA (promoter sequence) or cDNA (coding sequence).*

(h)

Primer	Sequence
20ox1F	GCGACGACATGAGCCGCTCAAAATC
20ox1R	CTCTCTAAAGTAGTCCCGTTTTACG
20ox1F2	CATGAATACACGAGCCGCTTC
LBa1	TTTTTCGCCCTTTGACGTTGGA
20ox2F3	CGATCTCTCAAGCCAAGACTCG
20ox2R3	TCTCTATTCACAACCGCTCTATG
GABI-kat LB	CCCATTTGGACGTGAATGTAGACAC
20ox3dCAPF1	CACTAACCATGGTGTCGATGAGAG
20ox3dCAPF1	TTAGAAACAAAGTCTTTAACGGCTT
ET10670genoF	CGATCTTCGATGCAAAGCTCC
ET10670genoR2	CTGAGCCTTCTGCTTCTCACAAG
Ds3-4	CCGTCCCGCAAGTTAAATATG
20ox4dCAP368F	GAATCGATATTTAGATTAAATTACTAG
20ox4dCAP368R	GGATTGATTGCCACTGG
GA20ox4Bur-genoF	GGTTCTAAATCATCAACCAGACCATATAT
GA20ox4Bur-genoR	CGTCAACTCCGTGGTTGGTG
20ox5F	TTTTCGTCAGGTGATTTAGCG
20ox5R	TGAGGGTTTTAGGTCCAAACC
RGAgenoF	CGATTGTCCAACCACGGG
RGAR-201	CAGCTAAGCATCCGATTTGC
rga28-244	ATGGCGGAGGTTGCTTTGAAACTCGAACA
LB (rga-28)	GGCAATCAGCTGTTGCCCGTCTCACTGGTG
GAI_TDNA_LP3	CGGTAACGGCATGGATGAG
GAI_TDNA_RP	AGCTTCGGCGAAGTAAGTAGC
LB3	TAGCATCTGAATTTCATAACCAATCTCGATACAC
ERWTF	CAAAGACCAGTCAGTTGACACAAATC
er105F	AGCTGACTATACCCGATACTGA
er105R2	CTGGAGATTAAGAAGTCATTCAAAGATG
GID1A-1F	GAATTATCGGCGTGCACCA
GID1A-1R	TGATTGTTATTAGGCAAGAGGTAAAACC
LBa1 (T-DNA iso)	TGGTTCACGTAGTGGGCCATCG
GID1B-1F	TCTCCTGTCCACCAAACATTG
GID1B-1R	CTGGGTTTTGGAGACTATGGC
SLAT3'	CTTATTTCAGTAAGAGTGTGGGGTTTTGG
GID1C-1F	ATGGCTGGAAGTGAAGAAGTTAATCT
GID1C-1R	CAGGGCGACGCAGGAG

(i)

Primer	Sequence
GUSintF5	CACACTTTGCCGTAATGAGTGAC
20ox1HseqF2	CTCCAATTCCCAATGAATAGATTAGAC
20ox2seqF	CATGGCAATTTGTTTGTTGGAC
20ox3seqF2	CTATCACATGCTTGACTTCACTGAATC
20ox4seqF	CATTCCCCTATTAAATAAATATGGTGC
pGWBF	CCTCTTCGCTATTACGCCAGC
LTP12seqR	CTTATGTTATTCTTGGGTACATGTCAAAC
LAT52seqR	GAAGTGATTGTAGCAATTGACTCGG
RGAseqF	CAAATCGGATGCTTAGCTGTGTC
GFP-F	CTGTCAGTGGAGAGGGTGAAGG
GFP-R	CATGCCATGTGTAATCCCAGC
GFP-R2	GCACACCGTAAGCGAAAGTAGTAAC

(j)

Primer	Sequence
20ox1promHindF	CATGATTGAGTTGAGGAACTGCAC
20ox1promSpeR	CAACATGGACAATTACCACTATTCC
20ox1promSpeF	CCAGTTTTGAATGAATGGTTAGAGC
20ox1promNdeR	CTAGCATATGTTTGAGAGATTATAGTAAAGTGAGTAGTAGTATTGC
20ox2promXma2F	CTACCCGGGCACATATCATTCGTGGGTGC
20ox2promNdeR	CTAGCATATGTTCTTTTCTTTTTTTTTTCTTGAGAG
20ox3promSalF	CATCAATATACGCTCGTCAGTAAAGC
20ox3promXmaATGR	CTACCCGGGTTTTTTTTAATTATCGTAGATCCTTTTAAGG
20ox4promSal2F	CTAGTCGACGAAAACTTTCTACTGAGTAACGGGAC
20ox4promjoinBamR	CTACCAAATGGATCAAATACTCTTTGG
20ox4promjoinBamF	CTTTAGAGAAACAAGTATCATAATCCTAAATTG
20ox4promNdeR2	CTACATATGTTTAGGTAGAGACTAAAAGATGTTTCATC
20ox5promshortXmaF	CTACCCGGGCAATCACCAATCACAACGTTTTTTAG
20ox5promNdeR	CTAGCATATGATTGTTTTTTTAGTTTTATCCTTTTTTAATATCTTATC
20ox5promXma2F	CTACCCGGGCTTAAATCGTTTATCTTCTTGTAAACACTCTC

(k)

Primer	Sequence
GA20ox1CDSSalF	CACGTCGACATGGCCGTAAGTTTCGTAAC
GA20ox1CDSNotR	CAGCGGCCGCTTAGATGGGTTTGGTGAGC
20ox3F-BamHI	GATCGGATCCATGGCAACGGAATGCATTG
20ox3R-NotI	CTAGTAACGGCCGCCAGTG
GA20ox5CDSSalF	CACGTCGACATGTGCATATATGCATCTAGACAG
GA20ox5CDSNotR	CAGCGGCCGCTCAAGTTGATTTCTTGTCGG
GA20ox1amp-EcoF	CGAATTCCTCAAAATGGCCGTAAGTTTCGTAACAAC
GA20ox1amp-BamR	CGGATCCTTAGATGGGTTTGGTGAGCCAATC
GA20ox5cDNAamp2-XhoF	CCTCGAGCTTATGTGCATATATGCATCTAGACAGAC
GA20ox5cDNAamp-KpnR	CGGTACCCTCAAGTTGATTTCTTGTCGGAG
LTPXbaF	CTCTAGACATGCACTAGATCGATTTACG
LTPXbaR	CTCTAGAGCTTTTACTTTGTTGAGGTCG
LAT52promXbaF	CTCTAGAGTCGACATACTCGACTCAGAAGGTATTG
LAT52promXbaR	CTCTAGATAATTGGAATTTTTTTTTTTGGTGTGTGTAC
rga17SalF	CGTCGACATGAAGAGAGATCATCACCAATTCC
rga17NotR	CGCGGCCGCATGTACGCCGCCGTCGAGAG

Tables (h)-(k). Primer sequences for the genotyping of mutant alleles (h) and of transgenic lines (i), for the amplification of GA20ox promoter fragments for GA20ox::GUS reporter lines (j) and other transgenic lines (k) created during this project.

Sequence within the primer highlighted in red indicates non-native sequence, underlining indicates non-native terminal restriction sites introduced via incorporation into the primer sequence.